2014

UNDERSTANDING HYDROTHERMAL CARBONIZATION OF MIXED FEEDSTOCKS FOR WASTE CONVERSION

Xiaowei Lu
University of South Carolina - Columbia

UNDERSTANDING HYDROTHERMAL CARBONIZATION OF MIXED FEEDSTOCKS FOR WASTE CONVERSION

by

Xiaowei Lu

Bachelor of Engineering
Harbin Institute of Technology, 2007

Master of Engineering
Chinese Academy of Sciences, 2010

Submitted in Partial Fulfillment of the Requirements

For the Degree of Doctor of Philosophy in

Civil and Environmental Engineering

College of Engineering and Computing

University of South Carolina

2014

Accepted by:

Nicole D. Berge, Major Professor

Jorseph R. V. Flora, Committee Member

Yeomin Yoon, Committee Member

Perry J Pellechia, Committee Member

Lacy Ford, Vice Provost and Dean of Graduate Studies

ACKNOWLEDGEMENTS

I would like to gratefully thank my advisor, Dr. Nicole D. Berge for her guidance, patience, and most importantly, the confidence in me during my three-year PhD studies at USC. Her mentorship was paramount in providing a comprehensive experience consistent my long-term career goals. She provides me a model of an instructor and independent thinker with her integrity, mindedness, and most importantly, delicateness and enthusiasm in her career. She trained me to not only be as a seriously experimentalist but also as an independent thinker and researcher. Always make plans for the future, set a goal in life, and push yourself to do hard work, through which you can discover your potential. Without her guidance and help, I will never achieve what I have today. For everything you have done for me, Dr. Berge, thank you so much!

I would like to thank Dr Jorseph R. V. Flora, Dr Yeomin Yoon and Dr Navid B.Saleh. I am very grateful for the guidance and help from Dr Flora in my classes and research, as well as his humor and optimism. I would also like to thank Dr Yoon for his help in my qualify exam, proposal and dissertation defense. Learning from Dr Saleh in class is one of the best experiences I had in USC. I wish you all the best in Texas!

I also owe a big “thank you” to Dr Perry Pellechia, who taught me all the stuff about NMR. I am so grateful about your patience! I wish I will become a researcher like you who is willing to share what you have with others.

I would like to thank the department of Civil and Environmental Engnineering, especially, Karen D. Ammarell, Tina Anderson, Andrea Campbell and Patrick Blake, for all the patience, expertise and help.

I want to thank my workmates, Beth Quattlebaum, Ryan Nelson, Ryan Diederick, Nate Bowman, Petra Olsen, Justine Flora and William Spears. Thank you for your help! Also, I want to thank Paula Lozano Masa, Iftheker Ahmed Khan, Chanil Jung, Linkel Boateng, Jiyong Heo, Nirupam Aich, Nabiul Rafi and Jaime Plazas Tuttle. I will miss you guys

Thank you, Liang Li, Yang Cao, Ke Zhou, Jinzhu Zhou, Marilyn Basset, Tom Basset, Qinghui Huang and Hongquan Wang, for your friendship and generous help during the three years. The beautiful memories with you will be the life-time treasure for me. I would like to especially thank Liang Li, the best workmate and roommate, and Yang Cao who inspired me with her life style. I wish to reunite with you in the future!

Thank you, my dear mother Shuyun Kang, father Zeng Lu, little sister Xiaoyu Lu, my beloved grandmother Shunzhen Zhang and grandfather Zhenjiang Lu. Thank you for shaping what I am today!

Last and most importantly, I want to thank my husband Rixiang Huang, who just got his PhD at the same time with me. There is so much tough time since we got married. Both of us have grown a lot from it. I am looking forwards to experiencing whatever God give us in the future!

ABSTRACT

Hydrothermal carbonization (HTC) is an environmentally beneficial means to convert waste materials to value-added solid and liquid products with minimal greenhouse gas emission. Research is lacking on understanding the influence of critical process conditions on product formation and environmental implication associated with HTC of waste streams. This work was conducted to determine how reaction conditions and heterogeneous compound mixtures (representative of municipal wastes) influence hydrothermal carbonization processes. The specific experiments include: (1) determine how carbonization product properties are manipulated by controlling feedstock composition, process conditions, and catalyst addition; (2) determine if carbonization of heterogeneous mixtures follows similar pathways as that with pure feedstocks; and (3) evaluate and compare the carbon and energy-related implications associated with carbonization products with those associated with other common waste management processes for solid waste.

TABLE OF CONTENTS

LIST OF TABLES

LIST OF FIGURES

CHAPTER 1.

INTRODUCTION

1.1 MOTIVATION

Hydrothermal carbonization (HTC) is a wet thermal conversion process that has been shown to transform organic compounds (such as biomass and organic waste) to value-added products in closed systems under autogenous pressures and over relatively low temperatures (180 - 350 ^{o}C) (Berge et al., 2011). During carbonization, feedstocks undergo a series of reactions, including hydrolysis, dehydration, decarboxylation, aromatization and condensation, ultimately resulting in the generation of gas, liquid and solid (referred as hydrochar so as to differentiate it from solids generated from dry conversion processes) products. These products have garnered significant study, with the majority of studies conducted evaluating the properties of the generated hydrochar. Because the majority of carbon present in feedstock remains integrated within the hydrochar, the recovered solids energy density is enhanced (Berge et al., 2011; Hwang et al., 2012). In addition, the hydrochar has been reported to be attractive for use in many different applications, including soil augmentation, environmental remediation and as an alternative energy source (Goto et al., 2004; Hwang et al., 2012; Liu et al., 2010; Paraknowitsch et al., 2009). Carbonization has also been found to be more energetically

advantageous than other dry thermal conversion processes (e.g., pyrolysis) for the conversion of wet materials.

HTC was first experimentally explored as a means to produce coal from cellulose in 1913 by Bergius (Bergius, 1913). During the past few decades, carbonization studies have reemerged and explored as a means to create novel low-cost carbon-based nanomaterials/nanostructures from carbohydrates (e.g., Hwang et al., 2012). More recently, HTC has been proposed as a potentially attractive municipal solid waste (MSW) conversion technique. Because, during HTC, a large fraction of the carbon remains integrated within the solid material, successful carbonization of wastes has the potential to substantially reduce fugitive greenhouse gas emissions associated with current waste treatment/management processes, including MSW landfills and compost and incineration facilities (Berge et al., 2011; Sevilla et al., 2011b) (Erlach et al., 2012; Escala et al., 2013; Hao et al., 2013; Kruse et al., 2013; Liu et al., 2013; Malghani et al., 2013; Ramke et al., 2009). HTC of waste streams has also emerged as a potential alternative strategy to produce a solid fuel source from waste streams. Ramke et al. (2009), Hwang et al. (2010), and Berge et al. (2011) have all reported that the produced hydrochar has an energy density equivalent to different types of coals (e.g., brown, lignite, etc.). Other advantages associated with carbonization include that emerging compounds, such as pharmaceuticals, personal care products, and endocrine disrupting compounds, may be thermally degraded or transformed during carbonization (Libra et al., 2011). In addition, HTC of waste materials has been shown to require less solids processing/treatment, such as chemical or mechanical dewatering of biosolids (Ramke et al., 2009). HTC of waste

materials also results in considerable waste volume and mass reduction, ultimately requiring less ultimate storage/disposal space.

To date, carbonization has been conducted on limited varieties of model feedstocks and more complex biomass, such as cellulose, lignin, hemicelluloses, starch and wood (Gao et al., 2012; Kang et al., 2012; Kobayashi et al., 2008; Sevilla and Fuertes, 2009b; Yan et al., 2009). There has been little work evaluating the carbonization mechanisms of complex waste materials or complex heterogeneous mixtures of compounds (e.g., lignin, cellulose, hemicellulose, sugars). Before adopting HTC as a waste management technique, it is important to understand the potential benefits and environmental application of HTC products and the influence of feedstock properties and processing parameters (such as time, temperature and processing liquid) on carbonization products.

1.2 Research Objectives

There is a distinct need for mechanistically understanding how reaction conditions and heterogeneous compound mixtures (representative of municipal wastes) influence hydrothermal carbonization processes. The overall objective of this dissertation work is to systematically investigate the carbonization of model compounds of varying complexity and the carbonization of heterogeneous waste materials to evaluate the feasibility of using HTC as a waste management tool. The specific objectives of this work include:

1. Determine how carbonization product properties are manipulated by controlling feedstock composition (Chapters 2, 3, and 5), process conditions (i.e., reaction time and temperature, Chapters 2 - 5), and catalyst addition (Chapter 4).
2. Determine if carbonization of heterogeneous mixtures follows similar pathways as that with pure feedstocks (Chapter 5).
3. Evaluate and compare the carbon and energy-related implications associated with carbonization products with those associated with other common waste management processes for solid waste (Chapter 2).

1.3 DISSERTATION ORGANIZATION

This dissertation is divided into six chapters. Chapters 2 – 5 contain results from laboratory experiments aimed at meeting the specific research objectives of this work. Chapter 6 contains overall conclusions from this study. The following outlines the information provided in each chapter:

In *Chapter 2*, results from the carbonization of solid waste materials (e.g., model food waste, paper and artificially mixed MSW) are reported and the carbon and energy-related implications associated with the carbonization products are compared to those associated with the landfilling, composting, and anaerobic digestion of the same materials. This work has been published in the journal *Waste Management* (Lu et al., 2012).

In *Chapter 3*, cellulose carbonization was conducted under different temperatures (225– 275 ^{o}C) and over a range of reaction times (up to 96 hrs). The gas, liquid and solid properties were measured to determine how changes in carbonization process parameters

influence carbonization. This work has been published in the journal *Bioresource Technology* (Lu l, 2013).

To explore the impact of catalyst addition on carbonization, laboratory experiments were conducted in which HCl, H_2SO_4, NaOH, NaCl, $CaCl_2$, or acetic acid was added to the initial process water. It is anticipated that the addition of catalysts to the carbonization process will occur via the use of alternative initial process waters. Thus the catalysts and their respective concentrations were chosen to mimic those likely found in domestic and industrial wastewaters. Carbonization of cellulose was conducted at 250^{o}C for a period of up to 3 hours. Results from these experiments are included in *Chapter 4*. The chemical composition of the carbonization products were evaluated and used to understand the influence of each on the process. This work has been accepted for publication in the journal *Bioresource Technology*.

Results from the carbonization of several individual pure compounds (e.g., xylose, lignin, starch and glucose) and mixtures of these compounds (e.g., cellulose/xylolse/lignin and starch/glucose) are presented in *Chapter 5*. Results from these experiments were compared to results obtained when carbonizing more complex feedstocks (e.g., paper, pine wood, and corn) of similar chemical composition. These experiments were conducted at 250^{o}C and for reaction times up to 96 hours. These results are used to help understand the influence of feedstock chemical composition (e.g., cellulose, lignin, starch) and complexity on carbonization products, as well as the interaction between the constituents. This work will be submitted to the journal *Bioresource Technology*.

Chapter 6 includes the conclusions of the present research and recommendations on future studies.

CHAPTER 2.

THERMAL CONVERSION OF MUNICIPAL SOLID WASTE VIA HYDROTHERMAL CARBONIZATION: COMPARISON OF CARBONIZATION PRODUCTS TO PRODUCTS FROM CURRENT WASTE MANAGEMENT OF TECHNIQUES[1]

[1] Thermal conversion of municipal solid waste via hydrothermal carbonization: Comparison of carbonization products to products from current waste management techniques, Lu, X., Jordan, B., Berge, N.D., 2012. Waste Management, 32, 1353-1365. Reprinted here with permission of publisher.

ABSTRACT

Hydrothermal carbonization (HTC) is a novel thermal conversion process that may be a viable means for managing solid waste streams while minimizing greenhouse gas production and producing residual material with intrinsic value. HTC is a wet, relatively low temperature (180 – 350 ^{o}C) thermal conversion process that has been shown to convert biomass to a carbonaceous residue referred to as hydrochar. Results from batch experiments indicate HTC of representative waste materials is feasible, and results in the majority of carbon (45 – 75% of the initially present carbon) remaining within the hydrochar. Gas production during the batch experiments suggests that longer reaction periods may be desirable to maximize the production of energy-favorable products. If using the hydrochar for applications in which the carbon will remain stored, it appears that the gaseous products from HTC result in fewer g CO_2-equivalent emissions than the gases associated with landfilling, composting, and incineration. When considering the use of hydrochar as a solid fuel, more energy can be derived from the hydrochar than from the gases resulting from waste degradation during landfilling and anaerobic digestion; however the carbon emissions are greater (for all wastes except for paper). Carbon emissions resulting from the use of the hydrochar as a fuel source are smaller than those associated with incineration, suggesting HTC may serve as an environmentally beneficial alternative to incineration. Results from this study suggest that HTC may play a beneficial role in waste management schemes.

2.1 INTRODUCTION

Hydrothermal carbonization (HTC) is a novel thermal conversion technique that may serve as an environmentally beneficial waste management/treatment process. During HTC, a feedstock is heated in subcritical water (temperatures typically ranging from 180 – 350^{o}C) and at autogenous pressures. As a result, the feedstock is decomposed by a series of simultaneous reactions, including hydrolysis, dehydration, decarboxylation, aromatization, and recondensation (Libra et al., 2011). A carbonaceous residue, referred to as hydrochar, is formed. Research has demonstrated that conversion via HTC of feedstocks ranging from pure substances (e.g., glucose, cellulose) to those more complex in nature (e.g., walnut shells, paper) results in promoting the integration of carbon in the hydrochar.

The predominant focus of the majority of work associated with the development and use of HTC has stemmed from the desire to create sustainable carbon nanomaterials/nanostructures (e.g., Cui et al. 2006; Demir-Caken et al. 2009; Fang et al. 2006; Wang et al., 2001), with applications ranging from hydrogen storage to chemical adsorption (e.g., Chang et al., 1998; Sevilla et al., 2011a). The significant potential environmental benefits associated with this process has led to the recent exploration of waste stream carbonization (Berge et al., 2011; Funke and Ziegler. 2010; Libra et al., 2011; Ramke et al., 2009). HTC has shown promise as a sustainable waste conversion technique, ultimately converting waste materials to value-added products, while promoting integration of carbon in the solid-phase (e.g., Berge et al., 2011; Funke and Ziegler. 2010; Hwang et al., 2010; Libra et al., 2011; Ramke et al., 2009). The ability to recover and reuse waste materials is advantageous, as it promotes the desired waste

management hierarchy prevalent in many countries. Proposed uses of hydrochar include: an adsorbent for environmental remediation (Lui et al., 2010), a novel carbon material (Cui et al., 2006; Demir-Caken et al., 2009; Titirici et al., 2007a,b), a solid fuel source (Cao et al., 2007; Paraknowitsch et al., 2009), and soil augmentation (Libra et al., 2011).

There are many potential advantages associated with using HTC as a solid waste treatment tool. Because, during HTC, a large fraction of the carbon remains integrated within the solid material, successful carbonization of wastes has the potential to substantially reduce fugitive greenhouse gas emissions associated with current treatment/management processes, including MSW landfills and compost (including N_2O) and incineration facilities. Ramke et al. (2009), Hwang et al. (2010), and Berge et al. (2011) carbonized solid waste materials (including paper, food waste, and mixed materials) at different temperatures (180 – 300 ^oC) and report that the majority of carbon initially present remains integrated within the hydrochar material (50 – 90% of initially present carbon). In each of these studies, less than 20 % of the initially present carbon was transferred to the gas-phase, with the balance of carbon being transferred to the liquid-phase. The carbon fractionation reported by these carbonization studies suggests that the hydrochar produced via MSW carbonization may serve as a significant carbon sink. It is important to note that the final use of the hydrochar will dictate the degree of ultimate carbon storage.

HTC of waste streams has also emerged as a potential alternative strategy to produce a solid fuel source. Many of the experiments evaluating the conversion of MSW via HTC have focused on evaluating the energy-related properties of the hydrochar. Ramke et al. (2009), Hwang et al. (2010), and Berge et al. (2011) have all reported that

the produced hydrochar has an energy density equivalent to different types of coals (e.g., brown, lignite, etc.). Lu et al. (2011) report that carbonization results in enhancing the solid energy content by 1.01 to 1.41 times. On a volume basis, the enhancement is more significant and reportedly ranges from 6.39 to 9.0 times (Lu et al. 2011).

Other advantages associated with HTC include that emerging compounds, such as pharmaceuticals, personal care products, and endocrine disrupting compounds, which currently pose significant environmental concerns in landfills, animal wastes, and wastewater may be thermally degraded or transformed during carbonization (Berge et al. 2011). In addition, HTC of waste materials requires less solids processing/treatment (such as chemical or mechanical dewatering of biosolids, Ramke et al. 2009).

To date, there have been relatively few experiments focused on evaluating the HTC of solid waste (e.g., Berge et al. 2011; Ramke et al. 2009). The majority of the studies conducted have evaluated the carbonization of model wastes at a few, somewhat arbitrary, times. These experiments have provided valuable information regarding HTC feasibility and potential environmental benefits. However, the studies lack the data necessary to understand how carbonization product composition (e.g., carbon fractionation, hydrocarbons in the gas-phase) and reaction extent change with time. Solid yields and carbonization extents have been shown to change with time during other thermochemical conversion processes (e.g., Bridgwater 2006). During pyrolysis, solids yields increase with increases in residence time (e.g., Bridgwater 2006). It is unknown if a similar relationship is true for HTC. Understanding how carbonization proceeds over time is also important when assessing overall process needs/requirements (e.g., energy). The specific objectives of this study were to: (1) evaluate the carbonization of model

solid waste streams over time to assess impact of reaction time on product (e.g., solid, liquid, and gas) composition and (2) use the carbonization experiment results to conduct a preliminary assessment of how products formed during HTC compare to those formed during currently utilized waste management processes (e.g., landfills and compost and incineration facilities). Although it is expected that carbon emissions from products formed during HTC will be lower than those produced during other processes, such comparisons have not yet been conducted. In addition, it is unknown how the energy associated with hydrochar compares with the energy associated with gaseous products from landfilling, incineration, and anaerobic digestion.

2.2 MECHANISMS OF HYDROTHERMAL CARBONIZATION

2.2.1 Mechanisms of Hydrothermal Carbonization

HTC is a thermal conversion process that has been reported to convert biomass (and other organics) to a carbon-rich, energy-dense char. HTC has been shown to be exothermic in nature for pure compounds (Funke and Ziegler 2009; Funke and Ziegler 2010; Titirici et al. 2007a) and energetically more advantageous than dry carbonization processes (i.e., pyrolysis), particularly for feedstocks containing moisture (Erlach and Tsatsaronis 2010; Libra et al. 2011; Ro et al. 2008). A requirement of HTC is that the solid feedstock be completely immersed in liquid during carbonization, requiring the process occur in a closed system under saturation pressures. The presence of sufficient water is a critical element associated with HTC because as temperatures increase, the physical and chemical properties of water change significantly, ultimately mimicking that of organic solvents (Siskin and Katritzky 2001; Akiya and Savage 2002; Wantanabe et al. 2004). At 200^{o}C, for example, water behavior approaches that of methanol (Akia and

Savage 2002; Siskin and Katritzky 2001; Watanabe et al. 2004). The elevated temperatures promote ionic reactions and increase the saturation concentrations of dissolved inorganic and organic components (Funke and Ziegler 2010). The heated water has also been shown to have an autocatalytic effect on feedstock carbonization (Funke and Ziegler 2010), facilitating hydrolysis, ionic condensation, and bond cleavage (Funke and Zeigler 2009). This has been observed when evaluating the conversion of cellulose. Cellulose conversion has been reported to occur at lower temperatures (< 220 ^{o}C) under wet conditions than those reported for dry processes (300 – 400 ^{o}C) (Libra et al. 2011).

The mechanisms associated with HTC are currently being explored. Titirici et al. (2007a), Sevilla and Fuertes (2009a,b), and Funke and Zeigler (2010) report that a series of hydrolysis, condensation, decarboxylic, and dehydration reactions occur during HTC. Accordingly, during HTC, the hydrogen and oxygen content of the feedstock decrease (Funke and Ziegler 2009; Libra et al. 2011). Sevilla and Fuertes (2009b) used HTC to produce carbon materials from cellulose and propose the following hydrochar production steps: (1) cellulose hydrolysis, (2) dehydration and fragmentation, (3) polymerization or condensation, (4) polymer aromatization, (5) nucleation, and (6) particle growth.

As the feedstock is converted to hydrochar, a fraction of organics is solubilized in the liquid-phase. The pH of the process water is generally low (< 5, commonly ~2) resulting from the production of organic acids, such as acetic acid. The chemical oxygen demand (COD) and total organic carbon (TOC) of process waters resulting from the carbonization of waste materials has been measured for a limited number of feedstocks (Berge et al. 2011; Ramke et al. 2009). Concentrations of these parameters are in the range of a typical young landfill leachate (Berge et al. 2011; Ramke et al. 2009). A

fraction of carbon is also transferred to the gas-phase, likely a result of decarboxylation (Funke and Zeigler 2009). The evolved gas is small and consists primarily of carbon dioxide. Other hydrocarbons have also been detected in appreciable concentrations (e.g., methane, ethane, propene) (Berge et al. 2011).

The rate and extent of these conversion processes likely depend on process conditions including temperature, time, feedstock composition, and water to solid ratio (Funke and Zeigler 2009). Few studies have evaluated how process conditions influence HTC of different feedstocks. Titirici et al. (2008) compared properties of hydrochar resulting from HTC of various pentoses and hexoses and report that no significant difference in hydrochar composition/properties exists between feedstocks of mono- and polysaccharide carbons, suggesting that the complexity of different sugars does not influence carbonization mechanisms. Yao et al. (2007) found the mechanism of HTC of fructose to be greatly influenced by temperature. At temperatures between 120 – 140^{o}C, fructose formed 5-hydroxymethlfurfural (HMF) by intramolecular dehydration, while at temperatures between 170-180 ^{o}C, HMF was not observed.

To date, there have been a limited number of studies evaluating the carbonization of waste materials. Notable studies evaluating HTC of wastes include Ramke et al. (2009), Hwang et al. (2010), and Berge et al. (2011). Carbonization temperatures (180 – 300^{o}C), times (50 sec – 20 hours), feedstock, and feedstock solid concentrations (20 – 50%) varied from study to study. Reported results from these experiments indicate that the majority of carbon does remain in the solid material, with smaller fractions being transferred to the liquid- and gas-phases. These experiments also evaluated the energy-related properties of the hydrochar, and report energy densities equivalent to lignite coals

or higher, ranging from 15 - 30 MJ/kg (Berge et al. 2011; Hwang et al. 2010; Lu et al. 2011; Ramke et al. 2009). It is important to note, however, that none of these studies have evaluated how product composition changes with time.

2.2.2 Comparison to Other Thermal Conversion Processes

The purpose of this section is to compare HTC with more common thermal waste conversion processes, including pyrolysis, gasification, and incineration. Operational and product distribution data associated with each technique can be found in Table 2.1. The quality and quantity of generated products (e.g., gas, liquid and solid) associated with each conversion technique depends highly on feedstock composition and operational parameters, particularly reaction time and temperature), thus the values presented in Table 2.1 represent typical reported ranges.

Table 2.1 Comparison of Operational Parameters and Product Distribution for Pyrolysis, Gasification, Incineration, and HTC.

Process	Reaction Temp. (^oC)[1, 2]	Reaction Time (hr)[1]	Reaction Atmosphere	Feedstock Moisture Content	Product Distribution						
					Char			Liquid		Gas	
					Dist. (%, wt.)[1]	Carbon (%, wt.)	Energy (MJ/kg)[c]	Dist. (%, wt.)[1]	Energy (MJ/kg)	Dist. (%, wt.)[1]	Energy (MJ/m^3)
Pyrolysis	300 - 500	seconds – weeks[b]	inert	dry	12 - 35	24 – 95[1,3,4]	11 – 35[6,7]	30 - 75	10 – 35[6,9]	13 - 35	5 – 30[6,9,11]
Gasification	500 - 800	seconds	air/O_2	dry	10	4 – 46[2,5]	not avail	5	not avail	85	2 – 20[2,10,11]
Incineration	850 - 1200	seconds-minutes	air/O_2	dry	15 - 20	2-10[12]	NA	NA	NA	80 - 90	12 – 16 MJ/kg_{wast}[d,12] e
HTC[a]	180 - 250	hours - days	inert/limited O_2; sat press	wet	50 - 80	58 - 83[1]	18-36[1,8,13]	5 – 20 (as TOC)	not avail	2 - 5	not avail

[a]note that HTC explorations have been limited, optimization has not yet occurred; [b]depends on process (fast, slow, intermediate, flash); [c]depends on feedstock energy; [d]based on typical MSW found in Tchobanoglous et al. 1993.

[1]Libra et al. 2011; [2]Bridgwater 2006; [3]Wu et al. 1997; [4]Zhang et al. 2010; [5]He et al. 2008; [6]Buah et al. 2007; [7]Ryu et al. 2007; [8]Berge et al., 2011; [9]Phan et al. 2008; [10]Gang et al. 2007; [11]Bosmans and Helsen 2010; [12] Tchobanoglous et al. 1993; [13]Mumme et al. 2011.

NA = not applicable

HTC differs from combustion, gasification, and pyrolysis in that the process occurs at comparatively lower temperatures, is simpler (e.g., compared to fluidized bed gasification), and requires a wet feedstock and/or addition of supplemental liquid (Table 2.1). During HTC, the feedstock is decomposed by reaction mechanisms similar to those in pyrolysis (e.g., hydrolysis, dehydration, decarboxylation, aromatization, and recondensation, Demirba 2000; Libra et al. 2011). In contrast to pyrolysis (and the other conversion processes), HTC produces higher solid (i.e., hydrochar) yields and more water soluble organic compounds. Gaseous oxidation products, particularly carbon dioxide, resulting from HTC are small because unlike combustion and gasification, exposure to oxygen is limited to that initially present in the reactor headspace and any dissolved oxygen in the water. It should also be noted that the total gas produced during HTC is small in comparison to other thermal conversion processes, and thus with a smaller fraction of carbon being transferred to the gas (Table 2.1). The composition of the gas resulting from HTC has only recently been explored; results show presence of energy rich hydrocarbons.

An advantage of HTC over dry conversion processes is that heterogeneous wet organic residues and waste streams can be processed without preliminary separating and drying. Pyrolysis, gasification, and combustion require the feedstock be dried prior to conversion. Energy required to dry feedstocks can be significant, obviously depending on feedstock moisture content. Because, during HTC, the phase change from water to steam is largely avoided, the required energy to heat the water (in a closed system to saturation conditions) is small in comparison to that required to evaporate the same mass of water (Berge et al. 2011). In addition, hydrochar quality and quantity (e.g., structure, size and

functionality) can be varied by changing the carbonization time, feedstock type and concentration, as well as by using additives and stabilizers.

The chemical structure of hydrochar more closely resembles natural coals than pyrolysis-derived chars (Libra et al. 2011; Schumacher et al 1960), which is important when considering the future hydrochar applications. This has prompted investigation of using hydrochar as a substitute for fossil fuels in conventional combustion processes or in novel fuel cells and engines (e.g., Cao et al., 2007; Paraknowitsch et al., 2009). Typical energy contents of chars resulting from each process are shown inTable 2.1. Note that the energy content is dependent on feedstock composition and reaction conditions.

The majority of products produced from thermal conversion products are used for energy-related applications. There has been a lot of recent exploration is using char resulting from pyrolysis as biochar (terminology commonly used to denote char application in soils) to increase soil fertility, while providing a long-term carbon sink (e.g., Lehmann and Joseph 2009). Because HTC is still a fairly new technique, potential uses of the char are still being explored/developed. Hydrochar may serve as a solid fuel source or as an environmental adsorbent. Hydrochar also has the potential to also serve as a valuable soil amendment. Land application of hydrochar, particularly when rich in carboxyl group.

2.3 MATERIALS AND METHODS

2.3.1 Carbonization Experiments

Model feedstocks were chosen to represent components of typical municipal solid waste (MSW). The following feedstocks were chosen: paper (33% (wt.) of waste discarded in landfills), food waste, and mixed MSW. Discarded office paper was used as

the paper feedstock; it was shredded (2 by 10-mm rectangles) prior to use. Rabbit food was used to simulate food wastes discarded in landfills and was crushed prior to use. Mixed MSW was simulated using representative waste materials and mixed to achieve distributions typically landfilled (USEPA 2006). Composition of the mixed MSW (wt. basis) is: 45.5% paper (shredded discarded office paper), 9.6% glass (crushed glass bottles), 16.4% plastic (shredded discarded plastic bottles), 17.6% food (crushed rabbit food), and 10.9% metal (shredded discarded aluminum cans). An ultimate analysis of each initial feedstock is included in Table 2.1 (conducted by Hazen Research, Inc., Golden, CO).

Batch carbonization experiment procedures follow those of Berge et al. (2011). Briefly, the batch experiments were conducted in 160-mL stainless steel tubular reactors. Each reactor consisted of a one-inch diameter stainless steel pipe nipple and end-caps, equipped with a gas sampling valve to allow controlled collection of gas samples. A solids concentration of 20% (wt.) of each feedstock was carbonized. A series of reactors containing the feedstocks were prepared and heated at 250^{o}C. Reactors were sacrificially sampled over a period 5 days. At each sampling time, the reactors were placed in a cold water bath to quench the reaction. After reactors were cooled, gas samples were collected and volume measured. The hydrochar was separated from the process liquid via vacuum filtration and subsequently dried at 80^{o}C to remove residual moisture.

Gas samples were collected in 3-L foil gas sampling bags. Gas volumes were measured by evacuating the gas sampling bag with a 1.0-L gas-tight syringe. Gas samples (0.05 – 0.1 mL) were injected to a GC/MS (Agilent 7890 equipped with a mass spectrometer) for determination of carbon dioxide concentration, as well as identification

of other components in the gas stream (identification via the NIST 2008 library). Gas samples for this analysis were routed through a GS-CarbonPlot column (30 m long and 0.53 mm id, J&W Scientific). Initial oven temperature was 35^{o}C. After 5-min, the temperature was increased at a rate of 25^{o}C/min until a final temperature of 250^{o}C was achieved. Carbon dioxide gas standards were obtained from Matheson Trigas.

After separating the solids from the liquid (via vacuum filtration), the liquid samples were weighed and analyzed for typical water quality parameters, including: pH, conductivity, chemical oxygen demand (COD) and total organic carbon (TOC), following procedures outlined by Berge et al. (2011). Dried solids were weighed to determine hydrochar yields, and carbon (Perkin Elmer 2400 Elemental Analyzer) and energy content (IKA C-200 bomb calorimeter) were measured.

2.3.2 Carbon Emission Calculations

Calculations were performed to provide a preliminary estimate of how the total carbon emissions associated with products from HTC compare to products associated with other waste management processes, including landfills (gas), composting (gas) and incineration (gas). All calculations are focused purely on products from these processes; a systems level analysis was not performed. In addition, in all analyses, total carbon emissions are reported; emissions from biogenic sources are not neglected. These calculations also assume that the char material remains stable over time, with negligible carbon being emitted following carbonization. It should be noted that there has been little work evaluating carbon retention in the hydrochar over time.

Methane and carbon dioxide emissions resulting from waste degradation during landfilling of the waste materials were modeled using the EPA Landfill Gas Emissions

Model (LandGEM), a first order decay model (USEPA 2005), and typical gas collection efficiencies. The methane yields (Lo), decay rates (k), and moisture contents for each material used in this analysis were taken from Levis and Barlaz (2011) and Eleazer et al. (1997), and are listed in Table 2.3. Obviously, gas collection efficiencies play a major role in the determination of fugitive emissions. Collection efficiencies change over time at landfills, ranging from no collection during waste placement to 90 - 95% collection after placement of the final cover (e.g., Levis and Barlaz 2011; Spokas et al. 2006). For the purposes of this study, a hypothetical waste placement/gas collection scenario was adopted, mimicking a scenario reported by Levis and Barlaz (2011). It is assumed that a temporary cover is placed on the waste after year 5 (collection efficiency of 75%), and a final cover during year 15 (collection efficiency of 95%). It is also assumed that there is no gas collection during year 1. The gas collection efficiencies used are reported in Table 2.4. The landfill gas is assumed to be 50% (vol.) methane and 50% (vol.) carbon dioxide. Methane emissions were converted to carbon dioxide equivalents using a global warming potential (GWP) of 25. Gas generation calculations were performed over a period of 75 years, although it is unlikely active gas collection will be sustained for that period of time.

The maximum gaseous emissions from waste degradation during composting were calculated via stoichiometry (elemental analysis of initial waste materials is included in Table 2.2) and assuming that the majority carbon in the biodegradable fraction of the waste is released as CO_2. Appreciable levels of methane and nitrous oxide also are emitted during composting. The contributions of these gases were included in the analysis and calculated using ratios provided by USEPA (2011): 0.0003 g nitrous oxide/g

wet waste and 0.004 g methane/g wet waste. The GWP of nitrous oxide is 310. Carbon emission calculations were performed over a range of waste biodegradation efficiencies (0 – 100%).

Table 2.2 Waste Material Elemental Analysis.

Waste Material	%C ($\%_{db}$)	%H ($\%_{db}$)	%O ($\%_{db}$)	%N ($\%_{db}$)	Moisture Content (%)
Paper	36	5	48.1	0.04	7.6
Food[1]	42.5	5.8	40.8	3.2	12.6
Mixed MSW	28.5	3.8	38.7	0.56	6.3

[1]values in this table are for rabbit food. Typical food waste generally has a much larger moisture content.
db = dry basis

Similar to composting, the maximum gaseous emissions resulting from waste conversion during incineration of the waste materials were calculated using stoichiometry (data in Table 2.6), assuming that all carbon present in the waste is released as CO_2. Carbon emissions from waste conversion were calculated for a range of waste conversion efficiencies. Although conversion efficiencies associated with incineration are typically high, these calculations were performed for illustrative purposes. Carbon emissions calculated from HTC are based on the carbon dioxide measured in the gas-phase. Methane concentrations were below the detection limit.

Table 2.3 Gas Generation Parameters.[1]

Waste Material	Lo (mL CH_4/g dry waste)	Moisture Content (%)	Decay rate (yr^{-1})
Paper	217	6	0.029
Food	300	70	0.144
Mixed MSW	92	21	0.04

[1]values taken from Levis and Barlaz 2011 and Eleazer et al. 1997

Table 2.4 Gas Collection Efficiencies.[1]

Time (year)	Gas Collection Efficiency (%)
1	0
2	45
3	60
4	65
5	70
6	75
7	75
8	75
9	75
10	75
11	79
12	83
13	87
14	91
15	95
>15	95

[1]based on values reported by Levis and Barlaz 2011

2.3.3 Energy Calculations

Energy associated with the products from landfilling, incineration, and anaerobic digestion were calculated and subsequently compared to those associated with hydrochar produced during HTC. It is important to note that complete energy balances of each process were not conducted; a systems analysis was not performed.

Using the predicted methane generation resulting from the LandGEM model (and the gas collection efficiencies reported in Table 2.4) and the energy content of methane (38 MJ/m^3), the energy generation expected from landfilling of each material was calculated by summing yearly energy production for each waste material. It is assumed that 100% of the collected gas will be used to generate energy at 100% efficiency. Energy resulting from waste incineration was calculated using typical energy contents of

the waste materials, assuming 100% conversion of waste, and assuming that all heat in the combustion gas is converted to energy with 100% efficiency. Energy from the anaerobic digestion of food waste was calculated based on the maximum amount of biogas measured at anaerobic digestion facilities reported by Levis et al. (2010) (136 m^3 gas/Mg waste) and assuming 100% of the gas is collected and subsequently converted to energy at 100% efficiency. Energy derived from the HTC process is via the resulting hydrochar. The measured hydrochar energy contents were used with the hydrochar yields to determine the total energy associated with the hydrochar. Any energy that may be derived from the gas- and liquid-phases resulting from HTC is neglected in this analysis.

When using the hydrochar as a fuel source, the carbon integrated within the solid during HTC will be released. The HTC-related carbon emissions when using the hydroch as an energy source include the carbon released during combustion (assuming 100% of the carbon is released) plus the carbon dioxide produced during HTC. For comparison, landfill gas combustion emissions (assume the methane is converted to CO_2 and water) were added to those associated with fugitive emissions previously calculated.

2.4 RESULTS AND DISCUSSION

2.4.1 HTC of waste materials

2.4.1.1 Carbon Distribution

Carbon in the gas, liquid and solid-phases was measured during the carbonization of each feedstock. Carbon fractionations resulting from carbonization are shown in Figure 2.1. Carbon recoveries in these experiments ranged from 85 – 110 %. For all feedstocks, the carbon content of the liquid-phase decreased slightly over time, while the carbon in the gas increased slightly (Figure 2.1). Following an initial decline of carbon in

the solid-phase (likely due to feedstock solubilization and/or leaching of carbon from the waste material), the solid-phase carbon content remained high (approximately 45-75% of the initially present carbon remained within the solid material) and relatively constant for all feedstocks over the 120 hour reaction period. Carbonization of food waste and mixed MSW resulted in the highest fraction of initial carbon remaining in the solid-phase (~64 - 67 %, Figure 2.1), while paper resulted in the smallest solid-phase carbon retention (~44 %). Carbon retention in the hydrochar from MSW carbonization is skewed by the carbon in the inert, uncarbonizable materials. Carbon distributions associated with the food and mixed MSW appear to stabilize after 20 hours, suggesting that the majority of carbonization occurs relatively fast, during the first 8 - 16 hours. Carbon distributions associated with paper did not stabilize until after approximately 72 hours (Figure 2.1). These differences may be due to changes in feedstock composition.

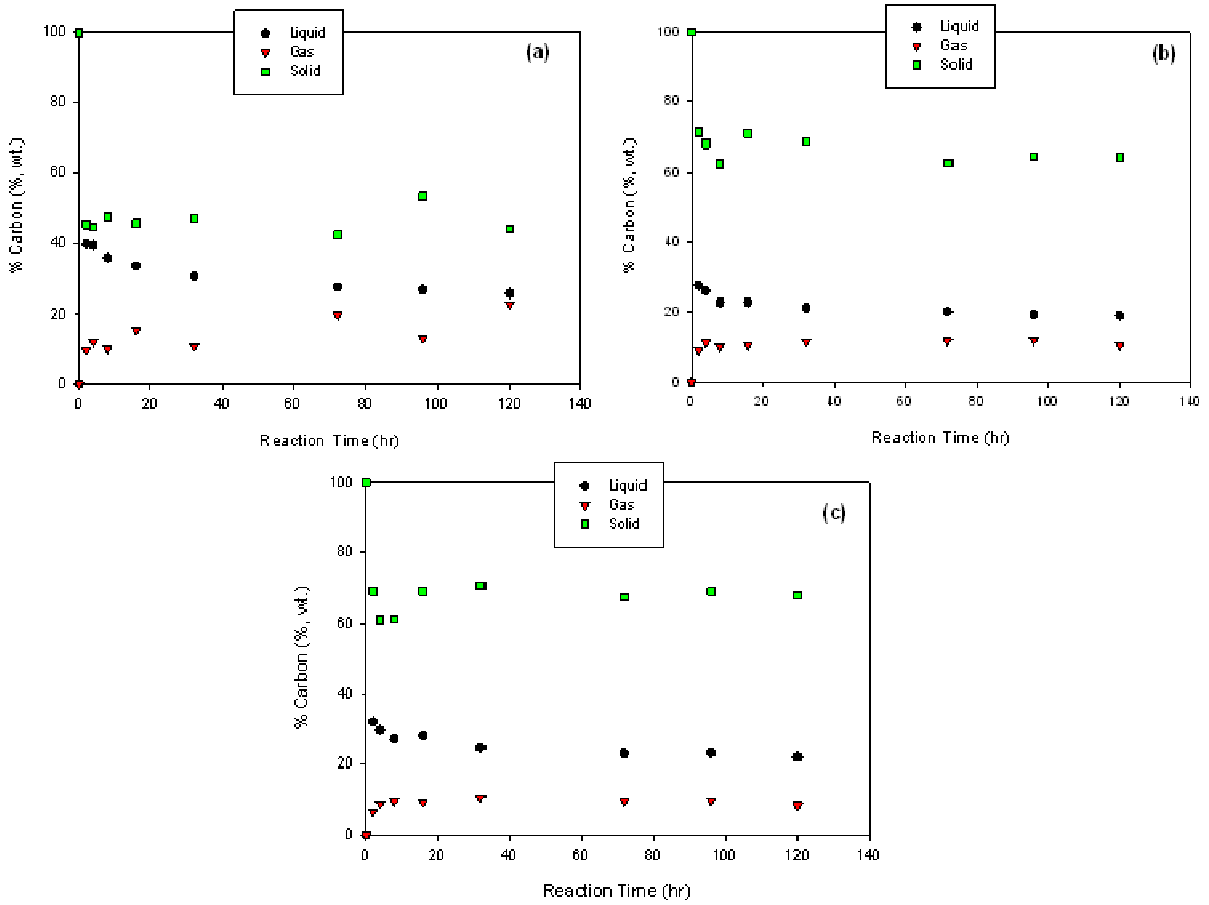

Figure 2.1 Changes in carbon distribution during HTC of (a) paper, (b) food, and (c) MSW.

Portions of the initially present carbon are transferred to the liquid- and gas-phases. The COD/TOC ratios associated with the process water are presented in Figure 2.2. The high ratios suggest that there is a high fraction of easily oxidizable organics in the water. This observation is consistent with reports that the liquid-phase contains significant organic acids, such as acetic acid (Berge et al., 2011; Funke and Zeigler 2009, 2010). The ratios change with time, suggesting the types of organics released into the process water are either changing or transforming. Increases in this ratio suggest that higher concentrations of easily oxidizable organics may be present. The pH of the process waters were < 5.5.

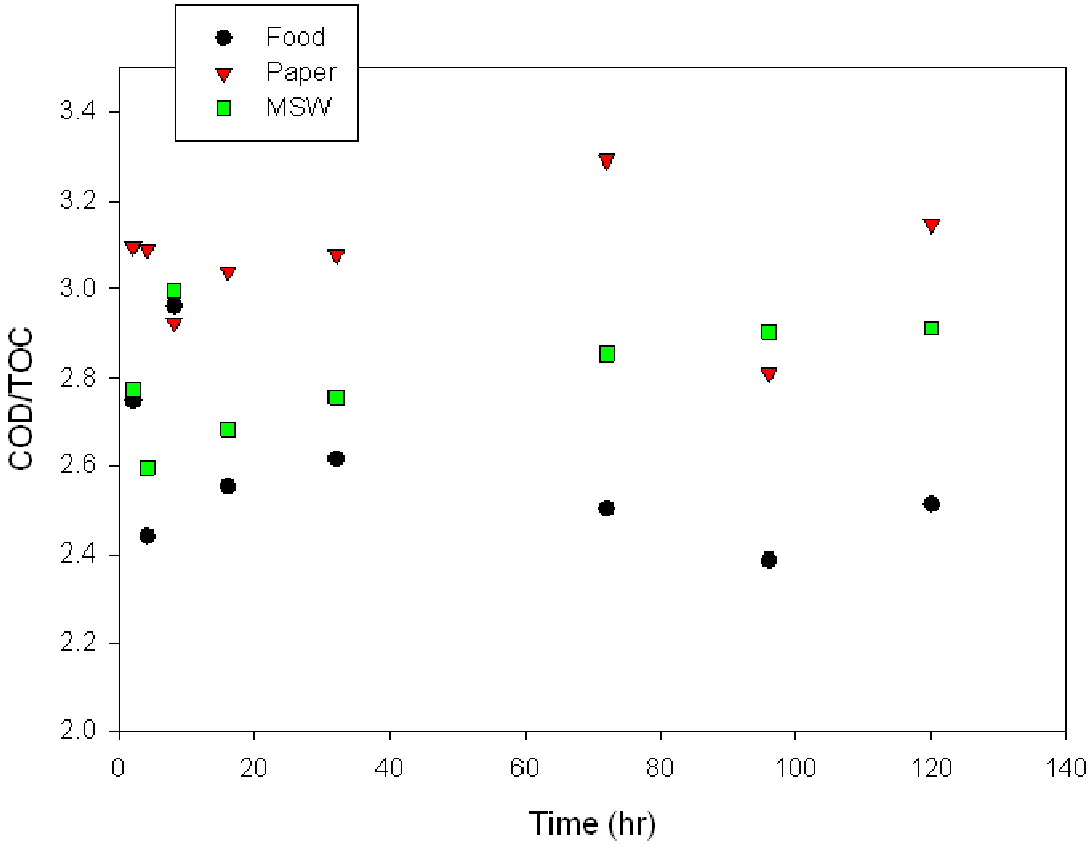

Figure 2.2 COD/TOC ratios in the process water resulting from the carbonization of paper, food waste, and mixed MSW.

The gas produced during carbonization is predominantly carbon dioxide, with trace amounts of other gases such as ethane, propene, and butane. Carbon dioxide has been reported as the predominant gas in other studies, and indicates that decarboxylation occurred (e.g., Berge et al. 2011; Ramke et al. 2009). Gas composition was found to change with reaction time (Figure 2.3). Although trace gas concentrations (or masses) were not quantified, qualitative comparisons of component peak areas can be used to compare gas production between feedstocks. To normalize for changes in gas production over time (gas volume increases with time), each component peak area was multiplied by the corresponding gas volume at the sample time. Interestingly, the mass of several of the trace gases, including propene, propane, butane, ethane, and ethylene, increase with reaction time, which may have a favorable impact on future potential energy recovery. Several of these trace gases have appreciable energy densities: propene: 49 MJ/kg; butane: 50 MJ/kg, and propane: 50 MJ/kg. Propene masses are significantly greater when carbonizing paper or MSW than food waste. Furan was also detected in the MS scans and appears to decrease with time. More analysis is required to confirm furan identification. These gas results suggest that longer reaction periods may be desirable to maximize the production of energy-favorable products.

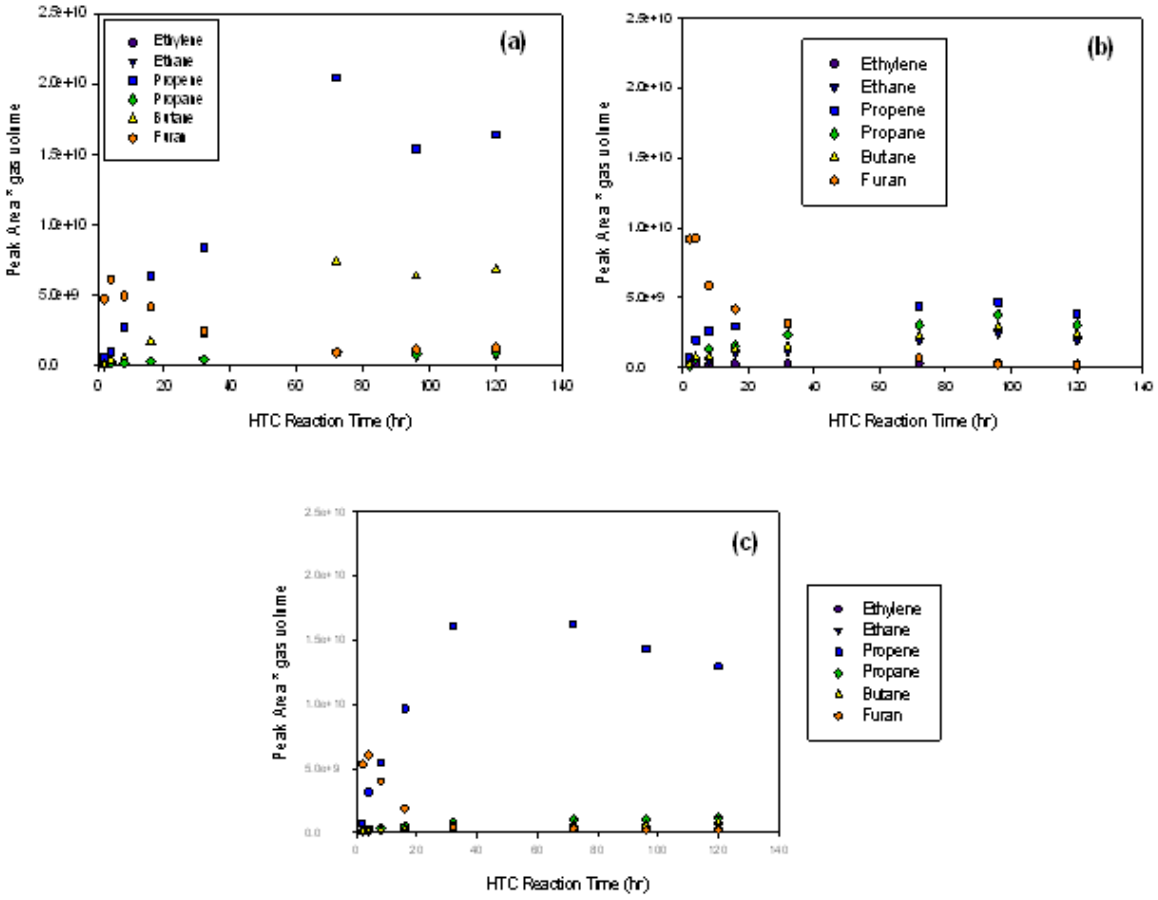

Figure 2.3 Gas composition over time as a result of carbonization of (a) paper, (b) food, and (c) mixed MSW.

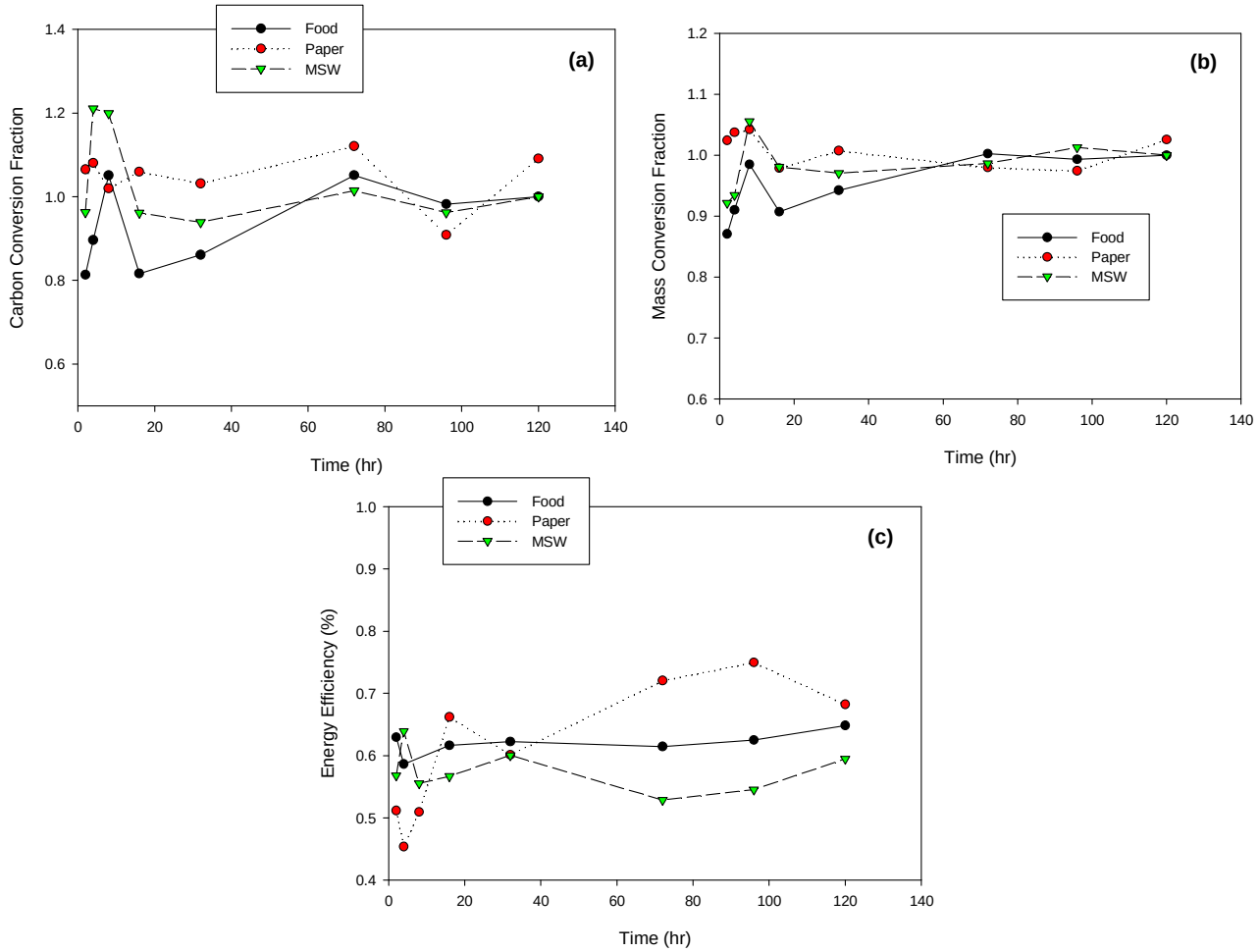

Figure 2.4 Carbon conversion fraction, mass conversion fraction, and energy efficiencies for the carbonization associated with (a) paper, (b) food waste, and (c) mixed MSW. Note that the lines are provided for visual guidance only.

Carbon conversion fractions ($\eta_{c,s}$) were calculated to compare conversion between feedstocks using the relationship provided in equation 1:

$$\eta_{c,s} = \frac{C_{feed} - C_t}{C_{feed} - C_{s,\infty}} \quad (1)$$

where C_{feed} is the mass of carbon in the initial feedstock, $c_{t,s}$ is the mass of carbon in the recovered solids at time t, and $c_{s,\infty}$ is the final carbon mass in the recovered solids. This relationship is analoglous to that often used in solid-state and pyrolysis models to describe gravimetric conversion fractions (e.g., Aggarwal and Dollimore 1996; Khawam and Flanagan 2006). Comparison of conversion fraction trends reveals an interesting phenomenon (Figure 2.4). The carbonization fraction associated with food waste initially increases, and then abruptly decreases. The initial increase is likely a result of initial feedstock solubilization. An initial decline in hydrochar yield (see Figure 2.5a) corroborates this hypothesis. It is likely that feedstock solubilization and char formation occur simulataneously. The abrupt decline in conversion fraction is indicative of more char production than feedstock solubilization. This analysis suggests that carbonization of food waste follows the hypothesized pathways of carbonization: feedstock solubilization followed by carbon partitioning to the gas and/or solid-phase. Different trends in carbonization fraction are observed for paper and MSW. The paper carbon conversion fraction trend changes little over time, suggesting that either solubilization of paper is very fast, char formation is very fast, or solubilization of the paper is insignificant and carbonization follows a pathway different than that observed for food waste. The trend associated with mixed MSW is representative of changes in carbon distribution associated with the paper and food waste. The conversion fraction exceeds 1.0 during early times, corresponding to early time food waste solubilization. The impact

of char production is dampened by the small changes in paper conversion fraction and the recovery of carbon in the inert materials that are not transformed during HTC (e.g., glass, metal).

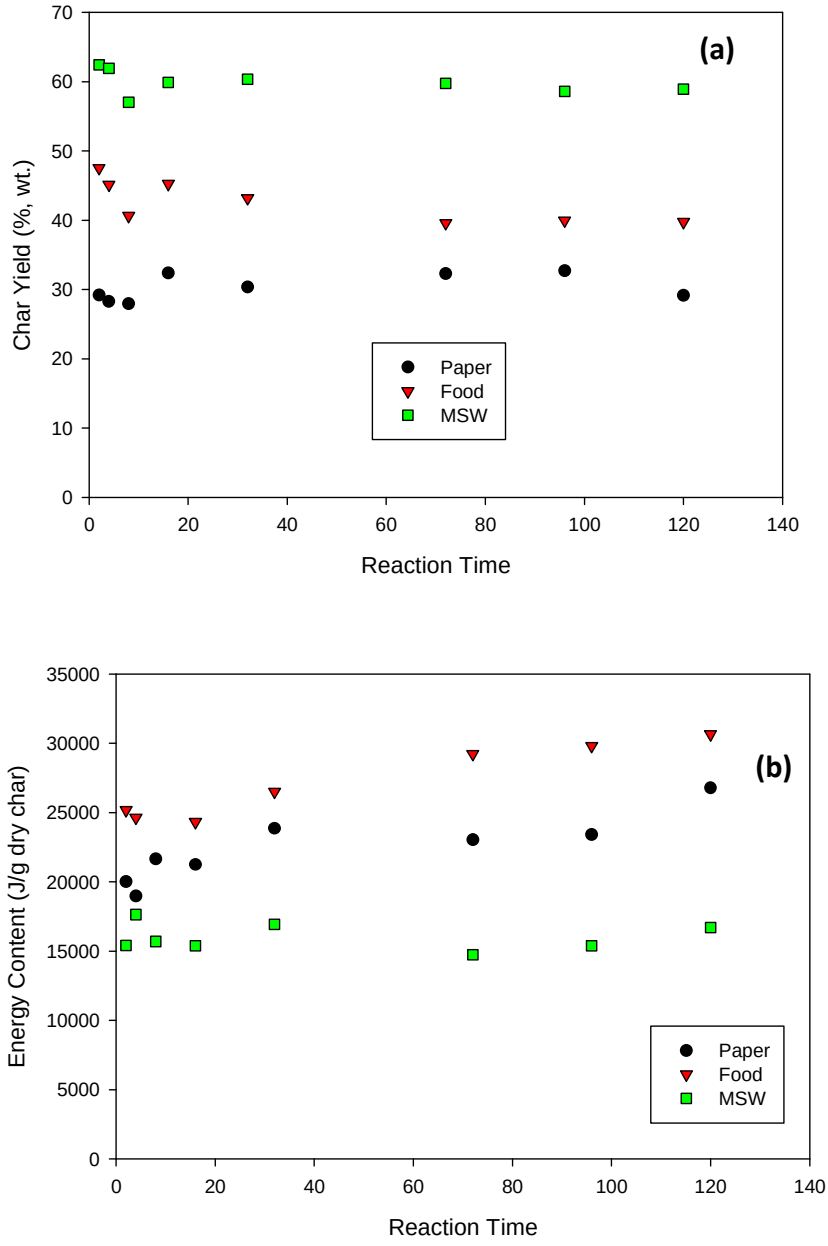

Figure 2.5 Hydrochar yields (a) and energy contents (b) associated with the carbonization of paper, food, and mixed MSW.

Barlaz (1998) developed carbon storage factors (CSFs, mass of carbon remaining in the solid following biological decomposition in a landfill/dry mass of feedstock) as a means to compare the mass of carbon remaining (stored) within solid material following biological decomposition in landfills. When compared with CSFs reported by Staley and Barlaz (2009) for landfilling of paper, food, and MSW, it appears carbonization of similar wastes may result in greater carbon storage. The calculated CSFs associated with the carbonization of each feedstock over the 120 hour reaction period were greater than those reported by Staley and Barlaz (2009) (Figure 2.6). The CSFs associated with carbonization appear to remain relatively stable over time, suggesting that time of carbonization has little impact on carbon storage. Global implications from this analysis should be used with caution, as long-term stability of carbon in the hydrochar is not well understood.

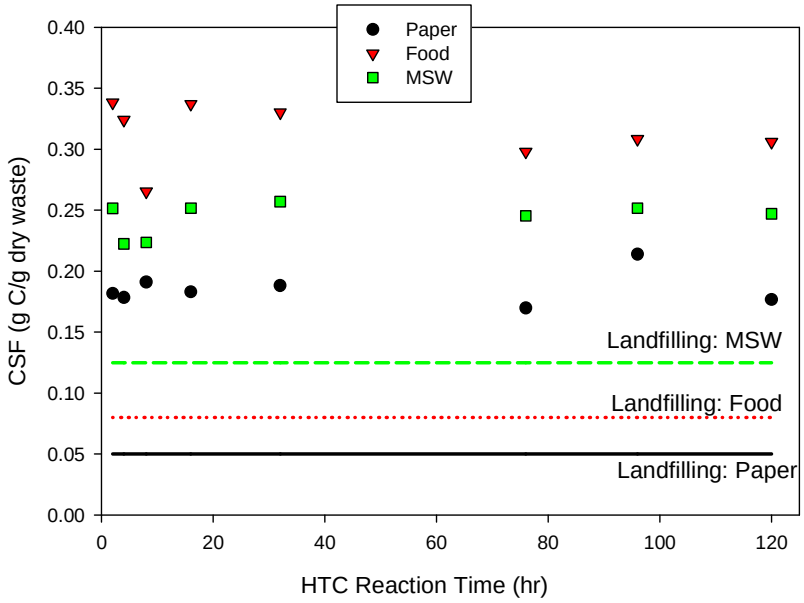

Figure 2.6 Changes in the carbon storage factors (CSFs) over time for each feedstock during carbonization. The lines represent the CSFs associated with the same waste materials during landfilling (reported by Staley and Barlaz 2009).

2.4.1.2 Hydrochar Yield and Energy Value

Because of the inherent value in the char material resulting from carbonization, solids recovery (often refered to as hydrochar yield) and energy content of the char material are important to assess over time. Hydrochar yields are calculated based on the total solids recovered at each sampling time divided by the mass of the initial feedstock. During early sampling time, it is possible (and likely) that the solids recovered will consist of both hydrochar and unreacted feedstock. The solid recoveries ranged from 30 – 60%, and fit within the reported range of hydrochar yields associated with various feedstocks (e.g., Berge et al. 2011; Ramke et al. 2009). The solid recoveries change over time. Initially a decrease (likely a result of initial feedstock solubilization) in solid recovery is observed, followed by a slight increase and subsequent stabilization (Figure 2.5a). The initial decline is more pronounced for food waste, likely a result of significant initial feedstock solubilization. The largest char yield is attained for the MSW, which is likely skewed because of the high recovery of uncarbonizable items (Berge et al. 2011). The lowest yield is associated with paper, following that reported by Berge et al. (2011).

Mass conversion fractions (M_s) following those used in solid-state reactions and in pyrolysis were calculated using equation 2:

$$M_s = \frac{M_{feed} - M_{s,t}}{M_{feed} - M_{s,\infty}} \qquad (2)$$

where M_{feed} is the mass of the initial feedstock, $M_{s,t}$ is the mass of solids recovered at time t, and $M_{s,\infty}$ is the final solid residue mass. The trends associated with mass

conversion fraction closely mimic those observed for carbon conversion fractions and char yields (see Figure 2.4), corroborating previous hypotheses.

The energy content of the solid material resulting from the carbonization of paper and food increases with time (Figure 2.5b), which is important when considering optimal reaction periods. The energy content associated with the solids resulting from carbonization of mixed MSW remained fairly constant with time, likely a result of the lack of conversion of glass/metals. Previous studies have reported that the produced hydrochar has an energy density equivalent to different types of coals (e.g., Ramke et al. 2009; Hwang et al. 2011) and report that the hydrochar energy content correlates well with carbon content of the solids. The same is true in this study. The hydrochar resulting from carbonization of food waste contained the highest energy content (~30MJ/kg). The MSW energy content was the lowest of the three wastes, and is likely skewed by the glass and aluminum energy contents. Greater energy conversion efficiencies (equivalent to the energy in the char divided by the energy in the feedstock), however, were obtained during the carbonization of paper (Figure 2.4).

Utilization of this char as an energy source is one promising option for use of the solids. Although Muthuraman et al. (2010) report blending of thermally pretreated MSW and Indian coal resulted in significant reduction in coal ignition temperature, there has been relatively little work exploring the use of hydrochar for energy purposes. One notable exception to this is work conducted by Paraknowitsch et al. (2009). They found that hydrochar can be used as an energy source in an indirect carbon fuel cell. It is important to note that during combustion of the hydrochar, all carbon will be released (section 4.3).

2.4.2 Comparison of carbon emissions from products formed during HTC and other waste management processes

There are several potential uses for the hydrochar produced during HTC. Depending on the ultimate application, environmental implications will change. In this section, results from the HTC batch experiments are used to compare carbonaceous emissions associated with products from HTC to those associated with landfilling, composting, and incineration. It is important to note that this discussion is only valid if the hydrochar is used as a soil amendment, adsorbent for environmental remediation, and/or simply as a material for storage of carbon. If the intent of hydrochar use is for energy generation (discussed in section 4.3), the hydrochar will be likely combusted and all integrated carbon released to the atmosphere.

2.4.2.1 Landfilling

The fugitive emissions in carbon dioxide-equivalents associated with waste degradation during landfilling of paper, food, and mixed MSW are shown in Figure 2.7. Comparing results from LandGEM and those obtained from the HTC laboratory experiments, it is evident that HTC results in significantly fewer g CO_2-equivalent emissions per gram of wet waste for each waste material (Figure 2.7). This is expected, as the majority of carbon during HTC is integrated within the solid material. Carbonizing paper, food and mixed MSW results in saving approximately 0.25, 0.44, and 0.13 g CO_2-equivalents per gram of wet waste, respectively, than if the materials were landfilled.

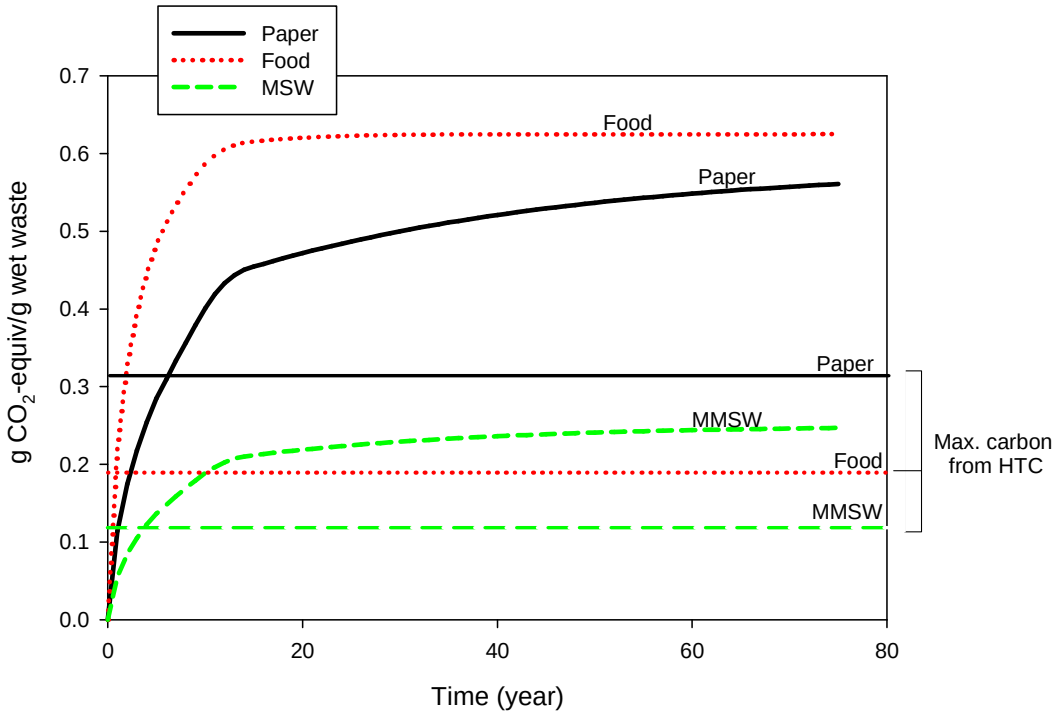

Figure 2.7 Comparison of carbon emissions between landfilling and carbonizing paper, food waste, and mixed MSW. Emissions from landfilling were estimated using first-order decay.

Emissions when landfilling waste materials exceed those associated with waste carbonization after 6.2, 0.83, and 3.5 years for paper, food, and mixed MSW, respectively (Figure 2.7). Compared to landfilling, the impact of waste carbonization is greater for waste materials that degrade quickly, such as food waste, because of the lack of initial landfill gas collection. When considering the mass of food waste generated in the US (28.8 million Mg/year, Levis et al. 2010) and assuming the majority of the food is landfilled, the CO_2-equivalents that can be avoided by carbonization are significant (~12.7 million Mg of CO_2-equivalents each year). Significant reductions in CO_2-equivalents will also result when carbonizing MSW and paper. Using the reported mass of MSW landfilled in 2009 (297 Tg, USEPA 2011), ~38 million Mg of CO_2-equivalents may be avoided each year by carbonizing MSW.

Obviously both gas collection and extent of degradation greatly influence the g CO_2-equivalents emitted as a result of landfilling the materials. The greater the collection efficiency, the fewer emissons. To evaluate how changes in the degree of waste degradation and gas collection efficiencies influence the comparison of carbon emissions between landfills and HTC, calculations were performed over a range (from 0 – 100%) of reported methane yields and over a series of gas collection efficiencies (representing average landfill life collection efficiencies). As would be expected, when the extent of waste degradation is low and gas collection efficiencies are high, carbon emissions from waste degradation in landfills approach those associated with HTC (Fgure 2.8).

Factors not included in this analysis that may have an impact on these calculations include methane oxidation in landfill covers. Levis and Barlaz (2011) report methane oxidation to range from 10 - 55%. A decrease in emissions because of oxidation will reduce the difference between HTC and landfilling. Using the percentage recommended by US EPA (10%, USEPA 1998), the overall conclusion that fewer carbon emissions generally result from carbonization than landfilling will not change. In addition, nitrous oxide emissions from landfills have been reported (e.g., Bogner et al. 2011 and Scheutz et al. 2011). Depending on landfill operation (e.g., aerobic bioreactor), nitrous oxide emissions may be significant. These emissions are not included in this analysis.

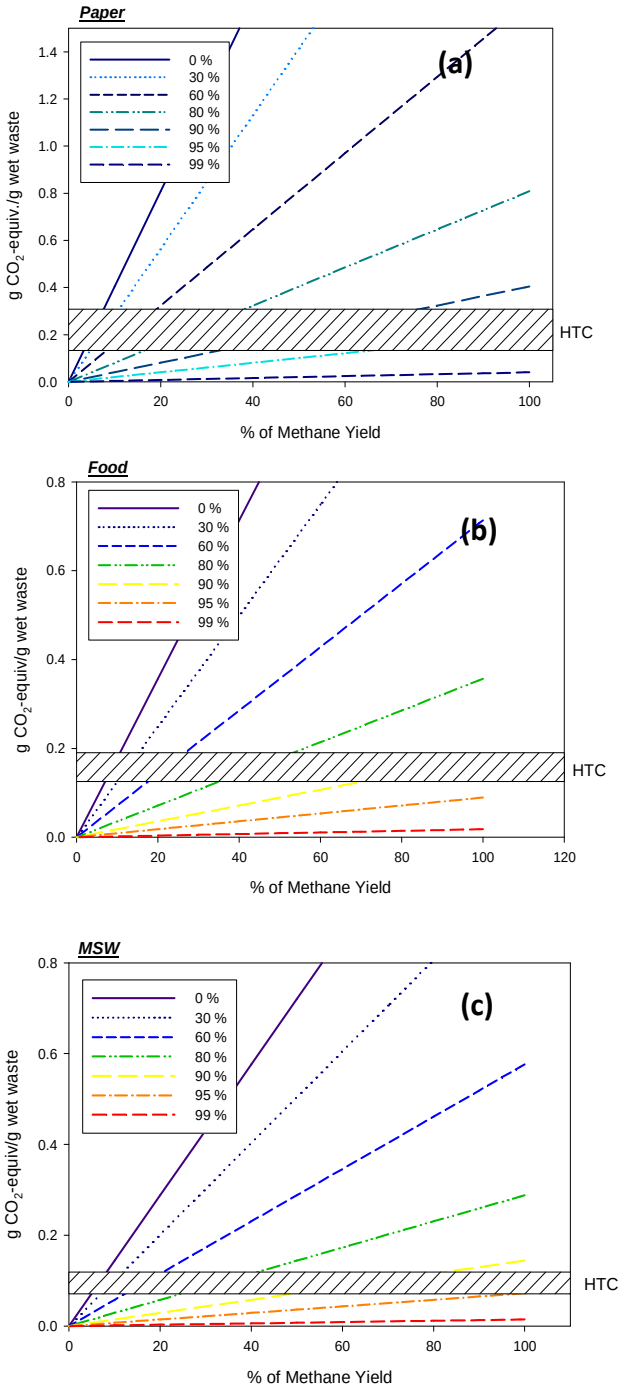

Fgure 2.8 Influence of average landfill gas collection efficiencies on fugitive carbon emissions associated with (a) paper, (b) food waste, and (c) mixed MSW.

2.4.2.2 Composting

Carbon emissions from waste degradation during composting were calculated over a range of waste biodegradation efficiencies (0 – 100%) (Figure 2.9a). In all cases, at high levels of waste biodegradation, gas emissions (in g CO_2-equivalents) from composting are significantly larger than those associated with HTC. This is not surprising, as gas collection does not usually occur during composting. Waste biodegradation via composting is only favorable in terms of carbon emissions when waste degradation is less than 17, 10, and 13% for paper, food, and mixed MSW, respectively. Typically, 50 – 80% of the degradable carbon is degraded during composting (Hermann et al. 2011). Compost is often used as a soil amendment, during which s smaller fraction of the carbon is slowly degraded (~20 – 30% of carbon remains sequestered, Hermann et al. 2011). The long-term stability of hydrochar is currently unknown. After being applied in a soil, hydrochar degradation would need to be substantial to reach the level of carbon emissions associated with the compost.

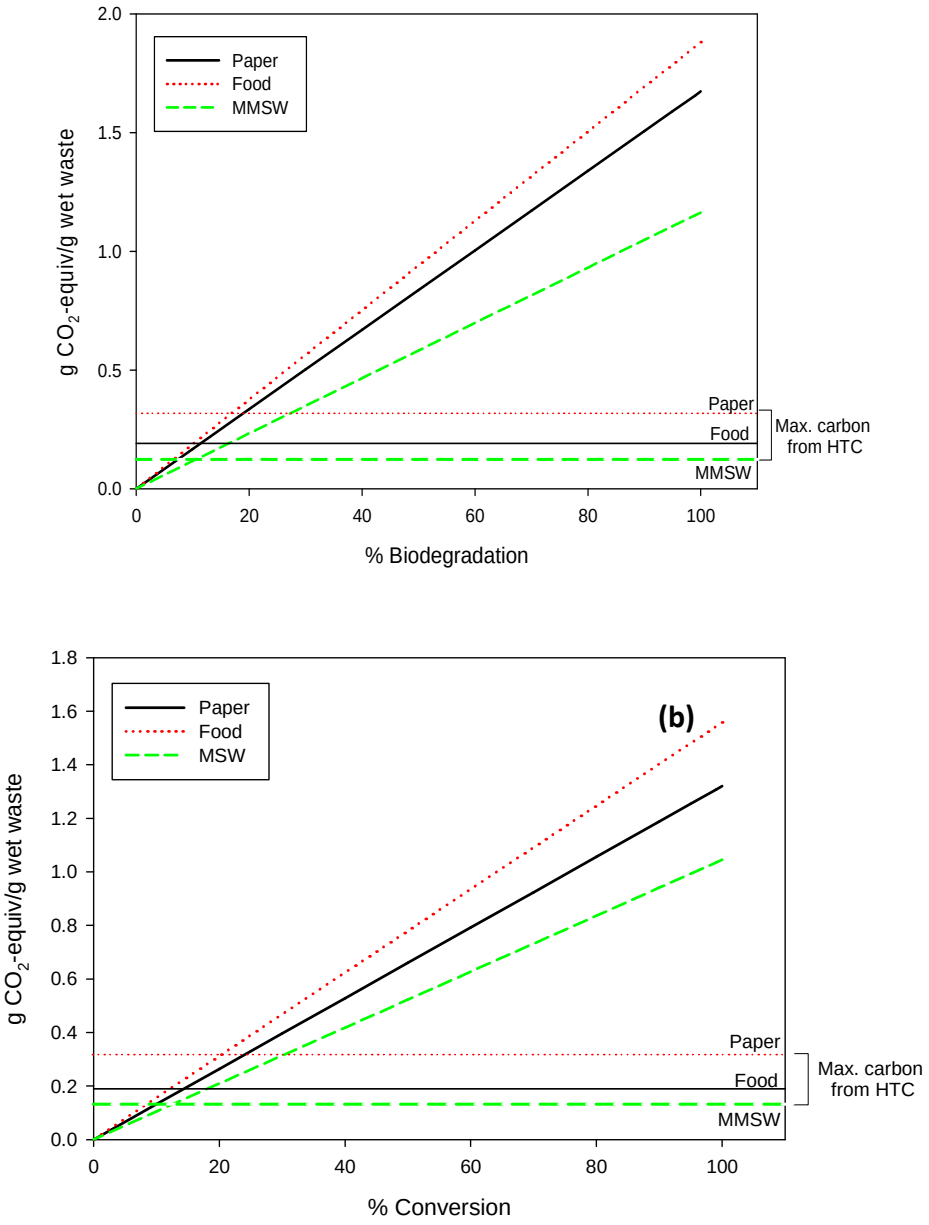

Figure 2.9 Comparison of carbon emissions from (a) composting and carbonization of paper, food, and mixed MSW and (b) incinerating and carbonization of paper, food, and mixed MSW.

2.4.2.3 Incineration

Carbon emissions from combustion gas resulting from waste conversion via incineration were calculated for a range of waste conversion efficiencies (Figure 2.9b). Although waste conversion is typically around 100%, a range of efficiencies were used for illustrative purposes. Results indicate that gas emissions (in g CO_2-equivalents) from incineration are significantly larger than those associated with HTC, assuming there is no capture or storage of the emitted CO_2 from incineration. This result is not surprising. In terms of g CO_2-equivalents, incineration would only be favorable with waste conversions below 20%. Conversions of such low efficiency are not desirable when incinerating waste. It should be noted that the only gaseous emission accounted for in this analysis during incineration is carbon dioxide. Trace gases produced during both incineration and HTC were not included in this analysis. Trace gas production associated with HTC is still fairly unknown.

2.4.3 Comparison of energy generation from products associated with HTC and other waste management processes

An advantage associated with HTC is the generation of a high energy content hydrochar. The energy that may be potentially derived from the hydrochar was compared to that expected from the products from landfilling (methane), incineration (combustion gas), and anaerobic digestion (methane) of the same waste materials. Results from this analysis are presented in Table 2.5**.**

Table 2.5 Potential Energy generation from Waste Management Processes (10^{-3} MJ/g wet waste).[1]

Waste Material	Landfilling[2]	Composting	Anaerobic Digestion[5]	Incineration	HTC[3]
Paper	5.7	0	-	12.9	7.8
Food	1.98	0	2.6 – 3.6	5.43[4]	11.94
Mixed MSW	2.1	0	-	15.5	9.76

[1]assuming 100% conversion to energy and energy content of methane is 38 MJ/m^3
[2]using gas calculations with gas collection efficiencies reported in Table 2.3
[3]maximum energy over a 120 hr period
[4]based on typical food waste, with a moisture content of 70%.
[5] based on the maximum amount of biogas measured at anaerobic digestion facilities reported by Levis et al. (2010): 136 m^3 gas/Mg waste and assuming 50 – 70% of the gas is methane; 100% of the gas is collected

The energy associated with the hydrochar resulting from carbonization is greater than that expected as a result of landfilling each waste material (Table 2.5). The energy generation as a result of carbonization of food waste is 6 times greater than that associated with landfilling of the same material. As discussed previously, a large fraction of methane is lost when landfilling food because of fast waste degradation at a time in which landfill gas collection efficiencies are small. Carbonization of MSW is expected to result in 4.6 times more energy than landfilling. These calculations assume the conversion to electricity is equivalent for all products (e.g., char and gas). It should also be noted that the use of all of the energy predicted as a result of landfilling is unlikely. Because of changes in energy generation over time, it is often not economically feasible to use 100% of the methane from a landfill to generate energy (Berge et al. 2009). There is, however, greater likelihood that 100% of the energy potential can be recovered from the char material, as it is storable and can be used as needed.

Table 2.6 Comparison of Carbon Emissions Resulting from Using the Hydrochar as a Solid Fuel (g CO_2-equivalents/g wet waste).

Waste Material	HTC [1]	Landfill [2]								Incineration [3]
		100% Waste Degradation Collection Efficiencies:				90% Waste Degradation Collection Efficiencies:				
		60%	70%	80%	95%	60%	70%	80%	95%	100% Conv.
Paper	0.91	2.10	1.77	1.45	0.96	1.89	1.60	1.30	1.01	1.32
Food	1.24	0.88	0.74	0.59	0.36	0.80	0.66	0.53	0.39	1.56
MSW	1.00	0.79	0.69	0.58	0.42	0.71	0.62	0.52	0.42	1.05

[1]emissions account for carbon release during combustion (100% of the carbon) and the carbon emissions during HTC; [2]carbon emissions include fugitive emissions and those associated with landfill gas combustion; [3]these values are provided for comparison.

A disadvantage to using hydrochar as an energy source is the release of carbon integrated within the solid during HTC. Table 2.6 contains the total carbon dioxide equivalent emissions when using the hydrochar as a fuel. Carbon emissions associated with landfilling of the same waste materials are also listed in Table 2.6. The landfill gas calculations were conducted for 100 and 90% waste degradation over a series of life-time average gas collection efficiencies. As shown, carbonization of paper still results in lower CO_2-equivalent emissions when using the hydrochar as a solid fuel. This is not the case, however, for food and MSW. In these instances, the carbon emissions are larger. The energy associated with the hydrochar is significantly larger. A systems level analysis is necessary to better understand the trade-offs between energy generation and carbon emissions. It should also be noted that the energy from HTC in this analysis does not include any energy that may be derived from the gas and liquid-phases. This information is not currently known for HTC.

A comparison of energy derived from the methane generated during anaerobic digestion of food waste was also conducted (Table 2.5). Using anaerobic digestion data provided by Levis et al. (2010), food waste digestion will result in 2.6 – 3.6 (10^{-3}) MJ/g wet waste. This is significantly lower than that derived from the hydrochar. The range of energy values results from a range of reported methane contents of the digestion gas, suggesting that HTC may be an attractive alternative for energy purposes.

When considering incineration of these waste materials, it appears that the energy derived from the combustion gas during incineration is greater for paper and MSW than from the hydrochar. Energy associated with the hydrochar from food waste carbonization is greater than that associated with its incineration. It should be noted that the energy value associated with food waste incineration depends highly on the moisture content of the food. The incineration calculations in Table 2.6 assume a moisture content of typical food (~70%). Carbon emissions from incineration of the wastes remain lower than those associated with using the hydrochar as a fuel source (Table 2.6). This suggests that the energy from hydrochar may serve as a more beneficial alternative to incineration.

2.5 CONCLUSIONS

Results from the batch experiments indicate HTC of waste materials results in the majority of carbon (45-75% of the initially present carbon) remaining within the hydrochar. Carbon distributions associated with food waste and MSW stabilized after 20 hours, while carbonization of paper was slower, stabilization observed after 72 hours. Conversion fraction trends illustrate that food waste solubilization occurs prior to/simultaneously with hydrochar formation, following hypothesized char formation

mechanisms, while conversion mechanisms associated with paper are still unclear. Gas production from HTC suggests that longer reaction periods may be desirable to maximize production of energy-favorable products. More data is necessary to determine potential energy yields from the gas.

If using the hydrochar in application in which the carbon will remain stored (such as an environmental adsorbent, soil amendment, or a novel material), it appears that the gaseous product from HTC results in fewer g CO_2-equivalent emissions than those associated with landfilling, composting, and incineration. This conclusion is expected, as the majority of carbon remains integrated in the hydrochar. Converting wastes via HTC to usable materials in which carbon remains integrated (such as an environmental adsorbent) there are definite advantages when comparing emissions from the products of waste treatment processes

When using the hydrochar as a solid fuel, more energy can be derived from the hydrochar than the gases resulting from waste degradation during landfilling and anaerobic digestion. However, there is a trade-off, as higher carbon emissions may result. Carbonization of paper results in lower CO_2-equivalent emissions when compared to degradation of the paper in a landfill. However, this is not the case for food and MSW. Incineration of paper and MSW results in more energy than that from the hydrochar, while the hydrochar resulting from the carbonization of food waste results in more energy than incinerating the food. Carbon emissions resulting from the use of the hydrochar as a fuel source are smaller than those associated with incineration, suggesting HTC may serve as an environmentally beneficial alternative to incineration.

Results from this study suggest that HTC may play a beneficial role in waste management schemes. The type and extent of environmental benefits will be dependent on hydrochar use/the purpose for HTC (e.g., energy generation or carbon storage). Research evaluating conversion of wastes via HTC is still in its infancy, and much work is needed to better understand the environmental implications associated with HTC. There is also a need for more information regarding the energy characteristics of the gas and liquid-phases. Once the necessary data are obtained, a life cycle assessment of each process is required and will provide greater insight to overall system environmental impact

CHAPTER 3.

INFLUENCE OF REACTION TIME AND TEMPERATURE OF PRODUCT FORMATION AND CHARACTERISTICS ASSOCIATED WITH THE HYDROTHERMAL CARBONIZATION OF CELLULOSE[2]

[2] Influence of reaction time and temperature on product formation associated with the hydrothermal carbonization of cellulose, Lu, X., Pellechia, P; Flora, J. R. V.; Berge, N. D., 2013. Bioresource Technology 138. 180-190. Reprinted here with permission of publisher.

ABSTRACT

Studies have demonstrated that hydrothermal carbonization of biomass and waste streams results in the formation of beneficial materials/resources with minimal greenhouse gas production. Data necessary to understand how critical process conditions influence carbonization mechanisms, product formation, and associated environmental implications are currently lacking. The purpose of this work is to hydrothermally carbonize cellulose at different temperatures and to systematically sample over a 96-hour period to determine how changes in reaction temperature influence product evolution. Understanding cellulose carbonization will provide insight to carbonization of cellulosic biomass and waste materials. Results from batch experiments indicate that the majority of cellulose conversion occurs between the first 0.5 to 4 hours, and faster conversion occurs at higher temperatures. Data collected over time suggest cellulose solubilization occurs prior to conversion. The composition of solids recovered after 96 hours is similar at all temperatures, consisting primarily of sp^2 carbons (furanic and aromatic groups) and alkyl groups.

3.1 INTRODUCTION

Recent studies demonstrate that hydrothermal carbonization (HTC) of biomass and solid and liquid waste streams (e.g., municipal solid waste, and human and animal liquid wastes) results in the formation of beneficial materials/resources with minimal greenhouse gas production (e.g., Berge et al., 2011; Falco et al., 2011b; Fuertes et al., 2010; Goto et al., 2004; Hoekman et al., 2011; Hwang et al., 2012; Knežević et al., 2009; Libra et al., 2011; Lu et al., 2012; Sevilla and Fuertes, 2009b; Titirici et al., 2007a; Xiao

et al., 2012). HTC is a wet thermal conversion process that occurs at relatively low temperatures (180 – 300^{o}C) in closed systems under autogenous pressures. During carbonization, a series of simultaneous reactions, including hydrolysis, dehydration, decarboxylation, aromatization, and recondensation occur, leading to the generation of a carbon-rich, high energy density, value-added material referred to as hydrochar. This functionalized carbon material has been the focus of many HTC-related investigations (e.g., Baccile et al., 2009; Cao et al., 2011; Falco et al., 2011b; Fuertes et al., 2010; Hwang et al., 2012; Kang et al., 2012), which have demonstrated that it may be used in several environmentally-relevant applications, such as soil augmentation, environmental remediation, and energy source generation (Goto et al., 2004; Hwang et al., 2012; Kammann et al., 2012; Liu et al., 2010; Paraknowitsch et al., 2009).

Carbonization investigations have been performed on feedstocks ranging from pure substances, such as glucose and cellulose (Falco et al., 2011a; Kang et al., 2012; Knežević et al., 2009; Pińkowska et al., 2011; Sevilla and Fuertes, 2009a,b), to more complex feedstocks, such as paper, food waste, and animal waste (Berge et al., 2011; Cao et al., 2011; Goto et al., 2004; Hwang et al., 2012). These carbonization studies have demonstrated that a large fraction of carbon initially present in the feedstock remains integrated within the hydrochar material during carbonization (Funke and Ziegler, 2010; Libra et al., 2011) and that hydrochar energy-related properties and structure resemble that of a low-grade coal (Berge et al., 2011; Hwang et al., 2012). Although these results provide valuable information regarding HTC feasibility and potential environmental benefits, few have described the time-dependent evolution of the solid, liquid, and gas-

phase carbonization products or how environmental implications associated with carbonization change with reaction time and temperature.

The majority of carbonization studies have been conducted over somewhat arbitrary and limited time frames, detailing the characterization of products at the selected times (e.g., Berge et al., 2011; Falco et al., 2011a; Falco et al., 2011b; Hwang et al., 2012; Kang et al., 2012; Sevilla and Fuertes, 2009a,b). With the exception of a few studies (e.g., Hoekman et al., 2011; Knežević et al., 2010; Knežević et al., 2009; Lu et al., 2012; Mumme et al., 2011; Pińkowska et al., 2011), data describing solid, liquid, and gas-phase product formation ranging from early time to reaction completion is lacking. Because carbonization kinetics likely vary between published studies, reports of only a few measurements at arbitrary time frames complicate comparisons between published data. Reaction time is an important carbonization process parameter requiring a more in-depth exploration to better understand product formation.

A distinct need for a detailed understanding of carbonization product formation/evolution over time at different reaction temperatures remains. Such an understanding will allow for optimization of carbonization, ultimately resulting in lower energy requirements, greater potential energy recovery, and minimal environmental impact. The purpose of this work is to understand the evolution of carbonization product formation and environmental implications associated with cellulose carbonization. Cellulose was chosen because it is a relatively simple feedstock and will provide insight to carbonization of cellulosic biomass and waste materials. The specific objectives of this work include: (1) understanding time dependent carbon distribution in carbonization products at different reaction temperatures; (2) evaluating how reaction temperature and

time influence liquid and gaseous product formation and composition; and (3) characterizing changes in the chemical composition and structure of hydrochar over time at different carbonization temperatures.

3.2 MATERIALS AND METHODS

3.2.1 HTC batch experiments

Microcrystalline cellulose derived from the Western redcedar plant (Thuja plicata, with average particle size of 50 µm, Acros Organics) was used as the feedstock in all experiments. Cellulose carbonization was conducted in 160-mL gas-tight stainless steel tubular reactors (MSC, Inc.) rated to withstand anticipated pressures and temperatures. Each reactor was equipped with a gas-sampling valve to allow controlled collection of gas samples. The in-situ liquid temperature was measured with a pipe-fitting thermocouple probe (Type J) inserted in the reactor and a data logger (Temp-300, Oakton Instruments). Temperatures were recorded every two minutes for the duration of the experiment. It should be noted that the reactors take between 80 and 100 minutes to reach the target reaction temperature (Figure 3.1), similar to other studies (e.g., Mumme et al., 2011). Although some studies define time zero when the reactor reaches the desired temperature, time zero in this work corresponds to the time the reactor is placed in the oven. The length and rate of reactor heating are not always clear in the published studies. As discussed in subsequent sections in this work, a significant fraction of conversion occurs during this heating period. Thus this period is important, potentially representing that in industrial implementation.

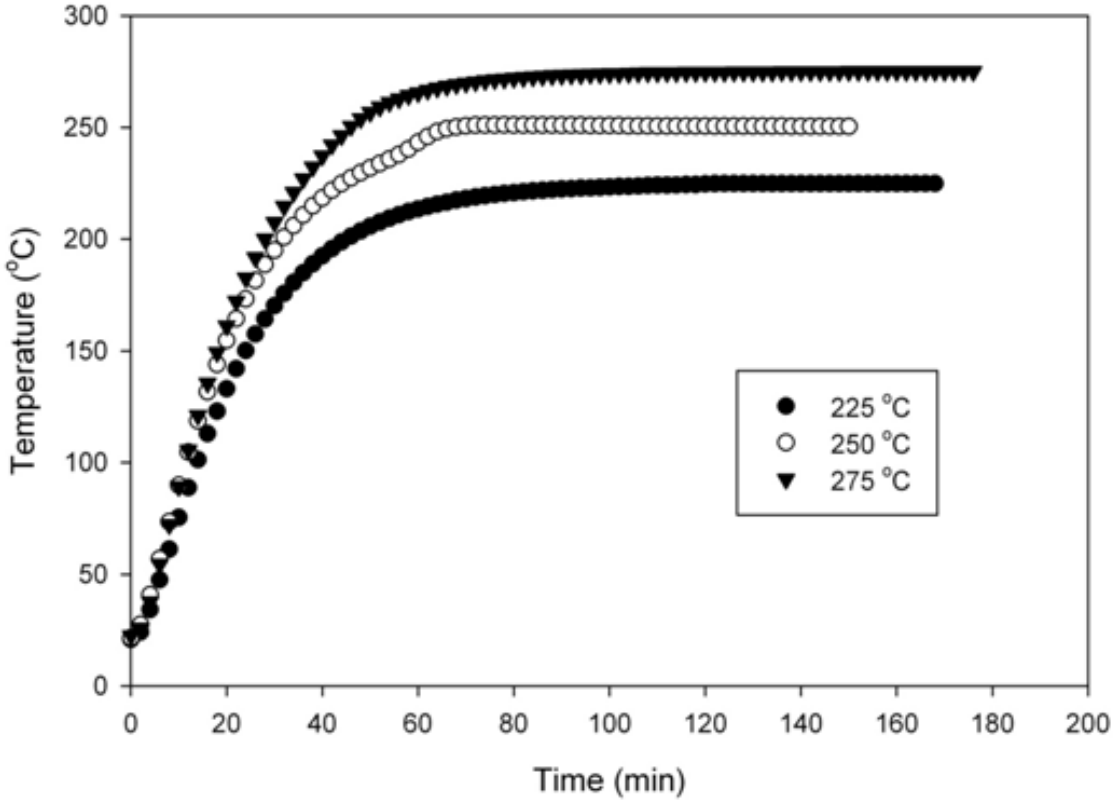

Figure 3.1 Heating profile associated with the three evaluated temperatures.

The batch experiments were conducted following procedures previously described (Berge et al., 2011; Lu et al., 2012). Briefly, a series of reactors containing cellulose (20 %, wt.) and deionized (DI) water were prepared. Reactors were sealed (unstirred) and heated in a laboratory oven to the desired temperature. Three reaction temperatures were evaluated: 225, 250 and 275^{o}C. At each sampling time, the reactors were removed from the oven and subsequently placed in a cold-water bath to quench the reaction. After reactors were cooled, gas samples were collected in either 1 or 3-L foil gas sampling bags (SKC, Inc.) and volume measured using a 1-L gas tight syringe (Hamilton Co.), following procedures previously described by Berge et al. (2011). Solids were separated

from the process liquid via vacuum filtration (0.22 um nitrocellulose filters, Millipore) and subsequently dried at 80^{o}C to remove residual moisture. All experiments (at each temperature and time) were conducted in duplicate.

Samples from the solid (ultimate analysis for solids at 250^{o}C, energy content, carbon content, ^{13}C solid-state NMR), liquid (total organic carbon (TOC), pH, chemical oxygen demand (COD), ^{1}H NMR), and gas phases (gas volume and composition) were taken to evaluate carbonization product evolution at different temperatures. These collected data were used to calculate carbon and energy-related properties associated with the recovered solids, including: carbon fraction, carbon densification, carbon conversion fraction, energy density, and energetic retention efficiency (see Table 3.1 for parameter definitions and equations).

3.2.2 Analytical techniques

Collected gas samples were analyzed for carbon dioxide and other trace gases. Carbon dioxide was quantified using GC-MS (Agilent 7890 equipped with a mass spectrometer). Gas samples were routed through a GS-CarbonPlot column (30m long and 0.53 mm id, J&W Scientific). Initial oven temperature was 35^{o}C. After 5-min, the temperature was increased at a rate of 25^{o}C/min until a final temperature of 250^{o}C was achieved. Carbon dioxide standards were purchased from Matheson Tri-gas. Trace gases were also identified (via the NIST 2008 library) using this technique. Quantification of trace gases was not conducted. The relative amount of gas species was determined by multiplying the peak area by the total gas volume generated at each sample time.

Table 3.1 Terminology and associated equations.

Term	Definition	Equation
Carbon fraction	Mass of carbon in the solid, liquid or gas-phase normalized by mass of initially present carbon. Values are based on carbon mass balances and reported on a dry basis	$\frac{\text{mass carbon in solid, liquid or gas phase}}{\text{mass of carbon in initial feedstock}}$
Carbon conversion fraction	Measure of the extent of solid-phase carbon conversion (defined by Lu et al. 2012)	$\eta = \frac{C_{feed} - C_t}{C_{feed} - C_\infty}$ where C_{feed} is the mass of carbon in the initial feedstock, C_t is the carbon in the recovered solids at time t, and C_∞ is the average carbon in the recovered solids after 96 hours
Carbon densification	Densification of carbon in the recovered solids (dry basis)	$\frac{\%\text{ carbon in the recovered solids}}{\%\text{ carbon in the initial feedstock}}$
Carbon content	Measured carbon concentration in solids (%, dry basis)	$\frac{\text{mass of carbon in solids}}{\text{mass of dry solids}}$
Solids recovery	Mass of solids recovered normalized by mass of initial feedstock (dry basis)	$\frac{\text{mass of dried solids recovered}}{\text{mass of dry initial feedstock}}$
Energy densification	Densification of solid energy content (dry basis)	$\frac{\text{measured energy content of recovered sol}}{\text{measured energy content of feedstock}}$
Energetic retention efficiency	Measure of the fraction of feedstock energy retained within the solid material (based on dry basis)	$\frac{\text{Energy content of recovered solids}}{\text{Energy content of feedstock}} \times \text{solids recovery}$

After separating the solids from the liquid (described previously), the liquid samples were weighed and analyzed for typical water quality parameters, including: pH, total organic carbon (TOC), conductivity, and chemical oxygen demand (COD) (following methods outlined by Berge et al., 2011). Conductivity and pH were measured using electrodes (Thermo Scientific Orion). COD was measured using HACH reagents (HR + test kit, Loveland, CO). TOC was measured using a TOC analyzer (TOC-Vcsn, Shimadzu). To determine composition of organics in the liquid-phase, samples were also analyzed using ^{1}H NMR. Liquid samples (0.6 mL) were analyzed with on a Varian Mercury/VX 400 MHz spectrometer. All samples were spiked with 0.1 mL deuterium oxide (D, 99.9 %, Cambridge Isotope Laboratories, Inc.) to allow ^{2}H field frequency locking. The vendor supplied WET1D pulse sequence was used to suppress the dominant resonance from H_2O. Spectra were collected with a 2.18 s acquisition time over a 16 ppm spectra width with 16 transients and a 10 s relaxation delay between each scan.

All dried solids were weighed and solids recoveries calculated (mass of dry solids recovered divided by the mass of initial dry solids). Carbon content in the solid samples from all times and temperatures was measured with an elemental analyzer (Perkin Elmer 2400). Samples of recovered solids at 250^{o}C were sent to Hazen Research, Inc. (Golden, CO) for ultimate analysis (carbon, hydrogen, oxygen, moisture, and ash content). Recovered solids energy contents were measured using a bomb calorimeter (C-200, IKA). Carbon mass balances were conducted by quantifying the carbon content in the gas (as carbon dioxide), liquid (as total organic carbon) and solid phases (solid-phase carbon content and solids recovery).

Recovered solids were also analyzed using ^{13}C-NMR to identify and provide semi-quantitative information associated with functional groups at each reaction temperature and time. Cross-polarization with magic angle spinning (CP-MAS) spectra were collected on a Varian Unity-Inova 500 MHz spectrometer using a Doty Scientific XC4 4mm MAS probe. The spectra were collected at ambient temperature with sample rotation rate of 8 kHz. TOSS sideband suppression was used as well as TPPM decoupling at a ^{1}H field strength of 62.4 kHz. Contact time of 1.5 ms had a linear amplitude ramped on the ^{13}C RF channel. Spectra were collected with a 50 ms acquisition time over a 400 ppm spectra width. The number of transients varied from 2,000 to 50,000 with a 1.5 s relaxation delay between each scan.

Each NMR spectrum was subsequently deconvoluted using MestRenova software (MestreLab Research, Version 7.0). Four main regions are detected in the ^{13}C NMR spectra (Table 3.3), following that reported by Baccile et al. (2009) and Falco et al. (2011b) . Peaks within Region I (0 − 48 ppm) result from the production of nonpolar alkyl carbons. Region II (60 − 105 ppm) represents C-O bonds associated with cellulose (Dudley et al., 1983). The peaks within this region can be further subdivided to describe individual components of cellulose. Region III (110 − 151 ppm) is representative of sp^2 hybrid carbons, containing peaks associated with furanic and aromatic carbons. The four peaks at 110, 118, 140 and 150 ppm are associated with furanic compounds. The peaks at 110 and 150 ppm correspond to β-carbons and α-carbons connected to H or alkyl chains, respectively. The peak at 118 ppm is attributed to two β-carbons connecting two furan rings. The peak at 143 ppm is assigned to the two α-carbons connecting two furan rings. The peak at 126 and 133 ppm represents aromatic compounds. Peaks within Region IV

(175 − 207 ppm) are attributed to C=O bonds (carbonyl groups). Peak intensities, width and the Gaussian/Lorentzian ratio were allowed to vary during deconvolution. Carbon distributed in the identified functional groups are calculated based on the percent area of each peak and normalized to the amount of carbon in the solid-phase (measured as described previously).

3.3 RESULTS AND DISCUSSION

3.3.1 Carbon distribution

Mass balance analyses indicate that cellulose carbonization results in a significant fraction (> 77%) of initially present carbon retained within the solid-phase over the 96-hour reaction period at all temperatures evaluated (Figure 3.2). This observation is consistent with observations at shorter time frames in other cellulose carbonization studies reported in the literature (e.g., Kang et al., 2012; Sevilla and Fuertes, 2009b). Between 7 and 30% of initially present carbon is transferred to the liquid-phase. A smaller fraction (<10%) of initially present carbon is transferred to the gas-phase, consistent with observations at selected times in previous studies (Berge et al., 2011; Hoekman et al., 2011; Lu et al., 2012). Carbon recoveries in all experiments range from 90-115%.

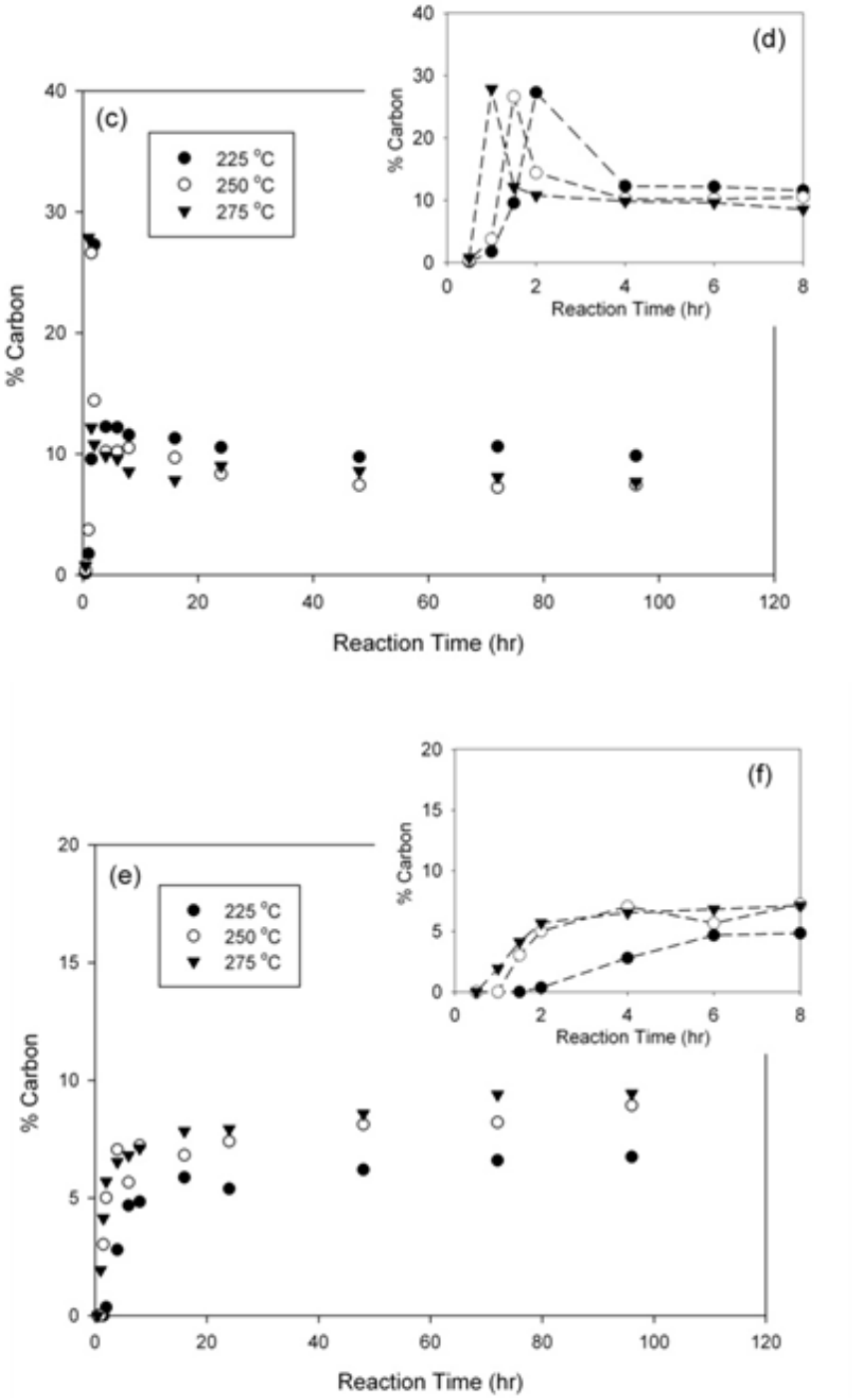

Figure 3.2 Carbon distribution over time at 225, 250, and 275°C in the solid (a and b), liquid (c and d), and gas-phases (e and f). Data points represent averages from duplicate experiments.

3.3.2 Influence of reaction time

Carbon distribution (defined in Table 3.1) changes with reaction time and provides insight to carbonization pathways/mechanisms. At each temperature (225, 250, and 275^{o}C), carbon distribution follows two distinct rates/trends, similar to that reported by Knezevic et al. (2010; 2009) for the conversion of wood, pyrolysis oil, and glucose. The first period, associated with early time data (time ranges from 0 to 6-8 hours), is characterized by significant changes in carbon distribution (Figure 3.2b,d,f). During this period and following an initial lag, a rapid decline in solid-phase carbon is observed, likely due to feedstock solubilization. Lu et al. (2012) and Knezevic et al. (2010) also observed solubilization of feedstock components followed by char formation when carbonizing rabbit food and wood, respectively. This decrease in carbon integrated within the solid-phase is coupled with a simultaneous increase in liquid and gas-phase carbon (see Figure 3.2b,d,f) as well as with a decrease in solids recovered (Figure 3.3), supporting this hypothesis. Carbon conversion fractions (as defined by Lu et al. (2012), Table 3.1) were calculated and reflect the extent of solid-phase carbon conversion. Carbon conversion fractions greater than one are likely indicative of feedstock solubilization. Conversion fraction results suggest the rate and/or extent of initial feedstock solubilization is dependent on heating rate (and thus final reaction temperature), as illustrated in Figure 3.4. A more significant initial decrease in solid-phase carbon, in conjunction with larger carbon conversion fractions, was observed at 225^{o}C than that observed at 250 and 275^{o}C. At 275^{o}C, calculated carbon conversion fractions never exceed one, suggesting that either: (1) the rate of feedstock solubilization and subsequent char production increases as temperature increases and is not captured by

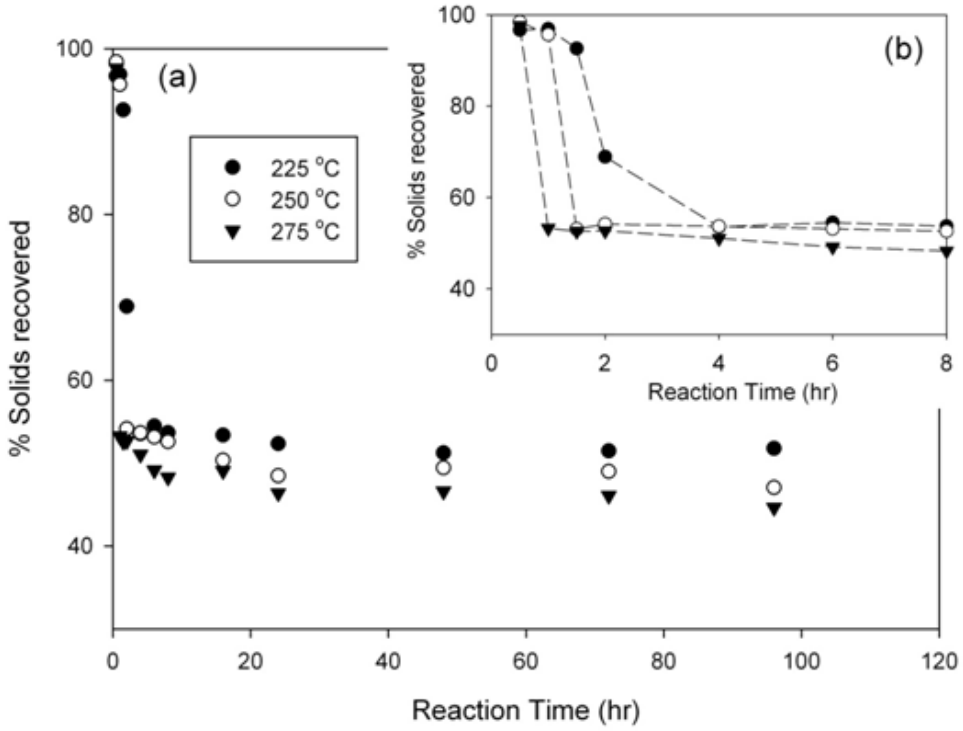

Figure 3.3 Solids recovery at 225, 250, and 275 ^{o}C over: (a) 96 hours and (b) the first 8 hours. Data points represent averages from duplicate experiments.

the sampling frequency or (2) the pathway of carbonization changes with temperature and the significance of feedstock solubilization declines as temperature increases. Falco et al. (2011a; 2011b) report that at temperatures below 200^{o}C, feedstock hydrolysis followed by char production is the predominant carbonization pathway, while at temperatures above 200^{o}C, solid-state reactions predominate. Although the final reaction temperature in these experiments exceeds 200^{o}C, it takes at least 30 minutes for the internal reactor temperature to reach 200 ^{o}C and between 80 and 100 minutes to reach the target reaction temperature (Figure 3.1). This slow heating rate likely increases the extent and significance of feedstock solubilization during cellulose carbonization at final reaction temperatures greater than 200^{o}C. This pathway would likely be of importance when the

process is scaled up for industrial implementation. Solubilization of components of wood prior to char formation has also been observed, even at temperatures above 200°C (Knežević et al., 2010). The second distinct period (at times exceeding 8 hours) is characterized by slower and less significant changes in carbon distribution (Figure 3.2).

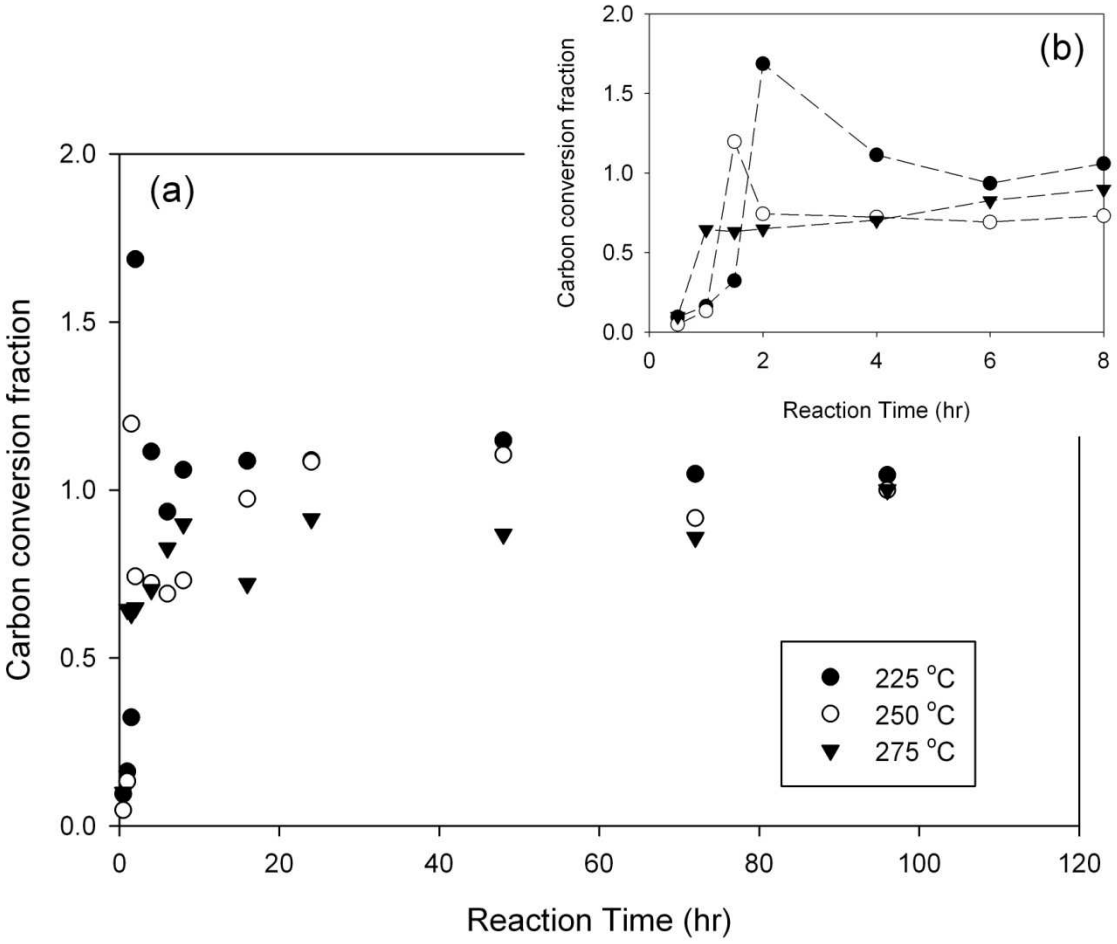

Figure 3.4 Carbon conversion fractions (defined in Table 3.1) at 225, 250, and 275 °C over (a) the entire reaction period and (b) over the first 8 hours. Data points represent averages from duplicate experiments.

3.3.3 Influence of reaction temperature

Carbon distribution (defined in Table 3.1) is also influenced by reaction temperature. The fraction of carbon ultimately transferred to the gas-phase increases with reaction temperature (Figure 3.2). At 225^{o}C and after 96 hours, approximately 6.7% of the initially present carbon was transferred to the gas, while approximately 9 and 9.5% of carbon was transferred to the gas after 96 hours at 250 and 275^{o}C, respectively. The fraction of carbon present in both the liquid and solid-phases is also influenced by reaction temperature. It is expected that at higher temperatures, gas evolution via decarboxylation and/or volatilization of organics is increased, thus greater retention of carbon in the liquid and solid-phases results at lower temperatures (Falco et al., 2011a). This hypothesis is substantiated, as the fraction of carbon (after 96 hours) remaining in the liquid-phase at 225^{o}C is greater than that observed at 250 and 275^{o}C. In addition, the fraction of carbon present within the solids is greater (~86%) at 225^{o}C (Figure 3.2).

Similar trends in carbon distribution as a result of variations in reaction temperature have been observed in other hydrothermal carbonization studies (Table 3.2; **Error! Reference source not found.**Figure 3.5) (Falco et al., 2011a; Hoekman et al., 2011; Knežević et al., 2010; Knežević et al., 2009; Pińkowska et al., 2011). Comparing experimental results from different studies is difficult because changes in operational parameters (e.g., heating rates, reactor configurations, feedstock mass concentrations, and reaction times) may significantly influence carbonization processes. Although it may be difficult to compare absolute numerical values between studies, comparison of reported experimental trends is valuable. Carbon fraction data from hydrothermal carbonization studies at different reaction temperatures and for several types of feedstocks (including

cellulose, glucose, starch, and lignocellulosic biomass) were compiled (Table 3.2 and **Error! Reference source not found.**Figure 3.5). Similar to this study, the fraction of initially present carbon found in the recovered solids decreases with increases in reaction temperature. One set of data deviate from this trend. Sevilla and Fuertes (2009a,b) report a decrease in carbon integrated within the solid-phase when carbonizing cellulose, glucose and starch at temperatures ranging from 170 – 250^{o}C. This reason for this difference is unclear, but could be due to differences in operational parameters, reactor size, reaction kinetics, or reaction time.

Table 3.2 Information from selected hydrothermal carbonization laboratory studies.

Feedstock Information		Reaction Information			Solid information									Liquid information		Gas information		Ref.
Type	Conc.	Temp. (°C)	Time (hrs)	Volume (mL)	Yield (%)	C fraction (%)	C densification[d, e]	HHV (MJ/kg)	Element analysis					C fraction (%)	Comp.	C fraction (%)	Comp.	
									C (% wt)	H (% wt)	O (% wt)	O/C	H/C					
cellulose	40 g L^{-1}	230	4	NR	33.5	53.8	1.61	NM	71.35	4.34	24.31	0.256	0.730	NM	NM	NM	NM	(Sevilla & Fuertes, 2009b)
		250	2		34.0	54.7	1.61	NM	71.51	4.30	24.19	0.254	0.722					
		250	4		36.5	59.6	1.63	NM	72.52	4.36	23.12	0.239	0.721					
	160 g L^{-1}	250	2		44.0	70.8	1.61	NM	71.46	4.38	24.16	0.254	0.736					
			4		52.3	84.3	1.61	NM	71.66	4.55	23.79	0.249	0.762					
	320 g L^{-1}	250	2		42.7	68.0	1.59	NM	70.72	4.48	24.80	0.263	0.760					
glucose	0.5 mol L^{-1}	170	4.5	NR	1.5	2.4[b]	1.62	NM	64.91	4.20	30.89	0.357	0.752	NM	NM	NM	NM	(Sevilla & Fuertes, 2009a)
		180			5.1	NR	NR	NM	NM	NM	NM	NM	NM					
		190			9.4	NR	NR	NM	NM	NM	NM	NM	NM					
		210			28	46.4[b]	1.66	NM	66.29	4.15	29.56	0.334	0.751					
		230			36	NR	NR	NM	NM	NM	NM	NM	NM					
		170	15.0		6.0	NR	NR	NM	NM	NM	NM	NM	NM					
		180			15	NR	NR	NM	NM	NM	NM	NM	NM					
	1 mol L^{-1}	190	4.5		26	NR	NR	NM	NM	NM	NM	NM	NM					
		230	1.0		31	NR	NR	NM	NM	NM	NM	NM	NM					
		240			43	NR	NR	NM	NM	NM	NM	NM	NM					
		240	0.5		37	NR	NR	NM	NM	NM	NM	NM	NM					
starch	0.25 mol L^{-1}	180	4.5		5.1	7.4[b]	1.44	NM	64.16	4.1	31.74	0.371	0.768					
		200			25	37.0[b]	1.48	NM	65.85	3.99	30.16	0.343	0.727					
glucose	10 wt/v (9.1 % wt)	140 to 200	24	50	0[a] to 38[a]	0[b] to 62.9[b]	1.05 to 1.68	NM	42[a] to 67[a]	NR	NR	NR	NR	NM	NM	NM	NM	(Falco et al., 2011)
		200			38.6[a]	64.4[b]	1.67	NM	66.7[a]	4.8[a]	26.3[a]	0.287[d]	0.844[d]					
		220			38.3[a]	66.2[b]	1.73	NM	69.1[a]	4.3[a]	25.6[a]	0.275[d]	0.738[d]					
		240			36.5[a]	63.4[b]	1.74	NM	69.6[a]	4.5[a]	24.5[a]	0.260[d]	0.762[d]					
		260			31.8[a]	56.6[b]	1.78	NM	71.3[a]	4.6[a]	21.9[a]	0.223[d]	0.755[d]					
		280			30.3[a]	54.9[b]	1.81	NM	72.4[a]	4.3[a]	20.3[a]	0.202[d]	0.688[d]					
alcell lignin		160 – 240	24		88[a] to 75[a]	90.5[b] to 81.7[b]	1.03 to 1.09	NM	68 [a] to 72 [a]	NR	NR	NR	NR					
rye straw		120 – 280	24		84[a] to 28[a]	86.1[b] to 47.0[b]	1.02 to 1.68	NM	47 [a] to 77 [a]	NR	NR	NR	NR					
wood	50/500 (wt/v)	150	8	1000	89.37	90.88[b]	1.02[b]	NM	53.63	6.03	40.32	0.564[d]	1.349[d]	NM	NM	NM	NM	(Tsukashi .H, 1966)
			72		84.33	88.84[b]	1.05[b]	NM	55.56	5.85	38.55	0.520[d]	1.263[d]					
		170	8		83.39	86.88[b]	1.04[b]	NM	54.95	5.83	39.19	0.535[d]	1.273[d]					
			72		82.81	92.78[b]	1.12[b]	NM	59.09	5.89	34.98	0.444[d]	1.196[d]					
		200	8		79.47	90.11[b]	1.13[b]	NM	59.80	6.17	33.91	0.425[d]	1.238[d]					
			32		71.93	89.01[b]	1.24[b]	NM	65.26	5.86	28.76	0.331[d]	1.078[d]					
			40		69.57	88.22[b]	1.27[b]	NM	66.88	5.99	26.99	0.303[d]	1.075[d]					
			72		66.22	88.88[b]	1.34[b]	NM	70.79	5.73	23.36	0.247[d]	0.971[d]					
		250	8		55.48	77.46[b]	1.40[b]	NM	73.63	5.57	20.62	0.210[d]	0.908[d]					
			72		55.84	80.83[b]	1.45[b]	NM	76.34	5.71	17.81	0.175[d]	0.898[d]					
		260	8		55.99	79.52[b]	1.42[b]	NM	74.90	5.77	19.16	0.192[d]	0.924[d]					
			72		53.36	78.45[b]	1.47[b]	NM	77.54	5.64	16.65	0.161[d]	0.873[d]					
		270	8		55.47	79.42[b]	1.43[b]	NM	75.51	5.44	18.93	0.188[d]	0.865[d]					
			72		50.73	74.19[b]	1.46[b]	NM	77.13	5.29	17.55	0.171[d]	0.823[d]					
		280	8		53.04	75.33[b]	1.42[b]	NM	74.90	5.10	19.90	0.199[d]	0.817[d]					
			72		46.61	68.69[b]	1.47[b]	NM	77.72	4.78	17.31	0.167[d]	0.738[d]					

		300	8		44.93	68.09[b]	1.52[b]	NM	79.93	5.44	14.63	0.137[d]	0.817[d]					
		325	72		39.86	62.49[b]	1.57[b]	NM	82.68	4.83	12.49	0.113[d]	0.701[d]					
		350	72		31.10	49.76[b]	1.60[b]	NM	84.39	4.52	11.09	0.099[d]	0.643[d]					
glucose	8.8 % wt (feedstock/water)	300	0 to 1	0.5	0 to 31[a]	0 to 47[a]	NR	NM	NR	NR	NR	0.2[a]	1.1[a]	40[a]	NM	10[a]	CO_2, CO, H_2 and CH_4 (by GC/MS)	(Knežević et al., 2009)
		350	0 to 1		0 to 22[a]	0 to 40[a]	NR	NM	NR	NR	NR	0.1[a]	1.2[a]	17.0[a]		18.0[a]		
			16.7		28[a]	50[a]	NR	NM	NR	NR	NR	0.21[a]	0.93[a]	22.3[a]		19.1[a]		
			166.7		29[a]	53[a]	NR	NM	NR	NR	NR	0.14[a]	0.97[a]	16.7[a]		19.1[a]		
glucose	1.5 % wt	300	9.9 to 60.6 sec	NR	0 to 4.5	NR	NR	NM	NR	NR	NR	NR	NR	NM	5-HMF, BTO, furfural, glucose,fructose,glycolaldehyde, anhydroglucose, and dehydroxyacetone (by HPLC))	NM	CO_2, CO, CH_4, C_2H_4, C_2H_6 (by GC)	(Chuntanapum & Matsumura, 2010)
		350	1.0 to 49.2 sec		0 ro 9.0	NR	NR	NM	NR	NR	NR	NR	NR					
		400	0.5 to 19.8		0 to 0	NR	NR	NM	NR	NR	NR	NR	NR					
Mixture of Jeffrey pine and White Fir	1/8 wt (feedstock/water)	215	0.5	hold time at the target T	69.1	76.92[b]	1.11	22.58	54.57	5.89	34.89	0.480[d]	1.295[d]	9.17	higher concentration of organic acids (by IC)at higher temperature; Lower concentration of sugars (by HPAEC-PAD) at higher temperature	NA	CO and CO_2 (by GC)	(Hoekman et al., 2011)
		235			63.7	78.67[b]	1.24	24.37	60.54	5.66	31.59	0.391[d]	1.122[d]	9.17		7.9		
		255	0.083		57.7	73.74[b]	1.28	25.10	62.65	5.43	32.31	0.387[d]	1.040[d]	11.40		5.5		
			0.167		55.5	71.31[b]	1.28	26.04	62.98	5.40	30.72	0.366[d]	1.029[d]	12.02		5.8		
			0.5		50.3	71.89[b]	1.43	28.26	70.06	5.19	23.42	0.251[d]	0.889[d]	11.27		8.5		
			1		52.1	76.41[b]	1.47	29.17	71.89	5.15	22.26	0.232[d]	0.860[d]	8.56		9.5		
		275	0.5		50.9	72.77[b]	1.43	29.02	70.08	5.31	21.14	0.226[d]	0.909[d]	8.47		10.7		
		295			50.1	74.62[b]	1.49	29.52	73.01	5.14	19.87	0.204[d]	0.845[d]	7.75		11.8		
cellulose	1/3 wt (feedstock/water)	225	20 (hold time at the target temperature)	50	53.3[a]	83.6	1.57	NM	66.40	5.11	28.49	0.32[d]	0.92[d]	NM	NM	NM	NM	(Kang et al., 2012)
		245			51.9[a]	85.0	1.65	NM	69.70	4.99	25.31	0.27[d]	0.86[d]					
		265			49.0[a]	83.4	1.70	NM	72.10	5.05	22.85	0.24[d]	0.84[d]					
Lignin		225			60.0[a]	84.1	1.41	NM	63.95	5.21	27.30	0.32[d]	0.98[d]					
		245			56.9[a]	82.6	1.46	NM	66.15	5.01	25.55	0.29[d]	0.91[d]					
		265			53.7[a]	80.5	1.51	NM	68.43	4.65	23.59	0.26[d]	0.82[d]					
D-xylose		225			50.0[a]	85.8	1.73	NM	68.85	4.66	26.69	0.29[d]	0.81[d]					
		245			49.5[a]	85.7	1.75	NM	69.78	4.69	25.53	0.27[d]	0.81[d]					
		265			47.6[a]	85.2	1.83	NM	72.80	4.93	22.27	0.23[d]	0.81[d]					
Pine wood meal		225			58.4[a]	87.0	1.50	NM	67.55	5.60	24.94	0.28[d]	0.99[d]					
		245			55.4[a]	85.4	1.55	NM	69.86	5.41	22.69	0.24[d]	0.93[d]					
		265			52.6[a]	86.3	1.65	NM	74.22	5.54	17.91	0.18[d]	0.90[d]					
Cellulose	20 % wt	225	0 to 96	160	100 to 51.8	100 to 86.1	1 to 1.60	16.14 to 25.02	46.06 to 73.50	NM	NM	NM	NM	0 to 9.83	Organic acids, glucose, sucrose, formate and HMF after 2 hrs; organic acids after 96 hrs (by ^{1}H NMR)	0 to 6.74	CO_2, C_2H_4, C_2H_6, C_3H_6, C_3H_8, C_4H_{10}, and furan (by GC/MS)	This work
		250			100 to 47.1	100 to 80.3	1 to 1.67	16.14 to 25.35	46.06 to 76.71	5.55 to 4.29	48.20 to 18.38	0.785 to 0.180	1.447 to 0.671	0 to 7.44	Organic acids, formate and HMF after 2 hrs; organic acids after 96 hrs (by ^{1}H NMR)	0 to 8.94		
		275			100 to 44.1	100 to 78.1	1 to 1.68	16.14 to 25.10	46.06 to 77.40	NM	NM	NM	NM	0 to 7.68	Organic acids and formate after 2 hrs; organic acids after 96 hrs (by ^{1}H NMR)	0 to 9.44		

[a] data obtained from the figures in the literature; [b] calculated based on the information in the literature ((carbon content of solids/carbon content of initial feedstock)*solids recovery); [c] information of liquid and gas is not reported in the reference; [d] calculated based on the information in literature.; NM: not measured; NR: not reported; NA: not available.

Comparison between studies reported in the literature and this work

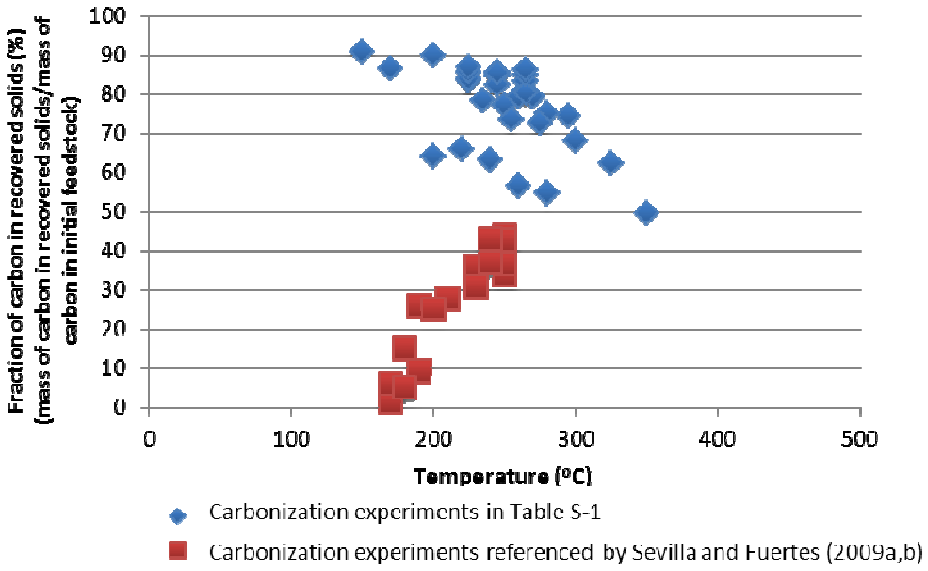

Figure 3.5 The influence of reaction temperature on the fraction of carbon present in the recovered solids. Data were collected from the literature and are listed in Table 3.2.

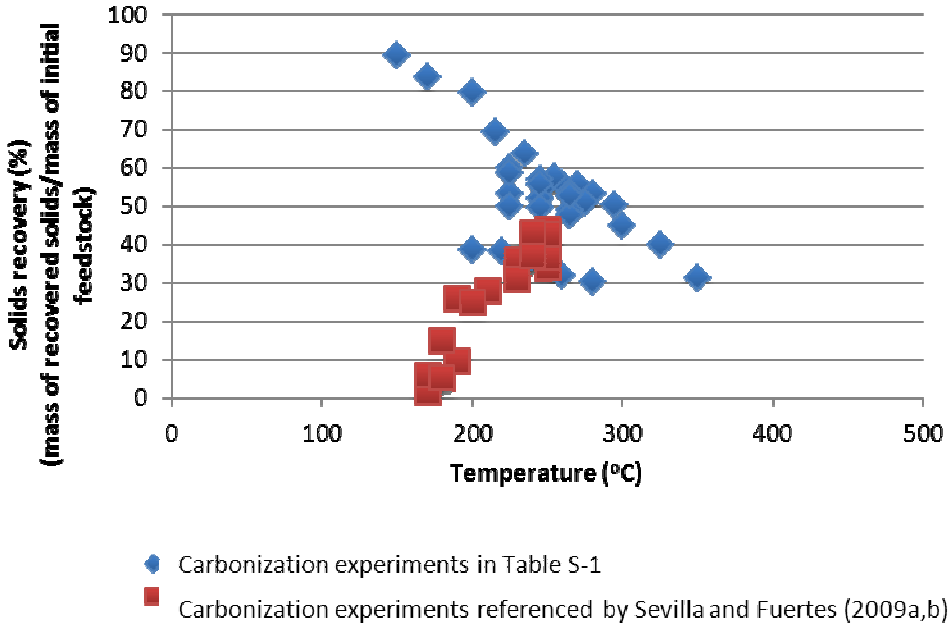

Figure 3.6 The influence of reaction temperature on solids recovery. Data were collected from the literature and are listed in Table 3.2.

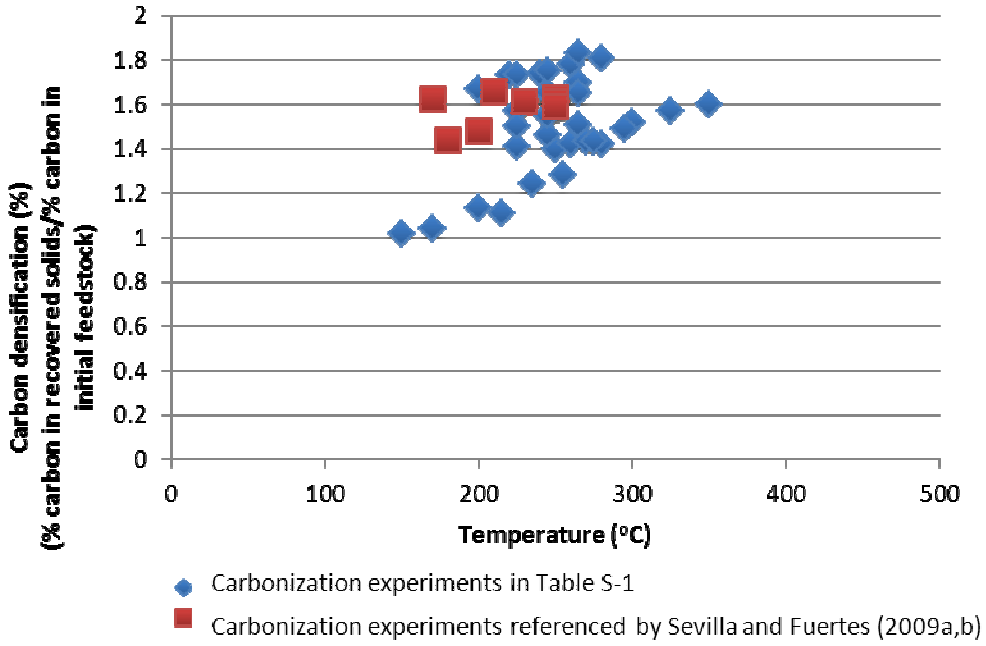

Figure 3.7 The influence of reaction temperature on solids carbon densification. Data were collected from the literature and are listed in Table 3.2.

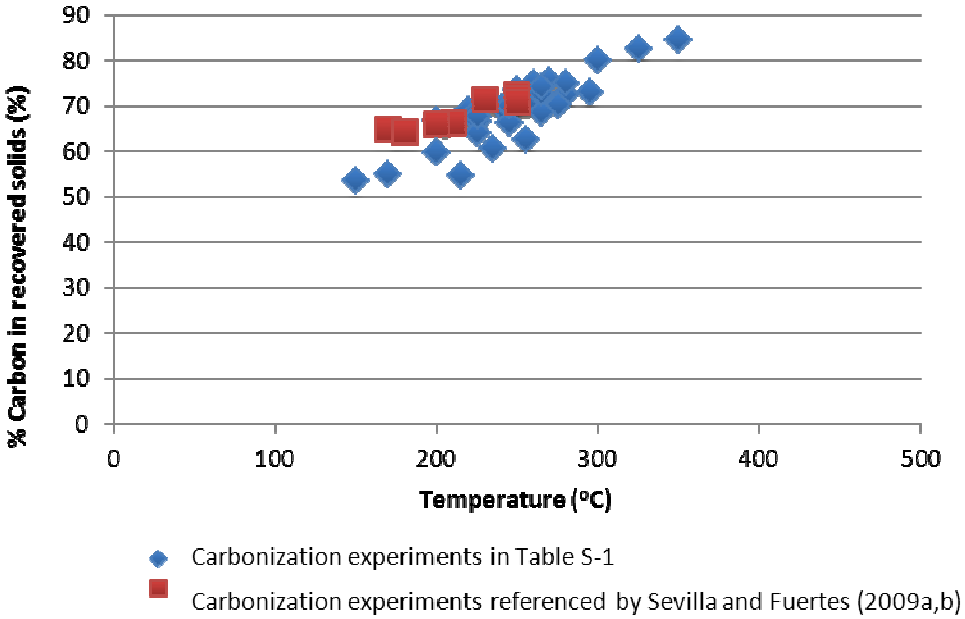

Figure 3.8 The influence of reaction temperature on the percentage of carbon in the recovered solids. Data were collected from the literature and are listed in Table 3.2.

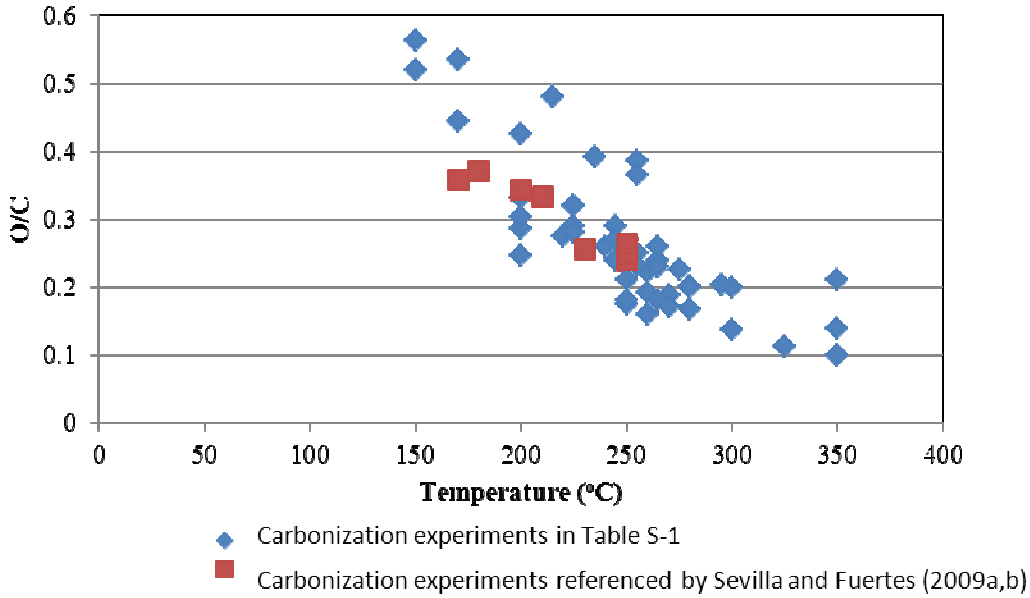

Figure 3.9 The influence of reaction temperature on the hydrochar O/C ratio. Data were collected from the literature and are listed in Table 3.2.

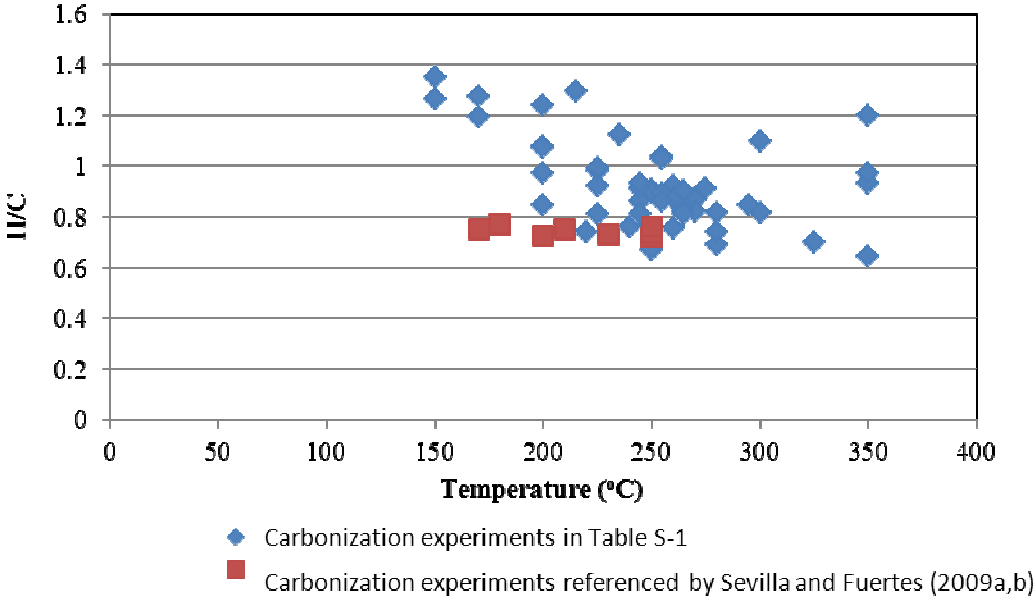

Figure 3.10 The influence of reaction temperature on the hydrochar H/C ratio. Data were collected from the literature and are listed in Table 3.2.

Changes in the gas composition as a result of temperature are also similar to those reported in the literature (Table 3.2), although fewer studies have evaluated changes in the carbon content of the gas and liquid-phases. Hoekman et al. (2011) report carbon dioxide yields increase from 7.9 to 11.1% over temperatures ranging from 235 to 295^{o}C. Trends associated with carbon partitioning to the liquid-phase at different temperatures are not reported as frequently (Table 3.2). Hoekman et al. (2011) observed a decrease in dissolved sugars as temperatures increased from 215-235^{o}C to 255 to 295^{o}C, while the acetic acid concentration increased.

Examination of carbon distributions and carbon conversion fractions at early times (< 6-8 hours) also indicates temperature plays a role in overall carbonization kinetics, which is critical in defining optimal carbonization time frames/conditions. When comparing early time data, the fraction of carbon integrated within the solid phase decreases at a faster rate as temperatures increase, coupled with subsequent faster increases in the fraction of carbon integrated within the liquid and gas-phases. This observation is not surprising, as reaction rates generally increase with reaction temperature.

3.3.4 Carbonization product characterization

3.3.4.1 Gas

Approximately 6.7 – 9.4% of carbon was transferred to the gas-phase. The predominant gas produced is carbon dioxide, accounting for approximately 70 - 80% (vol.) of the gas at all temperatures (**Error! Reference source not found.Error! Reference source not found.**Figure 3.5). Trace gases account for approximately 15% (vol.) of the produced gas. The most predominant trace gases identified (via GC/MS)

include ethylene, ethane, propene, propane, butane and furan (Figure 3.11). Quantification of these gases was not performed; identification was performed via the NIST library. It should be noted that there may be additional significant trace gases present that have not been identified with current analytical methods. The current analysis, however, can be used as a tool to qualitatively compare detected/identified gases over time. The gas peak areas were multiplied by the gas volume produced at each sampling time to represent changes in individual gas mass with time and temperature (Figure 3.11), suggesting greater cracking of long-chain hydrocarbons as reaction severity increases. Masses of released hydrocarbons increase with time at each temperature. The mass of hydrocarbons produced at 250^{o}C and 275^{o}C are generally greater than those produced at a reaction temperature of 225^{o}C, likely a result of increased reaction of organics at higher temperatures. This is consistent with lower solids recoveries at higher temperatures. Furan mass in the gas initially increases and then decreases with time at each reaction temperature (Figure 3.11f). Gas-phase furan content is likely related to the presence of furfurals (such as HMF) in the liquid. As furfural is heated, it decomposes to form furan (Asghari and Yoshida, 2006). Over time, gas-phase furans may be incorporated into the solid-phase carbon (Baccile et al., 2009; Titirici et al., 2008).

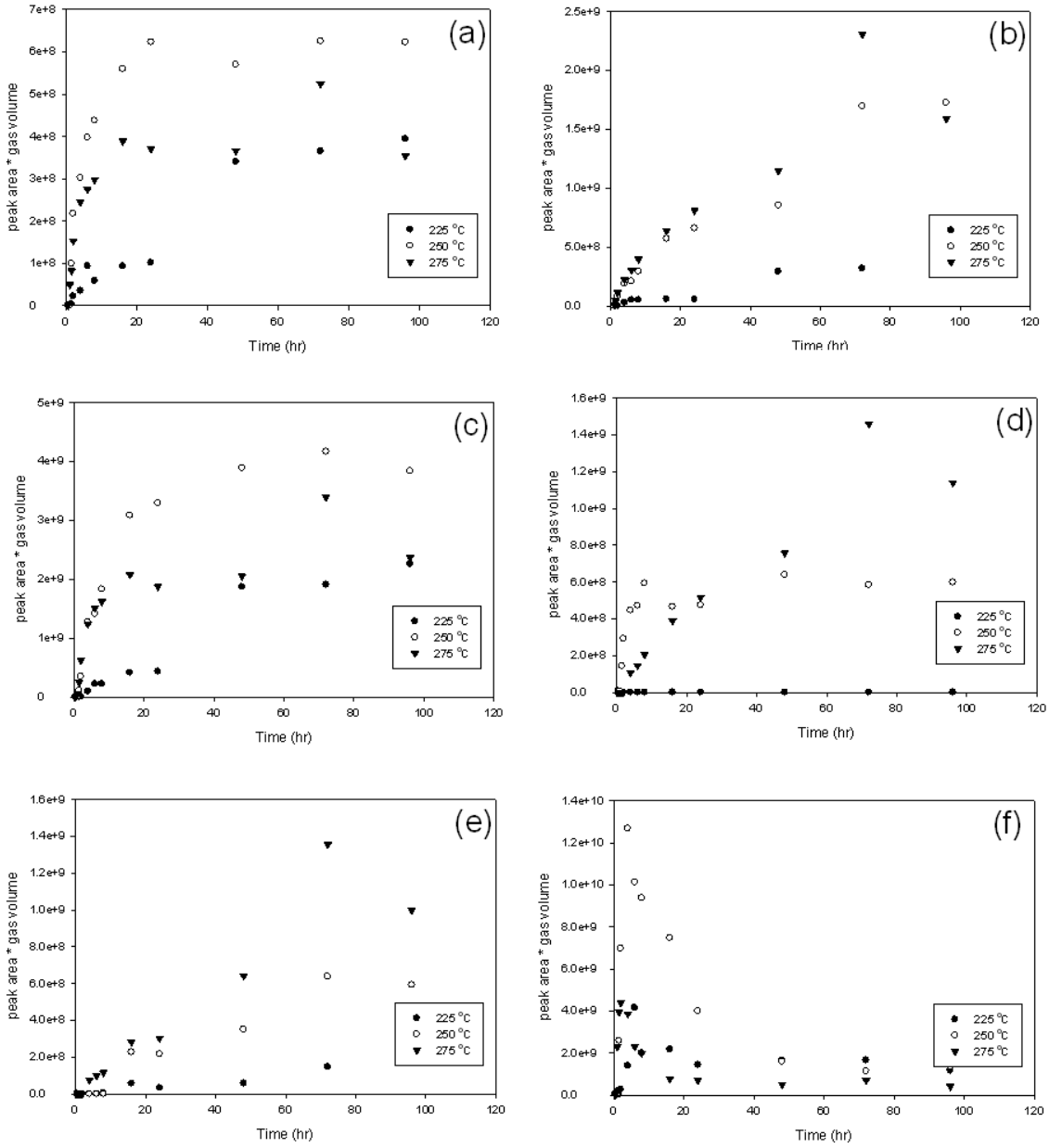

Figure 3.11 Trace gases produced as a result of cellulose carbonization: (a) ethylene, (b) ethane, (c) propene, (d) propane, (e) butane and (f) furan. Data points represent averages from duplicate experiments.

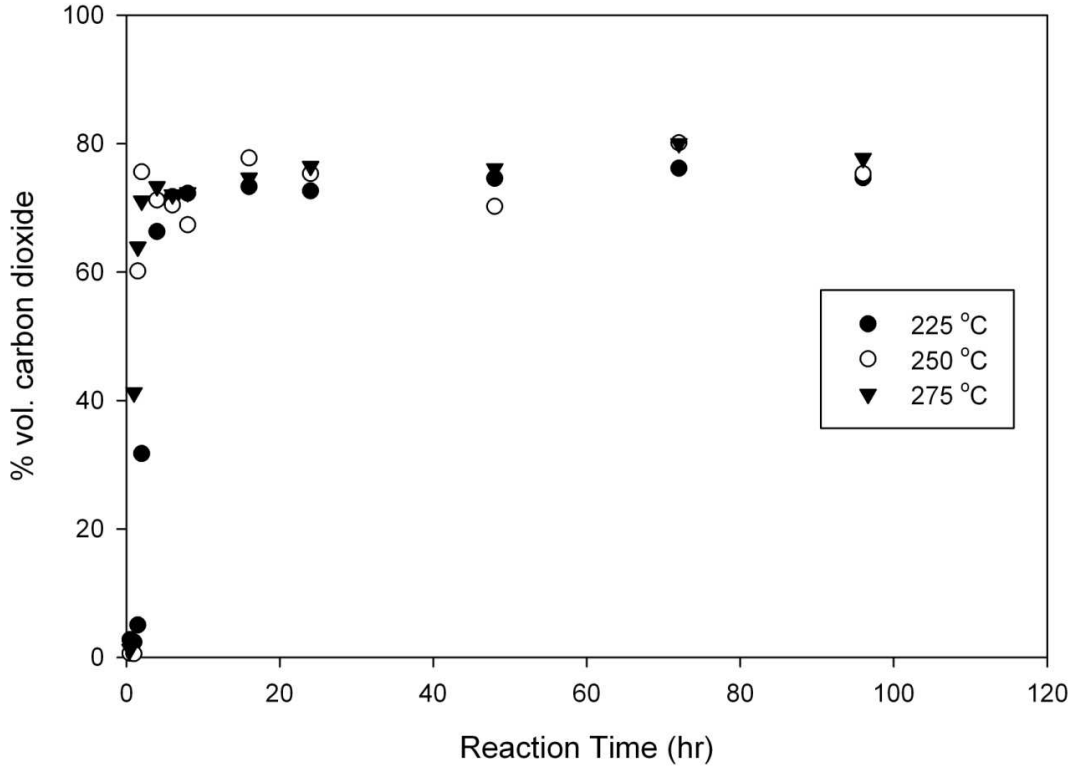

Figure 3.12 Carbon dioxide (%. vol) produced at each temperature. Data points represent averages from duplicate experiments.

Recovery of the detected hydrocarbons may represent a source of energy, as they have appreciable energy contents (e.g., ethane: 51.9 kJ/g, propane: 50.4 kJ/g, butane: 49.5 kJ/g). Actual concentrations of these gases were not measured, thus the magnitude of energy in the gas-phase is unknown. Results suggest longer reaction times and higher temperatures may provide greater potential energy recovery. Detected hydrocarbons appear to reach a constant level after 48-72 hours. The presence of furan in the gas is of environmental concern, unless it is collected and used in an industrial application. Lower gas-phase furan concentrations were observed at longer reaction times and higher temperatures, remaining fairly constant after 48 hours. These results suggest longer reaction times and higher temperatures will yield greater potential for energy recovery

from the gas-phase and lower gas-furan concentrations. As noted previously, there may be additional significant trace gases present that have not been identified with current analytical methods that may also result in negative environmental implications and/or greater energy value.

3.3.4.2 Liquid

Proton NMR was performed on liquid samples taken after carbonization at 2 and 96 hours at the three temperatures evaluated. Results (

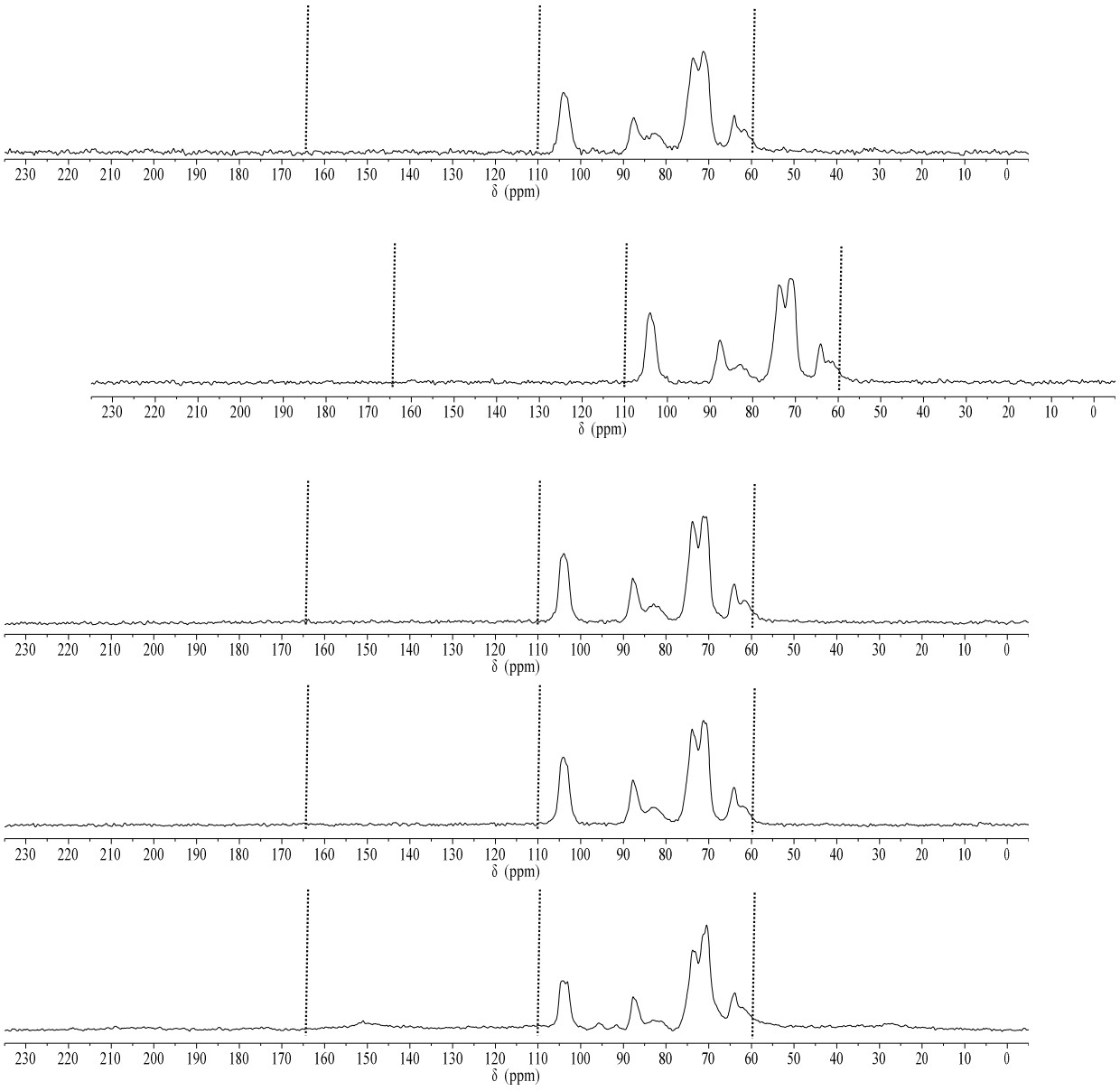

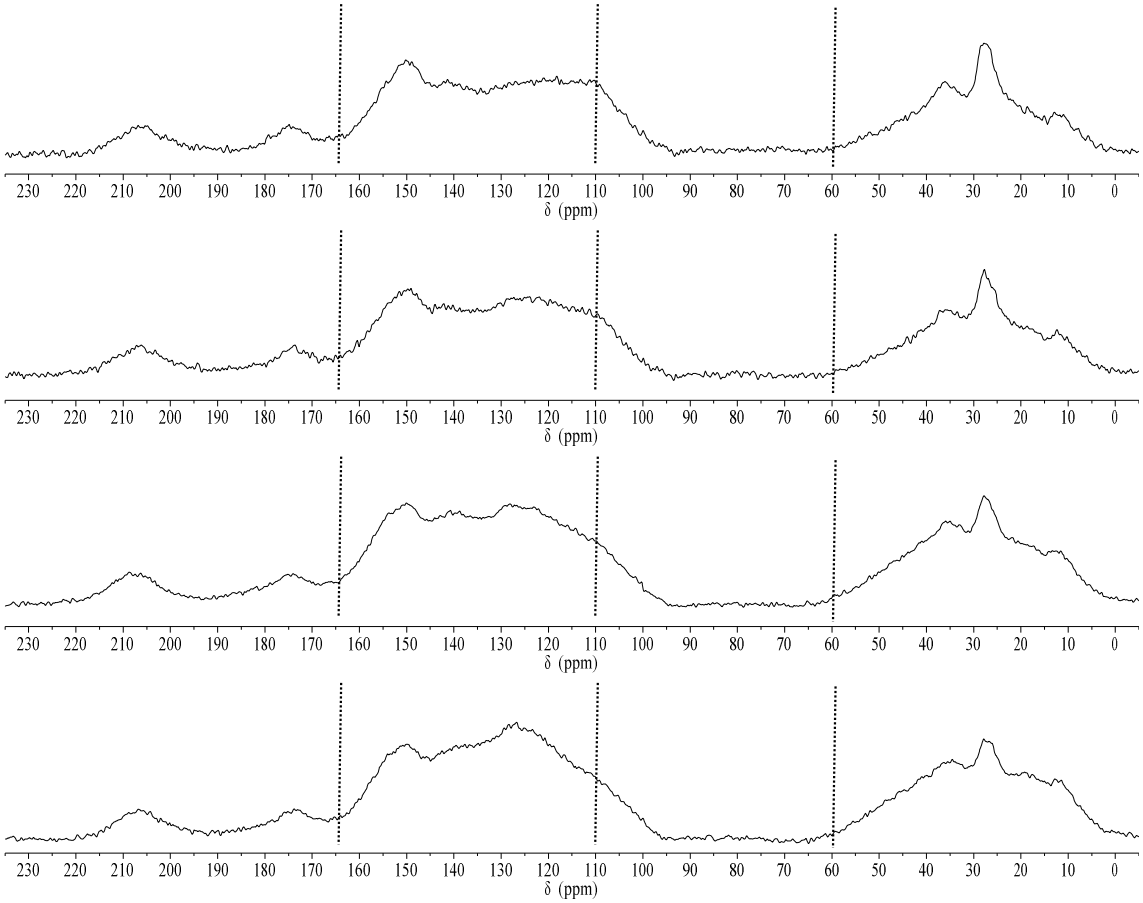

Figure 3.19 ^{13}C NMR of hydrochar at 225 ^{o}C.

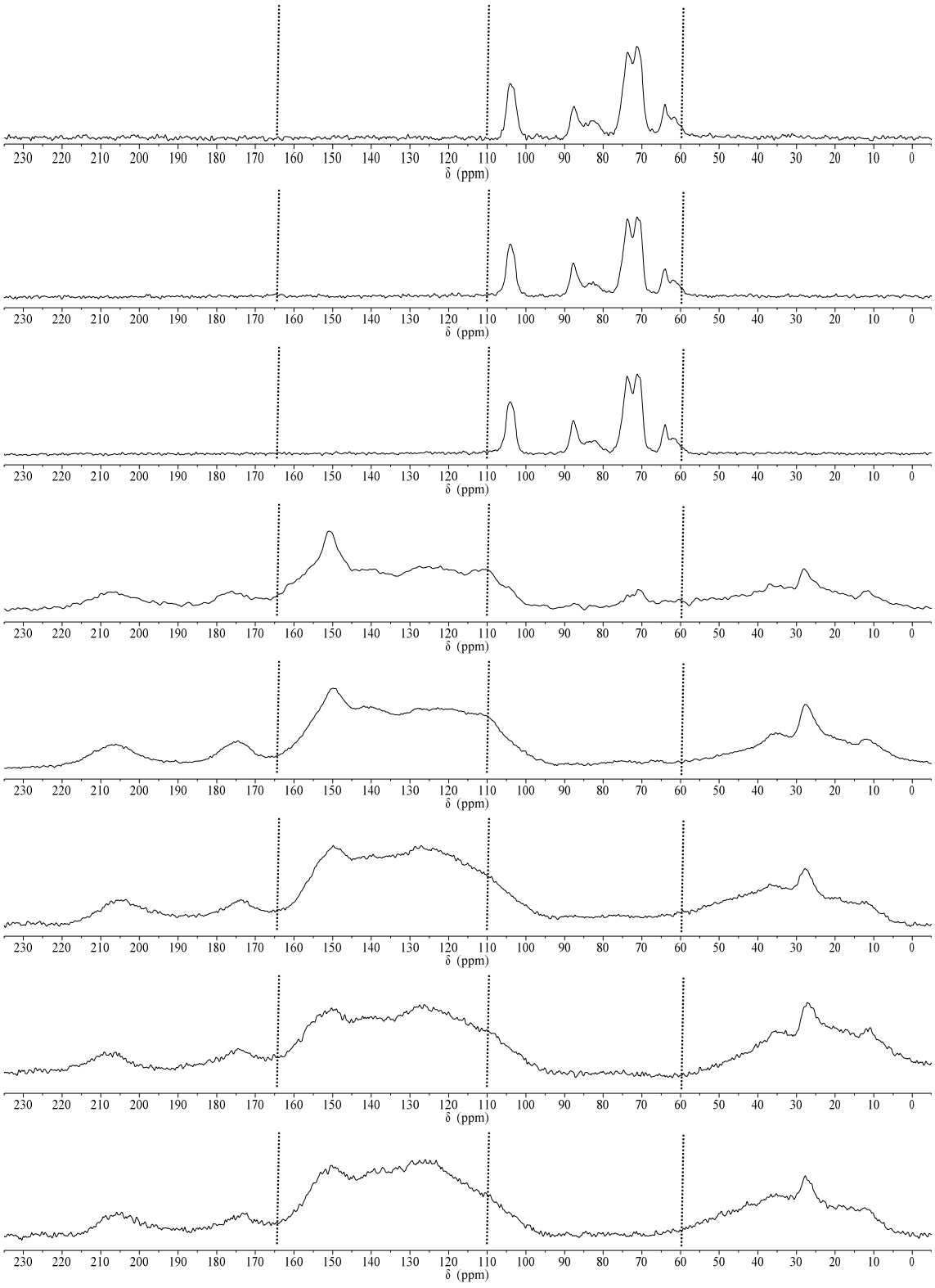
230 220 210 200 190 180 170 160 150 140 130 120 110 100 90 80 70 60 50 40 30 20 10 0
δ (ppm)

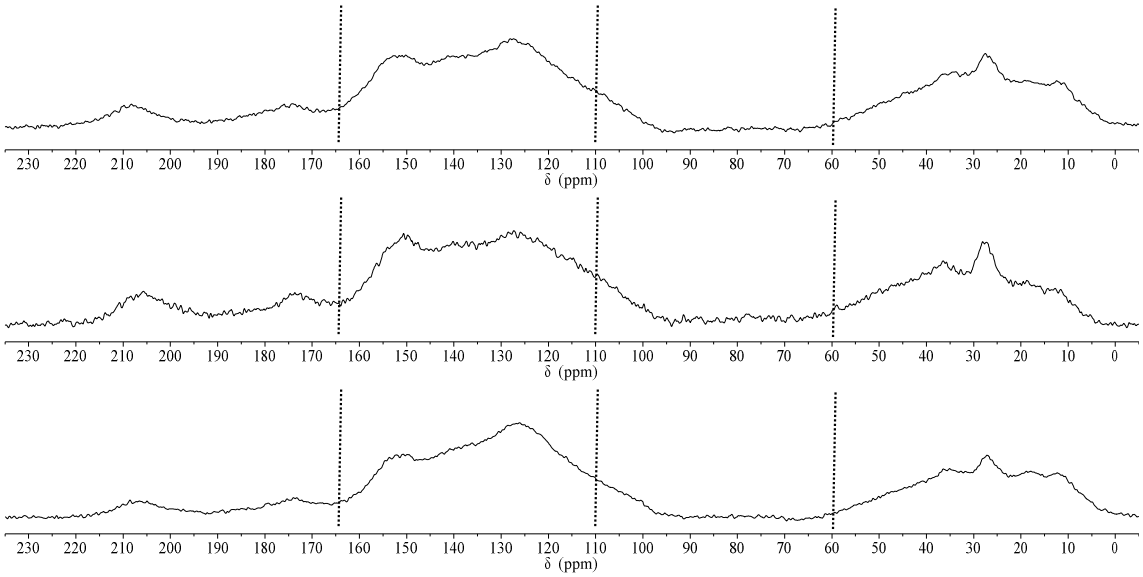

Figure 3.20 ^{13}C NMR of hydrochar at 250 ^{o}C.

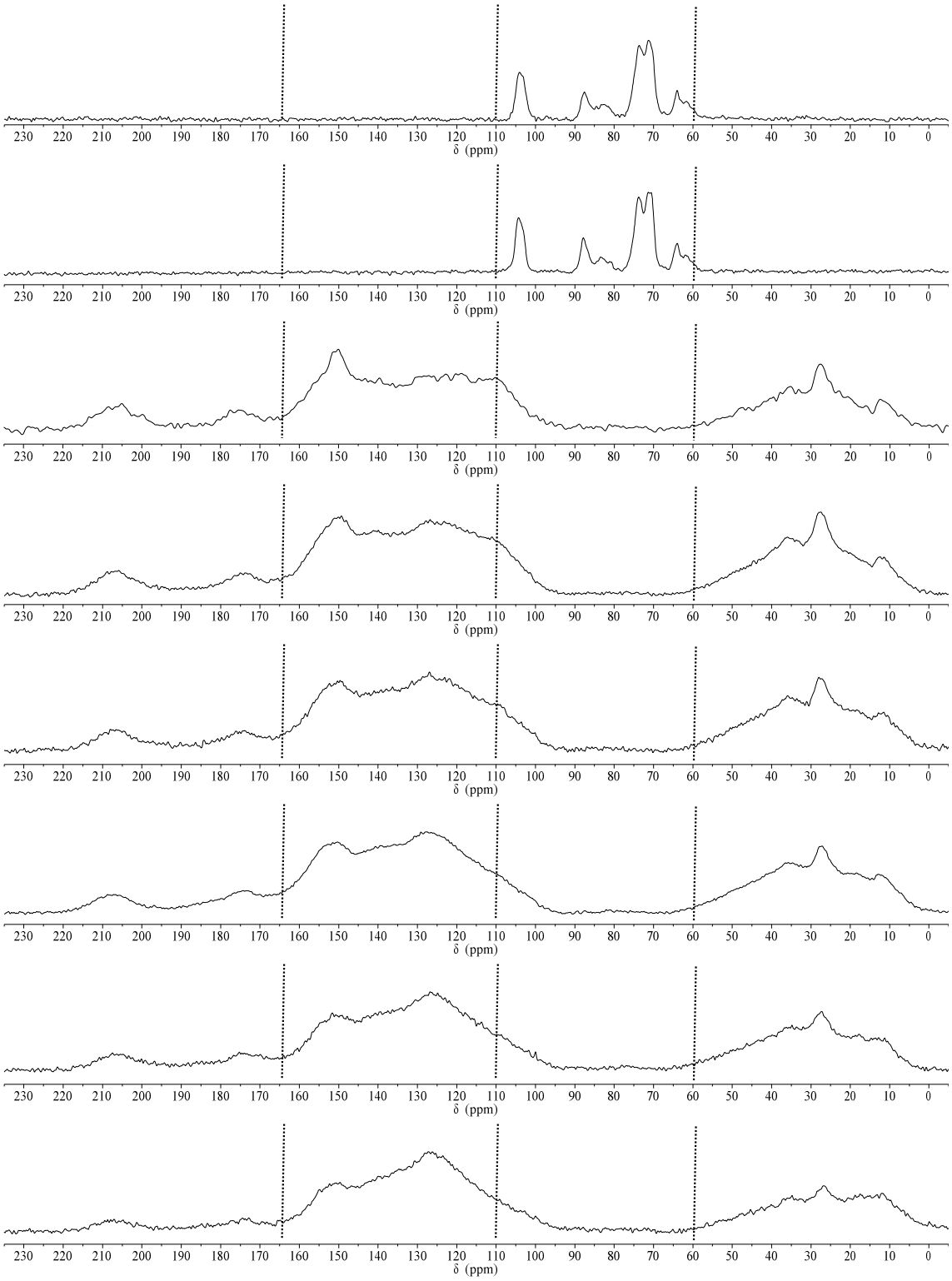
230 220 210 200 190 180 170 160 150 140 130 120 110 100 90 80 70 60 50 40 30 20 10 0
δ (ppm)

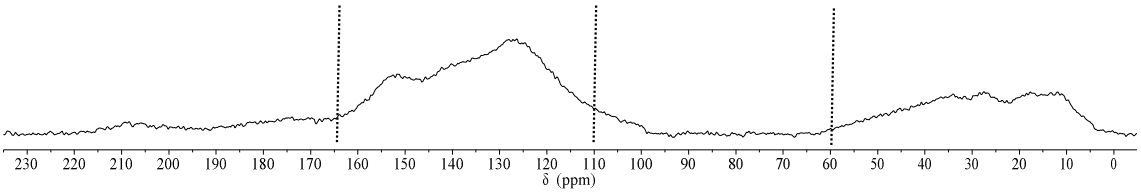

Figure 3.21 ^{13}C NMR of hydrochar at 275 ^{o}C.

Table **3.4** and Figure 3.13) from samples taken at 2-hours indicate the presence of aliphatics/alcohols, sugars, and aromatics. By the end of the 96-hour reaction period, the sugars and aromatics are not present; they likely either transformed/decomposed to other compounds or are integrated within the solid material.

At 225^{o}C, the liquid sample at 2 hours represents the point of the largest fraction of carbon in the liquid-phase (Figure 3.2) and contains several organic acids (e.g., acetic, citric, formic), as well as glucose and HMF. These data are consistent with reports that the liquid-phase contains high concentrations of sugars and organic acids (e.g., Baccile et al., 2009; Hoekman et al., 2011; Sasaki et al., 2000; Titirici et al., 2008). Sasaki et al. (2000) report that organic acids are hydrolysis products of cellulose in sub-/super critical water. Glucose was detected in the liquid, consistent with Baccile et al. (2009) that report glucose is an intermediate associated with cellulose carbonization. HMF is a dehydration product of glucose (Baccile et al., 2009). The composition of 2-hour samples taken at 250 and 275^{o}C do not indicate the presence of glucose (organic acids are detected). The absence of glucose is likely an artifact of changes in reaction rates; the 2-hour samples at

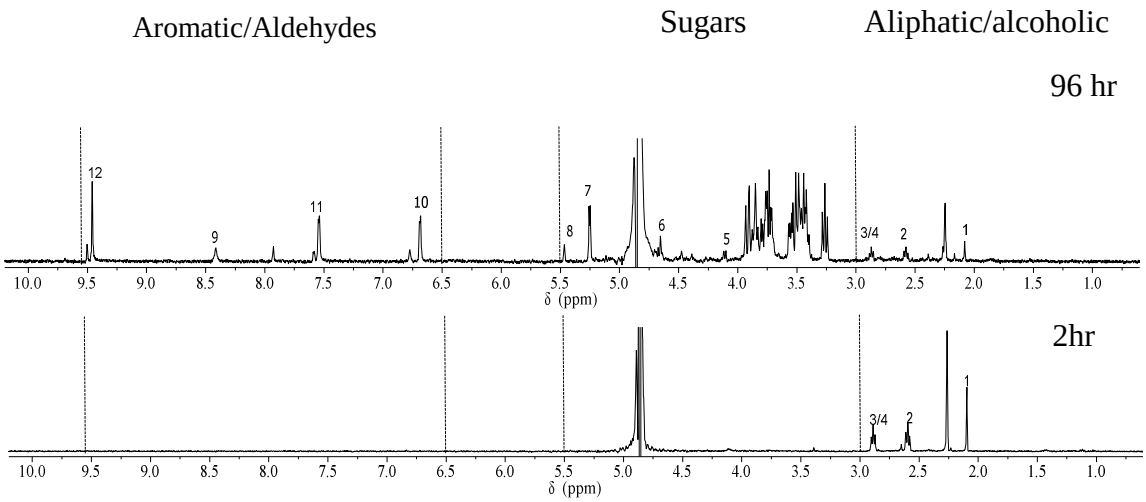

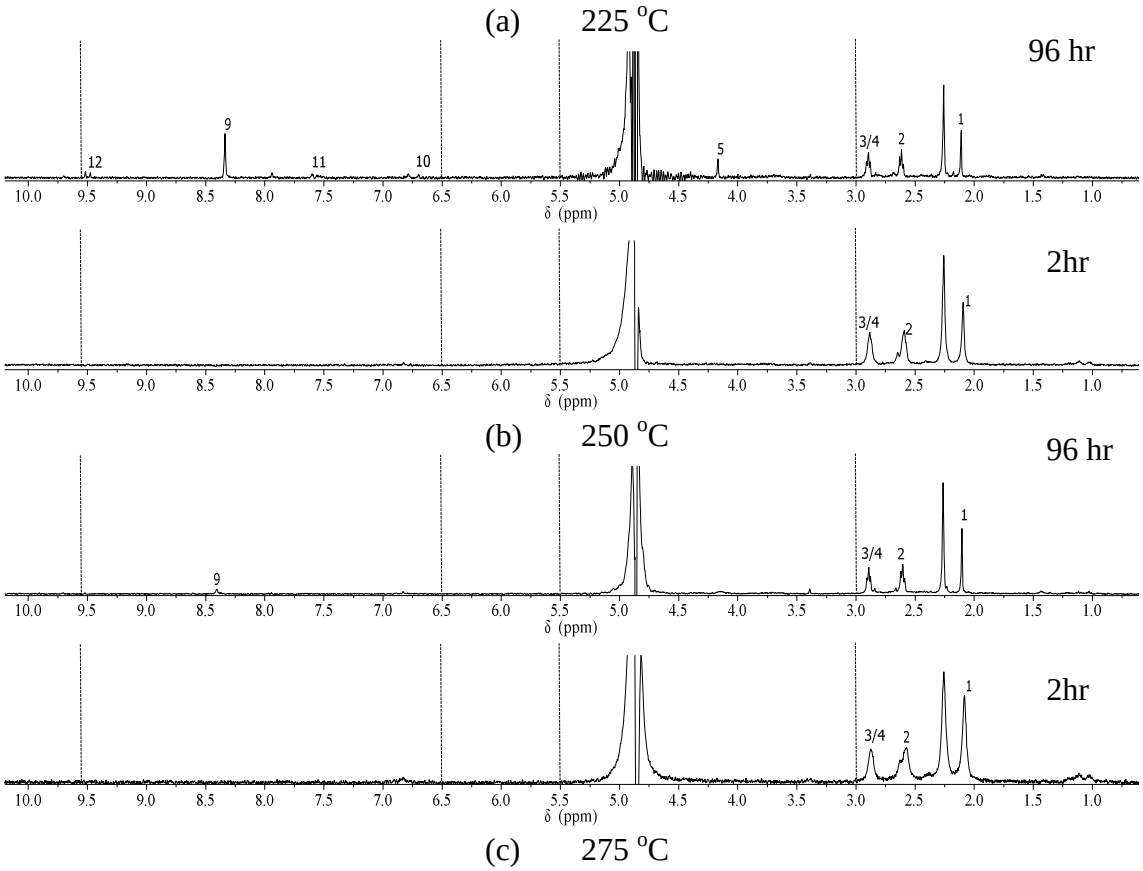

Figure 3.13 ^{1}H NMR spectra associated with liquid samples taken at 2 and 96 hours at reaction temperatures of: (a) 225, (b) 250 and (c) 275 °C. The numbers of the peaks represent carbons in related chemical structures (

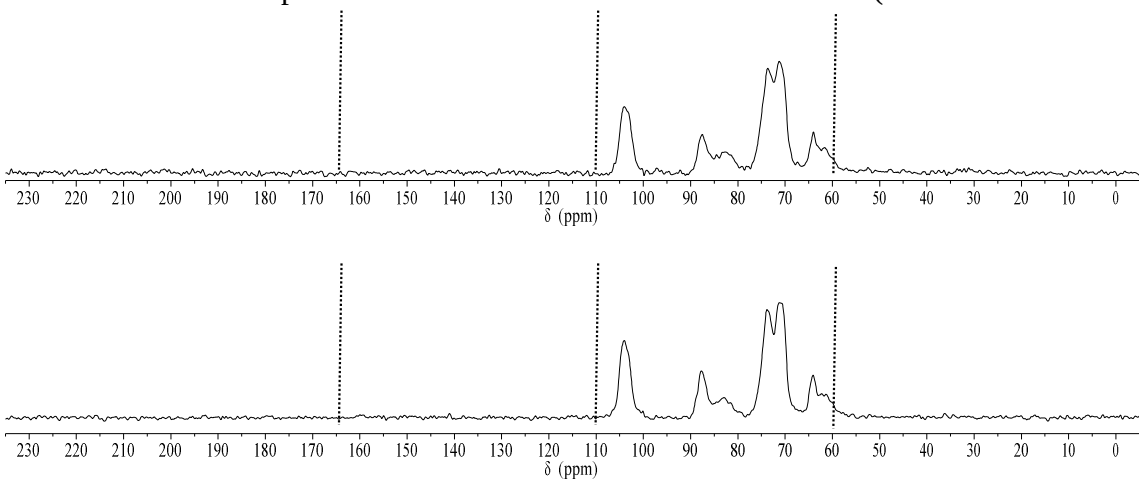

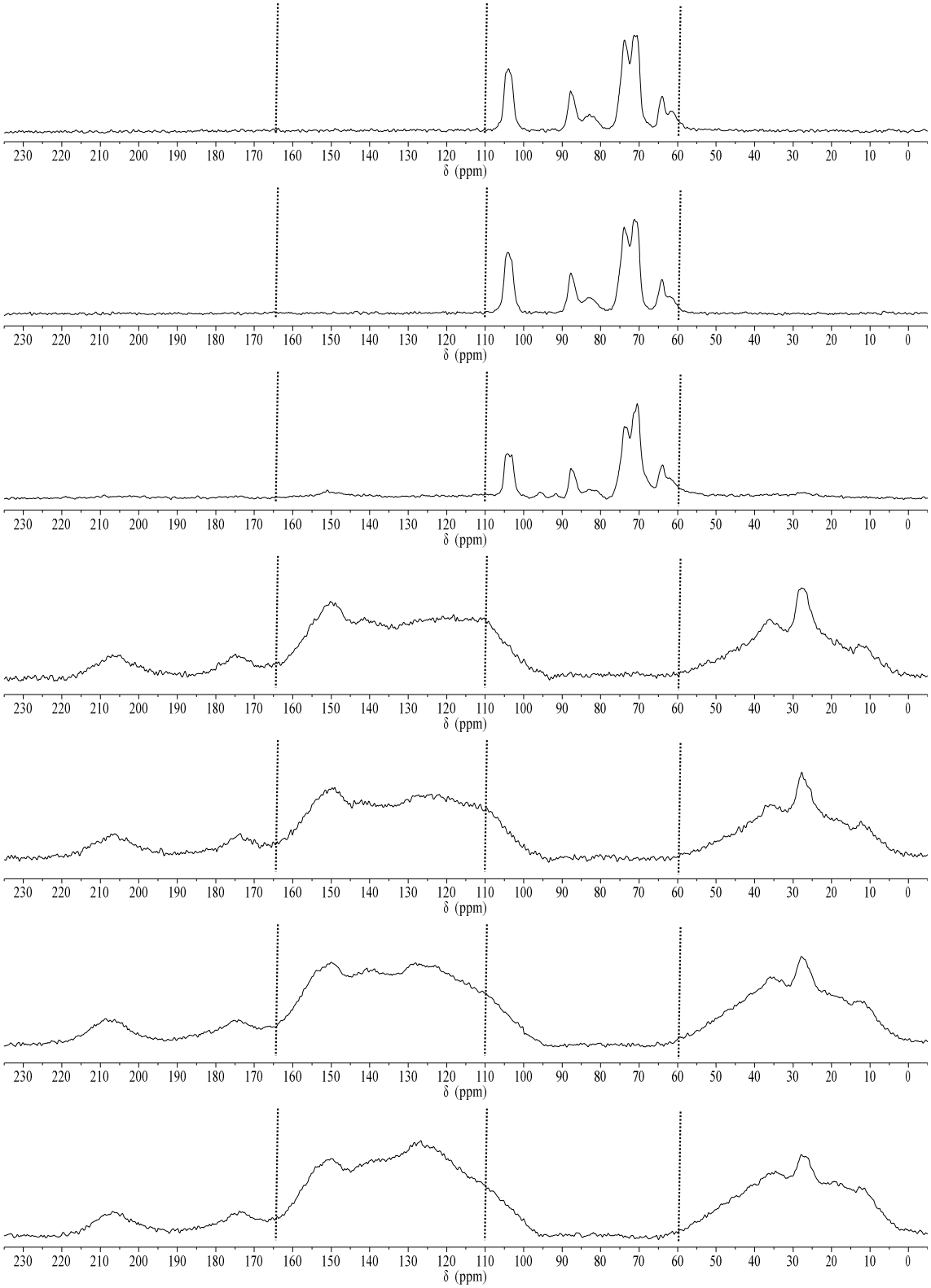

Figure 3.19 ^{13}C NMR of hydrochar at 225 ^{o}C.

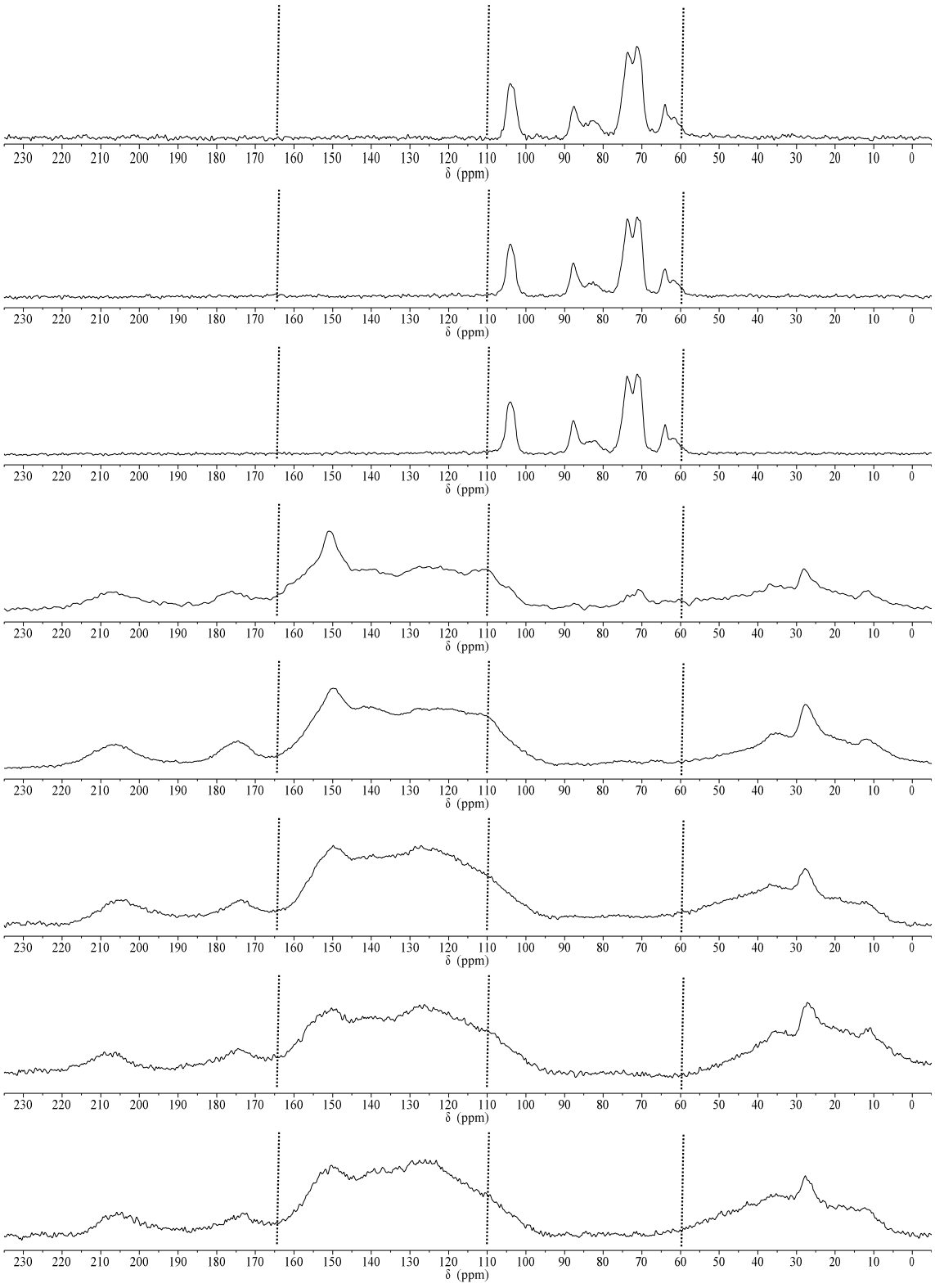
230 220 210 200 190 180 170 160 150 140 130 120 110 100 90 80 70 60 50 40 30 20 10 0
δ (ppm)

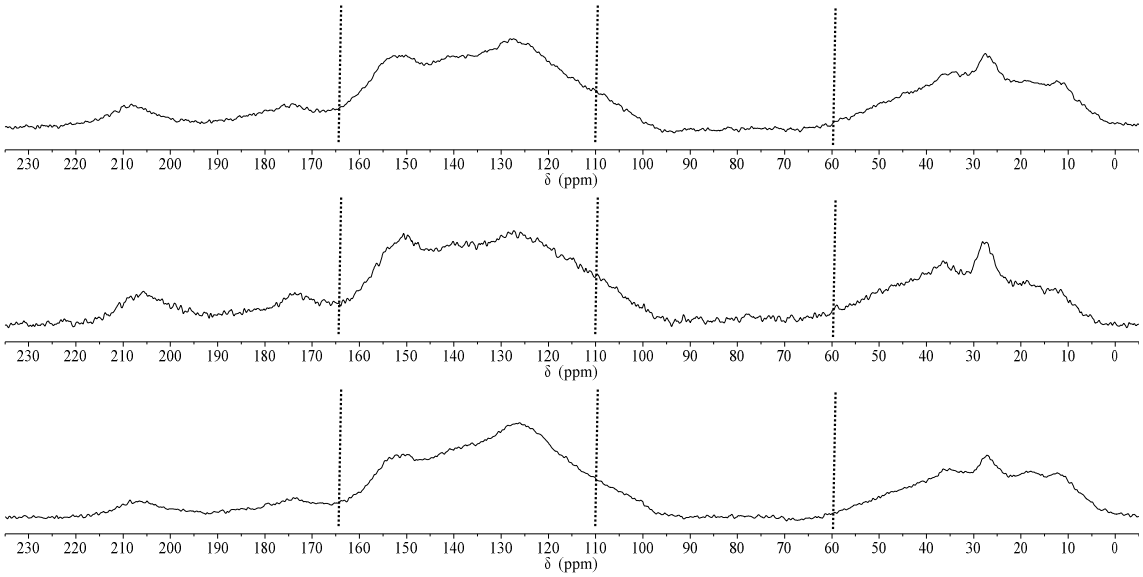

Figure 3.20 ^{13}C NMR of hydrochar at 250 ^{o}C.

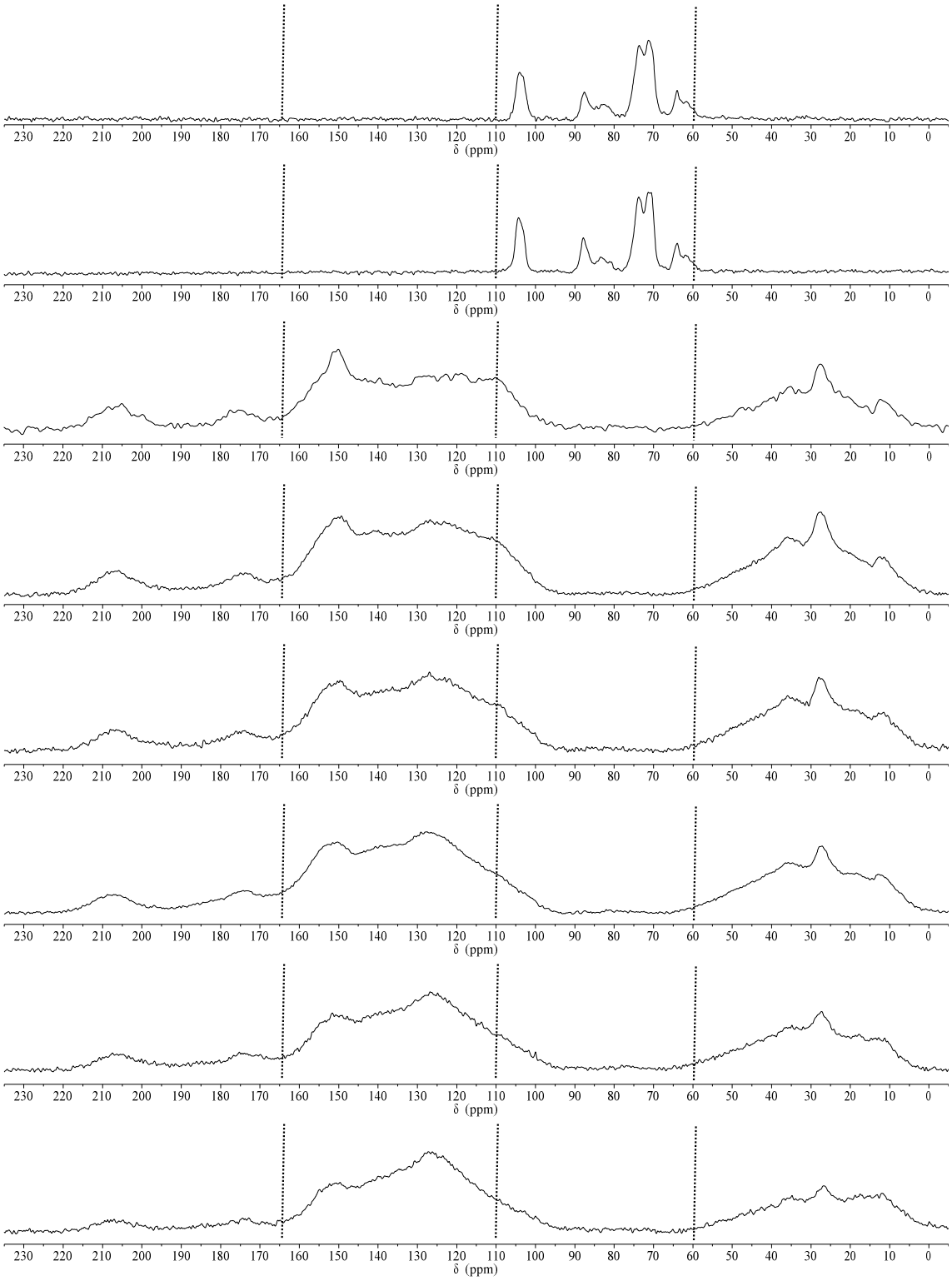
230 220 210 200 190 180 170 160 150 140 130 120 110 100 90 80 70 60 50 40 30 20 10 0
δ (ppm)

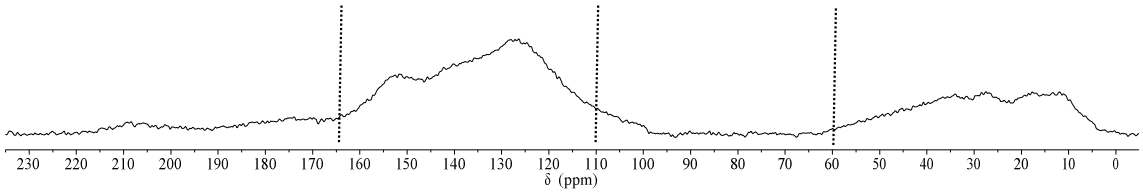

Figure 3.21 ^{13}C NMR of hydrochar at 275 ^{o}C.

Table 3.4). The peak present from 5.5 to 4.5 ppm represents water.

250 and 275^{o}C are taken following the large peak in liquid-phase carbon content (Figure 3.2). Sugars and aromatics are also present at higher temperatures, but at lower levels, likely due to changes in reaction rates at these temperatures. HMF is present at 250^{o}C at 2hrs, but not in the sample from the liquid at 275^{o}C. This lack of HMF is also likely a result of faster reactions at 275^{o}C.

The liquid composition at all temperatures is similar after 96-hours. The glucose detected in samples taken at 2-hours and at 225^{o}C is no longer present. HMF is also not present in any of the liquid samples after 96-hours. The decline in HMF is consistent with that reported by Asghari and Yoshida (2006). Over time, HMF likely becomes incorporated within the solids via polymerization-polycondensation (Baccile et al., 2009; Falco et al., 2011a), as it has been reported to play a role in solids formation (Falco et al., 2011a; Titirici et al., 2008). Acidic compounds remained in all liquid samples.

The COD/TOC ratio of the liquid at the three temperatures ranges from 1.5 – 3.5 (Figure 3.14). These relatively high COD/TOC ratios suggest there is a high concentration of oxidizable organics present (e.g., sugars, acetic acid, formate), corroborating the ^{1}H NMR data. The pH of the process water initially decreases, followed by a slight increase, ultimately resulting in a range of 2.9 – 3.4 (Figure 3.15). The most significant change in pH occurred before 4 hours, during the time in which the greatest change in carbon distribution occurred, likely resulting from the initial production of organic acids.

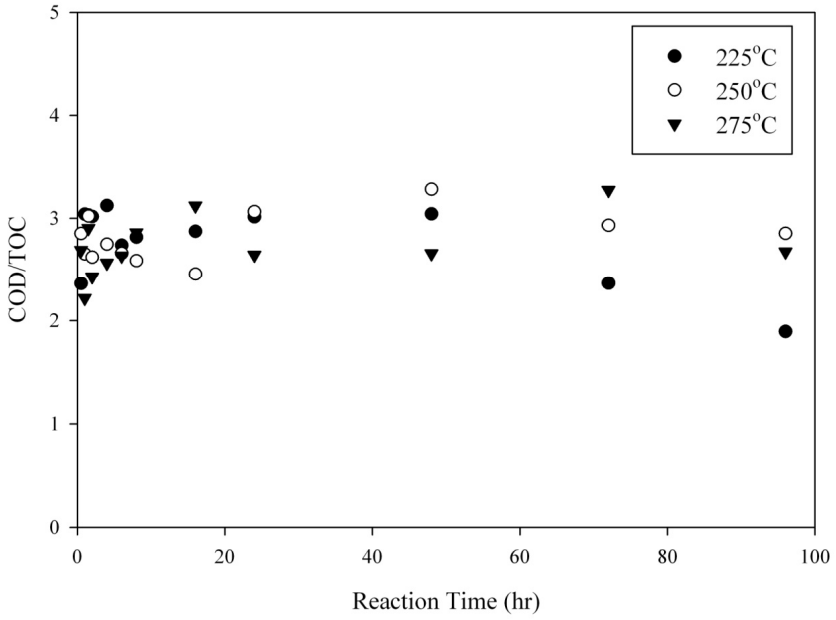

Figure 3.14 COD/TOC of liquid samples at 225, 250 and 275 °C. Data points represent averages from duplicate experiments.

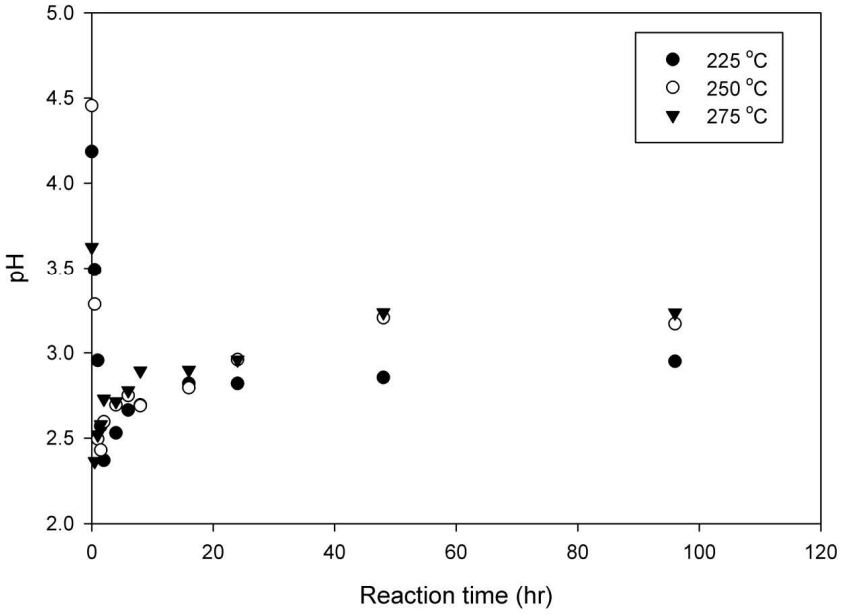

Figure 3.15 pH of liquid samples at 225, 250 and 275 °C. Data points represent averages from duplicate experiments.

3.3.4.3 Solids

3.3.4.3.1 Solids Recovery

Solids recovery (defined in Table 3.1) is calculated based on the total mass of dry solids recovered at each sampling time divided by the dry mass of the initial feedstock. It is likely that the solids recovered during early times (< 2 hours) are comprised of both unreacted and converted cellulose (e.g., hydrochar). Such differences cannot be distinguished via gravimetric or carbon measurements; results from ^{13}C NMR analysis confirm this phenomenon (discussed in detail in later sections). Solids recovery is influenced by both reaction temperature and time, and fit within the reported range of solids recovered following carbonization of various feedstocks at reported time intervals (Table 3.2 and Figure 3.3; e.g., Falco et al., 2011a; Hoekman et al., 2011; Knežević et al., 2009). The observed initial decrease in solids recovered results from a combination of initial feedstock solubilization and component partitioning to the gas and liquid-phases. As reaction temperatures increase, the rate of initial solids disappearance increases. In addition, as the target reaction temperature increases, the final solids recovery decreases (Figure 3.3). A similar influence of temperature on solids recovery has also been reported in the literature when carbonizing feedstocks such as cellulose, glucose and wood (measured over shorter time frames, Table 3.2 and Figure 3.6). Sevilla and Fuertes (2009a,b) report an opposite solids recovery trend when carbonizing cellulose, glucose and starch at temperatures ranging from 170 – 250^{o}C (Table 3.2). As discussed previously, this is likely an artifact of operational differences.

3.3.4.3.2 Hydrochar chemical composition

Elemental composition of solids recovered from experiments conducted at 250^{o}C was measured. Although the elemental composition of the solids recovered at 225 and 275^{o}C were not measured, it is assumed that the conversion mechanisms of cellulose are similar at different temperatures. The elemental composition of the solids recovered at 250^{o}C changes significantly during carbonization. Figure 3.16 illustrates the composition (normalized by solids recovery) of C, H, O and ash in the solids recovered over time at 250^{o}C. During the first hour, few changes in the elemental composition of the recovered solids occur. A significant change in elemental composition occurs between 1 and 1.5 hours, the time frame corresponding to significant changes in the carbon distribution and solids recovery (Figure 3.2 and Figure 3.3). Over this period, the mass of carbon in the recovered solids decreases by approximately 24%, while the solid-phase oxygen mass in the solids decreases by approximately 83%. Following 1.5 hours, smaller changes in the solids elemental composition occur. The decrease in solid-phase oxygen content represents the greatest change in the recovered solids composition and is the predominant component contributing to the decrease in mass recovery, similar to that observed at different temperatures for glucose (Falco et al., 2011a). A small fraction of the oxygen in the cellulose is transferred to the gas (based on carbon dioxide data), suggesting that the majority of the oxygen is transferred to the liquid-phase and is incorporated into dissolved organics or potentially the production of water. Deoxygenation occurs during both dehydration and decarboxylation and increases with temperature.

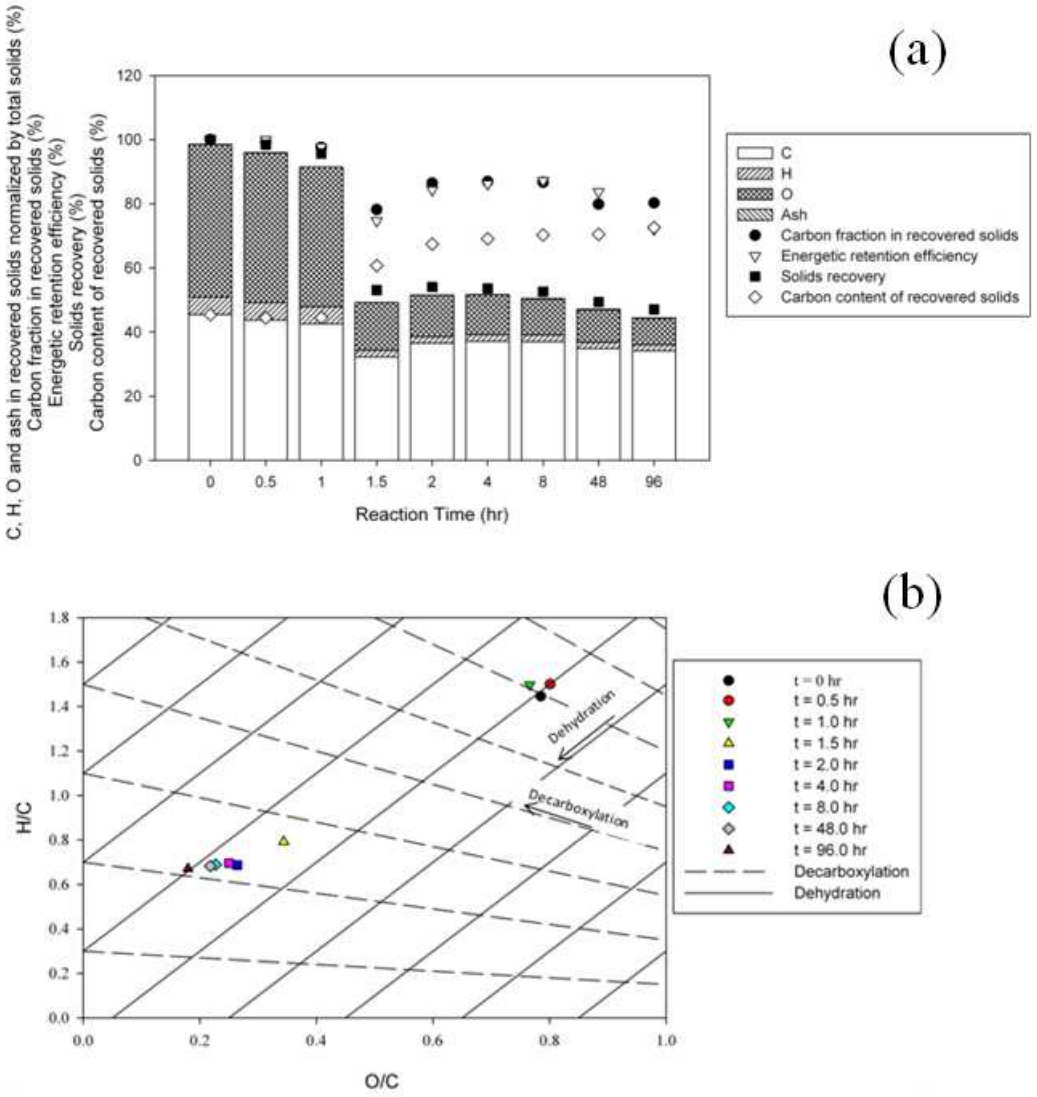

Figure 3.16 Elemental composition data associated with solids recovered at 250 ^{o}C: (a) recovered solids elemental composition, normalized by total initial solids, carbon fraction in recovered solids (percent of initially present carbon integrated within the solid-phase), energetic retention efficiency, and the carbon content (measured) of recovered solids over time at 250 ^{o}C and (b) Van Krevelen diagram associated with solids recovered at 250 ^{o}C. The lines represent the dehydration and decarboxylation pathways.

The carbon content of the recovered solids increases with time. This carbon densification (as defined in Table 3.1) is observed at all temperatures (Figure 3.17). Increases in carbon densification with temperature have also been observed in other studies (Table 3.2 and **Error! Reference source not found.**Figure 3.7 and Figure 3.8).

Carbon densification and deoxygenation have important energy-related implications (Channiwala and Parikh, 2002; Hwang et al., 2012).

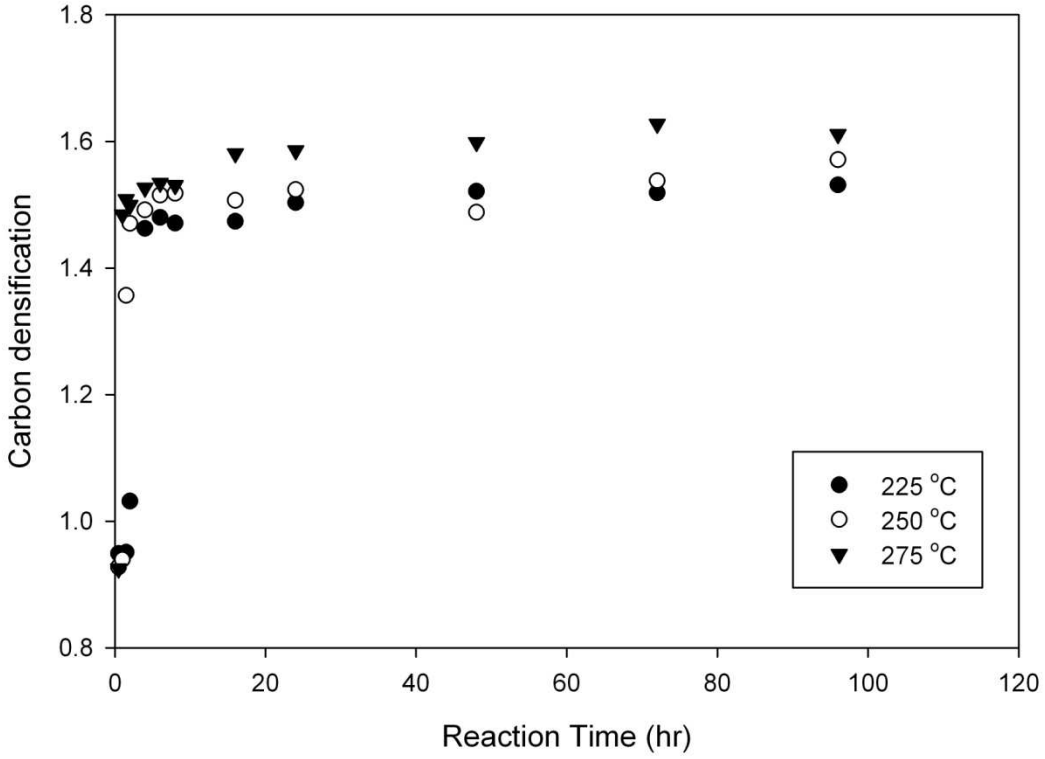

Figure 3.17 Solid-phase carbon densification at 225, 250, and 275 °C. Data points represent averages from duplicate experiments.

The energy value of the recovered solids increases over time at all temperatures evaluated (Figure 3.18a), following observations of increases in carbon and decreases in oxygen content. The energy content of the recovered solids after 96 hours varies by less than 5% at all reaction temperatures (average value is 25,000 J/g). The energy content of the recovered solids is greater at 250 and 275°C than that at 225°C. Except for one time (at one hour), the energy values at 250 and 275oC vary by less than 8%. A greater difference is observed when comparing with the energy measurements at 225°C (vary by

less than 20%). Energy densification increases with time and is slightly larger at 250 and 275^{o}C than at 225^{o}C after 96 hrs (Figure 3.18b). Solids energy densification has been reported when carbonizing a variety of feedstocks (Berge et al., 2011; Hoekman et al., 2011; Hwang et al., 2012; Roman et al., 2011). The energetic retention efficiency is a measure of the fraction of feedstock energy retained within the solid material (Figure 3.18c). The energetic retention efficiencies are similar at all reaction temperatures. Initial energetic retention efficiencies are high because no solids conversion has occurred, only cellulose solubilization. From 16 to 48 hours, the energy retained in the solids is slightly larger at 250^{o}C. Although the energy content of recovered solids after 96 hours at 225^{o}C is lower than that at 250 and 275^{o}C the energetic retention efficiency is greatest at 225^{o}C because the mass of recovered solids is greatest at that temperature. The energetic retention efficiency associated with the solids recovered at 250 and 275^{o}C decrease slighty with time because of the decreases in recovered solids mass.

The atomic H/C and O/C ratios were calculated using the elemental composition data. Results from this analysis are presented in a Van Krevelen diagram (Figure 3.16b). Van Kevelen diagrams allow for delineation of reaction pathways. Straight lines can be drawn to represent the dehydration and decarboxylation reaction pathways. As illustrated in Figure 3.16b for carbonization at 250^{o}C, as cellulose carbonization proceeds, the predominant process appears to be dehydration. Decarboxylation also occurs, as evidenced by the production of carbon dioxide. The atomic ratios change significantly during the period of greatest cellulose conversion (from 1 to 1.5 hours). These atomic ratios suggest little change during early times (0 – 1 hour), while dehydration is a predominant pathway following cellulose dissolution and subsequent initial hydrochar

formation. Decarboxylation also occurs during this time period, evidenced by the commencement of carbon dioxide production and the change in atomic ratios. Following this, during the period of less significant changes in carbon distribution (> 2 hours), decarboxylation appears to be a more predominant conversion pathway, as the H/C ratio remains relatively constant. Decarboxylation results in minimal carbon release with more significant oxygen release. The H/C and O/C ratios after 2 hours are within the range of values reported for hydrochars resulting from the carbonization of various feedstocks (Table 3.2) and are similar to that of a low grade coal . Based on data from studies reported in the literature (Table 3.2, Figure 3.9 and Figure 3.10), it appears that temperature has greater influence on the O/C than that on the H/C ratio.

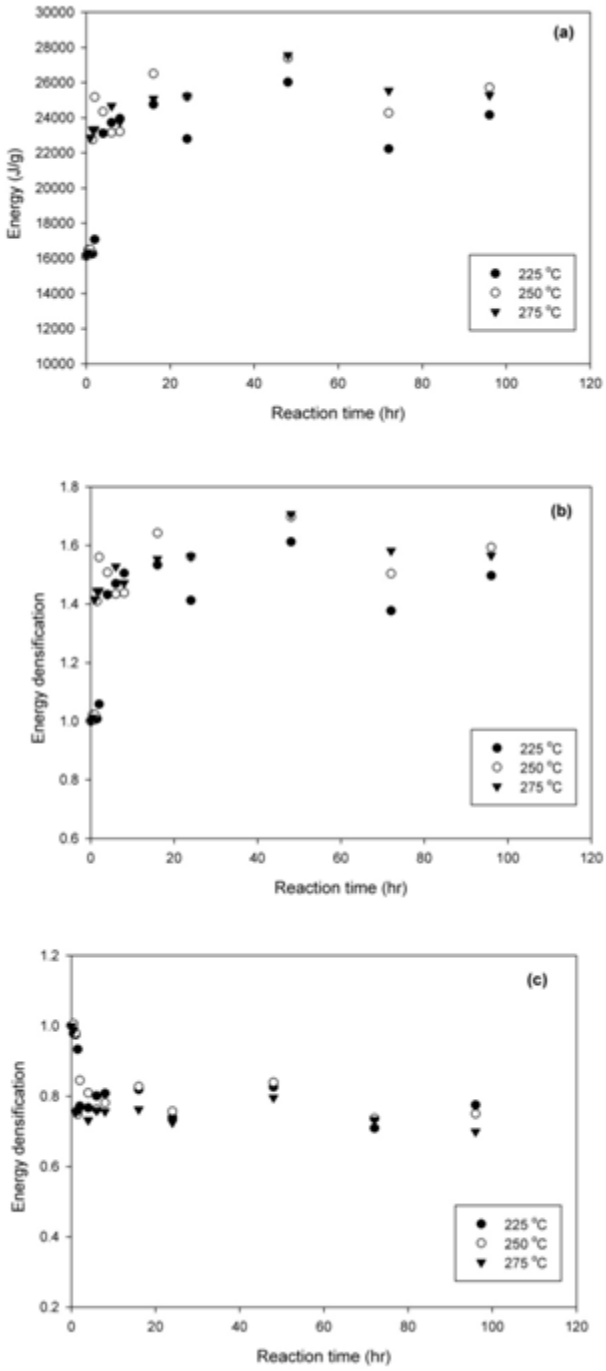

Figure 3.18 Solid-phase energy properties at 225, 250, and 275 ^{o}C: (a) energy content, (b) energy densification, and (c) energetic retention efficiency.

3.3.4.3.3 ^{13}C NMR analysis

Spectra from ^{13}C solid-state NMR of solids recovered over time at the three temperatures provide semi-quantitative solids structural information and insight to carbonization pathways/mechanisms. Four main regions are detected in these spectra (Figure 3.19 – 3.21 and Table 3.3), following that reported by Baccile et al. (2009) and Falco et al. (2011b): nonpolar alkyl carbons (0 - 48 ppm), cellulose (60 - 105 ppm), sp^2 hybrid carbons (furanic and aromatic carbons, deconvoluted between 110 – 151 ppm), and carbonyl carbons (175 – 207 ppm).

Table 3.3 Peak assignments for ^{13}C NMR spectra.

Spectral domain	Region (ppm)	Represented structure	Chemical shift (ppm)	Reference
I: alkyl	0 – 50	CH_x	0 - 50	Baccile et al., 2009
II: unconverted cellulose	60 – 105	C_6	59 – 64	Kono et al., 2002
		C_2, C_3, C_5	71 – 74	
		C_4	82 – 88	
		C_1 (O-C-O)	102 – 104.2	
III: sp^2 C	110 – 151	β -C in furan ring	110	Baccile et al., 2009; Falco et al., 2011b
		β-β bond connecting two furan rings	118	Falco et al., 2011b
		aromatic C	125	Falco et al., 2011b
		aromatic C	132	Baccile et al., 2009; Falco et al., 2011b
		α-α bond connecting two furan rings	140	Falco et al., 2011b
		α-C in furan ring	150	Baccile et al., 2009; Falco et al., 2011b
IV: carbonyl	175 – 210	H-C=O	175	Baccile et al., 2009
		R_2-C=O	207	Baccile et al., 2009

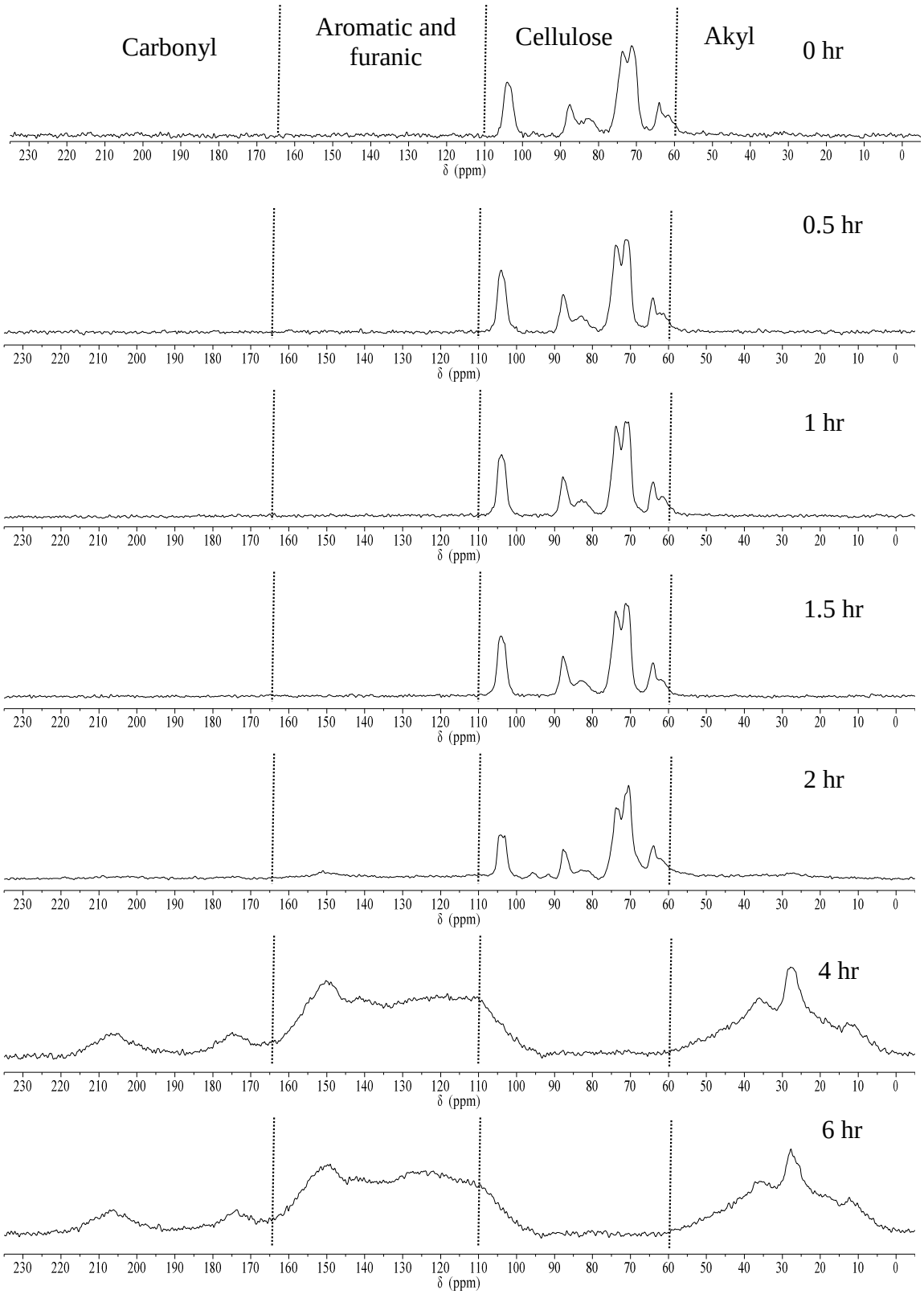
Carbonyl
Aromatic and furanic
Cellulose
Akyl
0 hr
0.5 hr
1 hr
1.5 hr
2 hr
4 hr
6 hr
230 220 210 200 190 180 170 160 150 140 130 120 110 100 90 80 70 60 50 40 30 20 10 0
δ (ppm)

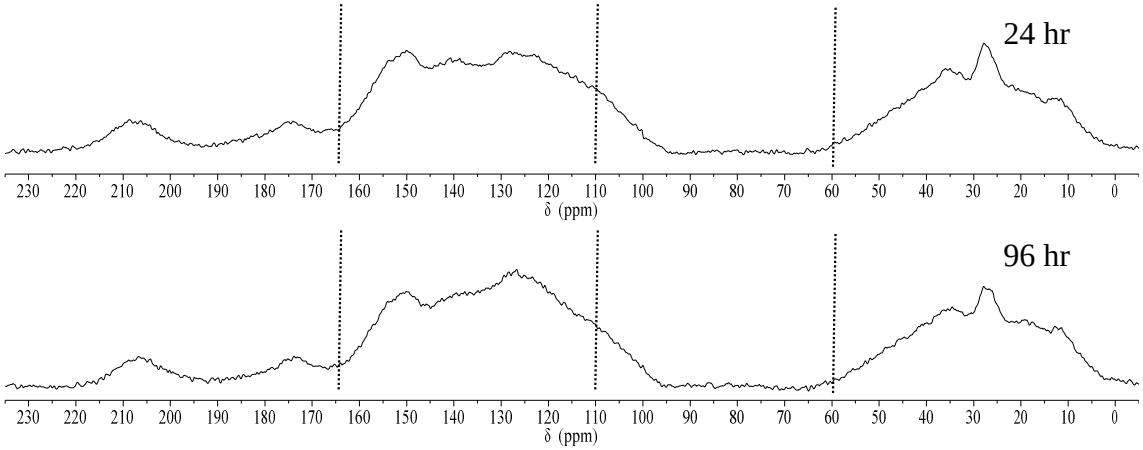

Figure 3.19 ^{13}C NMR of hydrochar at 225 ^{o}C.

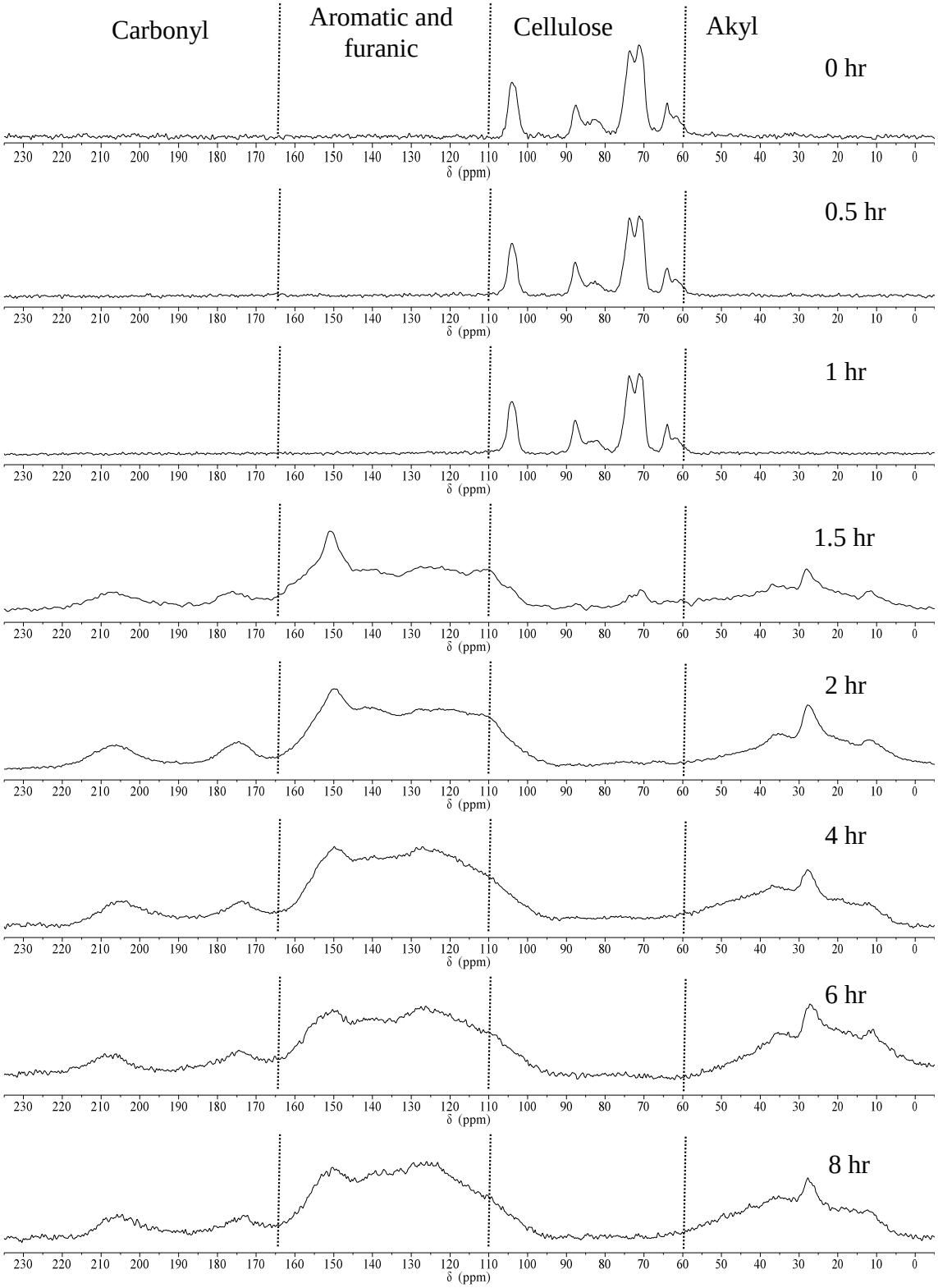
Carbonyl
Aromatic and furanic
Cellulose
Akyl
0 hr
0.5 hr
1 hr
1.5 hr
2 hr
4 hr
6 hr
8 hr
230 220 210 200 190 180 170 160 150 140 130 120 110 100 90 80 70 60 50 40 30 20 10 0
δ (ppm)

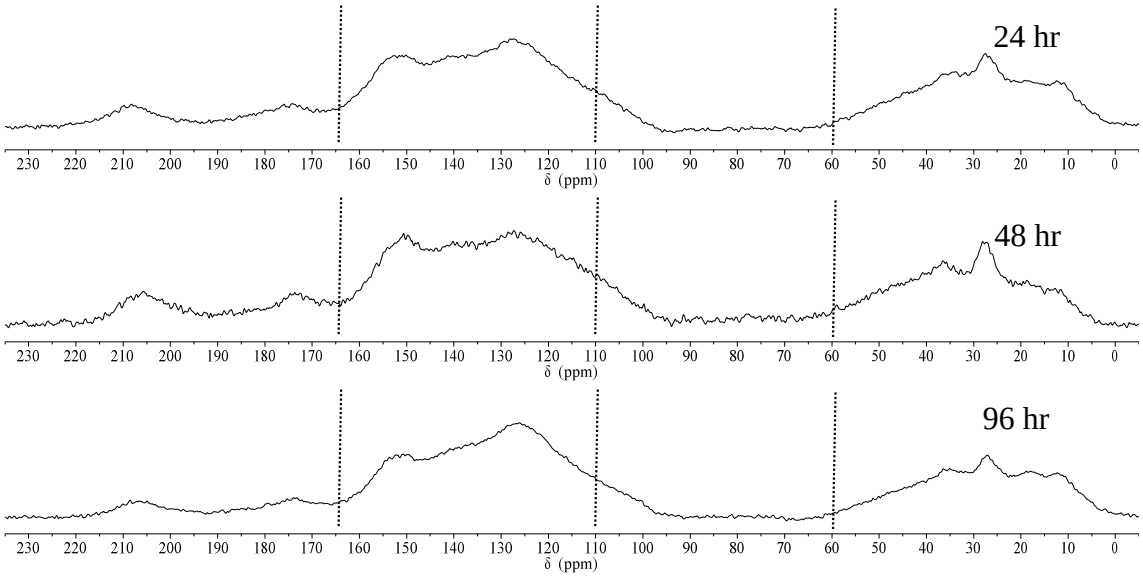

Figure 3.20 ^{13}C NMR of hydrochar at 250 ^{o}C.

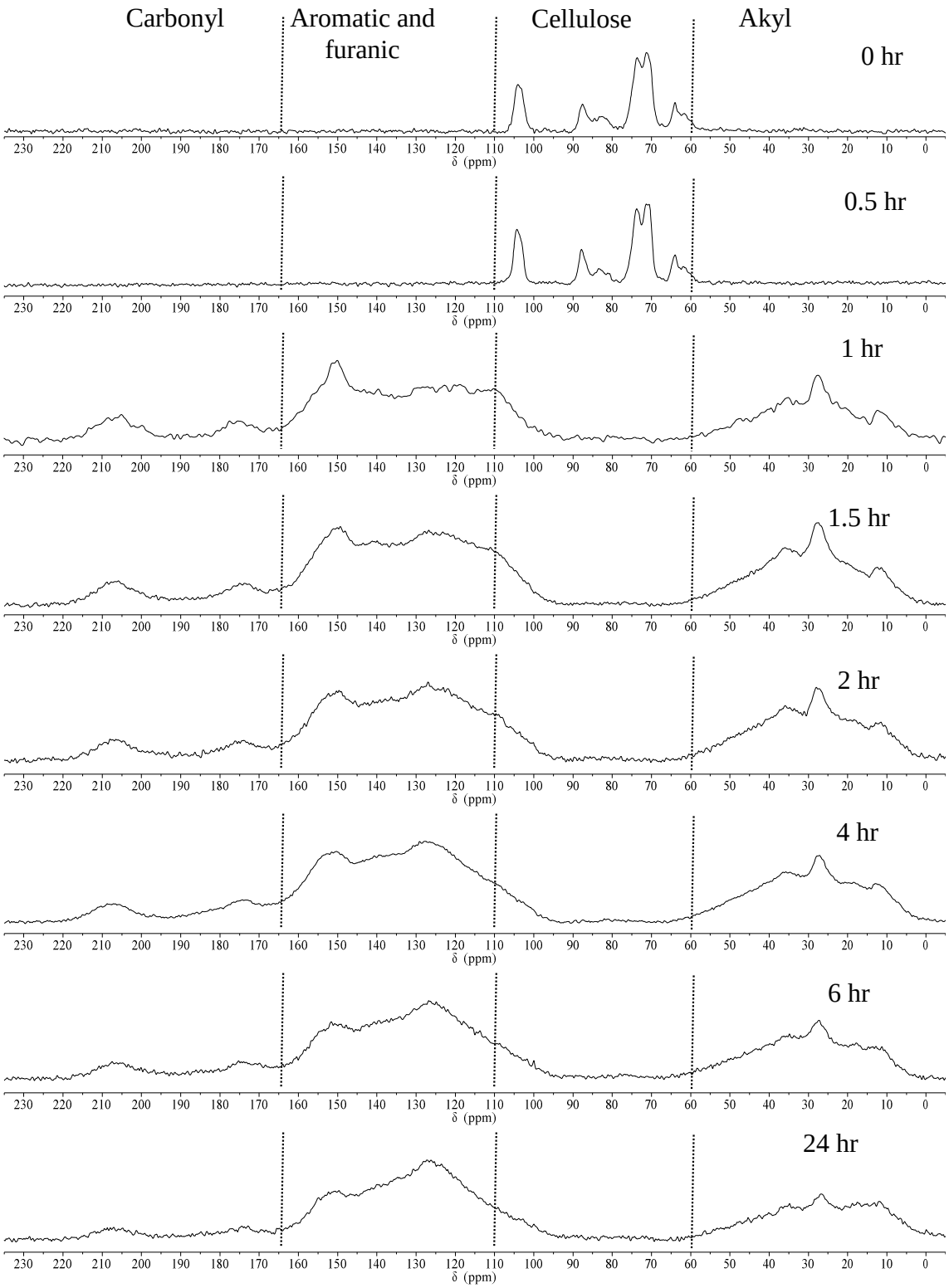
Carbonyl
Aromatic and furanic
Cellulose
Akyl
0 hr
0.5 hr
1 hr
1.5 hr
2 hr
4 hr
6 hr
24 hr
230 220 210 200 190 180 170 160 150 140 130 120 110 100 90 80 70 60 50 40 30 20 10 0
δ (ppm)

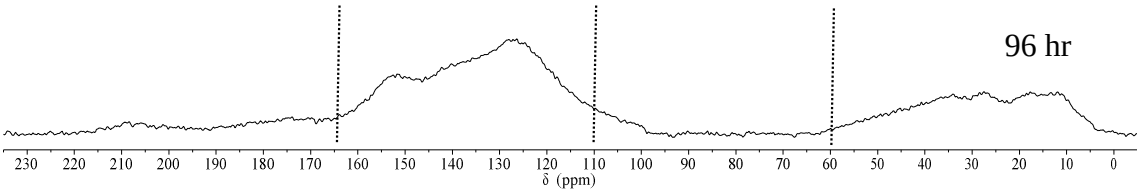

Figure 3.21 ^{13}C NMR of hydrochar at 275 ^{o}C.

Table 3.4 Chemical compounds associated with the peak numbers in ^{1}H NMR spectra of liquid samples (see Figure 3.13).

Region	Chemical shift range (ppm)	Compound	Chemical structure	Chemical shift (ppm)	Multiplicity	Reference
Aliphatic /alcoholic	0.8 — 3	Acetic acid	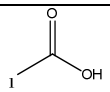	2.07	singlet	(Caligiani et al., 2007)
		Levulinic acid	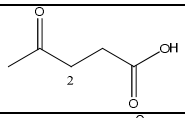	2.6 – 2.7	singlet	(Chalid, 2012)
		Succinic acid	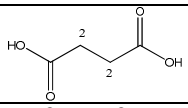			(Caligiani et al., 2007)
		Acetoacetate	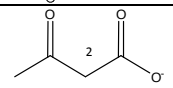			(Fan, 1996)
		Citric acid	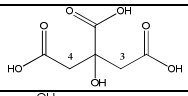	2.87	doublet	(Caligiani et al., 2007)
Sugars	3 – 5.5	Fructose	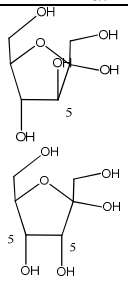 α-fructose β-fructose	4.11	multiplet	(Fan, 1996)
		β-glucose	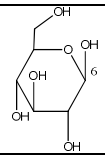	4.64	doublet	(Fan, 1996)
			The other protons	3.26 – 3.86		
		α-glucose	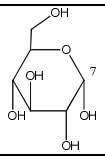	5.24	doublet	(Fan, 1996)
			The other protons	3.44 – 3.86		
		Sucrose	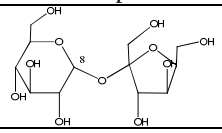	5.42	doublet	(Fan, 1996)
Aromatic/ aldehydes	6.5 – 9.5	Formate	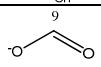	8.46	singlet	(Fan, 1996; Silwood et al., 1999)
		HMF	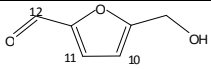	6.68 (C10)	doublet	(Caligiani et al., 2007)
				7.54 (C11)	doublet	
				9.46 (C12)	singlet	

The influence of reaction time on the carbon fractions in the recovered solids structure at each reaction temperature is shown in Figure 3.22. During the first 1 to 2 hours, the only peaks visible in the ^{13}C NMR spectra are those associated with cellulose, indicating solids conversion to hydrochar has not yet occurred. Decreases in the areas associated with these cellulose peaks coupled with carbon detection in the liquid-phase (Figure 3.2 and Figure 3.16), suggest cellulose dissolution occurs and is consistent with calculated carbon conversion fractions, solids recovery, and carbon distribution data (Figure 3.2, Figure 3.3 and Figure 3.4). The rate of cellulose disappearance/dissolution is greatest at 275 ^{o}C (3.4). As the peaks associated with cellulose decrease, the formation of peaks representative of alkyl, sp^2 and carbonyl carbons increase, suggesting commencement of hydrochar formation. Evidence of hydrochar formation is not apparent until after 4, 1.5 and 1 hour at reaction temperatures of 225, 250 and 275^{o}C, respectively. These data suggest cellulose dissolution, at least in part, is a precursor for hydrochar formation. Knezevic et al. (2010) also observed this phenomenon when carbonizing wood chips. Falco et al. (2011a), however, did not conclude that significant cellulose solubilization contributed to or was a precursor to hydrochar formation at temperatures greater than 200^{o}C. It should be noted that Falco et al. (2011a) did not evaluate cellulose carbonization during times of greatest conversion (they sampled at 4, 6, 24 and 72 hours). As discussed previously, the slow heating of the reactors utilized in this work increase the importance of cellulose dissolution.

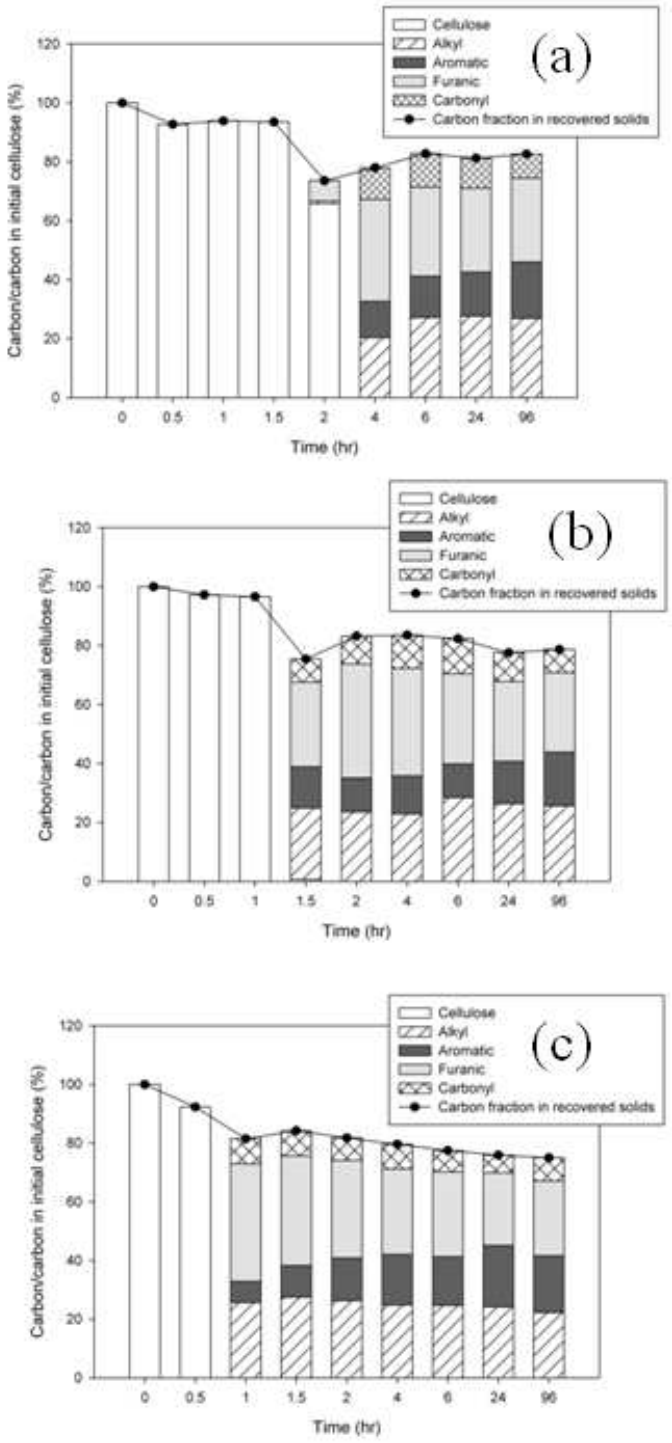

Figure 3.22 Solid-phase carbon distribution data derived from 13C NMR data over time at: (a) 225, (b) 250, and (c) 275 ^{o}C.

The ^{13}C NMR spectra at 225^{o}C from 0 – 2 hours suggest cellulose crystallinity changes during early reaction times. Initially, cellulose appears to be predominantly in the crystalline form of Iα (Atalla and Vanderhart, 1984; Kono et al., 2002). After 2 hours at 225^{o}C, the NMR spectra indicate a change in the peaks associated with cellulose, as a clear doublet at C-1 and a higher peak around 72 ppm at C-2,3,5 are present (see Table 3.3 and Figure 3.19). These differences suggest the Iβ crystalline form of cellulose is becoming more predominant (Atalla and Vanderhart, 1984; Kono et al., 2002). It is reported that the crystalline form Iα is less stable than Iβ, due to differences in hydrogen bonds (Watanabe et al., 2007). Yamamoto and Horli (1993) demonstrated that the crystalline form of Iα can be transformed into Iβ by hydrothermal treatment at 220 − 280 ^{o}C in NaOH and Debzi et al. (1991) report Iβ formation results from annealing at 260 – 280 ^{o}C in inert gases. This apparent formation/detection of Iβ is may be due to either: (1) the transformation of Iα into Iβ or (2) the dissolution of the Iα component of cellulose.

Following significant disappearance of cellulose, carbon is predominantly converted to furanic, aromatic and alkyl compounds (Figure 3.22). As reaction time increases, there is a slight decrease in furanic carbons, while the aromatic carbons increase. This observation is similar to hydrochar characterization reported by Falco et al. (2011a) from the carbonization of cellulose and glucose. Reduction of furanic groups may be a result of intramolecular condensation and dehydration, contributing to the generation of more condensed aromatic structures (Falco et al., 2011a; Falco et al., 2011b). This observation is also consistent with the carbon densification in solids observed over time. Decreases in the furanic groups also correlate with the observed loss

of oxygen in the recovered solids, possibly resulting from decarboxylation of the furanic rings.

Following cellulose conversion, the percent of carbonyl groups increases and then decreases slightly. After 96 hours, the intensity of carbonyl groups in the chars at all temperatures is similar. This observation differs from that reported by Falco et al. (2011a). Falco et al. (2011a) report a significant decline in the relative intensities of carbonyl groups as temperature increases from 240 to 280 ^{o}C. Differences are likely a result of process parameters, such as reaction time and solids concentration. The percent of aliphatic carbons remains fairly constant during carbonization at 225, 250 and 275 ^{o}C.

The overall char composition after 96 hours at all reaction temperatures is similar, consisting primarily of sp^2 carbons (furanic and aromatic groups), with a greater proportion of furanic groups than aromatic groups, and alkyl groups. Percent differences between the individual groups at the three temperatures generally differ less than ~5%. The hydrochar resulting from the carbonization of cellulose at 275^{o}C contains a slightly larger percentage of aromatic groups than those produced at 225 and 250^{o}C. The fraction of alkyl and carbonyl groups is slightly larger at lower temperatures. Falco et al. (2011a; 2011b) observed a higher degree of aromatization as temperatures increase. Although the fraction of carbon in the aromatic groups did increase with temperature, the increase was small. It is possible if a larger range of temperatures were evaluated the degree of aromatization would increase. The similar final structure of the hydrochar suggests similar conversion mechanisms at the temperatures evaluated. Although temperatures within the range evaluated in this study do not appear to influence carbonization pathways, temperature does influence conversion rates.

3.3.5 Implications on process optimization

Results from this work can be used to gain insight on critical process parameters and optimal carbonization conditions. Reaction time is an important parameter. The period of greatest carbon conversion occurs during the first 8 hours, with appreciable conversion continuing over a 24-hour period (Figure 3.2). Carbon conversion continues, but only varies by approximately 5% after 24 hours, suggesting reaction times of 24 hours are sufficient for the greatest integration of carbon in the solid. Higher reaction temperatures yield faster conversion.

The energy content of the recovered solids is greatest at higher temperatures (250 and 275^{o}C) throughout the majority of the experiment, with the energy value of recovered solids from all temperatures approaching a similar value after 96 hours. For the first 48 hours, the energetic retention efficiency is greatest at 250^{o}C. If operating to maximize energy recovery, it appears that operation at 250^{o}C for up to 48 hours is optimal, although it should be noted that the energetic retention efficiencies at the three temperatures vary by less than 6%. This time frame correlates well with the hydrocarbon masses in the gas-phase. Detected hydrocarbons reach their maximum value, and thus maximum energy content, around 48 to 72 hours. However, a balance between carbonization energy requirements and energy recovery in the solids and gas-phase needs to be evaluated for process optimization.

Potential environmental concerns associated with furanic compounds decreases with time. The carbon content of the liquid also decreases. These decreases, in part, occur because of compound incorporation into the solid-phase. Additional work is needed to evaluate potential compound desorption from the hydrochar over time and/or the time-

dependence on the release of volatiles during hydrochar combustion for energy generation.

3.4 CONCLUSIONS

Results from batch experiments indicate time and temperature impart the greatest impact on cellulose carbonization during the first 8 hours, the period of greatest conversion. Data suggest cellulose solubilization occurs prior to conversion. The composition of solids recovered after 96-hours is similar at all temperatures, consisting primarily of sp^2 carbons (furanic and aromatic groups) and alkyl groups. The composition of the gas-phase changes over time, with greater masses of energy-dense hydrocarbons and lower masses of furan detected at longer reaction times. Composition of the liquid-phase also changes with reaction time, ultimately resulting in the formation of organic acids.

CHAPTER 4.

INFLUENCE OF PROCESS WATER QUALITY ON HYDROTHERMAL CARBONIZATION OF CELLULOSE[3]

[3] . Influence of process water quality on hydrothermal carbonization of cellulose, Lu X.; Flora, J R. V.; Berge, N. D., 2014. Bioresource Technology 154. 229-239. Reprinted here with permission of publisher.

ABSTRACT

Hydrothermal carbonization (HTC) is a thermal conversion process that has been shown to be environmentally and energetically advantageous for the conversion of wet feedstocks. Supplemental moisture, usually in the form of pure water, is added during carbonization to achieve feedstock submersion. To improve process sustainability, it is important to consider alternative supplemental moisture sources. Liquid waste streams may be ideal alternative liquid source candidates. Experiments were conducted to systematically evaluate how changes in pH, ionic strength, and organic carbon content of the initial process water influences cellulose carbonization. Results from the experiment conducted evaluating the influence of process water quality on carbonization indicate that changes in initial water quality do influence time-dependent carbonization product composition and yields. These results also suggest that using municipal and industrial wastewaters, with the exception of streams with high $CaCl_2$ concentrations, may impart little influence on final carbonization products/yields.

4.1 INTRODUCTION

Hydrothermal carbonization (HTC) is a thermal conversion process that has been shown to be environmentally and energetically advantageous for the conversion of wet feedstocks, such as biomass and components of municipal solid waste (MSW), to a carbon-rich, energy-dense solid material often referred to as hydrochar. Results from the carbonization of a variety of feedstocks indicate that a large fraction of carbon initially present in the feedstock remains integrated within the hydrochar material (Berge et al., 2011a; Funke & Ziegler, 2010b; Li et al., 2013; Libra et al., 2011b; Lu, 2013; Titirici et

al., 2007a), potentially resulting in fewer carbon emissions than those associated with other conversion approaches. The generated hydrochar has sparked significant interest in carbonization processes, as HTC may serve as a sustainable means to create functional materials from renewable sources (Berge et al., 2011b; Hwang et al., 2012; Libra et al., 2011a; Román et al., 2013; Titirici & Antonietti, 2010; Titirici et al., 2012).). These functional materials have been used for use as a soil amendment, environmental adsorbent, and as an energy source (Flora et al., 2013; Kammann et al., 2012; Libra et al., 2011; Liu et al., 2010; Paraknowitsch et al., 2009).

During HTC, wet feedstocks undergo a series of simultaneous reactions, including hydrolysis, dehydration, decarboxylation, aromatization, and recondensation (Funke & Ziegler, 2010a; Libra et al., 2011a; Sevilla & Fuertes, 2009b; Titirici et al., 2007b). These reactions occur under autogeneous pressures, and at temperatures generally ranging between 180 – 300^{o}C. A requirement of the carbonization process is feedstock submersion in liquid (Funke & Ziegler, 2010a). To achieve feedstock submersion, supplemental moisture is often required, as few feedstocks contain sufficient moisture to meet this requirement. Water (often deionized) is the liquid most often used as the supplemental moisture source in the majority of reported laboratory HTC studies (e.g.,(Berge et al., 2011a; Funke & Ziegler, 2010a; Li et al., 2013; Libra et al., 2011a; Lu et al., 2012; Lu, 2013). From a practical perspective, however, the use of water as a moisture source is not sustainable and a disadvantage of the process, as it results in the depletion of an increasingly scarce and valuable resource. To improve process sustainability and flexibility, it is important to consider potential alternative supplemental moisture sources. Liquid streams, such as leachates, seawater, and wastewaters, are ideal

alternative liquid source candidates as they are plentiful and require some level of treatment prior to discharge to or subsequent use as a water source (e.g., drinking, irrigation, recreational). The composition of these waste streams, however, is complex and the impact of their composition on HTC has not been previously studied.

There has been some limited work investigating the addition of salts, acids, and bases during carbonization, but not at concentrations or ranges relevant to typical waste streams. Results from these previously conducted experiments suggest that changes in process water composition may favorably impact carbonization product yields and composition. Lynam et al. (2011) carbonized lignocelluosic biomass in the presence of high concentrations of acetic acid (0.4 g acetic acid per g of biomass) and found that the addition of the acid enhanced the energy content of the solid materials and reduced solid yields. In addition, it has been shown that solids recovered when carbonizing in the presence of calcium salts have larger energy contents and result in solids that have desirable properties when co-firing in existing coal boilers (Lynam et al., 2012). Stemann et al. (2013) evaluated the influence of recycled process water (rich in organics and rather acidic) on carbonization and found that carbonizing in the presence of concentrated organic acids catalyzes dehydration.

An important first step to identifying suitable alternative liquid sources is to understand how, and if, process water quality influences carbonization product composition and yields. Experiments were conducted to systematically evaluate how changes in initial process water quality influence cellulose carbonization. The specific objectives of this study were to evaluate how changes in initial process water pH (including addition of both acids and bases, HCl, H_2SO_4, NaOH, $Ca(OH)_2$), ionic strength

(NaCl and $CaCl_2$), and organic concentrations (modeled with acetic acid, AA) spanning ranges expected in municipal and industrial waste streams influence carbonization mechanisms and product composition, yields, and energy value.

4.2 MATERIALS AND METHODS

4.2.1 Bach HTC experiments

Microcrystalline cellulose (with average particle size of 50 µm, Acros Organics) was purchased from Fisher Scientific. Cellulose (with average particle size of 50 µm, Acros Organics) derived from the Western redcedar plant was used as the feedstock in all experiments. Cellulose serves as a model biomass compound and was chosen for use in this study because its carbonization has been explored extensively and the reaction pathways and mechanisms are well defined. Cellulose carbonization was conducted in 160-mL gas-tight stainless steel tubular reactors (MSC, Inc.) rated to withstand anticipated pressures and temperatures, similar to those reported by Lu et al. (2013). Each reactor was equipped with a gas-sampling valve to allow controlled collection of gas samples. The in-situ liquid temperature was measured as described by Lu et al. (2013); the heating profile if the reactor system can be found in the supporting information (see supplemental information of Figure 3.1). Time zero in this work corresponds to the time the reactor is placed in the oven.

The batch experiments were conducted following procedures previously described (Berge et al., 2011b; Flora et al., 2013; Lu et al., 2012). Briefly, a series of reactors containing cellulose (20 %, wt.) and deionized (DI) water were prepared. Reactors were sealed (unstirred) and heated in a laboratory oven to 250^{o}C. Reactors were sacrificially

sampled at 30, 60, 90, 120, and 180 minutes to assess how carbonization products/yields change with time. This time frame was chosen because it represents the time range of greatest cellulose conversion (Lu et al., 2013). At each sampling time, the reactors were removed from the oven and subsequently cooled in a cold-water bath to quench the reaction. Gas samples were collected in either 1 or 3-L foil gas sampling bags (SKC, Inc.) and volume measured using a 1-L gas tight syringe (Hamilton Co.). Solids were separated from the process liquid via vacuum filtration (0.22 um nitrocellulose filters, Millipore) and subsequently dried at 80^{o}C to remove residual moisture.

A series of batch experiments were conducted to systematically evaluate how process water composition influences carbonization product composition and yields. The concentration ranges evaluated simulate those found in municipal and industrial waste streams. All solutions were mixed prior to addition to the carbonization experiments. Acidic process water was created via the addition of either HCl (Fisher Scientific, Inc.) or H_2SO_4 (Fisher Scientific, Inc.) over a concentration range of 0.0001 N – 0.01 N (equivalent initial pH levels/H^+ concentrations), with initial pH values ranging from 4.3 – 2.2. Basic process water was created via the addition of NaOH (0.0001 – 0.01 N NaOH) and $Ca(OH)_2$ (0.00001 – 0.001 N $Ca(OH)_2$), with initial process water pH levels ranging from 7.5 – 11.8. The influence of salt concentration and type on carbonization is also evaluated; NaCl or $CaCl_2$ (Fisher Scientific, Inc.) was added to the initial process water over a concentration range of 0.01 N – 0.5 N (equivalent Cl^- concentrations). To evaluate the presence of simple organics on carbonization, experiments in which 500 – 5,000 mg/L acetic acid (AA) was added to the process water were conducted. A summary of the

initial process water composition used in these experiments is listed in **Table 4.1**. All experiments were conducted in duplicate.

Table 4.1 Process water compositions evaluated.

Type of Additive	Specific Additive	Concentrations Evaluated
DI Water	None	Control Experiment
Acid	HCl	0.0001, 0.001, 0.01 N
	H_2SO_4	0.0001, 0.001, 0.01 N
Base	NaOH	0.0001, 0.001, 0.01 N
	$Ca(OH)_2$	0.00001, 0.0001, 0.001 N
Salt	NaCl	0.01, 0.025, 0.5 N
	$CaCl_2$	0.01, 0.025, 0.5 N
Organic Carbon	Acetic Acid	500, 1,000, 5,000 mg/L

4.2.2 Analytical techniques

Samples from the solid (energy content, solid yields, and carbon and hydrogen content), liquid (total organic carbon (TOC), pH, chemical oxygen demand (COD), ^{1}H NMR), and gas phases (gas volume and composition) were taken to evaluate carbonization product evolution at different temperatures.

Collected gas samples were analyzed for carbon dioxide and other trace gases. Carbon dioxide was quantified using GC-MS (Agilent 7890 equipped with a mass spectrometer). Gas samples were routed through a GS-CarbonPlot column (30m long and 0.53 mm id, J&W Scientific). Initial oven temperature was 35^{o}C. After 5-min, the temperature was increased at a rate of 25^{o}C/min until a final temperature of 250^{o}C was achieved. Carbon dioxide standards were purchased from Matheson Tri-gas. Gas samples were also injected into a gas chromatograph (HP5890) equipped with a TCD and a Carboxen 1010 Plot column (30m x 0.53 mm i.d., Supelco) for determination of hydrogen concentration (carrier gas was argon). Initial oven temperature was held constant at 35^{o}C for 7.5 min and subsequently increased to 240^{o}C at a rate of 24^{o}C/min.

After separating the solids from the liquid (via vacuum filtration), the liquid samples were weighed and analyzed for typical water quality parameters, including: pH, total organic carbon (TOC), conductivity, and chemical oxygen demand (COD) (following methods outlined by Lu et al., 2013). Conductivity and pH were measured using electrodes (Thermo Scientific Orion). COD was measured using HACH reagents (HR + test kit, Loveland, CO). TOC was measured using a TOC analyzer (TOC-Vcsn, Shimadzu).

The composition of the organics in the liquid-phase was determined in the experiments containing the largest concentrations of each additive (Table 4.1) using ^{1}H NMR. Liquid samples (0.6 mL) were analyzed with on a Varian Mercury/VX 400 MHz spectrometer. All samples were spiked with 0.1 mL deuterium oxide (D, 99.9 %, Cambridge Isotope Laboratories, Inc.) to allow ^{2}H field frequency locking. TSP (2,2,3,3-d4-3-(trimethylsilyl)propionic acid sodium salt) was added as an internal standard to correct peak shifting. The vendor supplied WET1D pulse sequence was used to suppress the dominant resonance from H_2O. Spectra were collected with a 2.18 s acquisition time over a 16 ppm spectra width with 16 transients and a 10 s relaxation delay between each scan. Each NMR spectrum was subsequently deconvoluted using MestRenova software (MestreLab Research, Version 7.0).

All dried solids were weighed and solids recoveries calculated (mass of dry solids recovered divided by the mass of initial dry solids). Carbon and hydrogen contents of the solid samples from all times were measured with an elemental analyzer (Perkin Elmer 2400). The solids ash content was measured by placing a sample of char in a crucible in a muffle furnace at 500 ^{o}C for 2 hours and 750 ^{o}C for an additional 2 hours. The oxygen

content of the recovered solids was calculated by subtraction, assuming that the only constituents in the solids were carbon, hydrogen, ash and oxygen. Recovered solids energy contents were measured using a bomb calorimeter (C-200, IKA). Carbon mass balances were conducted by quantifying the carbon content in the gas (as carbon dioxide), liquid (as total organic carbon) and solid phases (solid-phase carbon content and solids recovery).

4.3 RESULTS AND DISCUSSION

4.3.1 Influence of initially acidic conditions on carbonization products

Results indicate that acidic process water influences carbonization product yields and composition. Cellulose dissolution appears to be accelerated in the presence of initially acidic process water (0.0001 N – 0.01 N HCl and H_2SO_4), as evidenced by lower solid recoveries at early reaction times (< 1.5 hrs, Figure 4.1a) than those measured in the control experiment (i.e., carbonizing in the presence of DI water). It should be noted that the initial lag in cellulose dissolution (0 – 0.5 hr) is likely due to the slow heating rate (and thus lower system temperature) associated with the reactor system (see Lu et al., 2013 and Figure 3.1). The observed acceleration of cellulose dissolution is correlated with acid concentration; as the acid concentration in the initial process water increases, the solids recovered at early reaction times decreases (Figure 4.1a). Analysis of variance (ANOVA) tests were conducted using SigmaPlot (version 11) to determine whether carbonization in the presence of initially acidic process water imparts a statistically significant ($p < 0.05$) impact on solid recoveries. Results from this analysis indicate that all solid recoveries obtained when carbonizing at all initial HCl concentrations evaluated

are statistically significant from those obtained in the control experiment at a reaction time of 1-hr (Table 4.2). Results from ANOVA tests also indicate that the differences between solid recoveries measured at all evaluated initial HCl concentrations are statistically significant from each other at a reaction time of 1-hr ($p<0.05$), confirming that HCl concentration also influences cellulose dissolution. ANOVA tests associated with solid recoveries obtained when carbonizing in the presence of the lowest H_2SO_4 concentration (0.0001 N) evaluated indicate that there is no statistically significant difference with the control (Table 4.2). However, carbonizing in the presence of the other H_2SO_4 concentrations evaluated does impart a statistically significant difference at a reaction time of 1-hr, similar to that observed when carbonizing in the presence of HCl. ANOVA test results also indicate that H_2SO_4 concentrations also influence solid recoveries ($p<0.05$).

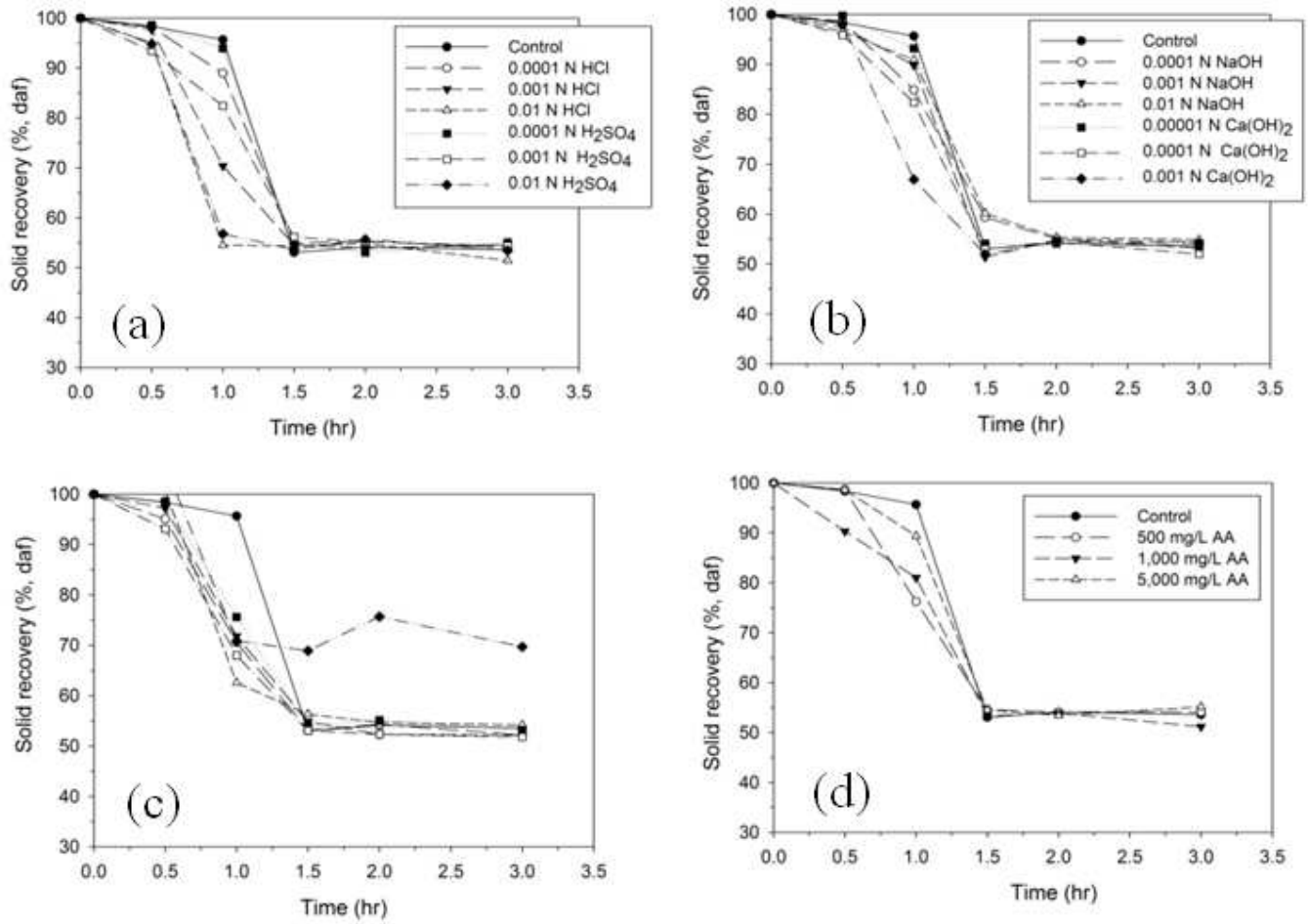

Figure 4.1 Solid recoveries over time for experiments in which the initial process water contains: (a) acids, (b) bases, (c) salts, and (d) organic carbon. Data points represent average values.

Table 4.2 Statistical significance compared with the control experiment when carbonizing in the presence of initially acid, basic, salt, and organic conditions.[a]

Additive	Conc. (N)	Solids Recovery					Carbon in Solids (%, ash-free)					% of initially present Carbon in liquid					% of initially present carbon in gas					Energy Content (J/g)					Solids Oxygen Content (%, ash-free)					Solids Hydrogen Content (%, ash-free)				
		0.5	1.0	1.5	2.0	3.0	0.5	1.0	1.5	2.0	3.0	0.5	1.0	1.5	2.0	3.0	0.5	1.0	1.5	2.0	3.0	0.5	1.0	1.5	2.0	3.0	0.5	1.0	1.5	2.0	3.0	0.5	1.0	1.5	2.0	3.0
HCl	0.0001		■						■				■	■					■		■				■				■								
	0.001		■						■				■	■					■	■	■								■								
	0.01		■					■	■				■	■				■	■	■	■			■				■	■				■			
H2SO4	0.0001								■		■		■								■		■		■						■					
	0.001		■								■		■						■		■				■						■					
	0.01		■						■		■		■	■				■	■	■	■		■	■	■	■				■		■					
NaOH	0.0001		■	■									■	■									■		■											
	0.001		■						■				■	■		■			■		■		■						■					■		
	0.01		■	■					■				■			■							■		■				■				■		
Ca(OH)2	0.00001								■				■	■		■			■				■		■				■			■		■		
	0.0001		■						■				■	■					■				■		■		■		■					■		
	0.001		■						■				■	■					■	■			■		■				■					■		
NaCl	0.01		■										■																							
	0.025		■										■	■				■			■				■											
	0.5		■					■					■	■				■	■				■		■				■		■					
CaCl2	0.01		■										■	■					■		■		■	■		■								■		
	0.025		■					■	■				■	■				■	■		■		■		■	■			■	■						
	0.5		■	■	■	■		■	■	■	■		■	■				■	■	■	■		■	■	■	■	■		■	■	■	■		■	■		
AA	0.008								■		■		■					■	■	■	■		■	■		■				■		■		■	■		■
	0.017		■						■				■	■					■	■	■									■			■	■	■		■
	0.083		■						■		■		■	■					■	■	■		■	■						■		■			■		■

[a]all shaded boxes represent a $p < 0.05$

The acid type also appears to influence cellulose dissolution. Lower solid recoveries are observed at early reaction times when carbonizing in the presence of HCl than when carbonizing in the presence of H_2SO_4 at equivalent H^+ concentrations. ANOVA test results confirm this phenomenon for one acid concentration. The solid recoveries obtained when carbonizing at an initial HCl and H_2SO_4 concentration of 0.001N are statistically significant from one another at a reaction time of 1 hour. This difference suggests that Cl^- and SO_4^{2-} may play a significant and different role in the cellulose dissolution and/or subsequent conversion process. The addition of Cl^- has been shown to disrupt the hydrogen bonding of cellulose, ultimately enhancing cellulose dissolution (e.g., Lynam et al., 2012; Remsing et al., 2006). These results also suggest that initial process water chemical properties (i.e., pH and ionic strength) may be insufficient in fully describing the influence of initial process water composition on carbonization. There was no statistically significant difference determined between the measured solid recoveries at 0.0001 N and 0.01 N HCl and H_2SO_4.

The ultimate solid recoveries (at a reaction time of 3 hours) when carbonizing in the presence of all concentrations of HCl and H_2SO_4 are similar to each other and the control experiment (Figure 4.1a). Although acid pretreatment of biomass has been shown to reduce ultimate solid recoveries, lower recoveries were likely not observed in these experiments because the cellulose contains little insoluble material (low ash content). Lynam et al. (2011) observed a decline in solid yields when carbonizing in the presence of acid, which was attributed to the dissolution of cellulose. It is likely that as biomass complexity increases the influence of initial acid concentration on ultimate solid recoveries may change. ANOVA test results confirm the lack of statistically significant

differences between the solid recoveries obtained at a reaction time of 3 hrs ($p > 0.05$, seeTable 4.2). These results suggest the influence of HCl and H_2SO_4 addition on solid recoveries may be kinetic in nature.

The influence of initial acid addition on the carbon content of the recovered solids (Figure 4.1a), as well as system carbon distribution (see Figure 4.2 – 4.4), was also evaluated. Results from ANOVA tests indicate that differences between the ash-free carbon contents of the recovered solids obtained when carbonizing in the presence of all evaluated HCl concentrations and the control experiment are statistically significant from one another at a reaction of 1.5 hours (Table 4.2). Measured differences between the final recovered solids carbon contents (at a reaction time of 3 hr), however, are not statistically significant. These results suggest, similar to that associated with the solid recoveries, the influence of HCl addition is kinetic in nature. Conclusions from ANOVA tests associated with the carbon content of recovered solids from experiments in which H_2SO_4 was added, however, differ. The differences between the solids carbon contents measured from the control experiment and those from experiments in which H_2SO_4 were added are all statistically significant from one another at a reaction time of 3 hr (Table 4.2). However, the only other solid carbon contents that are statistically significant from that obtained in the control experiment are those measured after carbonizing for 1.5 hr in the presence of 0.0001 N and 0.01N H_2SO_4. These results suggest the inclusion of H_2SO_4 in the initial process water does influence solids carbon content, but the influence may not be explained by reaction kinetics alone.

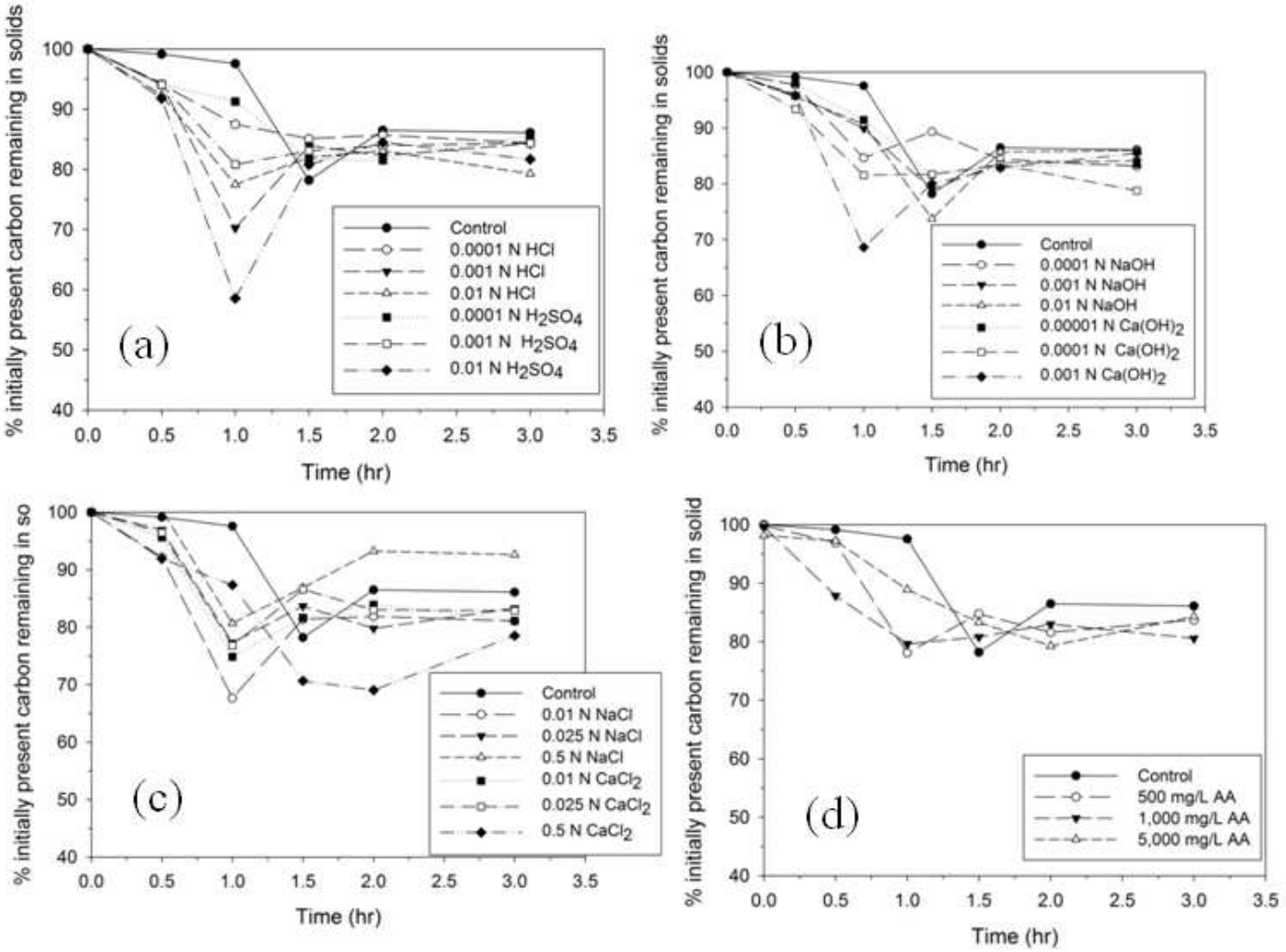

Figure 4.2 Percentage of initially present carbon remaining in the solid-phase over time when carbonizing in the presence of: (a) acids, (b) bases, (c) salts, and (d) organic carbon.

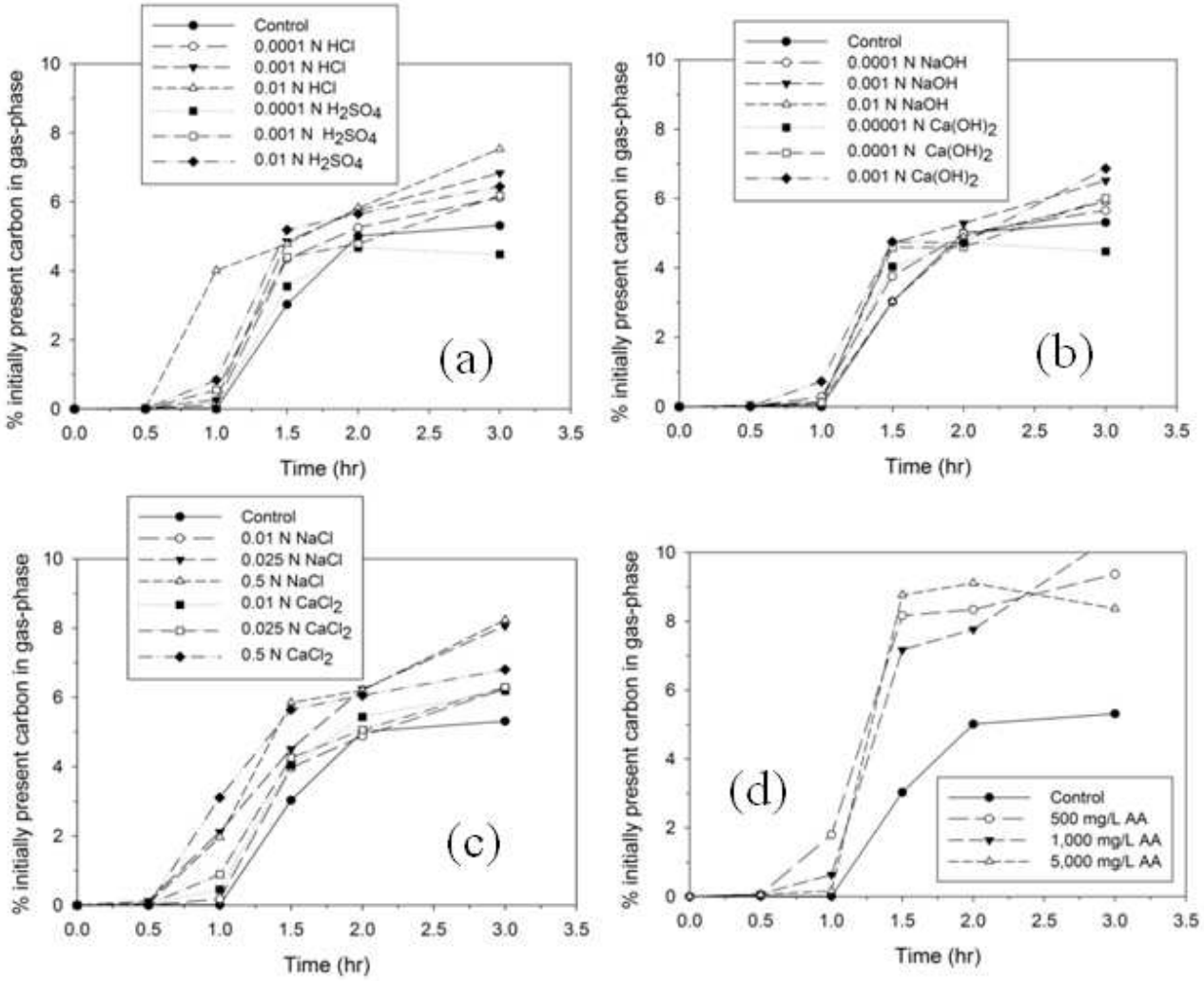

Figure 4.3 Percentage of initially present carbon remaining in the gas-phase over time when carbonizing in the presence of: (a) acids, (b) bases, (c) salts, and (d) organic carbon.

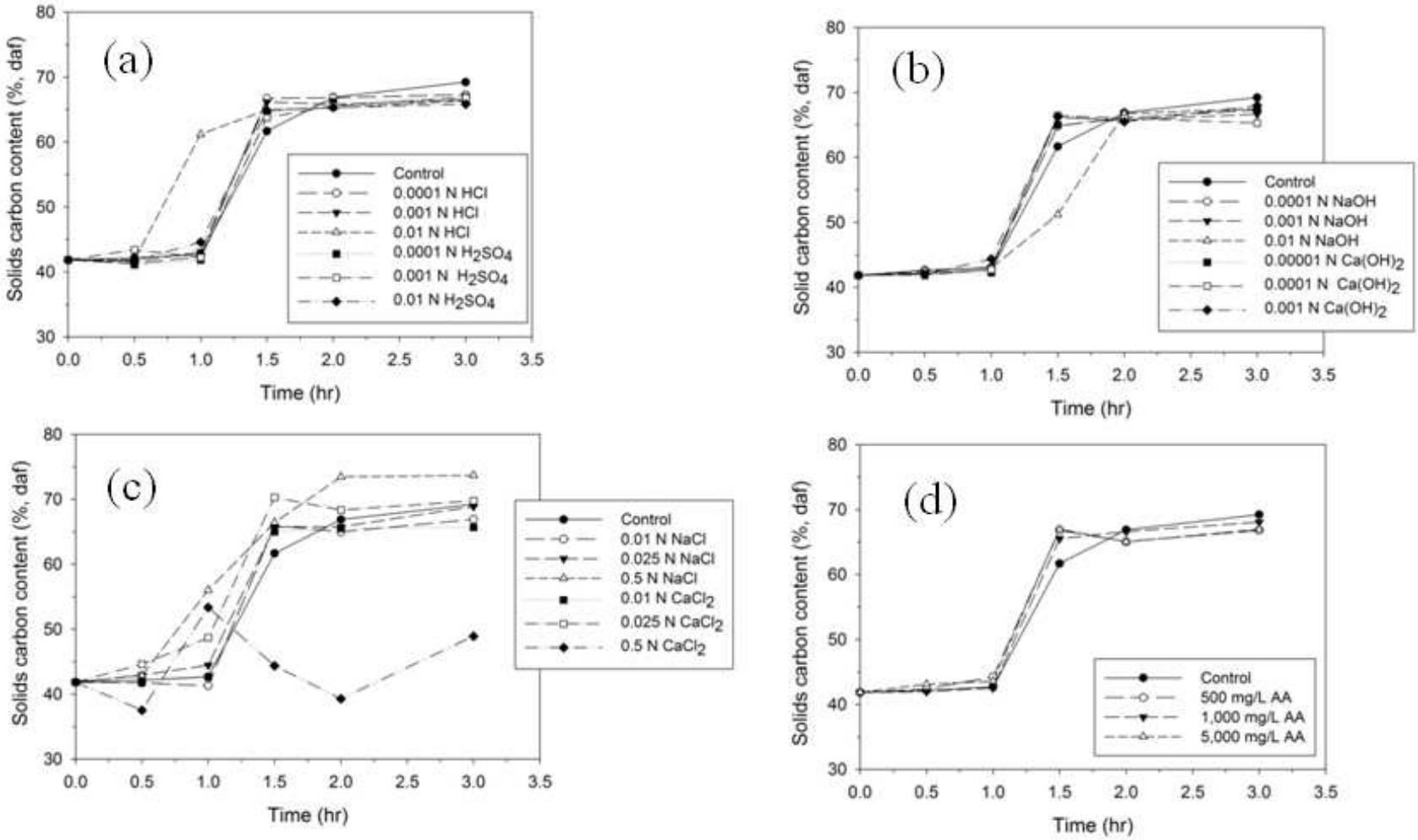

Figure 4.4 Solid carbon content (%, daf) over time for experiments in which the initial process water contains: (a) acids, (b) bases, (c) salts, and (d) organic carbon. Data points represent average values.

A statistical comparison between the percentage of initially present carbon in the gas-phase (Figure 4.3) measured in the control experiment and the experiments conducted in the presence of initially acidic conditions was conducted and indicate that, at a reaction time of 3-hr, the percentages of initially present carbon in the gas-phase is statistically significant from the control experiments (Table 4.2). Tests were also conducted evaluating the statistical significance of the liquid-phase carbon data (Figure 4.4a and Table 4.2). Although the values are noticeably different at a reaction time of 3 hours (Figure 4.4a), there is not a statistically significant difference between these values (Table 4.2).

ANOVA tests confirm that solids energy contents at a reaction time of 3 hours are not influenced by carbonizing in acidic conditions (Table 4.2 and Figure 4.5a). Inspection of ANOVA test results associated with the time-series energy data indicate that when carbonizing in the presence of HCl over the 3-hr reaction period, only 13% of the energy values are statistically different than the control (Table 4.2). However, when carbonizing in the presence of H_2SO_4, 47% of the energy values differ from the control (Table 4.2). These results suggest carbonization in the presence of H_2SO_4 imparts a greater influence on recovered solids energy content than HCl.

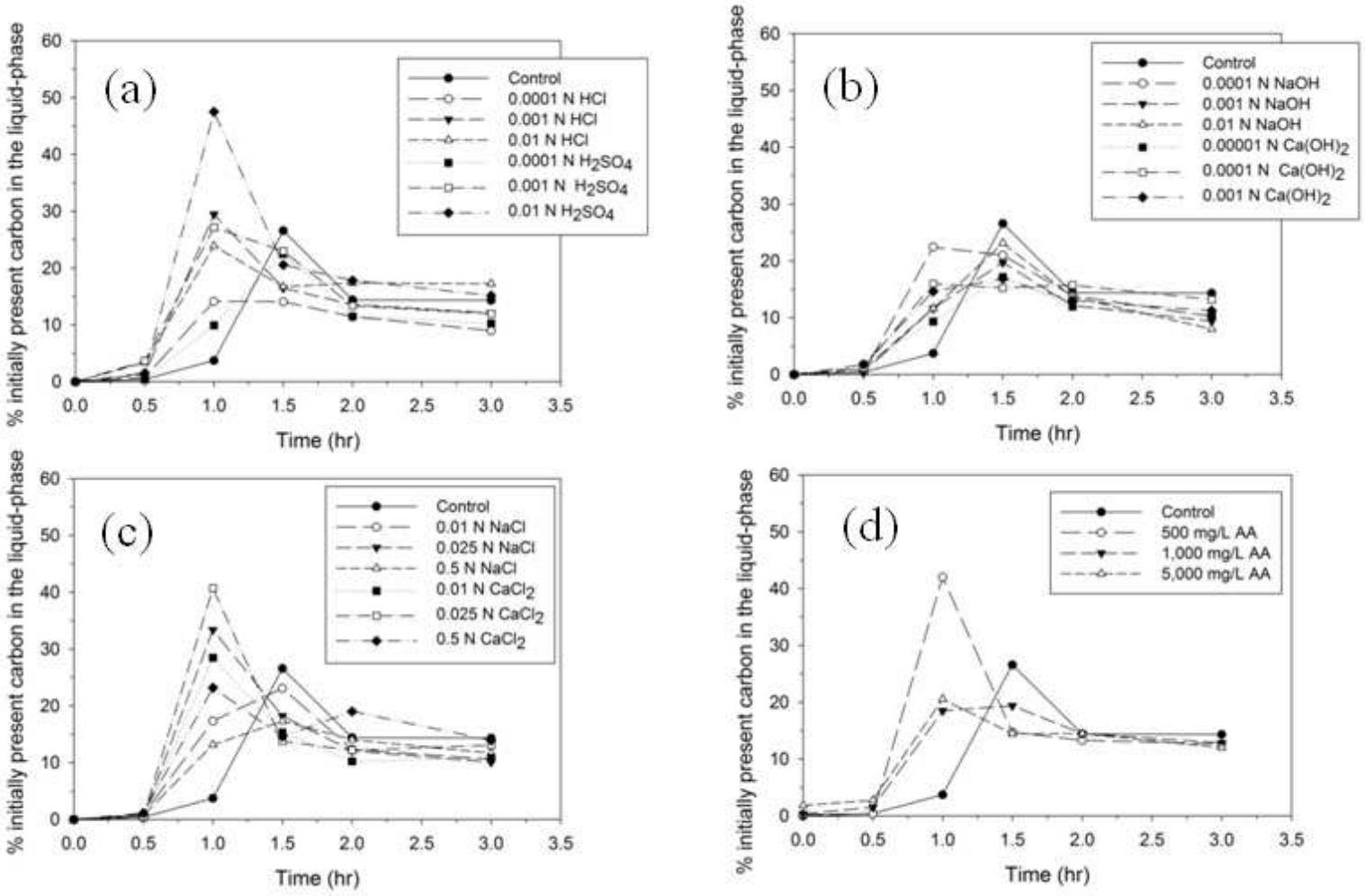

Figure 4.5 Percentage of initially present carbon in the liquid-phase over time for experiments in which the initial process water contains: (a) acids, (b) bases, (c) salts, and (d) organic carbon. Data points represent average values.

Evidence of liquid-phase reaction acceleration as a result of carbonizing in acidic conditions is inherent when comparing the final process water composition with that from the control experiment. Figure 4.4a depicts the fraction of initially present carbon found in the liquid-phase over time for all acids/acid concentration evaluated. In each experiment, including the control, the fraction of liquid-phase carbon increases and then decreases. The reaction time associated with the maximum liquid-phase carbon content occurs earlier (1 hour) when carbonizing in acidic conditions for all acid concentration, except for 0.0001 H_2SO_4, than when carbonizing in the presence of DI (1.5 hours). These differences are highlighted by results from ANOVA tests (Table 4.2). ^{1}H NMR was used to identify and determine the relative concentrations of organics in the liquid-phase from the 0.01 N HCl and 0.01 N H_2SO_4 concentrations (Figure 4.7 and Figure 4.8). Results from this analysis indicate that pathway of cellulose conversion in the presence of acidic conditions is similar to that reported in the literature for conversion in DI, but is accelerated. Literature reported mechanisms associated with cellulose carbonization in DI water, including production and conversion of liquid-phase intermediates, are detailed in **Error! Reference source not found.**Figure 4.9. Glucose (a hydrolysis product of cellulose) and/or its decomposition products (e.g., HMF, furfural) are observed after carbonizing for 1 hour and are no longer detected at 1.5 hours when carbonizing in acidic conditions. No glucose was detected in the experiment containing 0.01 N HCl, suggesting the liquid-phase reactions, particularly the decomposition of glucose, is faster than that associated with the experiment containing 0.01 H_2SO_4 and the control. In addition, the formation of organic acids (e.g., acetic acid, levulinic acid, and formic acid, Figure 4.7 and Figure 4.8 are detected earlier when carbonizing in the presence of acidic conditions.

The trend of formic acid production/consumption differs from that observed in the control. In the presence of DI water, the formic acid concentration increases as carbonization proceeds. However, when carbonizing in initially acidic conditions, the formic acid concentration decreases. It is likely that greater amounts of formic acid are being converted to gaseous carbon dioxide. Increases in carbon dioxide have been observed in these experiments at a reaction time of 3 hours (Figure 4.10), supporting this hypothesis.

The solids atomic H/C and O/C ratios were calculated using the elemental composition data and plotted on a Van Krevelen diagram (Figure 4.11a). Van Krevelen diagrams allow for delineation of reaction pathways. Straight lines can be drawn to represent the dehydration and decarboxylation reaction pathways. Atomic ratio data at each reaction time for each acid concentration evaluated were plotted. Initially, the H/C ratio increases due to increasing solids hydrogen content (Figure 4.12) during the first 60 minutes, suggesting that hydrogen enrichment occurs. Such enrichment has not been previously observed with solids recovered from the HTC process.

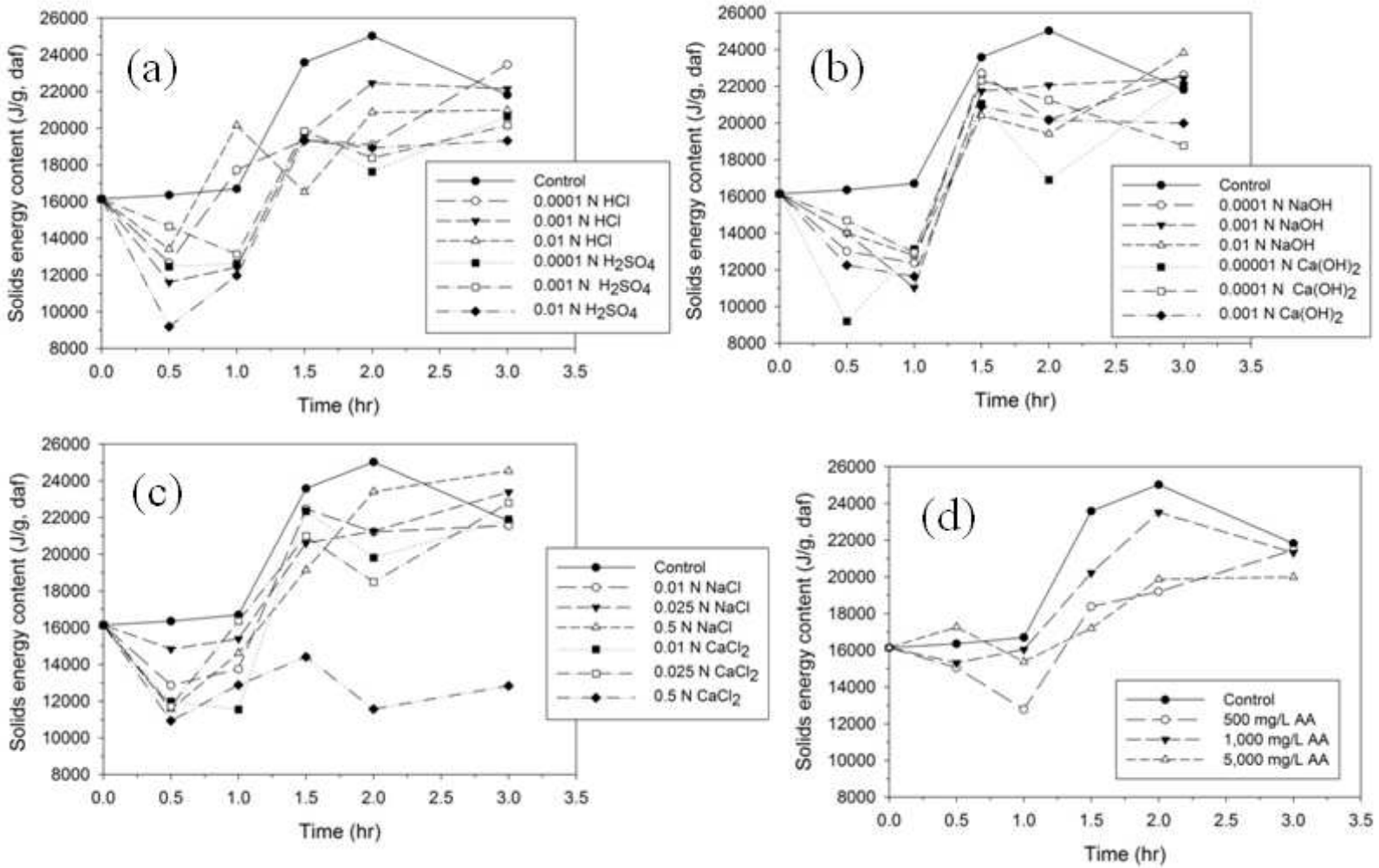

Figure 4.6 Solids energy content (dry, ash-free) over time for experiments in which the initial process water contains: (a) acids, (b) bases, (c) salts, and (d) organic carbon. Data points represent average values.

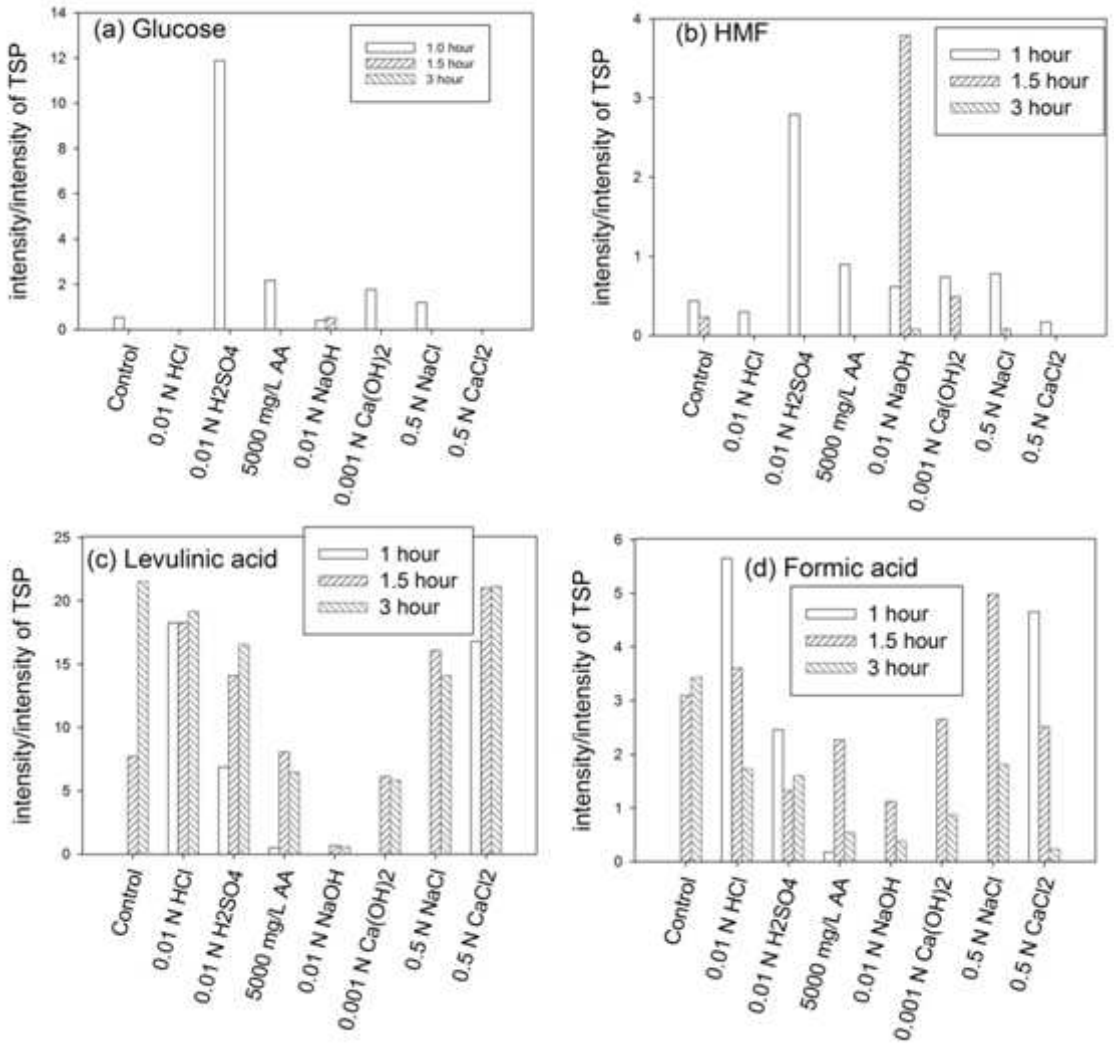

Figure 4.7 Constituents identified in the liquid-phase: (a) glucose, (b) HMF, (c) levulinic acid, and (d) formic acid

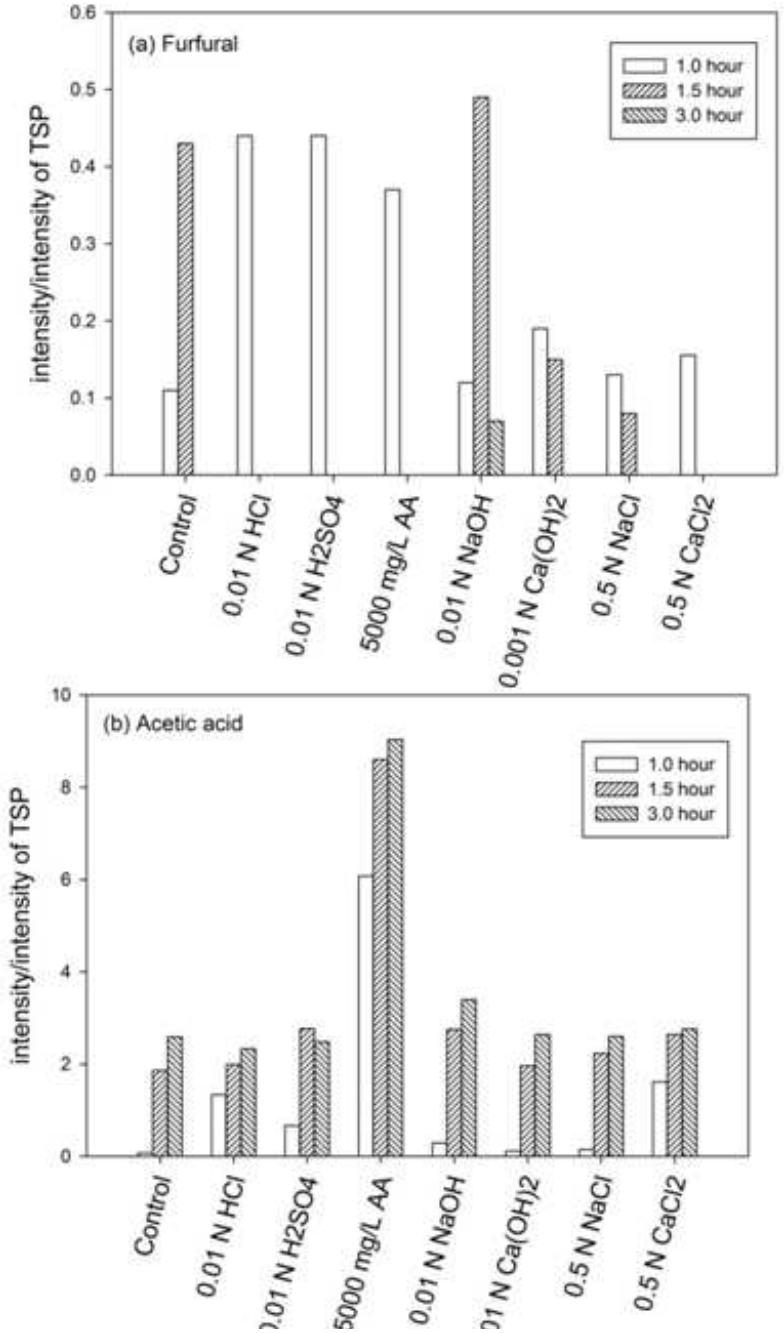

Figure 4.8 Furfural (a) and acetic acid (b) detected in the liquid-phase.

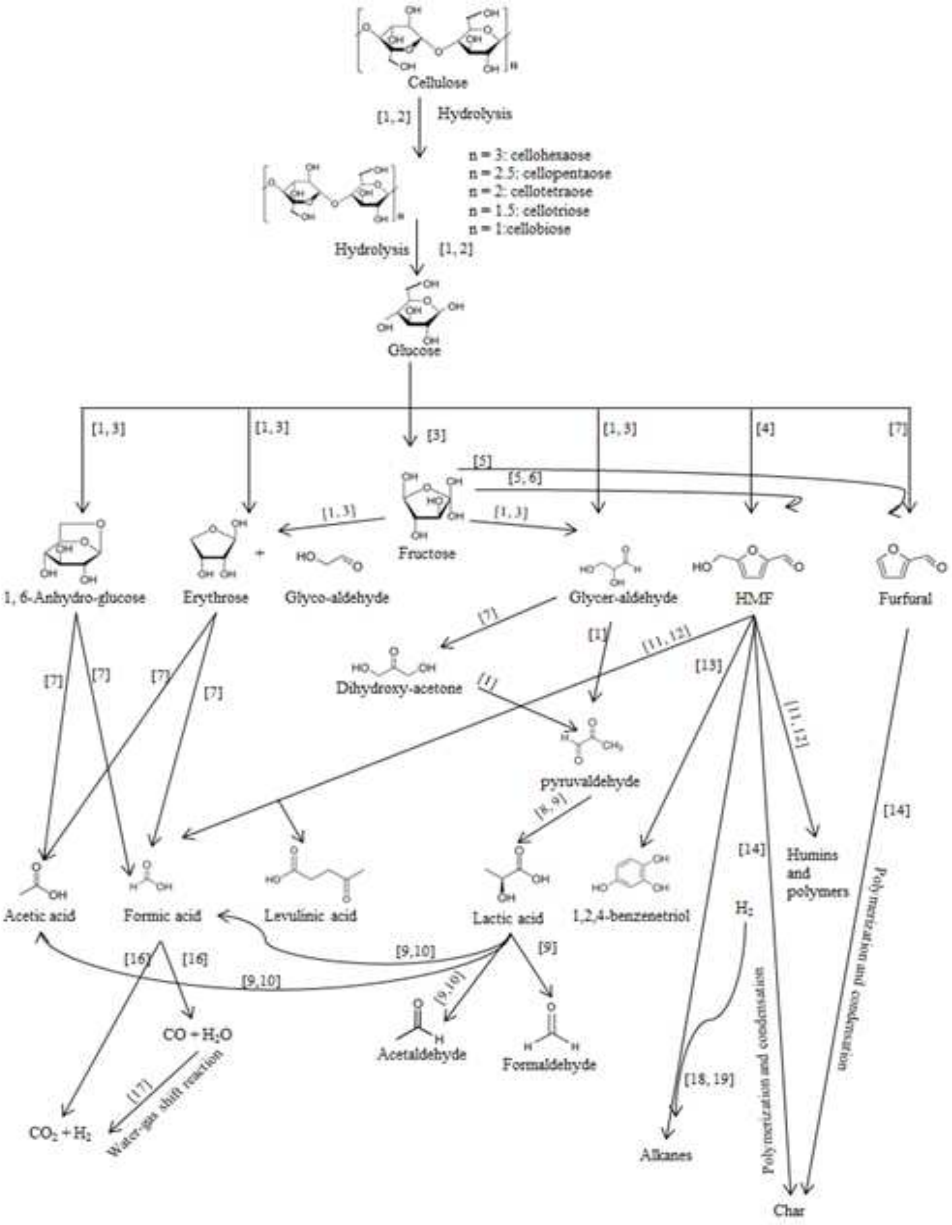

Figure 4.9 Literature reported pathways of cellulose carbonization. The numbers refer to references.

References:

1: (Sasaki, Kabyemela et al. 1998) 2: (Sasaki, Fang et al. 2000) 3: (Kabyemela, Adschiri et al. 1997) 4: (Scallet and Gardner 1945) 5: (Asghari and Yoshida 2006) 6: (Yao, Shin et al. 2007) 7: (Kabyemela, Adschiri et al. 1999) 8: (Antal Jr, Mok et al. 1990) 9: (Srokol, Bouche et al. 2004) 10: (Li, Portela et al. 1999) 11: (Horvat, Klaic et al. 1985) 12: (Patil a nd Lund 2011) 13: (Chuntanapum and Matsumura 2009) 14: (Falco, Caballero et al. 2012) 15: (http://online.sfsu.edu/tripp/SFSU/Chem335/Entries/2011/4/15_Presentations_files/ Dihydroxyacetone.pdf) 16: (Enthaler, von Langermann, et al. 2010) 17: (Newsome 1980) 18: (Huber and Chheda et al. 2005) 19: (Yin, Mehrotra et al. 2012).

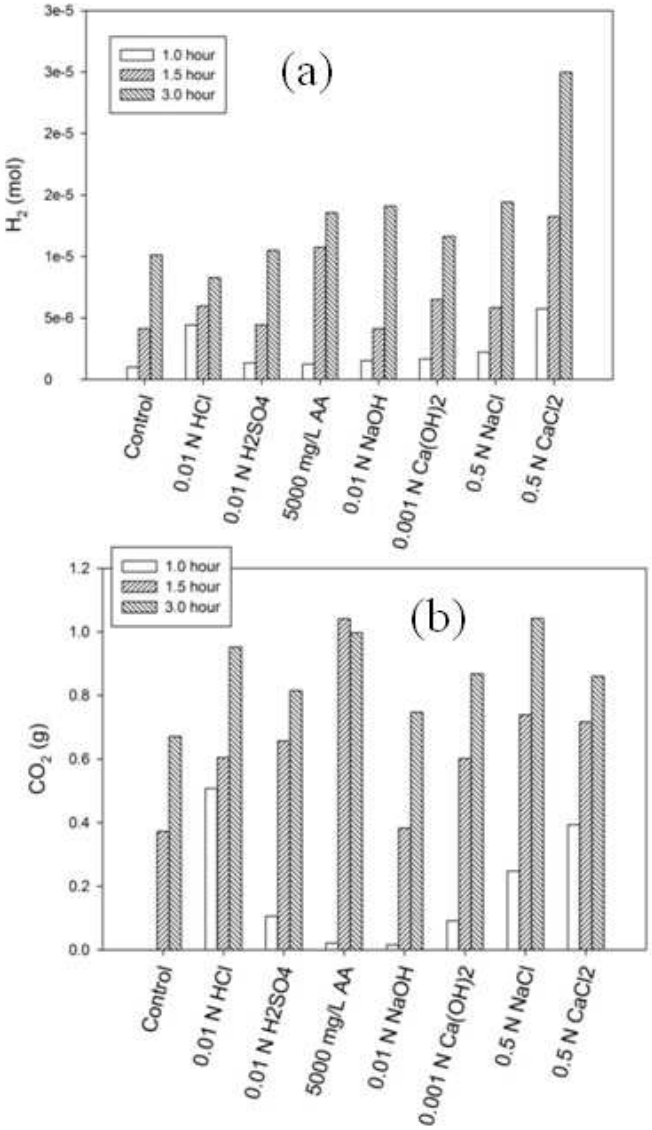

Figure 4.10 Gas-phase hydrogen (a) and carbon dioxide (b) concentrations over time

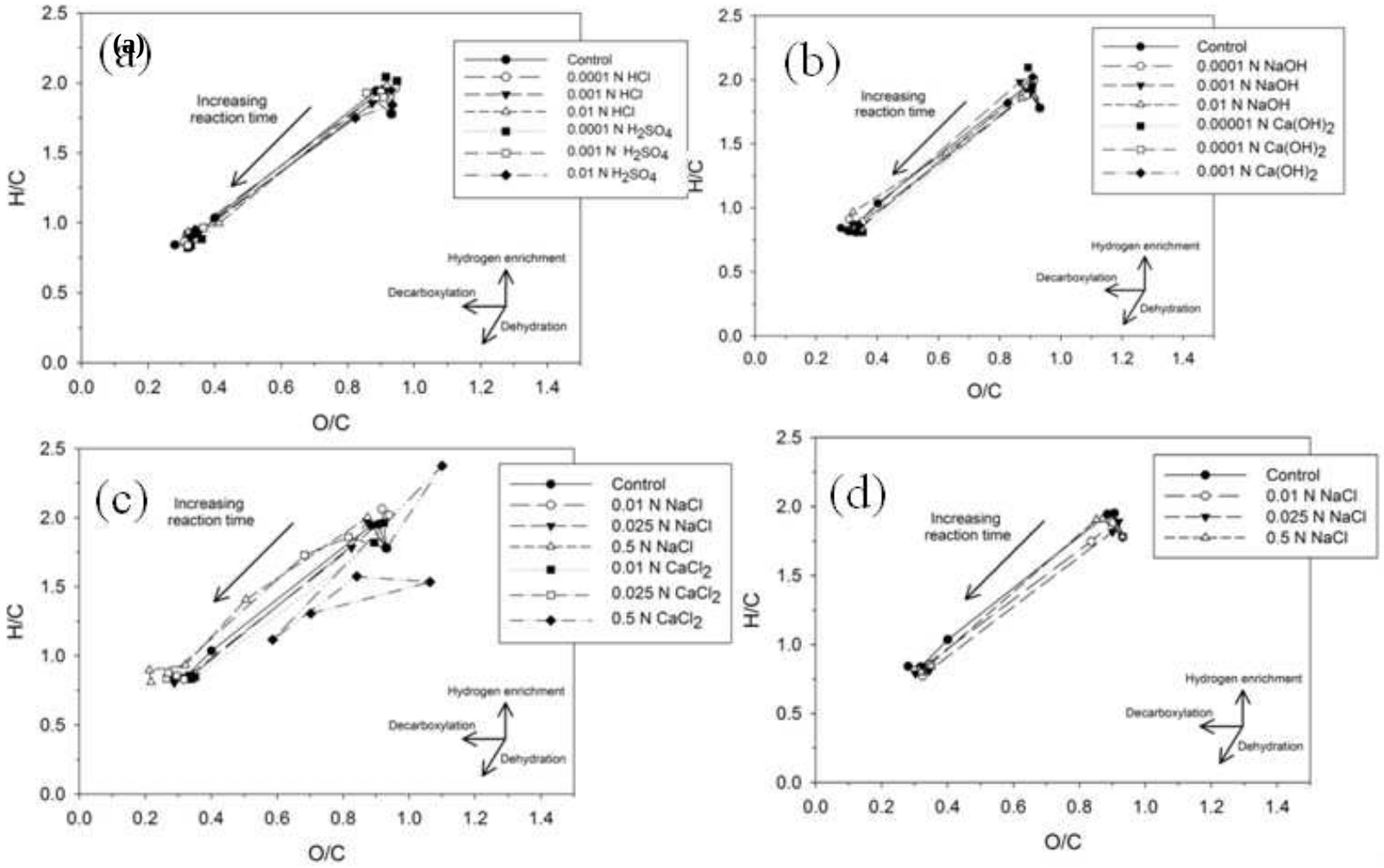

Figure 4.11 Van Krevelen diagrams containing atomic ratio data associated with all reaction times for experiments in which the initial process water contains: (a) acids, (b) bases, (c) salts, and (d) organic carbon.

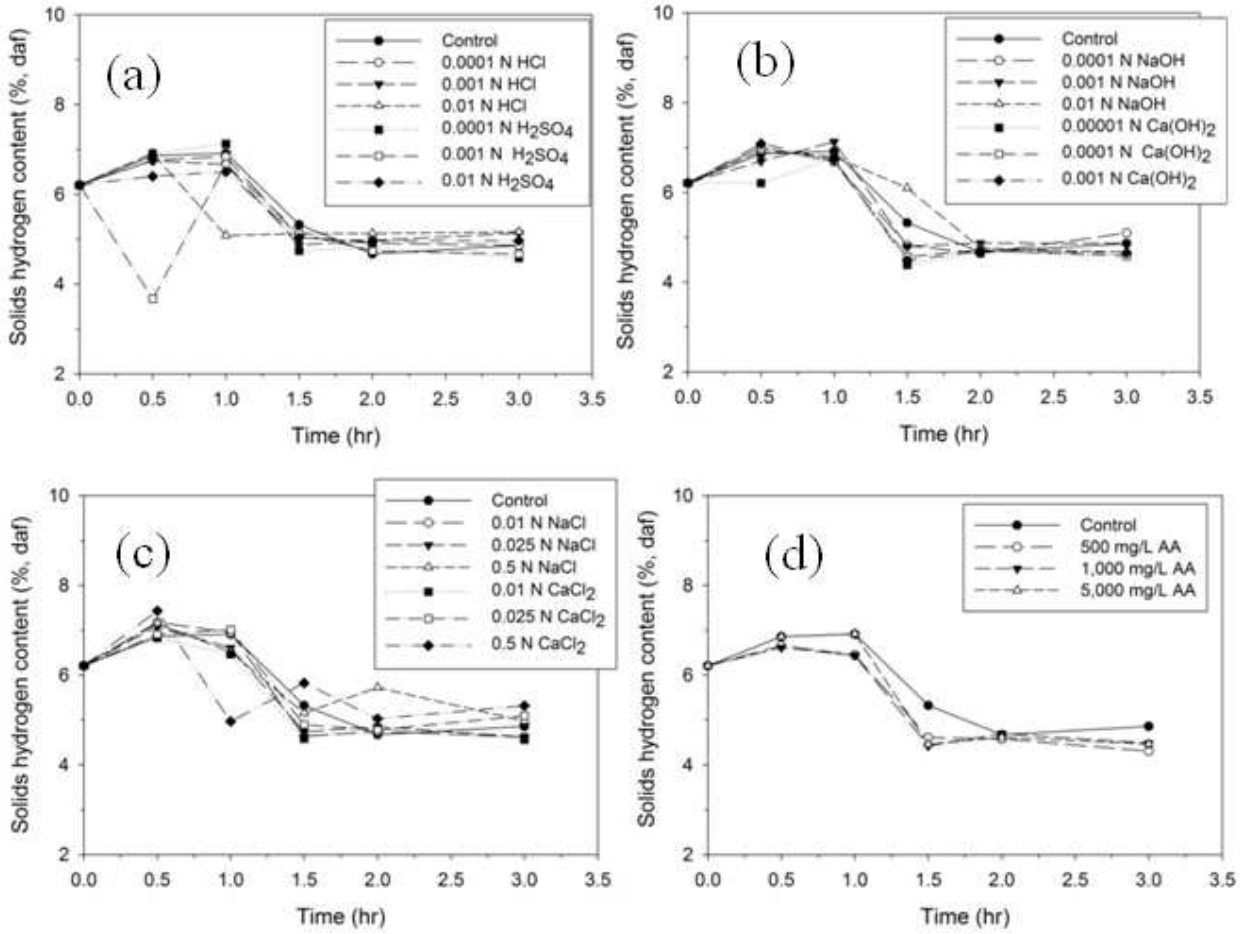

Figure 4.12 Solids hydrogen content when carbonizing in the presence of: (a) acids, (b) bases, (c) salts, and (d) organic carbon.

Data also indicate that as cellulose carbonization proceeds in the presence of acids, dehydration remains a predominant carbonization mechanism. Similar to that reported by Lu et al. (2013) the atomic ratios change significantly during the period of greatest cellulose conversion (from 0.5 to 1.5 hours), with oxygen contents of the solids decreasing significantly (Figure 4.13). Decarboxylation also occurs under acidic conditions, as evidenced by the production of carbon dioxide (Figure 4.10). The addition of 0.01 N H_2SO_4 appears to promote more decarboxylation than the 0.01 N HCl, as evidenced by the gas-phase carbon measurements. The carbon content of the gas-phases when carbonizing in the presence of equivalent initial concentrations of HCl and H_2SO_4 are statistically significant from one another, suggesting changes in initial acid type influences decarboxylation. ANOVA results also indicate there is no statistically significant difference between the H/C and O/C ratios obtained at a reaction time of 3-hr from all experiments conducted in initially acidic conditions and those obtained from the control experiment. These results also suggest the influence of Cl^- and SO_4^{2-} on carbonization kinetics may differ, but mechanisms remain similar.

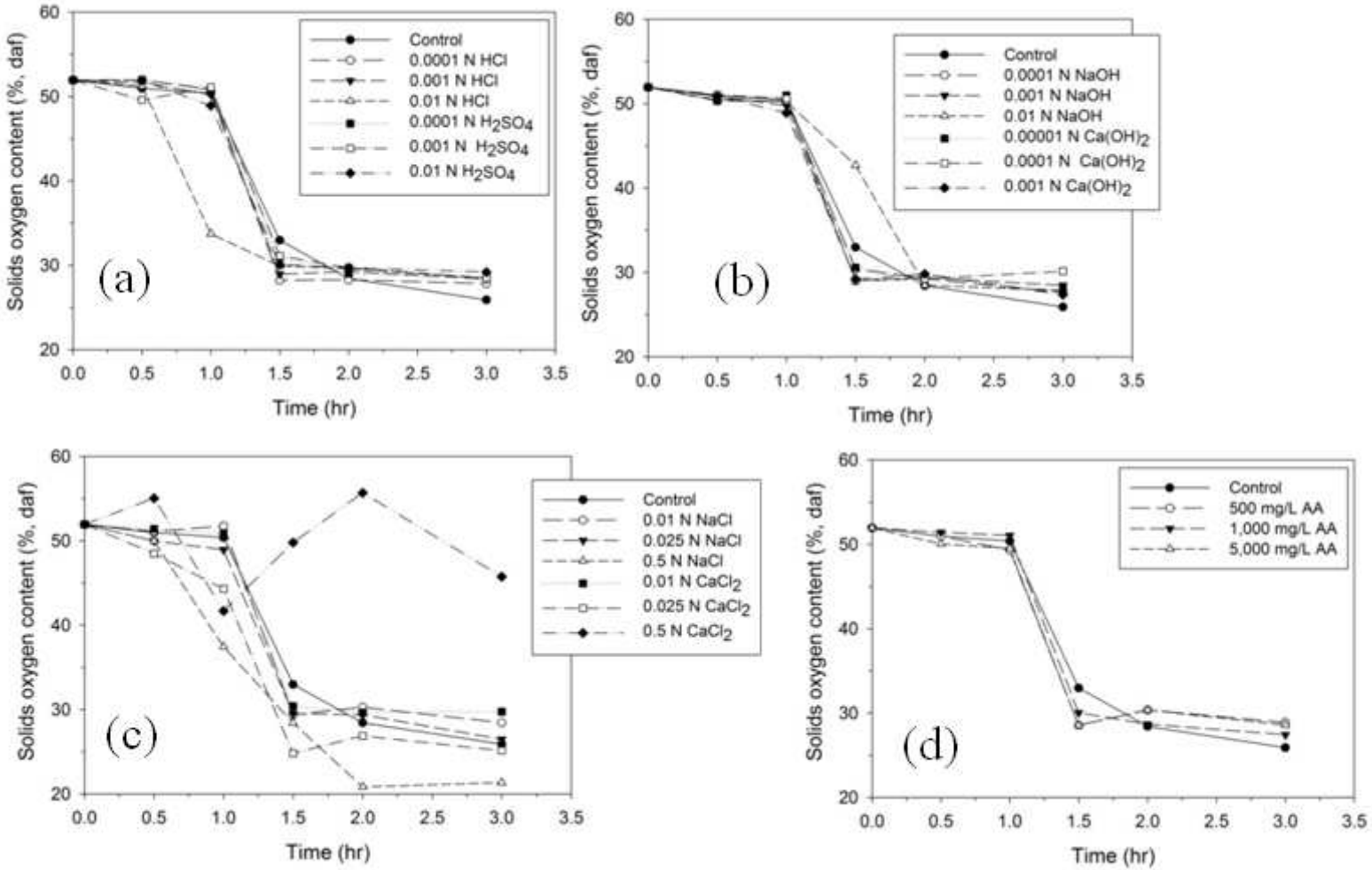

Figure 4.13 Solids oxygen content when carbonizing in the presence of: (a) acids, (b) bases, (c) salts, and (d) organic carbon

4.3.2 Influence of initially basic conditions on carbonization products

Carbonizing in initially basic conditions (0.001 – 0.01 N NaOH and 0.0001 – 0.001 N $Ca(OH)_2$) also influences initial cellulose dissolution (Figure 4.1b). $Ca(OH)_2$ has an effect similar to that observed when carbonizing in the presence of acids; initial cellulose dissolution increases as base concentration increases. ANOVA test results confirm there is a statistically significant influence when carbonizing in the presence of $Ca(OH)_2$. ANOVA results indicate that recovered solid yields are different from the control experiment when carbonizing in the presence of 0.0001 and 0.001 N $Ca(OH)_2$ ($p < 0.05$) at a reaction time of 1-hr (Table 4.2); however, there was no observed statistical significance between solid recoveries obtained from the control experiment and when carbonizing in the presence of 0.00001 N $Ca(OH)_2$ (Table 4.2).

Carbonizing in the presence of NaOH also influences initial cellulose dissolution (Figure 4.1b). At a reaction time of 1 hr, cellulose dissolution decreases as the NaOH concentration increases, while the solid recovery obtained when carbonizing in the presence of the largest NaOH concentration (0.01 N) is also similar to the control. Results from ANOVA tests confirm that at a reaction time of 1 hr, there is a statistically significant difference in recovered solids yields when carbonizing in the presence of all evaluated concentrations of NaOH (Table 4.2). These results also suggest the influence of initial base addition on carbonization is kinetic in nature.

The decreased initial cellulose dissolution at 0.01 N NaOH fits with previously reported observations. The degree of cellulose swelling has been shown to decrease with increasing alkali concentration (Krassig, 1993). These results indicate that Na^+ and Ca^{2+} influence cellulose dissolution/decomposition differently. Similar to that reported when

investigating the influence of acidic process water on cellulose carbonization, these results indicate that solution chemical properties (i.e., pH and ionic strength) of the process water may be insufficient to fully describe the time-dependent influence of process water composition on carbonization. Ultimate yields (at a reaction time of 3 hours) for all bases and base concentrations are similar to each other and that obtained from the control experiment (Figure 4.1b); the differences at this reaction time were not deemed statistically significant (Table 4.2), also suggesting base addition influences carbonization kinetics, not carbonization extent.

Solids carbon content and system carbon distribution are also influenced when carbonizing in the presence of basic process water. Recovered solids carbon content (%, ash-free) following carbonization in the presence of 0.001 and 0.01 N NaOH are statistically significant when compared with those obtained from the control experiment at a reaction time of 1.5 hr (Table 4.2). The solids carbon contents (%, ash-free) obtained from the experiment with the lowest concentration of NaOH evaluated (0.0001 N) is not statistically significant from the control experiment, suggesting that larger concentrations of bases are required to impart a statistically significant impact on carbon content. Reoveries obtained at a reaction time of 3 hours are not statistically significant from the control experiment (Table 4.2).

The solids carbon contents obtained when carbonizing in the presence of all $Ca(OH)_2$ concentrations were statistically significant when compared with the control at a reaction time of 1.5 hr. Results from ANOVA tests also indicate that concentration of $Ca(OH)_2$ did not statistically influence solids carbon content (all comparisons had $p > 0.05$). The ultimate solids carbon contents (at a reaction time of 3 hr) were not deemed

statistically significant form one another, suggesting the influence of carbonizing under basic conditions imparts a kinetic influence on solids carbon content (Table 4.2).

Carbonization under initially basic conditions influences the percentage of initially present carbon transferred to the liquid-phase (Figure 4.4b and Table 4.2), ultimately resulting in a lower concentration of carbon in the liquid-phase at a reaction time of 3 hr. Results from ANOVA tests confirm that base addition influences the transfer of carbon to the liquid-phase. At reaction times of 1 and 1.5 hr, the percentage of initially present carbon transferred to the liquid-phase under basic conditions (both NaOH and $Ca(OH)_2$) is statistically significant from that obtained in the control experiment (Table 4.2). After 3 hours, less of the initially present carbon is dissolved in the liquid than that observed in the control (e.g., carbonizing in the presence of DI water), confirmed by ANOVA test results. The percentage of initially present carbon transferred to the liquid-phase when carbonizing under 0.00001 N $Ca(OH)_2$ and 0.001 N and 0.01 N NaOH are statistically significant when compared with the control experiment (Table 4.2).

The influence of base addition on recovered solids energy content is variable (Table 4.2). At a reaction time of 3 hrs, no statistically significant differences in solids energy content were observed between that resulting from the control experiment and from the experiments containing all bases and base concentrations. When comparing the statistical significance of solids energy contents over time, approximately 33% of the solids energy data obtained when carbonizing in the presence of NaOH are statistically different from the control (Table 4.2). Carbonizing in the presence of $Ca(OH)_2$ imparts a greater influence on solids energy content. Approximately 53% of the solids energy data

are statistically significant from the control when carbonizing in the presence of $Ca(OH)_2$. Different from that observed with NaOH, changes in $Ca(OH)_2$ concentration do impart a statistically significant impact during carbonization.

Carbonization in the presence of 0.01 N NaOH appears to have slowed the liquid-phase carbonization reactions (Figure 4.7 and Figure 4.8). Glucose is still observed at a reaction time of 1.5 hours. In addition, the presence of 0.01 N NaOH appears to influence the decomposition pathway of HMF (a major decomposition product of glucose). High levels of HMF are observed at 1.5 hours, with a significantly lower amount detected at 3 hours. This accumulation may be due slower kinetics of the liquid-phase reactions. HMF has been reported to be converted to levulinic and/or formic acids, which has been shown to be more favorable under acidic conditions (Shen and Wyman, 2012; Weingarten et al., 2012). The yields of levulinic acid are significantly lower when carbonizing in the presence of 0.01 N NaOH. The lower yield of levulinic acid (and decreasing trend of formic acid) suggests that the pathway of HMF conversion differs from that observed in DI and acidic process water. It is possible a greater proportion of the HMF is integrated within the recovered solids when carbonizing in the presence of 0.01 N NaOH. In comparison, when carbonizing in the presence of 0.001 N $Ca(OH)_2$ there is appreciable glucose and HMF detected at 1.5 hours (Figure 4.7 4.6). However, these compounds are not detected at a reaction time of 3 hours, suggesting the liquid-phase reactions are faster with 0.001 N $Ca(OH)_2$ than 0.01 N NaOH.

Base addition does not appear to influence carbonization mechanisms. Atomic ratios of H/C and O/C were used in conjunction with van Krevelen diagrams (as discussed previously) to evaluate carbonization mechanisms (Figure 4.11b). Similar to

that observed in the when carbonizing under acidic conditions, hydrogen enrichment was observed at all base concentrations (Figure 4.12). The predominant carbonization mechanism remains dehydration.

4.3.3 Influence of initial salt process water on carbonization products

Salt addition to the initial process water also accelerates cellulose dissolution, as illustrated in Figure 4.1c. NaCl and $CaCl_2$ (at equivalent Cl^- concentrations) influence solid recoveries differently. Changes in NaCl concentration impact cellulose dissolution, but not ultimate solid yields, while changes in $CaCl_2$ concentration influence both cellulose dissolution and ultimate solid yields. Results from ANOVA tests confirm these differences. When carbonizing in the presence of NaCl, all solids recoveries obtained at a reaction time of 1 hr are only statistically significant from that obtained in control experiment at the same time (Table 4.2). The presence of $CaCl_2$ imparts a more significant impact on solid recoveries. At $CaCl_2$ concentrations of 0.01 and 0.025 N, solid recoveries are only statistically significant when compared to the control experiment at a reaction time of 1 hr. When carbonizing at 0.5 N, however, solid recoveries are statistically significant from those obtained during the control experiment at all reaction times except 0.5 hr. The solid recoveries obtained when carbonizing at 0.5 N $CaCl_2$ are also statistically significant when compared to all other $CaCl_2$ concentrations evaluated.

The acceleration of cellulose carbonization in the presence of salts has been observed by others. Lynam et al. (2012) also report that the addition of Ca^{2+} containing species accelerate carbonization. Ming et al. (2010) report that sodium slats drastically accelerate carbonization, specifically the inter/intra-dehydration, aromatization, and cross polymerization processes. The largest concentration of $CaCl_2$ (0.5 N) imparted the

greatest influence on solid recoveries (Figure 4.1c), resulting in the largest solid yields measured (ash-free). This result was unexpected. Ramsurn et al. (2011) gasified biochar in the presence of $Ca(OH)_2$ and report that the addition of Ca^{2+} may passivate the surface of the material, possibly rendering components of the feedstock insoluble. It is possible that a similar effect was observed when adding of 0.5 N $CaCl_2$. This was not observed when carbonizing in the presence of lower $CaCl_2$ concentrations. These differences indicate that solid yields are influenced by salt type/composition. Changes due to Na^+ and Ca^{2+} were also observed when carbonizing in the presence of NaOH and $Ca(OH)_2$.

The carbon content (% C, daf) of the recovered solids following carbonization in the presence of NaCl appears to uninfluenced (Figure 4.4c and Table 4.2). Carbonizing with $CaCl_2$ does influence solids carbon content. Solids recovered following carbonization in the presence of $CaCl_2$ always have lower carbon contents than that obtained when carbonizing in the presence of DI water (Figure 4.4c). The solids carbon contents obtained when carbonizing in the lowest concentration of $CaCl_2$ were not statistically significant from the control experiment (Table 4.2). However, statistical significance was observed when carbonizing in the presence of 0.025 and 0.5N $CaCl_2$; carbonization in the presence of 0.5N $CaCl_2$ results in statistically significant solids recoveries from a reaction time of 1 to 3 hr. These results suggest that salt addition influences carbonization kinetics and that addition of high concentrations of $CaCl_2$ influences carbonization extent/mechanisms. The carbon content of the solids generated in the presence of 0.5 N $CaCl_2$ is significantly lower than those generated in the presence of DI water or any of the other salts, acids, and bases evaluated. The largest concentration

of Ca^{2+} imparts a negative impact on solids carbon content (Figure 4.4), while the largest concentration of Na^{+} imparts a more positive impact.

The influence of salt addition on recovered solids energy content is variable (Figure 4.5c). Based on experimental data and results from ANOVA tests, the final solids energy contents are not statistically significant from one another at a reaction time of 3 hours, except when carbonizing with the largest $CaCl_2$ concentration. These results suggest that changes in NaCl concentration do not influence recovered solids energy contents. When carbonizing in the presence of 0.5 N $CaCl_2$, the solids energy are statistically significant from all data obtained from the control experiment at all reaction times (Table 4.2). The influence of carbonizing in the presence of 0.5N $CaCl_2$ is more significant that obtained when carbonizing in the presence of 0.5 N NaCl. The influence of these differences in solids energy content influence the system energetic retention efficiency. An energetic retention efficiency of 82% is associated with the solids recovered from the experiment containing 0.5 N NaCl; at 0.5 N $CaCl_2$, the energetic retention efficiency is only 55% (Figure 4.14). The largest difference between the solids generated in the presence of $CaCl_2$ and NaCl is the change in oxygen content (Figure 4.13), which generally has a significant impact on solids energy content. As the NaCl concentration in the initial process water increases, the oxygen content of the recovered solids at a reaction time of 3 hours decreases. The opposite trend exists when carbonizing in the presence of $CaCl_2$. The reduction in energy content with the addition of $CaCl_2$ differs from that reported by Lynam et al. (2012). It is possible this difference is a result of carbonizing at different temperatures and reaction times. These results suggest that the

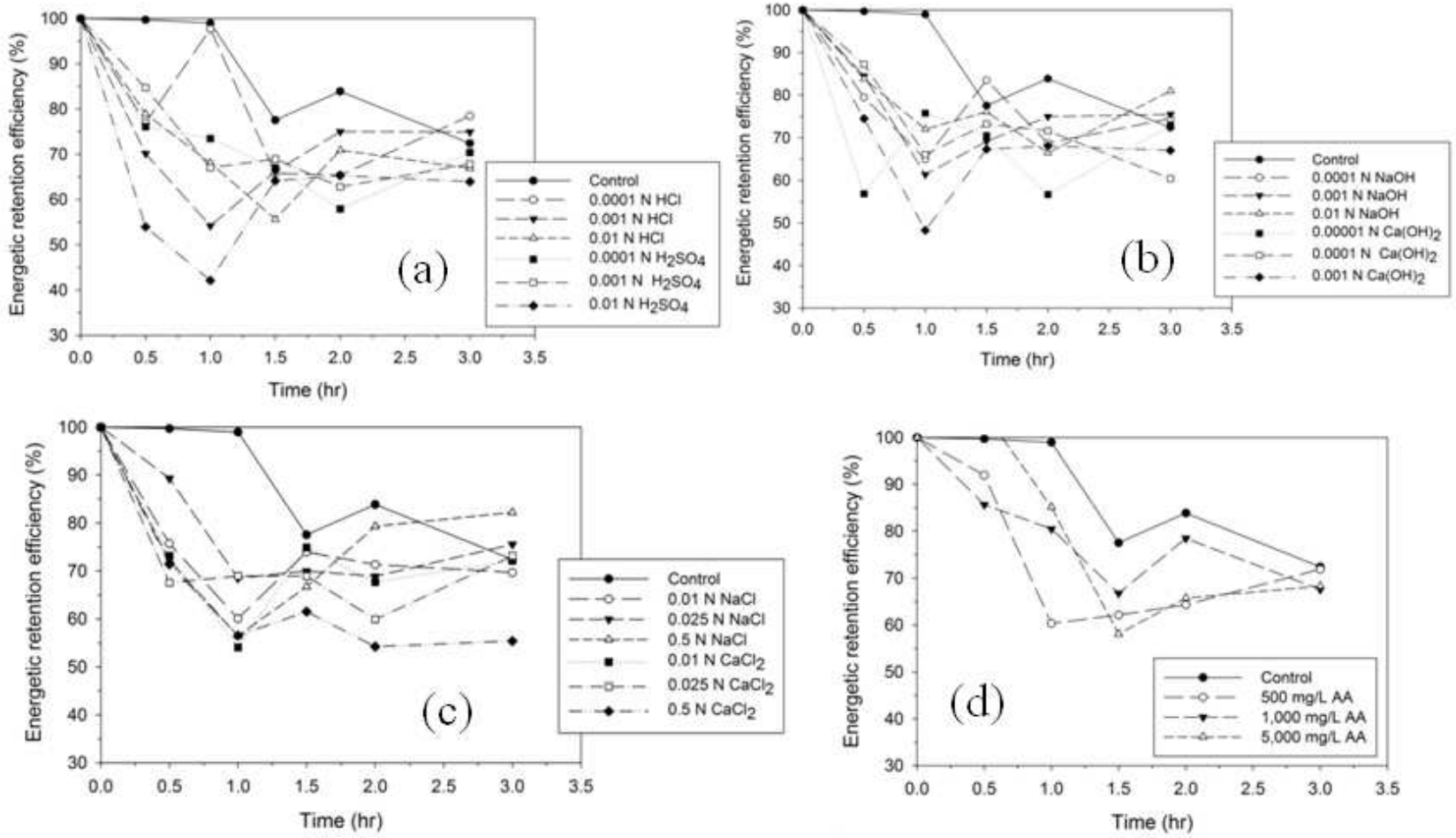

Figure 4.14 Energetic retention efficiency water when carbonizing in the presence of: (a) acids, (b) bases, (c) salts, and (d) organic carbon.

Na^+ and Ca^{2+} cations influence the transfer of oxygen from the solids to the liquid-phase, influencing solids energy content. Lu et al. (2013) report that the majority of oxygen initially present in the feedstock is transferred to the liquid-phase.

Liquid-phase composition results suggest that the liquid-phase reactions in the presence of 0.5 N $CaCl_2$ are accelerated (Figure 4.4c and Figure 4.7 4.6). No glucose is observed at all reaction times and the HMF is not detected at 1.5 hours (Figure 4.7 4.6). The levulinic acid yields are larger, while the formic acid is disappearing. It is likely the formic acid is being converted to hydrogen gas. Significantly more hydrogen was measured in the gas-phase when carbonizing in the presence of $CaCl_2$. It should be noted that although the liquid-phase reactions appear to be accelerated in the presence of 0.5 N $CaCl_2$, it is likely that the full extent of cellulose conversion to these liquid-phase intermediates has not occurred because of the solids surface passivation that is hypothesized to occur at this $CaCl_2$ concentration. Similar pathways are observed at 0.5 N NaCl. Patwardhan et al. (2010) report that mineral salt addition accelerates the pyrolysis of cellulose and the formation of low molecular weight compounds, including formic acid.

Atomic ratios of H/C and O/C were used in conjunction with van Krevelen diagrams (as discussed previously) to evaluate carbonization mechanisms (Figure 4.11). The influence of each salt differs. As NaCl concentrations increase, decarboxylation increases (Figure 4.11), confirmed by ANOVA test results (Table 4.2). The addition of $CaCl_2$ at 0.01 – 0.025 N exhibited little change in the atomic ratio data, indicating the level of decarboxylation and dehydration are similar. However, at a $CaCl_2$ concentration of 0.5 N, significant differences in the solids composition were observed (Figure 4.11c),

including the oxygen content of the recovered solids. The trend of the atomic ratio data also differ (Figure 4.11c). A greater amount of oxygen remains integrated within the recovered solids after 3 hours, suggesting the level of dehydration decreases at larger $CaCl_2$ concentrations.

4.3.4 Influence of initial AA process water on carbonization products

The presence of organics, simulated in these experiments with acetic acid (AA), in the initial process water accelerates cellulose dissolution, as illustrated in Figure 4.1d. The acceleration is greater than that observed in the presence of bases, but less than that observed in the presence of acids and salts. Changes in AA concentration influences cellulose dissolution; as the AA concentration increases, the acceleration of cellulose dissolution appears to decrease. Results from ANOVA tests indicate that carbonizing in the presence of 500 and 1,000 mg/L AA results in a statistically significant change in the recovered solids at a reaction time of 1 hr when compared with the control experiment (Table 4.2). Consistent with the data in .4.1d, the solids recovered at an initial AA concentration of 5,000 mg/L were not statistically significant from the control experiment. Ultimate solid yields, however, are not influenced by AA concentration and are similar to those obtained from the control experiment, as confirmed by results from the ANOVA tests (Table 4.2).

The carbon content (% C, daf) of the recovered solids following carbonization in the presence of AA is always lower than that obtained when carbonizing in the presence of DI water (Figure 4.4d). Results from ANOVA tests indicate that the solids carbon content obtained when carbonizing in the presence of AA are statistically significant when compared to that obtained with the control experiment at a reaction time of 1 hr.

Results als indicate that at a reaction time of 3 hr, the AA concentrations of 500 and 1,000 mg/L are different than that of the control experiments, suggesting the influence of initially organic acid presence is kinetic in nature. The percentage of initially present carbon (cellulose plus initially present AA) remaining in the solids after 3 hours is lower when carbonizing in the presence of AA than that observed when carbonizing in DI water. This observation is not surprising. The fraction of carbon present in the liquid-phase after carbonizing for three hours is similar to the control at all AA concentrations evaluated, while the percentage of carbon transferred to the gas-phase is significantly larger than that observed in the control experiment (8-11%, Figure 4.10) , as well as the that measured when carbonizing n the presence of the other additives. These observations are consistent with results from ANOVA tests. The fraction of carbon in the liquid-phase is not statistically significant from the control at a reaction time of 3 hrs, but is statistically significant from the control at a reaction time of 1 hr. The fraction of carbon in the gas-phase is statistically significant from the control experiment at reactions times ranging from 1.5 to 3 hr.

The influence of AA addition on recovered solids energy content is negative (Figure 4.5d). The energy content of recovered solids when carbonizing in the presence of AA is always slightly lower than that measured in the control experiment and decreases as the concentration of initially present AA increases. ANOVA test results indicate that at AA concentrations of 500 and 1,000 mg/L the solids energy content is statistically different than the control experiment at reaction times of 1.5 and 2 hr (Table 4.2).

The liquid-phase carbon content is shown in Figure 4.5 4.4d. The largest liquid-phase carbon concentrations when carbonizing in the presence of AA were observed at 1 hr. The AA appears to accelerate the conversion of produced HMF and subsequent formation of levulinic acid (Figure 4.6).

Atomic ratios of H/C and O/C were used in conjunction with van Krevelen diagrams (as discussed previously) to evaluate carbonization mechanisms (Figure 4.11d). Dehydration remains the predominant mechanism. The solids hydrogen and oxygen contents, however, do statistically differ from those obtained in the control experiment at a reaction time of 3 hours, suggesting carbonization mechanisms may differ when carbonizing in the presence of AA.

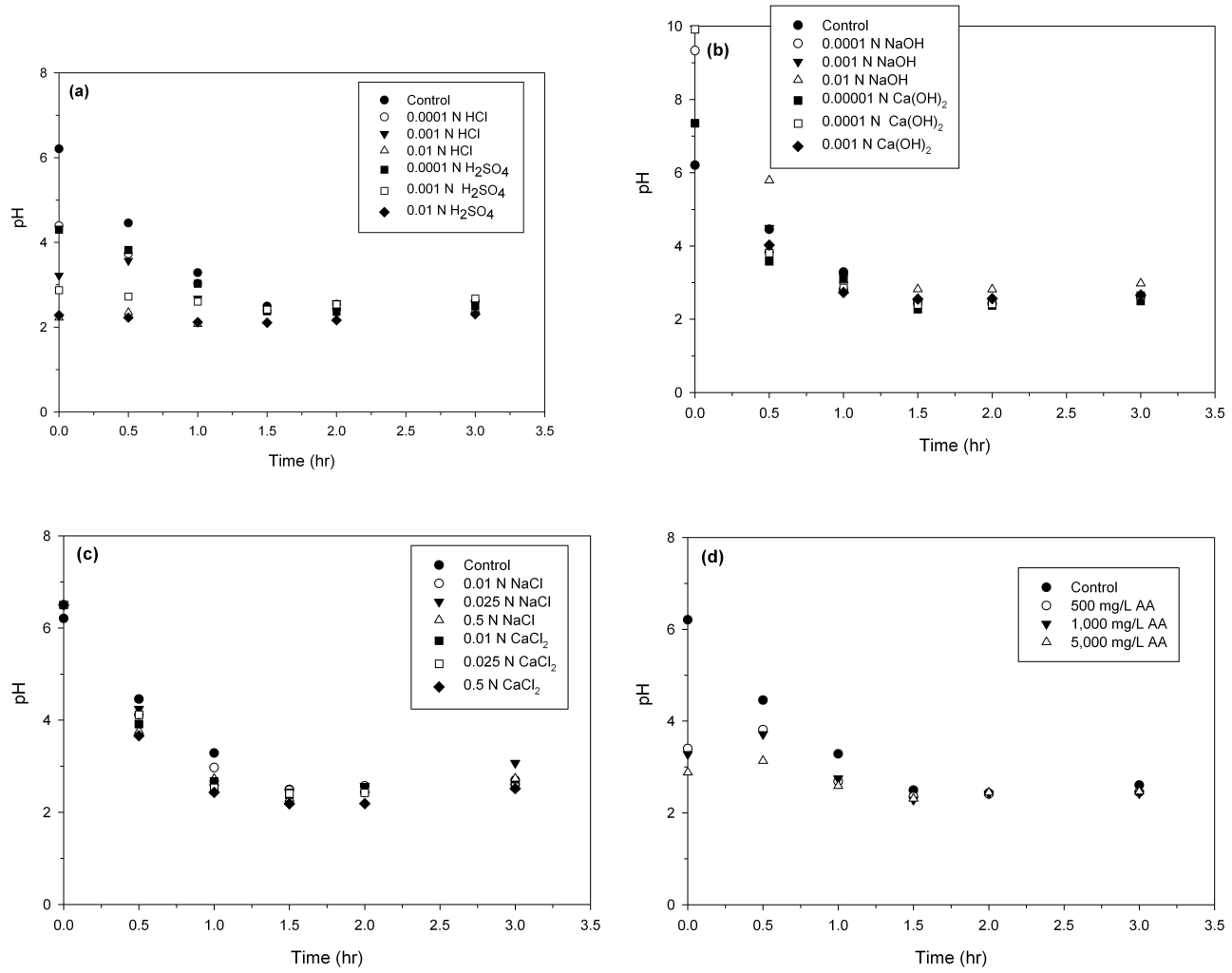

Figure 4.15 pH of the final process water when carbonizing in the presence of: (a) acids, (b) bases, (c) salts, and (d) organic carbon.

4.4 CONCLUSIONS

Experiments were conducted to determine how initial process water characteristics influence carbonization product composition and mechanisms. Results from the experiments conducted evaluating the influence of process water quality on carbonization indicate that changes in initial water quality do influence time-dependent carbonization product composition and yields. Changes in initial water quality appear to have the greatest influence on the carbon content transferred to the gas-phase, as 71% of the values are statistically significant from the control experiment at a reaction time of 3 hours. The additive that resulted in the greatest change in carbonization product yields/composition is the 0.5 N $CaCl_2$. At high salt concentrations, it is possible the solids surfaces become passivated, inhibiting the carbonization process and negatively influencing recovered solids energy and carbon content. Results from these experiments also indicate that when evaluating the time-dependent carbonization product production, the specific cations and anions impact product yields/composition differently.

These results suggest that changes in process water quality, with the exception of high salt concentrations, impart little influence on ultimate carbonization products/yields. Leachates with high ionic strength and saltwater sources, however, may result in lower solids yields and energy contents and may not be a preferred alterative liquid source. Experiments in the presence of multi-component process waters need to be conducted to determine whether interactions between the components in the process water influence carbonization product yields/composition.

CHAPTER 5.

INFLUENCE OF FEEDSTOCK CHEMICAL COMPOSITION ON THE HYDROTHERMAL CARBONIZATION OF MIXED FEEDSTOCKS[4]

[4] Influence of feedstock chemical composition on hydrothermal carbonization of mixed feedstocks, Lu X.; Flora, J R. V.; Berge, N. D.. Submitted to Bioresource Technology, 1/25/2014.

ABSTRACT

As the exploration of the carbonization of mixed feedstocks continues, there is a distinct need to understand how feedstock chemical composition and structural complexity influence their carbonization. Laboratory experiments were conducted on pure/model compounds, mixtures of the pure compounds, and complex feedstocks containing the pure compounds (e.g., paper, wood). Results indicate that feedstock properties do influence carbonization products. Carbonization product characteristics were predicted using results from the carbonization of the pure compounds and indicate that recovered solids energy contents are more accurately predicted than solid yields and carbon masses in each phase, while predictions associated with solids surface functional groups are more difficult to predict using this approach. To more accurately predict other carbonization products, compounds more closely representing the complex feedstocks need to be used as the basis for the predictions.

5.1 INTRODUCTION

Hydrothermal carbonization (HTC) has been extensively studied as a beneficial technique for biomass and waste conversion to value-added products (e.g., Berge et al., 2011; Lu et al., 2013; Kang et al., 2012; Sevilla and Fuertes, 2011). HTC is a wet relatively low temperature thermal conversion process that occurs under autogenous pressures. During carbonization, valuable solid, liquid, and gaseous products are generated through a series of simultaneous reactions, including hydrolysis, dehydration, decarboxylation, aromatization, and recondensation (e.g., Funke and Ziegler, 2010; Libra et al., 2011; Sevilla and Fuertes, 2009b). The generated solids material has sparked

considerable interest in this conversion technique. These solids, referred to as hydrochar to differentiate them from char produced from dry conversion processes, are carbon and energy-dense, and have been documented to be predominantly aromatic and/or furanic in nature (Baccile et al., 2009; Falco et al., 2011), with a structure resembling a low-grade coal (e.g., Berge et al., 2011). In addition, work has been conducted indicating the generated hydrochar may be used in several environmentally-relevant applications, such as soil augmentation and environmental remediation (e.g., Kammann et al., 2012; Liu et al., 2010).

Carbonization of a large variety of complex feedstocks has been studied, ranging from different types of biomass (e.g., wood, grass) to various heterogeneous municipal wastes (e.g., food waste, sludges, solid waste) (e.g., Berge et al., 2011; Li et al., 2013; Libra et al., 2011). Results from these studies indicate that a large fraction of carbon initially present in the feedstocks remains integrated within the hydrochar material during carbonization (e.g., Funke and Ziegler, 2010; Libra et al., 2011). Another advantage of carbonization is that initial feedstock drying is not required, resulting in an energetically advantageous conversion technique for wet feedstocks (Li et al., 2013). In addition, the resulting liquid stream contains appreciable concentrations of valuable compounds (e.g., organic acids, HMF, and nutrients, e.g., Hoekman et al., 2011; Li et al., 2013).

As the exploration of the carbonization of mixed feedstocks continues, there is a distinct need to understand how the chemical composition and structural complexity of these feedstocks influence the carbonization process. The major chemical composition of biomass and waste materials includes significant fractions of lignin, cellulose, hemicellulose, starch, and/or sugars. Although carbonization of these feedstocks has been

previously investigated independently (e.g., Carrier et al., 2012; Falco et al., 2011; Kang et al., 2013; Sevilla and Fuertes, 2009b; Yu et al., 2004), there is little information regarding the carbonization of mixtures of these compounds or how carbonization of these individual compounds correlates with the carbonization of biomass or waste materials containing these compounds. Dinjus et al. (2011) carbonized several mixed feedstocks (e.g., straw, grass, cauliflower, beechwood) to understand the influence of lignin on carbonization. Their results indicate that lignin may influence the release of carbonization intermediates and may impede carbonization by forming a protective shell around the feedstock (Dinjus et al., 2011). Kang et al. (2012) underpredicted the hydrochar yields of wood meal when using data from the carbonization of cellulose, lignin and xylose, suggesting compound interaction may occur during carbonization. Interactions between individual components in biomass have also been reported during pyrolysis and gasification (e.g., Carrier et al., 2012; Hosoya et al., 2009.

A need for understanding how chemical components of complex biomass or waste materials interact during carbonization remains. Development of such an understanding may lead to the development of predictive carbonization models based on feedstock chemical composition, ultimately leading to more purposefully designed carbonization work. The purpose of this work is to understand how changes in feedstock composition and complexity influence carbonization product quality. The specific objectives of this work include: (1) understanding the time dependent carbonization products from the carbonization of pure/model compounds (e.g., lignin, cellulose, xylose, glucose and starch), mixtures of the pure compounds, and complex feedstocks (e.g., pinewood, paper, and sweet corn); (2) comparing carbonization products associated with

those obtained from the carbonization of pure compounds with that of biomass/waste products comprised of the pure compounds; and (3) determine the predictability of carbonization product characteristics of complex, mixed feedstocks using results from the carbonization of the pure/model compounds.

5.2 MATERIALS AND MATHODS

5.2.1 Feedstock characteristics

Several individual feedstocks that represent major fractions of biomass and waste materials were evaluated in this study: cellulose, starch, lignin, glucose, and xylose. Microcrystalline cellulose derived from the Western redcedar plant (Thuja plicata, with average particle size of 50 µm, purchased from Acros Organics) was used as the cellulose source in all experiments. Powder potato starch (extra pure, Fisher Scientific) was used as the starch source in all experiments. Low sulfonate alkali lignin (from kraft process, Sigma-Aldrich, Inc.) was used as the lignin source. Glucose (Fisher Scientific, Inc.) was used to model the sugar content of biomass/waste materials and D-(+)-Xylose (> 98%, Alfa Aeser) was used to simulate hemicellulose.

The complex feedstocks used in this work include office paper, pine wood, and sweet corn. Before use, the office paper was shredded using a titanium paper shredder (25 by 4 mm strips). Pine wood chips were purchased locally. Approximate size of the wood chips, in all dimensions, is < 1mm. The wood chips were air-dried prior to use in the carbonization experiments. Frozen sweet corn kernels were purchased from a local grocery store (7 – 9mm). Before use, the corn was thawed. Feedstock lignin, cellulose, hemicellulose, starch, and sugar content were measured by the Soil and Forage Analysis

Laboratory at the University of Wisconsin. Feedstock properties are reported in Table 5.1.

5.2.2 Batch experiments

All batch carbonization experiments were conducted following procedures previously described (Li et al., 2013; Lu et al., 2013). Briefly, the feedstocks were placed in 160-mL stainless steel tubular reactors (2.54 cm i.d., 25.4 cm long, MSC, Inc.) fitted with gas-sampling valves (Swagelock, Inc.). A mass of 8 g of dry solids was added to all reactors. Deionized (DI) water was subsequently added to achieve the desired solid material concentration of 20 % (dry wt.). All reactors were sealed and heated in a laboratory oven at 250^{o}C. The in-situ liquid temperature was measured with a pipe-fitting thermocouple probe (Type J) inserted in the reactor and a data logger (Temp-300, Oakton Instruments). Temperatures were recorded every two minutes for the duration of the experiment. The desired in-situ temperature of the reactors was achieved after 90 min. Experiments for each feedstock were conducted over a carbonization period of 96 hours, with samples periodically taken over this period. These sampling times include the period of reactor heating.

Samples from the solid (energy content, carbon content, ^{13}C solid-state NMR, ash), liquid (total organic carbon (TOC), pH, chemical oxygen demand (COD)), and gas phases (gas volume and composition) were taken to evaluate carbonization product properties at different temperatures. These collected data were used to calculate solid yields and carbon and energy-related properties associated with the recovered solids.

Three sets of carbonization experiments were conducted. First, all individual compounds representing fractions of biomass/waste (e.g., cellulose, starch, lignin,

glucose, xylose) were carbonized (referred to as pure throughout this work). The second set of carbonization experiments were conducted with known mixtures of the chemical compounds. The following two mixtures of pure compounds were carbonized (%, by wt. of added compounds): (1) 52.5% cellulose, 30% xylose, and 17.5% lignin; and (2) 80% starch, 20% glucose. The last set of carbonization experiments was conducted with the mixed feedstocks (e.g., paper, pine wood, and sweet corn).

5.2.3 Analytical techniques

At each sampling time, reactors were removed from the oven and placed in a cold water bath. Following cooling, the produced gas was collected in either a 1 or 3-L foil gas sampling bag. Gas composition of these samples was analyzed using GC-MS (Agilent 7890). Gas samples were routed through a GS-CarbonPlot column (30m long and 0.53 mm id, J&W Scientific). Initial oven temperature was 35^{o}C. After 5-min, the temperature was increased at a rate of 25^{o}C/min until a final temperature of 250^{o}C was achieved. Carbon dioxide standards (Matheson Trigas) were used to determine concentrations in the gas. Gas volumes were measured with a large volume syringe (S-1000, Hamilton Co.).

The process liquid and solid were separated via vacuum filtration through a 0.22 µm cellulose nitrate membrane filter (Whatman International Ltd.). Liquid conductivity and pH were measured using electrodes (Thermo Scientific Orion). Liquid chemical oxygen demand (COD) was measured using HACH reagents (HR + test kit, Loveland, CO). Liquid total organic carbon (TOC) was measured using a TOC analyzer (TOC-Vcsn, Shimadzu).

Table 5.1 Feedstock properties

Feedstock Classification	Feedstock	Chemical Composition				Carbon (%, dry wt.)	Moisture (%, wet wt.)	Ash (%, dry wt.)	Particle Size
		ADL (%, dry wt.)	Cellulose[C] (%, dry wt.)	Starch (%, dry wt.)	Sugar (%, dry wt.)				
Pure Compounds	Lignin	41.08	52.97	NM	NM	48.1	NM	20.06	NA
	Cellulose	0.2	98.68	NM	NM	42.4	NM	0.002	NA
	Xylose	NM	NM	NM	NM	41.5	NM	0	NA
	Glucose	NM	NM	NM	NM	40.8	NM	0.003	NA
	Starch	NM	NM	>99.50	0.17	37.0	NM	0	NA
Pure mixtures	Mix 1:[a] C, X, L	NM	NM	NM	NM	44.0	NM	6.02	NA
	Mix 2:[b] S, G	NM	NM	NM	NM	37.7	NM	0	NA
Complex	Pine Wood	32.3	41.0	NM	NM	46.6	15	0.02	1 mm
	Paper	1.3	79.3	NM	NM	36.3	0.19	5.16	3 × 10 mm
	Corn	NM	NM	57.6	45.3	53.3	74.37	0.29	3 ×7 × 9 mm

[a]C = cellulose, X = xylose, and L = lignin; [b]S = starch, G = glucose; [c]cellulose measurement is based on the NDF method.
NM=not measured; NA=not applicable.

All collected solids were dried at 80℃. All dried solids were weighed and solids recoveries calculated (mass of dry solids recovered divided by the mass of initial dry solids). Solid carbon content (Perkin Elmer 2400 Elemental Analyzer) and energy content (C-200 bomb calorimeter, IKA, Inc.) were measured. In addition, the lignin, cellulose, and hemicellulose contents of the recovered solids were measured using the standardized acid detergent lignin (ADL, lignin), acid detergent fiber (ADF, combination of cellulose, lignin and ash) and natural detergent fiber (NDF, cellulose, hemicellulose, lignin and ash) techniques (conducted by the Soil and Forage Laboratory at the University of Wisconsin). A drawback of the ADL measurement is the acid soluble lignin dissolves during the test; thus the ADL often underpredicts the total lignin content (Hatfield et al., 2005; Yasuda et al., 2001). Recovered solids starch and sugar content was measured using a YSI 2700 Biochemistry Analyzer following solid hydrolysis (conducted at the Soil and Forage Laboratory at the University of Wisconsin). The initial feedstock ash content was measured by placing a sample of the material in a crucible in a muffle furnace at 500 ^{o}C for 2 hours and 750 ^{o}C for an additional 2 hours.

Recovered solids were also analyzed using ^{13}C-NMR to identify and provide semi-quantitative information associated with functional groups at each reaction temperature and time. Solid state ^{13}C CP-MAS spectra were collected on a Bruker Avance III-HD 500 MHz spectrometer fitted with a 1.9mm MAS probe. The spectra were collected at ambient temperature with sample rotation rate of 20 kHz. 1.5ms contact time with linear ramping on the ^{1}H channel and 62.5kHz field on the ^{13}C channel were used for cross polarization. ^{1}H dipolar decoupling was performed with SPINAL64

modulation and 145kHz field strength. Free induction decays were collected with a 27 msec acquisition time over a 300 ppm spectra width with a relaxation delay of 1.5s.

Each NMR spectrum was subsequently deconvoluted using MestRenova software (MestreLab Research, Version 7.0). Spectra are divided into five regions (Table 5.2): (1) aliphatic 0 – 50 ppm, (2) methoxyl: 50 – 60 ppm; (3) O-alkyl: 60 – 110 ppm; (4) aromatic, furanic and O-aromatic: 110 – 160 ppm; and (5) carboxyl and carbonyl (C=O): 160 – 215 ppm. These regions are based on previously conducted work (Baccile et al., 2009; Falco et al., 2011). Peak intensities, width and the Gaussian/Lorentzian ratio were allowed to vary during deconvolution. Carbon distributed in the identified functional groups were calculated based on the percent area of each peak and normalized to the amount of carbon in the solid-phase.

Table 5.2 Peak assignments for ^{13}C NMR spectra.

Spectral domain	Region (ppm)	Represented structure	Chemical shift (ppm)	Reference
Alkyl	0 – 50	CH_x	0 - 50	Baccile et al., 2009
Methoxyl	50 – 57	O-CH_3	50 – 60	Preston et al, 1998
O-alkyl	57 – 105	C-O	60 - 88	Preston et al, 1998
		O-C-O	102 – 104.2	
sp^2 C	110 – 160	β -C in furan ring	110	Baccile et al., 2009; Falco et al., 2011
		β-β bond connecting two furan rings	118	Falco et al., 2011
		aromatic C	125	Falco et al., 2011b
		aromatic C	132	Baccile et al., 2009; Falco et al., 2011
		α-α bond connecting two furan rings or O-aromatic	140	Falco et al., 2011, Preston et al, 1998
		α-C in furan ring or O-aromatic	150	Baccile et al., 2009; Falco et al., 2011, Preston et al, 1998
Carboxyl and carbonyl	175 – 210	H-C=O	175	Baccile et al., 2009
		R_2-C=O	207	Baccile et al., 2009

Calculations based on experimental results from the carbonization of pure compounds (i.e., lignin, cellulose, xylose, starch, glucose) were performed to predict the characteristics associated with the recovered solids from the experiments associated with the mixtures (e.g., cellulose + xylose + lignin and starch + glucose) and mixed feedstocks (i.e., wood, paper, corn). The following parameters were predicted: solid yields, solids energy content, carbon mass in the solid, liquid, and gas-phases, gas volume and solids surface functional groups. Specific details associated with these predictions can be found in the supporting information.

5.3 RESULTS AND DISCUSSION

5.3.1 Recovered solid yield

Solid yields (total mass of dry solids recovered at each sampling time divided by the dry mass of the initial feedstock) are influenced by reaction time and feedstock type (Figure 5.1). The observed initial changes in the mass of solids recovered results from a combination of initial feedstock solubilization, solids production, and component partitioning to the gas and liquid-phases. Solid yields generated from feedstocks that are soluble in water at room temperature initially increase with time, while those that are insoluble in water at room temperature initially decrease with time (Figure 5.1). Initially recovered solids (< 2 hours) are likely comprised of both unreacted feedstock and converted hydrochar, similar to that reported by Lu et al. (2013). Such differences cannot be distinguished via gravimetric or carbon measurements. After a period of approximately 1.5 to 24 hours, the yields stabilize. The time to reach these stable, final solid yields depends on feedstock type, with shorter times associated with the pure feedstocks (except for lignin) and larger stabilization times associated with the mixtures

of pure feedstocks and complex feedstocks. These observations suggest changes in feedstock type and complexity influence carbonization kinetics.

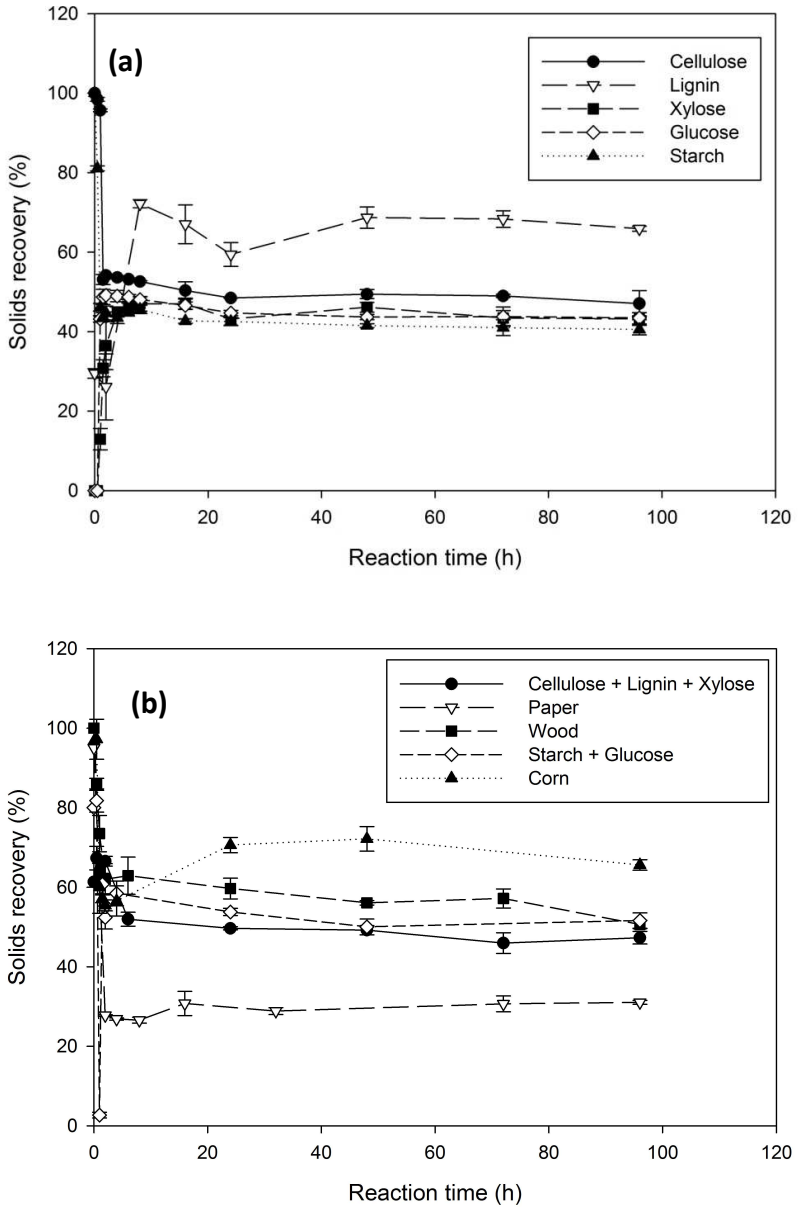

Figure 5.1 Solids recoveries from the carbonization of: (a) pure compounds and (b) mixtures of pure compounds and complex feedstocks.

5.3.1.1 Pure compounds

The solid yields generated from the carbonization of the pure feedstocks after a reaction time of 96 hours increase with feedstock carbon content (Figure 5.2), with

greater yields measured from the carbonization of lignin (~66%) than other pure feedstocks (~40 – 47%, Figure 5.1). Results from ANOVA tests confirm that yields associated with lignin are statistically different from those obtained when carbonizing the other pure feedstocks ($p < 0.05$). Larger solids yields associated with the carbonization of lignin have also been previously reported (Kang et al., 2012), but do not necessarily indicate lignin carbonization/conversion. Results from thermogravimetric analyses reported in the literature indicate that lignin has greater thermal stability than cellulose and hemicellulose (Kang et al., 2012), resulting in greater solids recovery. This greater stability is likely due to the abundant heat resistant phenolic structures found in lignin (Williams and Onwudili, 2006). These larger yields, coupled with a solids carbon densification close to one (Figure 5.3), suggest conversion of lignin under the conditions evaluated in this study is minimal, corroborating that reported by others (Dinjus et al., 2011; Kang et al., 2013). Measured ADL in the recovered solids confirm this hypothesis. After the initial measurement, the fraction of ADL in the recovered solids changes little over time (Figure 5.4).

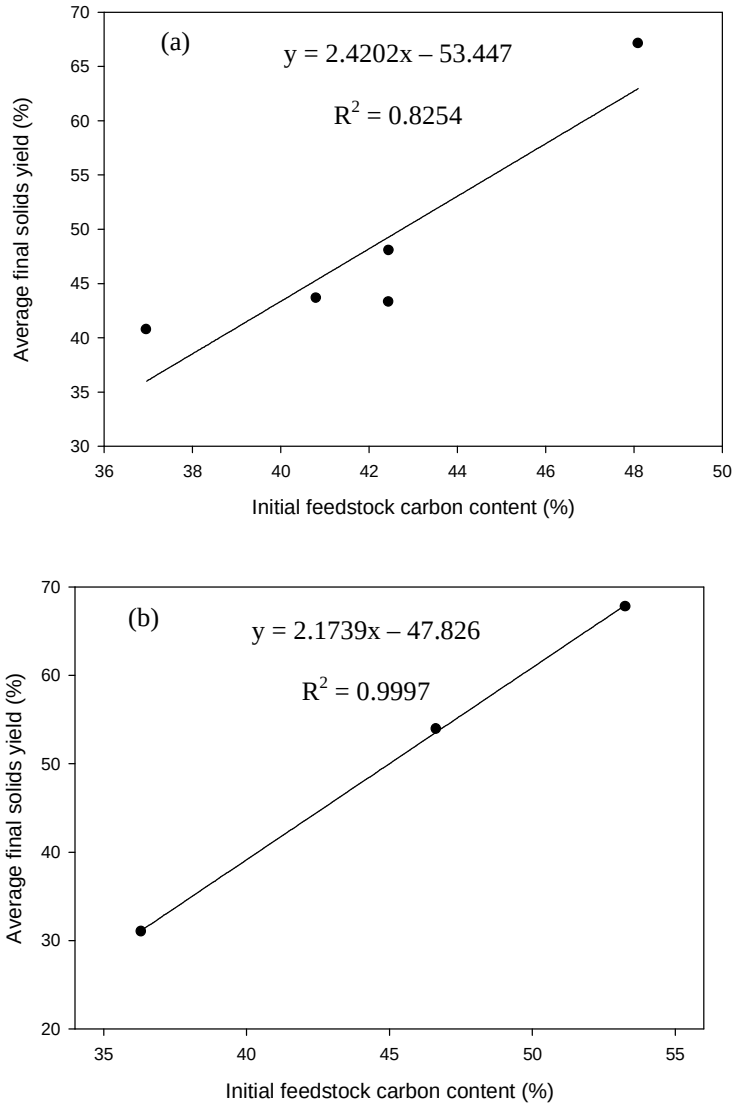

Figure 5.2 Linear relationship between solids yield and carbon content of the feedstock at 96 hours for: (a) pure feedstocks including cellulose, lignin, xylose, starch and glucose and (b) complex feedstocks including wood, paper and corn.

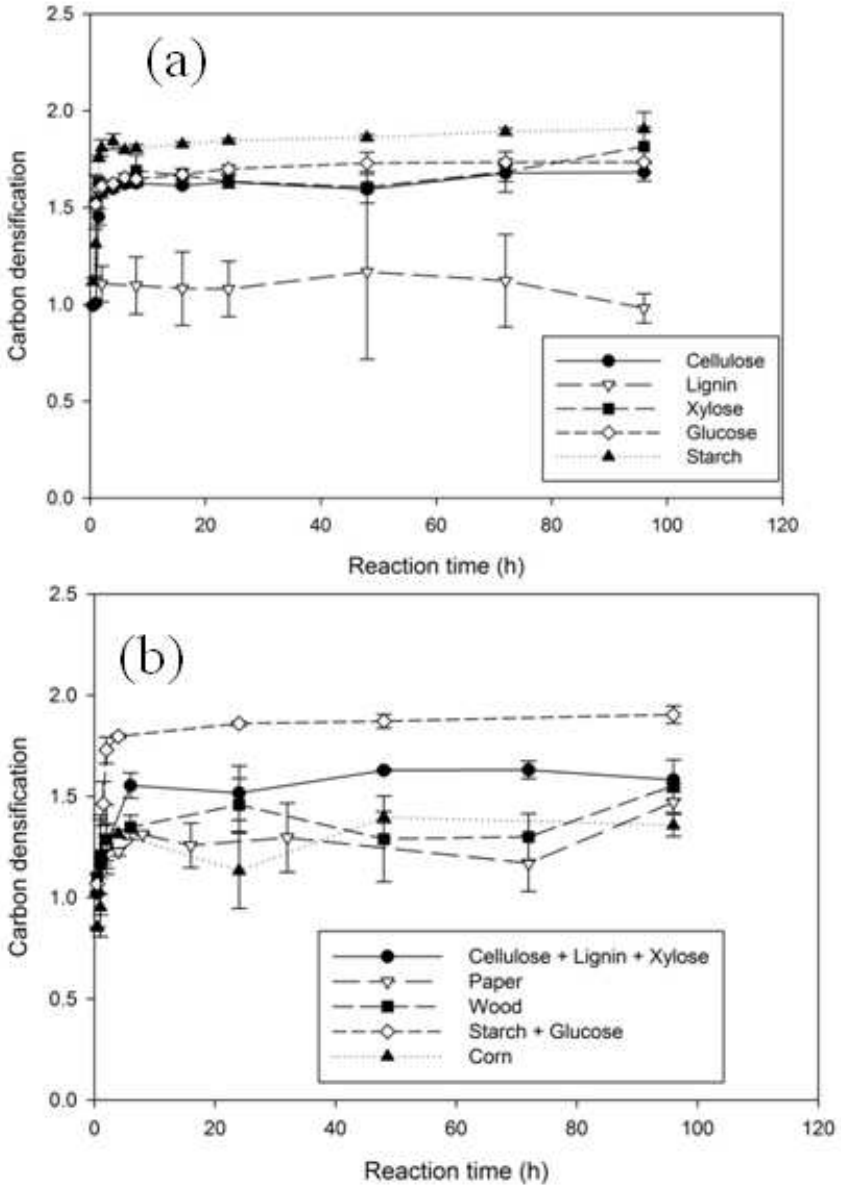

Figure 5.3 Carbon densification in recovered solids from the carbonization of: (a) pure compounds and (b) mixtures of pure compounds and complex feedstocks.

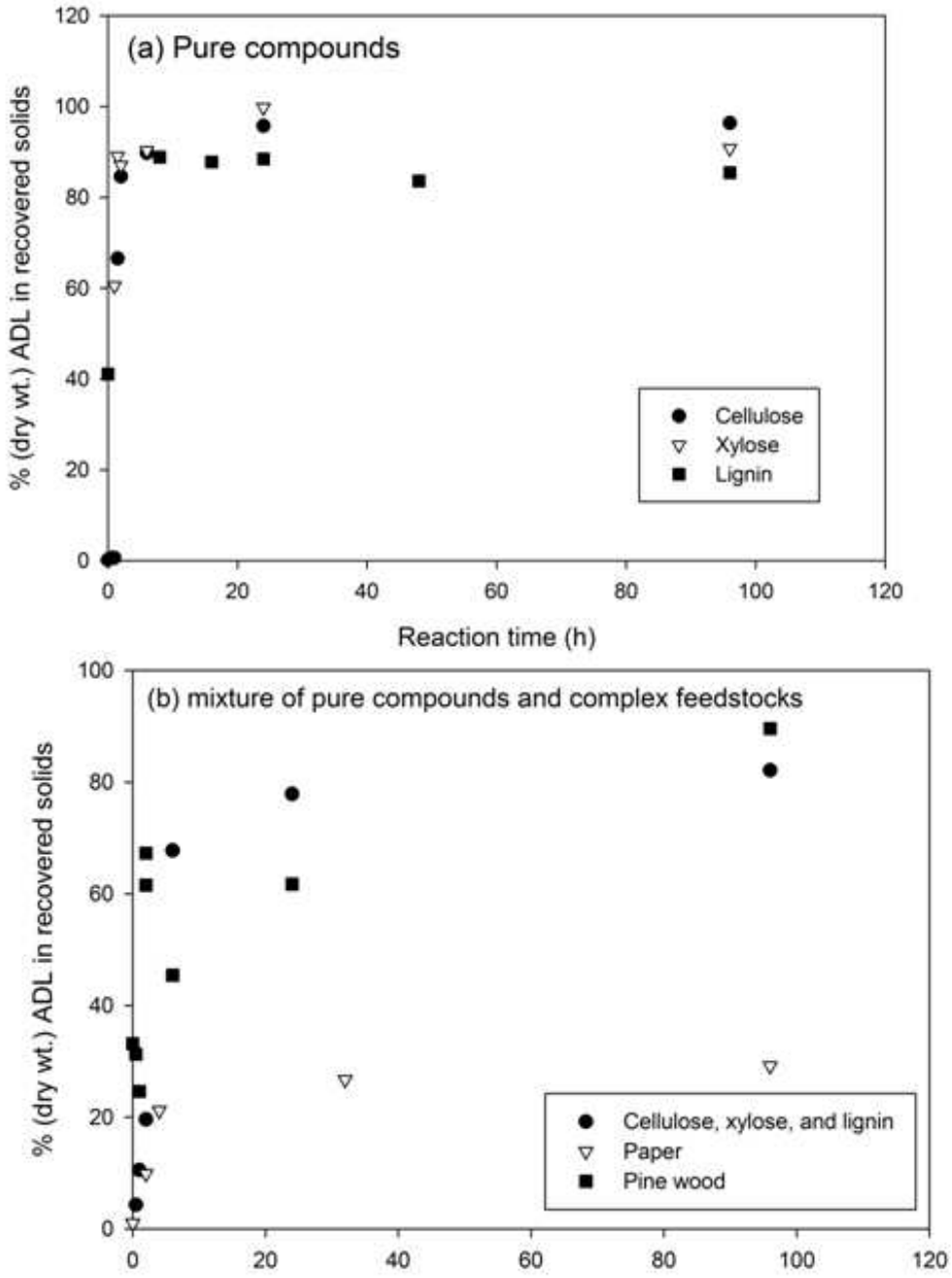

Figure 5.4 Percentage of ADL in the recovered solids from the carbonization of: (a) pure compounds and (b) mixtures of pure compounds and complex feedstocks.

Lower and similar yields result from the carbonization of the other pure compounds (e.g., cellulose, glucose, starch, and xylose). Results from ANOVA tests indicate that all final yields (at a reaction time of 96 hours) are statistically significant from one another ($p < 0.05$), except for the final yields resulting from the carbonization of glucose and xylose ($p > 0.05$). The yields associated with cellulose are greater than the other pure feedstocks (except for lignin), with those associated with the carbonization of glucose and xylose being statistically similar ($p > 0.05$). The lowest obtained yield resulted from the carbonization of starch. These results are similar to previous reports that carbonization of cellulose results in larger solids yields than that associated with the carbonization of starch (Williams and Onwudili, 2006).

Differences associated with the yields resulting from the carbonization of the pure compounds may be due to feedstock chemical and/or structural properties. As stated previously, a relationship between yield and carbon content of the feedstock exists (Figure 5.2), suggesting initial feedstock carbon content influences solids generation. These differences in yield may also result from changes in feedstock structure/properties. Cellulose has an unbranched crystalline structure, with a crystallinity degree ranging between 67 – 83% (Wang et al., 2013) and a degree of polymerization of 1000 - 2000 (Sweet and Winandy, 1999). Starch has a lower degree of polymerization than cellulose and a branched structure that is 15 – 45 % crystalline (Hoover, 2001; Oates, 1997; Waigh et al., 1999). The relatively lower yields associated with starch may possibly be explained by its gelatinization when heated. When heated, the starch granules undergo melting, swelling and eventually collapse (Xie et al., 2008; Zobel et al., 1988), destroying the crystalline structure of starch (Zobel et al., 1988). As a result, the glucosyl units

associated with the starch are likely distorted and form a less stable conformation (Oates, 1997) .

5.3.1.2 Mixture of pure compounds and complex feedstocks

The solid yields associated with the carbonization of the mixtures of pure compounds and the complex feedstocks (e.g., wood, paper, and corn) also differ. A longer reaction time is required for complex feedstocks to reach a stable mass of recoverable solids than that associated with the pure feedstocks, except for lignin, suggesting carbonization kinetics are slower for the complex feedstocks. The largest yields were generated when carbonizing the corn, the feedstock of greatest initial carbon. Similar to that associated with the pure compounds, a distinct and significant linear relationship between the initial carbon content of the complex feedstock and their final yields exists (correlation coefficient of 0.99, Figure 5.2). Results from ANOVA tests indicate the yields associated with these feedstocks are, for the most part, statistically significant from one another. The yields resulting from the mixture of cellulose, xylose, and lignin statistically differ from all other mixtures and complex feedstocks at all times, except for the corn and the starch and glucose mixture at 1 and 48 hours, respectively ($p > 0.05$). Yields resulting from carbonization of wood are statistically different from all other mixtures and complex feedstocks at all reaction times, except corn at 0.5 and 24 hours ($p > 0.05$). At early times, the yield obtained from the carbonization of the starch and glucose mixture is similar to that obtained when carbonizing corn (times less than 4 hours, $p > 0.05$).

The majority of the yields obtained when carbonizing these mixtures and complex feedstocks also statistically differ from that obtained when carbonizing the pure

compounds. Not surprisingly, at certain reaction times the yields obtained when carbonizing the cellulose, lignin, xylose mixture do not differ statistically ($p > 0.05$) from cellulose (24, 48 and 96 hours) and xylose (48, 72, and 96 hours), two of the major components of the mixture. The yields obtained when carbonizing the starch and glucose mixture are predominantly different from the pure feedstocks, except at a few reaction times (cellulose at 2 and 48 hours and starch at 0.5 hours, $p > 0.5$). Yields from the carbonization of wood are similar to those obtained from lignin at 48 and 72 hours, while the yields from paper are similar to lignin at a reaction time of 2 hours ($p > 0.05$).

5.3.1.3 Prediction of solid yields

The ash-free solid yields resulting from the carbonization experiments of the pure feedstocks were used to predict the yields resulting from the carbonization of the mixtures of pure compounds and the complex feedstocks. The ash was removed form the predictions because the feedstock ash contents vary. Results from this analysis are shown in Table 5.3 and Figure 5.5. For all mixtures and complex feedstocks, the predictions of ash-free solid yields remain fairly constant with time (similar to the measured values), with predictions more closely approximating the measurements at later times.

The predictions of solid yields obtained from the carbonization of mixtures of pure compounds are fairly accurate, with less than 20% error between the measured and predicted values at a reaction time of 96 hours. The yield prediction associated with the mixture of cellulose, lignin, and xylose closely approximates the measured value (~1% error between the measured and predicted values at a reaction time of 96 hours). Surprisingly, the yield prediction associated with the carbonization of the starch and glucose mixture at a reaction time of 96 hours is underpredicted by ~20% from the

measured value, suggesting compound-related interactions may occur during the carbonization of these compounds that catalyze solids production.

The predictions of solid yields from the carbonization of the complex feedstocks vary more significantly from the measured values (Table 5.3and Figure 5.5). The yields associated with wood (~39% error between the measured and predicted values at a reaction time of 96 hours) and corn (~36% error between the measured and predicted values at a reaction time of 96 hours) are underpredicted, while the yields associated with paper (~49% error between the measured and predicted values at a reaction time of 96 hours) are overpredicted. Interestingly, the yields associated with both the mixture of starch and glucose and the corn are greater than that predicted values, suggesting that intermediate compounds associated with the carbonization of these compounds may catalyze solids production. A similar phenomenon was observed for the starch and glucose mixture, suggesting when carbonizing feedstocks containing starch and sugars, solids generation is catalyzed.

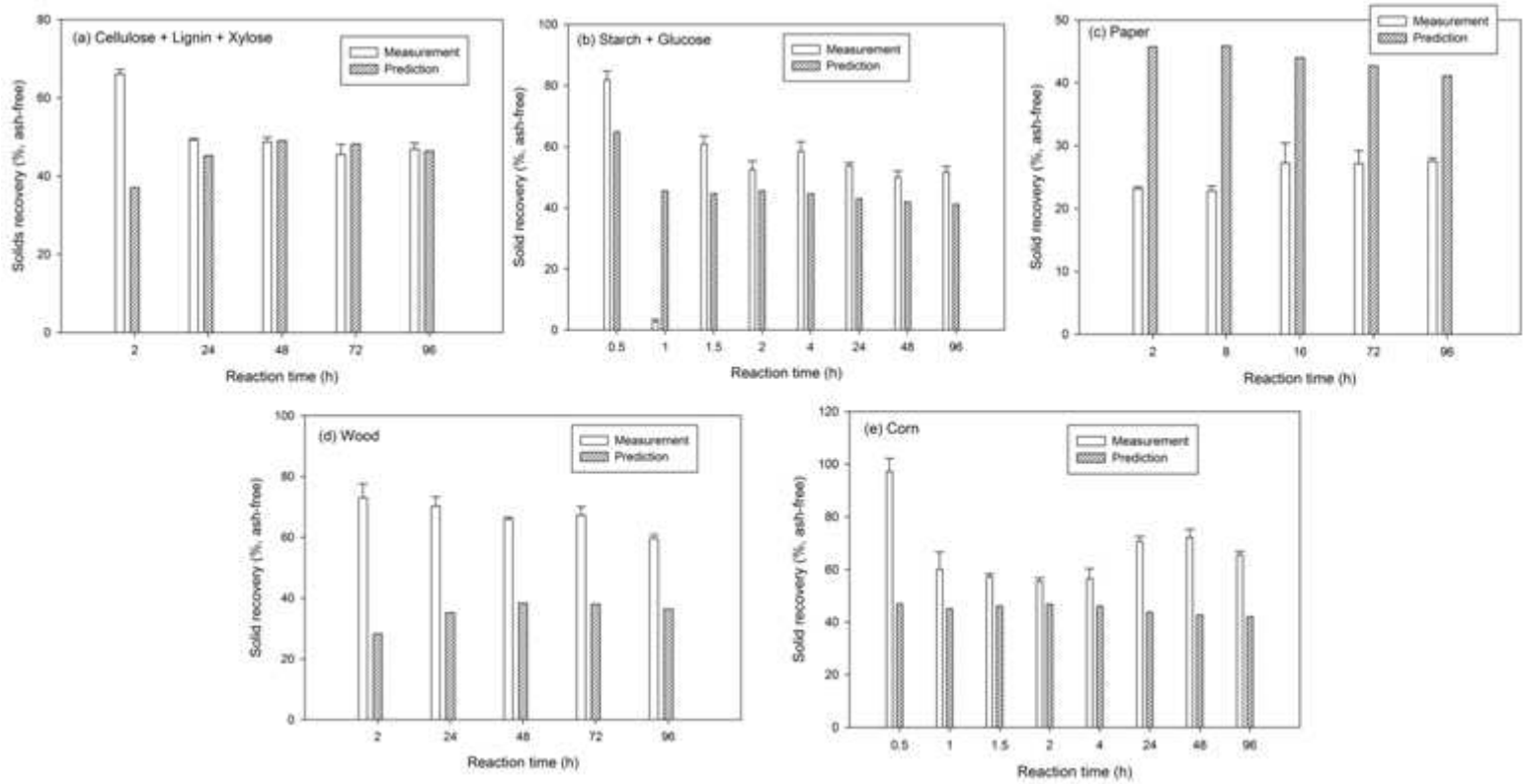

Figure 5.5 Predictions associated with solid recoveries for the carbonization of: (a) mixture of cellulose, lignin, and xylose; (b) mixture of starch and glucose; (c) paper; (d) wood; and (e) corn.

Table 5.3 Percent error between the prediction and measurement of solid recovery, mass of carbon in solid, liquid and gas phases, recovered solids energy content, and functional groups in recovered solids at a reaction time of 96 hours.[a]

Feedstock	Solid recovery (ash-free)	Carbon mass in recovered solids		Carbon mass in the liquid-phase		Carbon mass in the gas-phase		Energy Content (ash-free)	Distribution of functional groups in char					
	Meas. Value	Meas. values	Adj. meas. values	Meas. values	Adj. meas. values	Meas. values	Adj. meas. values	Meas. values	Aliphatic	OCH3	O-alkyl	Aromatic	Furanic/O - aromatic	C=O
C+L+X	0.90	-0.2	-0.2	41.9	41.9	30.8	30.8	-29.0	27.5	89.5	-49.6	-24.5	-16.8	-154.1
Wood	38.9	21.7	-10.6	43.6	20.3	9.2	-28.2	9.5	27.8	89.0	43.8	-82.2	20.3	-346.8
Paper	-49.3	-69.7	-96.5	68.7	63.8	26.0	14.3	18.9	43.3	NA	99.6	-79.2	-68.8	-97.2
S+G	20.3	2.2	2.2	23.1	23.1	-24.6	-24.6	-0.17	-4.8	NA	100	19.3	-21.0	-8.4
Corn	35.9	45.0	45.0	63.1	63.1	45.7	45.7	11.0	13.6	NA	NA	10.0	-71.6	-31.4

[a]positive values indicate an underprediction; negative values indicate an overprediction.

One potential reason for the large differences between the predicted and measured yields associated with the complex feedstocks may result from compound structural differences. The cellulose, hemicellulose (e.g., xylose) and lignin carbonized in this work serve as the basis for these predictions. It is likely, however, that the structure of each of these compounds differs from the structure of these compounds when located within the complex feedstocks. The cellulose, lignin and hemicellulose components of each complex feedstock are chemically bonded within each material by non-covalent bonds and cross-linkages that provide material structure (Iiyama et al., 1994; Saulnier et al., 1995). It is also known, for example, that the structural complexity of cellulose in paper decreases after its manufacture, as evidenced by a reduction in cellulose polymerization during kraft puling of paper (Berggren et al., 2003). Another structural difference that may cause these large prediction errors is related to hemicellulose. In this work, hemicellulose is modeled using xylose. When embedded in the complex materials, hemicellulose forms polymers, combining with cellulose (Kulkarni et al., 1999), resulting a structure different from xylose. It is also highly probable, because of different bonding mechanisms, that the structure of the lignin used in this work differs from the structure of lignin found in paper/wood.

5.3.2 Carbon mass distribution among carbonization products

Carbon mass in the solid, liquid and gas-phases was measured. The resulting carbon recoveries in all experiments range from 70-130%. Mass balance analyses indicate that distribution of the initially present carbon depends on feedstock type and reaction time (Figure 5.6). At early reaction times (< 2 hr), a large fraction of initially

present carbon exists in the liquid-phase. The magnitude of this fraction depends on feedstock characteristics; larger fractions of carbon are initially measured in the liquid-phases when carbonizing feedstocks that are soluble in water at room temperature. Mass balance analyses also indicate that carbonization results in a significant fraction (> 40%) of initially present carbon retained within the solid-phase for all feedstocks after a reaction time of 2 hours (Figure 5.6). Of all the feedstocks carbonized, the solids generated from the carbonization of paper contained the lowest fraction of initially present carbon (44 - 54%), while the solids generated from the carbonization of corn contained the largest fraction of initially present carbon (69 - 90%). Results from analysis of variance (ANOVA) tests indicate that the fractions of initially present carbon found in the solids resulting from the carbonization of paper are statistically different from those obtained when carbonizing all other feedstocks ($p < 0.05$). The fraction of initially present carbon found in the solids during the carbonization of the pure compounds and mixtures of pure compounds and complex feedstocks have statistical similarities. The fractions of initially present carbon found in the solids when carbonizing cellulose are statistically similar ($p > 0.05$) to the cellulose, xylose, lignin mixture (reaction times greater than or equal to 2 hours), wood (all reaction times), mixture of starch and glucose (reaction times greater than or equal to 2 hours), and corn (reaction times greater than or equal to 4 hours). The majority of the fractions of initially present carbon found in the solids recovered when carbonizing starch, xylose, lignin, and glucose are statistically similar to the mixtures of pure compounds and complex feedstocks ($p > 0.05$), except for paper. These results suggest that changes in feedstock complexity/chemical composition

do not impart statistically significant impacts on the fraction of carbon remaining in the solid-phase.

Fractions of initially present carbon transferred to liquid-phase, following initially large values (Figure 5.6), are low, generally less than 20%. Carbonization of paper results in the largest fraction of carbon remaining in the liquid-phase, suggesting the intermediates resulting from paper carbonization differ from those generated during the carbonization of the other evaluated feedstocks. These intermediates resulting from the carbonization of paper appear to have greater liquid-phase solubility. ANOVA test results confirm that the liquid-phase carbon contents resulting from the carbonization of paper are statistically different from the liquid-phase carbon contents resulting from the carbonization of all other feedstocks ($p < 0.05$).

Fractions of carbon are also transferred to the gas-phase as a result of carbonization, consistent with observations in previous studies (e.g., Berge et al., 2011; Hoekman et al., 2011; Li et al., 2013). The fraction of initially present carbon transferred to the gas-phase is below 10% for all feedstocks except paper (Figure 5.6). When carbonizing paper, a significant fraction of carbon was transferred to the gas-phase (between 10 and 25%), suggesting the carbonaceous components of paper are more volatile than those of the other evaluated feedstocks. The carbonization of lignin resulted in the lowest fraction of carbon transferred to the gas-phase, which is consistent with reports that little conversion of lignin occurs during carbonization (Dinjus et al., 2011; Kang et al., 2013) and previously described experimental results. Results from ANOVA tests confirm, with the exception of some early time carbon contents, that gas-phase

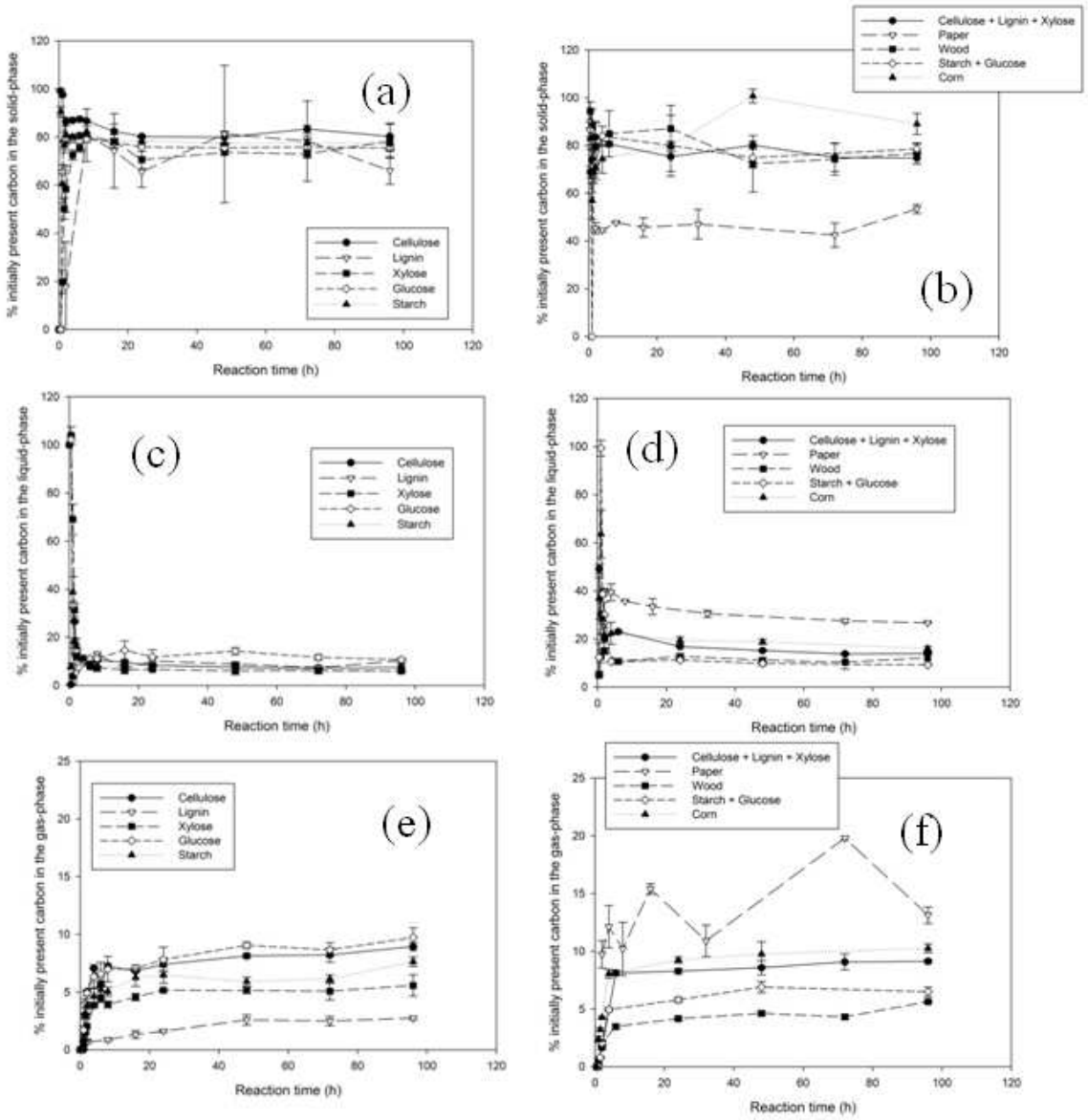

Figure 5.6 Carbon distribution associated with the carbonization of all evaluated feedstocks: (a) % carbon in the solid-phase when carbonizing pure compounds; (b) % carbon in the solid-phase when carbonizing mixtures of pure compounds and complex feedstocks; (c) % carbon in the liquid-phase when carbonizing pure compounds; (d) % carbon in the liquid-phase when carbonizing mixtures of pure compounds and complex feedstocks; (e) % carbon in the gas-phase when carbonizing pure compounds; and (f) % carbon in the gas-phase when carbonizing mixtures of pure compounds and complex feedstocks.

carbon contents are statistically different between all feedstocks ($p < 0.05$). Exceptions to this include a comparison between: (1) glucose and the cellulose, xylose, and lignin mixture at times > 24 hours, (2) glucose and the starch and glucose mixture at reaction times > 24 hours, (3) starch and the starch and glucose mixture at 96 hours, and (4) cellulose and the cellulose, xylose, and lignin mixture at reaction times greater than 16 hours.

5.3.2.1 Prediction of carbon mass in the solid, liquid and gas-phases

Carbon data from the carbonization experiments of the pure feedstocks (e.g., cellulose, lignin, xylose, glucose and starch) were used to predict the mass of carbon in the solid, liquid, and gas-phases resulting from the carbonization of the mixtures of pure compounds and the complex feedstocks (defined in Table 5.1). Results from this analysis are shown in Figure 5.7 – 5.9 and Table 5.3.

The predictions of the mass of carbon in the solid-phase resulting from the carbonization of the mixtures of pure compounds (Figure 5.7) are similar to the measured values at long reaction times (> 4 hours), while the predictions are less accurate at short reactions times (Figure 5.7). This observation suggests that carbonization kinetics are influenced when carbonizing the mixtures of pure compounds. Changes in carbonization kinetics are not surprising; previous work has detailed the influence of lignin presence on carbonization of several mixed feedstocks (e.g., straw, grass, cauliflower, beechwood) (Dinjus et al., 2011), supporting the conclusion that compound interactions may influence carbonization kinetics. The ADL fraction in the recovered solids from the carbonization of the mixtures and complex feedstocks increases with time (Figure 5.4). It is possible the ADL fraction of the solids influences carbonization kinetics. These predictions suggest

that there is no significant compound interaction that results in an overall increase or decrease in solid-phase carbon mass at times of reaction completion. The predictions associated with the final (at reaction times of 96 hours) solid-phase carbon masses for the mixtures of pure compounds vary by less than 3% from the measured values, suggesting such predictions are feasible when carbonizing mixtures of pure compounds that accurately reflect the material in the complex feedstock (Table 5.3).

Greater differences between the predicted and measured carbon masses (Table 5.3) in the solid-phase are observed for the mixed feedstocks (e.g., wood, paper, and corn). The predictions of solid-phase carbon mass from the carbonization of wood and paper are more complicated because the cellulose, hemicellulose, and lignin fractions of these feedstocks comprise only 77 and 88%, respectively, of the total feedstock mass (Table 5.1). To account for this discrepancy, the measured carbon mass was adjusted to only reflect the fraction of carbon represented in the prediction. This adjusted value more accurately reflects the relationship between the prediction and measurement. When considering this adjustment for the carbon found in the solids collected from the carbonization of wood, the accuracy of the prediction improves (~11% error between the measured and predicted values at a reaction time of 96 hours, Figure 5.7 and Table 5.3). When considering this adjustment for the carbon mass in the solids recovered when carbonizing paper, however, the accuracy of the prediction decreases (~97% error). The prediction of the carbon mass found in the solids resulting from the carbonization of corn do not require adjustment, as the starch and sugar contents account for 100% of the feedstock mass. The error associated with the prediction of carbon mass from the solids resulting from the carbonization of the corn at 96 hours is significant (~45%).

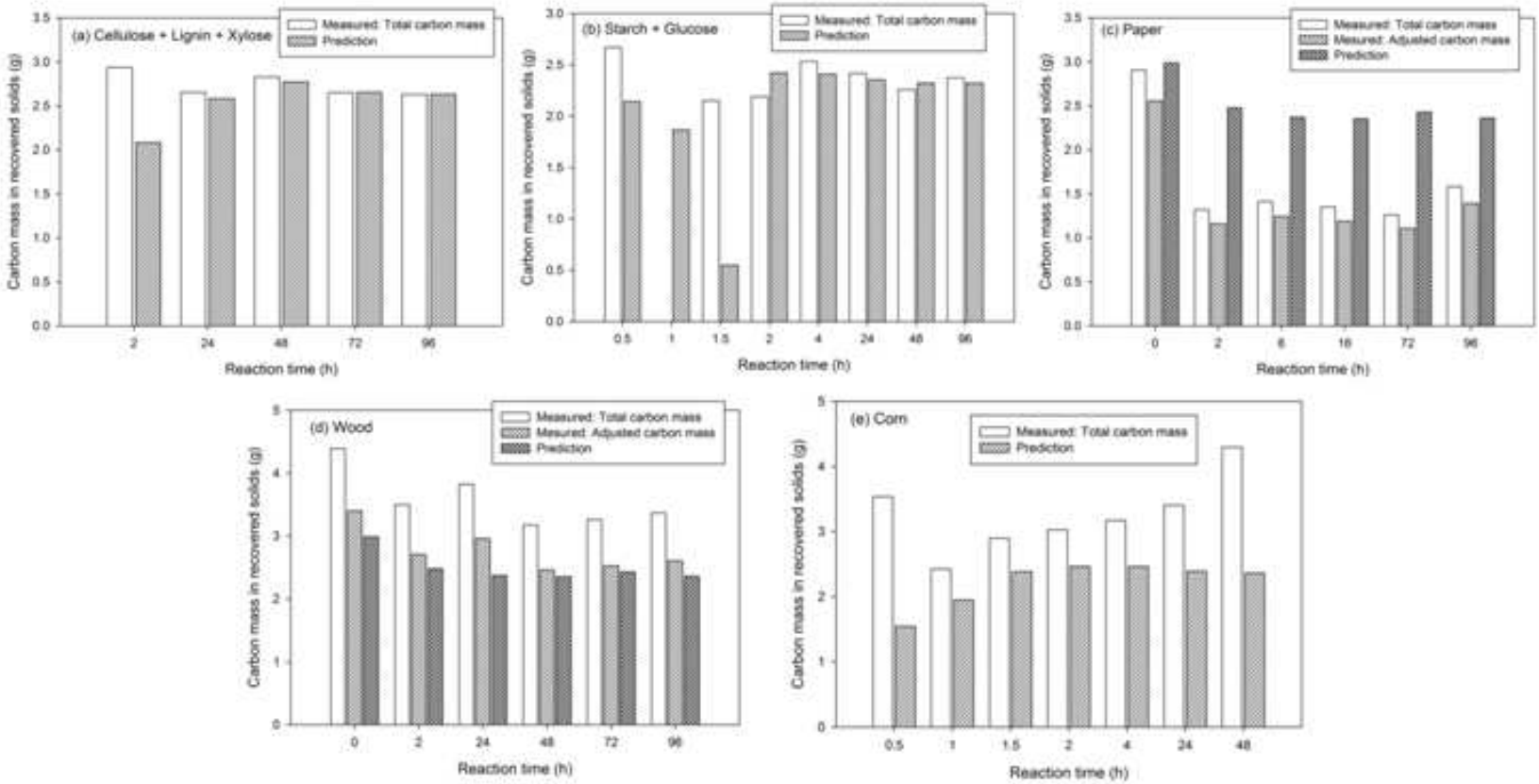

Figure 5.7 Predictions associated with carbon mass in the solid-phase for: (a) mixture of cellulose, lignin, and xylose; (b) mixture of starch and glucose; (c) paper; (d) wood; and (e) corn.

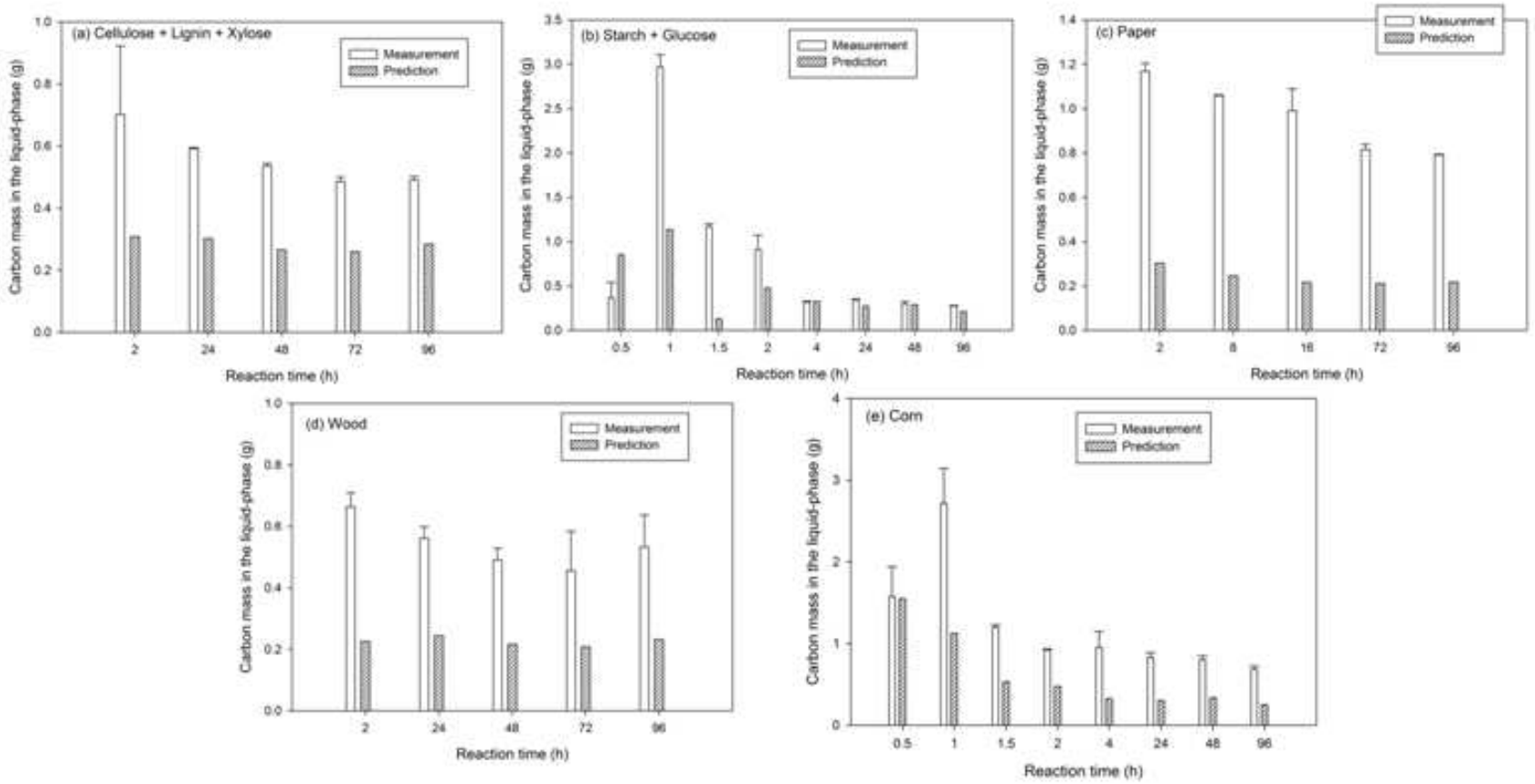

Figure 5.8 Predictions associated with carbon mass in the liquid-phase for: (a) mixture of cellulose, lignin, and xylose; (b) mixture of starch and glucose; (c) paper; (d) wood; and (e) corn.

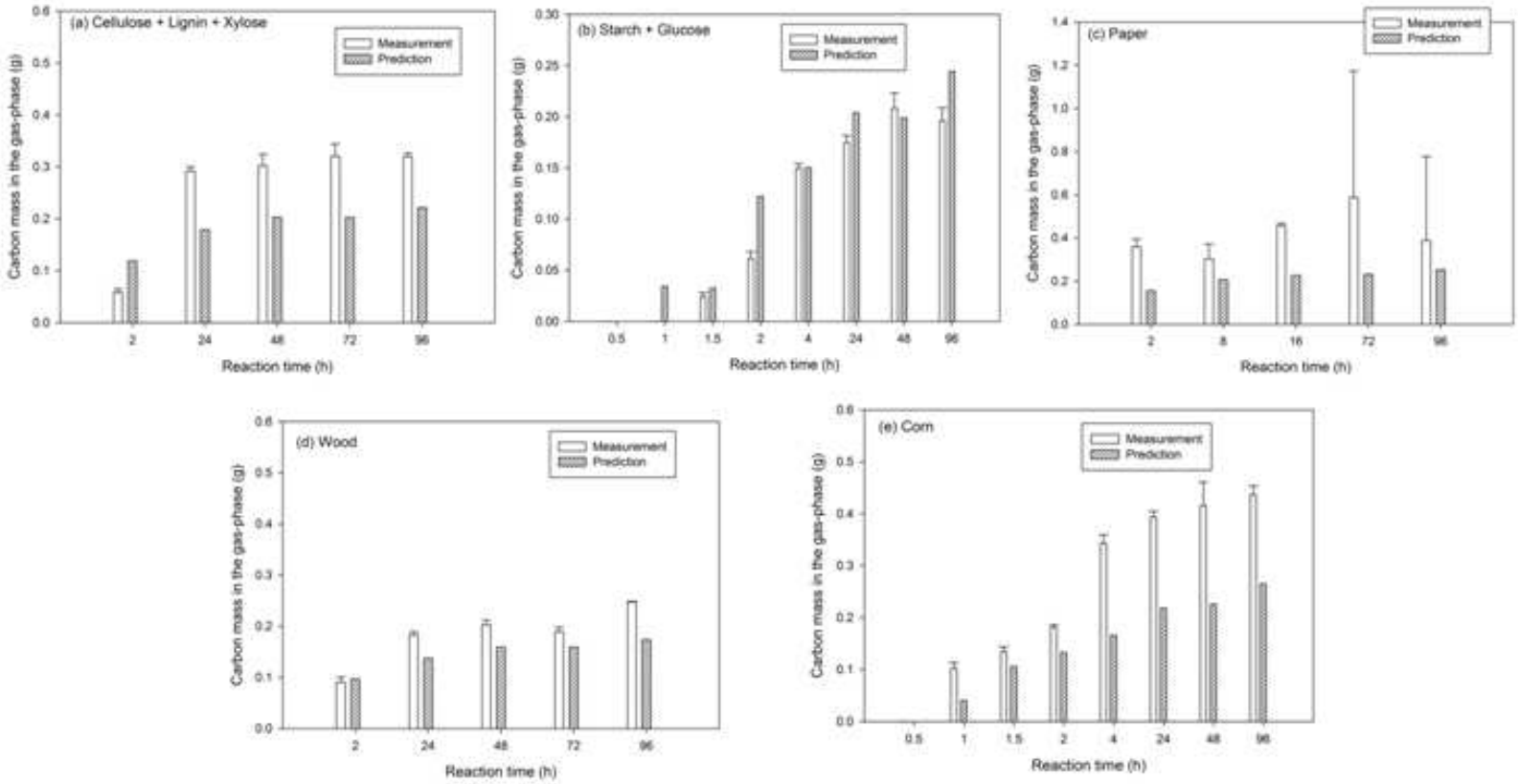

Figure 5.9 Predictions associated with carbon mass in the gas-phase for: (a) mixture of cellulose, lignin, and xylose; (b) mixture of starch and glucose; (c) paper; (d) wood; and (e) corn.

The significant errors associated with the predictive capability of the carbon mass in the solid-phase following the carbonization of complex feedstocks may result because (1) the cellulose, hemicellulose, and lignin fractions of the each feedstock differ in structure and carbon content from those of the pure compounds used in this study or (2) different intermediate products are formed during the carbonization of each feedstock (possibly a result from unaccounted fractions of each feedstock) that interact/influence carbonization. Underprediction of solids carbon mass may suggest that liquid-phase intermediates generated during carbonization catalyze solids formation, similar to that reported by Stemman et al. (2013), resulting in greater solids carbon mass than that expected from the results of pure compound carbonization. It is also important to note that the cellulose, hemicellulose, and lignin fractions of these feedstocks likely differ in structure and carbon content from those of the pure compounds used in this study, also likely contributing to the large prediction error. The components comprising the sugar and starch content of the corn also differ from those used in these experiments. Corn has been reported to contain fractions of fructose, sucrose and maltose (Ferguson et al., 1979); the carbonization of these sugars may result in different solid-phase carbon contents, leading to decreased prediction capabilities.

When predicting the mass of carbon in the solids generated from the carbonization of paper, the carbon mass is significantly overpredicted ~97% error between the measured and predicted values at a reaction time of 96 hours (Figure 5.7) especially when accounting for the fact only 88% of the initial paper composition is accounted for in the prediction. This gross overprediction suggests that the carbon components of the paper are either more amenable to liquid solubility (substantiated by

the greater liquid-phase carbon contents discussed previously), are more volatile, and/or that the model pure compounds used in this work vary significantly from those found in paper.

Predictions of the mass of carbon in the liquid-phase are always lower than the measured mass of carbon in the liquid-phases at a reaction time of 96 hours, even for the mixtures of pure compounds (Figure 5.8). This observation suggests that some interaction of compounds found in these feedstocks and mixtures of pure compounds influences intermediate liquid-phase solubility and may potentially also influence intermediate compound composition. Predicting liquid-phase carbon with the pure compounds used in this work does not appear reasonable, as the percent error between the measured and experimental values is > 20% for all feedstocks (including the mixtures of pure feedstocks) and as high as 64% for paper (Table 5.3).

Carbon mass in the gas-phase is underpredicted for all feedstocks evaluated (Figure 5.8), except for the mixture of starch and glucose and wood, suggesting that fractions of the feedstocks unaccounted for may be volatile in nature, resulting in greater carbon partitioning to the gas-phase. These results are consistent with predictions associated with gas volume (Figure 5.10). The errors associated with this prediction are significant (Table 5.3), suggesting this type of prediction (with the pure feedstocks carbonized in this work) cannot be accurately utilized. It is likely other factors must be included in such a prediction.

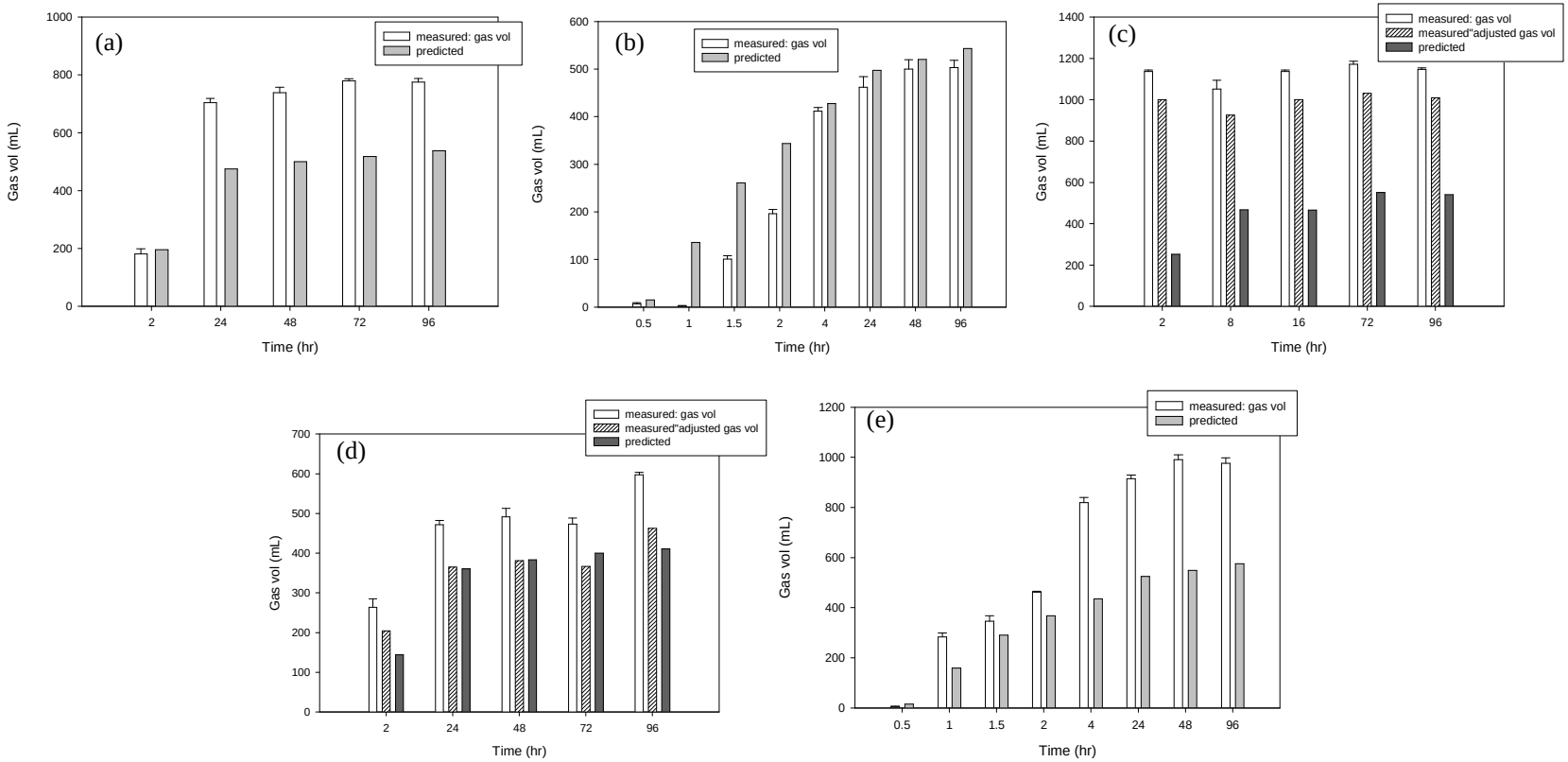

Figure 5.10 Predictions associated with gas volume from: (a) mixture of cellulose, xylose and lignin, (b) mixture of starch and glucose, (c) paper, (d) wood, and (e) corn.

5.3.2.2 Carbon densification

Carbonization results in carbon densification of the recovered solids, as shown in Figure 5.3. Solids recovered from the carbonization of lignin indicate little carbon densification (close to 1). This observation is in-line with the hypothesis that significant fractions of lignin are not converted during carbonization at 250^{o}C and is consistent with that reported by others (Dinjus et al., 2011; Kang et al., 2013) and the ADL results (Figure 5.4). The solids recovered from the carbonization of starch exhibit the largest carbon densification (1.9 after 96 hours) among the pure feedstocks. Evidence of the greater carbon densification associated with starch carbonization is also shown in the structure of the recovered solids (as discussed in subsequent sections). The carbon densification associated with the solids recovered from the carbonization of all pure feedstocks, except lignin, is greater than that associated with the complex feedstocks (e.g., wood, paper, and corn).

5.3.3 Energy content of recovered solids and associated predictions

The energy content of the recovered solids increases with time. The energy content of solids resulting from the carbonization of cellulose (25kJ/g dry solids) have the largest energy content, compared with those generated from the other pure compounds, while solids resulting from the carbonization of paper (26kJ/g dry solids) had the larger energy contents than those associated with the other complex feedstocks.

Ash-free solids energy contents resulting from the carbonization experiments of the pure feedstocks were used to predict the energy contents associated with the mixtures of pure compounds and the complex feedstocks. Results from this analysis are shown in Table 5.3 and Figure 5.11. As with previously described predictions, there are significant

differences between the measured and predicted values at short reaction times, suggesting carbonization kinetics vary between the pure compounds and mixtures/complex compounds. At late reaction times (96 hours), the predictions are significantly closer (Figure 5.11). With the exception of paper and the cellulose, xylose, and lignin mixture, the percent errors associated with all solids energy contents are less than 11% (at a reaction time of 96 hours), suggesting energy content is not as sensitive to changes in feedstock chemical and structural characteristics as other predicted carbonization products. Predictions associated with the energy content of solids recovered from the carbonization of paper and the cellulose, xylose, and lignin mixture vary from the measured values by less than 29%. These results suggest that solids energy content may be predicted based on the results of pure compound carbonization, even if the pure compounds carbonized differ in structure/properties. This is an important observation, providing an approach to predict energy content of the solids from feedstock chemical composition. Such predictions will allow for more informed feedstock selection.

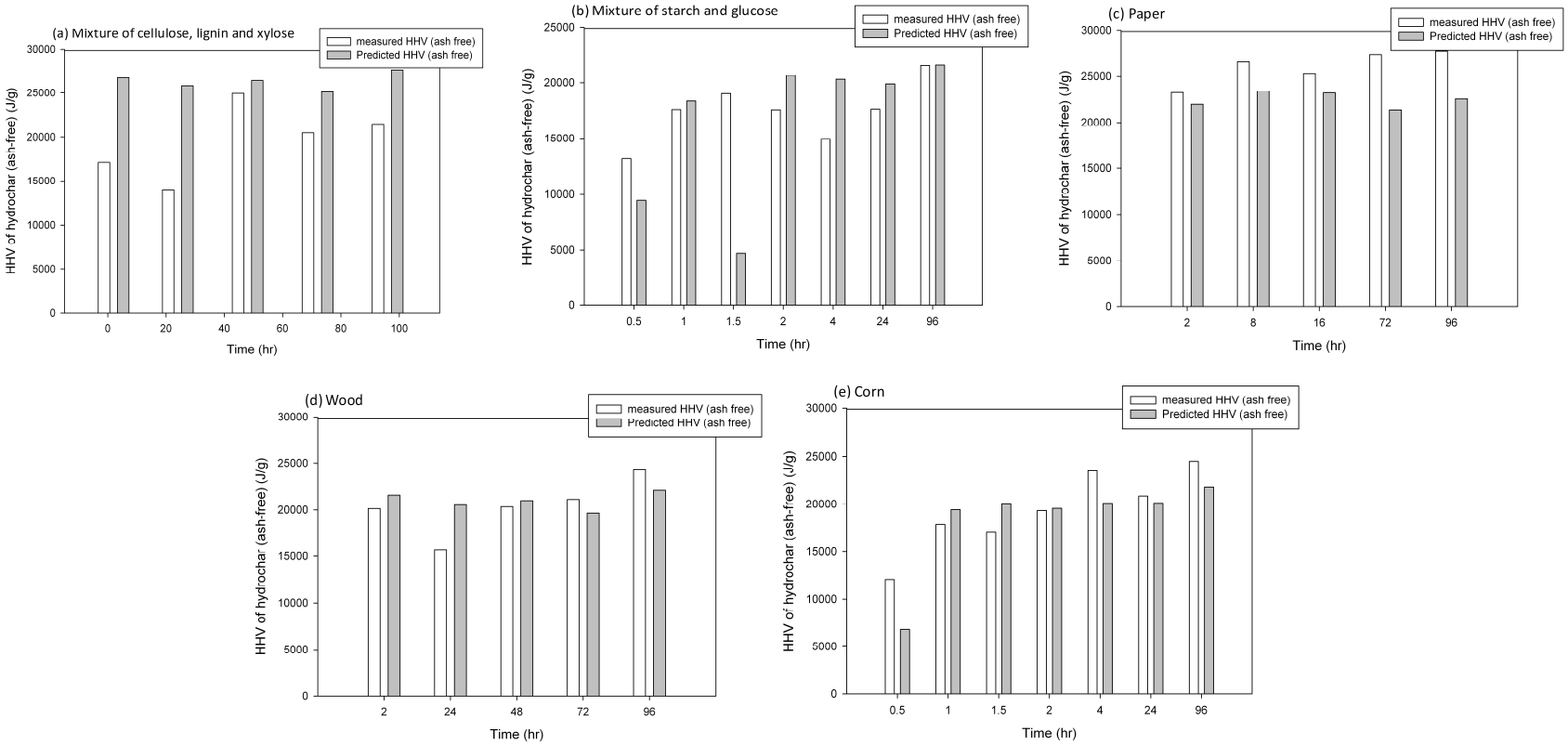

Figure 5.11 Predictions associated with the recovered solids energy content for: (a) mixture of cellulose, xylose and lignin, (b) mixture of starch and glucose, (c) paper, (d) wood, and (e) corn.

5.3.4 Recovered solids chemical characteristics

The ^{13}C NMR spectra of the feedstocks are shown in Figure 5.12 and indicate that cellulose, starch, glucose have peaks in the O-alkyl region (60 – 110 ppm). The peaks associated with glucose and xylose are sharp and narrow, suggesting they have high crystallinity. The spectra of lignin indicates it contains aliphatic, O-alky, aromatic and phenolic compounds, while wood contains compounds associated with lignin and holocellulose. Results indicate that paper contains cellulose/hemicellulose (peaks found in the O-alkyl region), while no compounds associated with lignin are present. The spectrum of corn indicates it mainly contains O-alkyl compounds, with smaller amounts of aliphatic and carboxyl compounds that are likely proteins (Duodu et al., 2001).

5.3.4.1 Pure Compounds

The time dependent characteristics of the solids formed during carbonization, normalized to the carbon content of the solids, for all pure feedstocks are shown in Figure 5.13. These data indicate that as a result of carbonization, the carbon is predominantly converted to furanic, aromatic and alkyl compounds (Figure 5.13). The trends associated with the conversion of cellulose, starch, xylose and glucose are similar. First, O-alkyl bonds associated with the initial feedstocks disappear and aliphatic and carboxyl/carbonyl compounds are subsequently formed. As reaction time increases, increases in the fraction of furanic carbons are observed. These furanic carbons likely result from the polymerization of liquid and/or gas-phase intermediates, such as HMF and furfural (Falco et al., 2011). As reaction times continue to increase, the furanic compounds decrease and

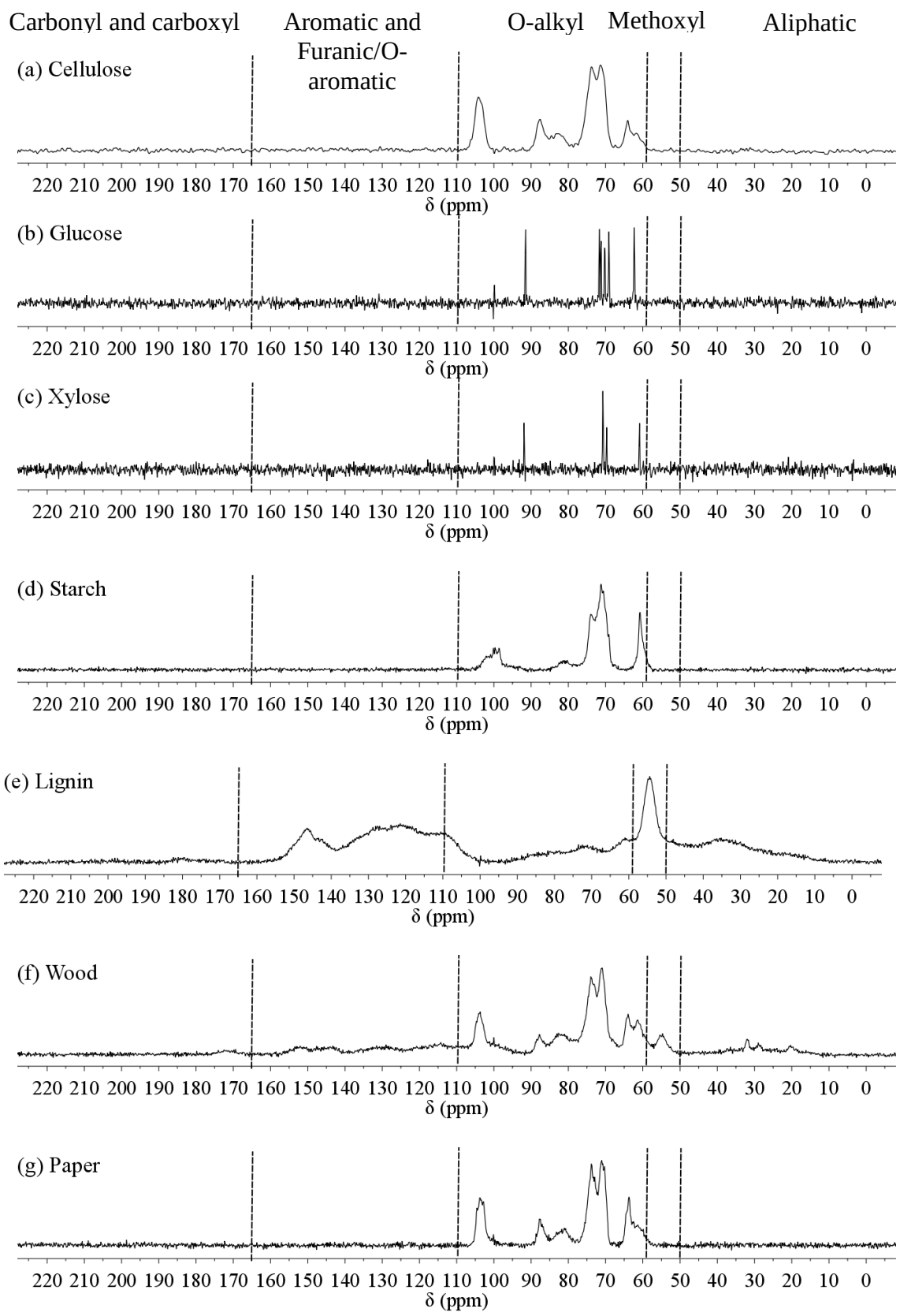
Carbonyl and carboxyl
Aromatic and Furanic/O-aromatic
O-alkyl
Methoxyl
Aliphatic
(a) Cellulose
(b) Glucose
(c) Xylose
(d) Starch
(e) Lignin
(f) Wood
(g) Paper
220 210 200 190 180 170 160 150 140 130 120 110 100 90 80 70 60 50 40 30 20 10 0
δ (ppm)

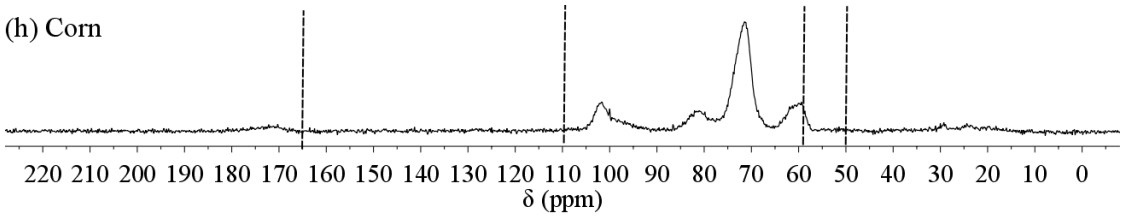

Figure 5.12 ^{13}C NMR spectra of initial feedstocks, (a) cellulose, (b) glucose, (c) xylose, (d) starch, (e) lignin, (f) wood, (g) paper, and (h) corn.

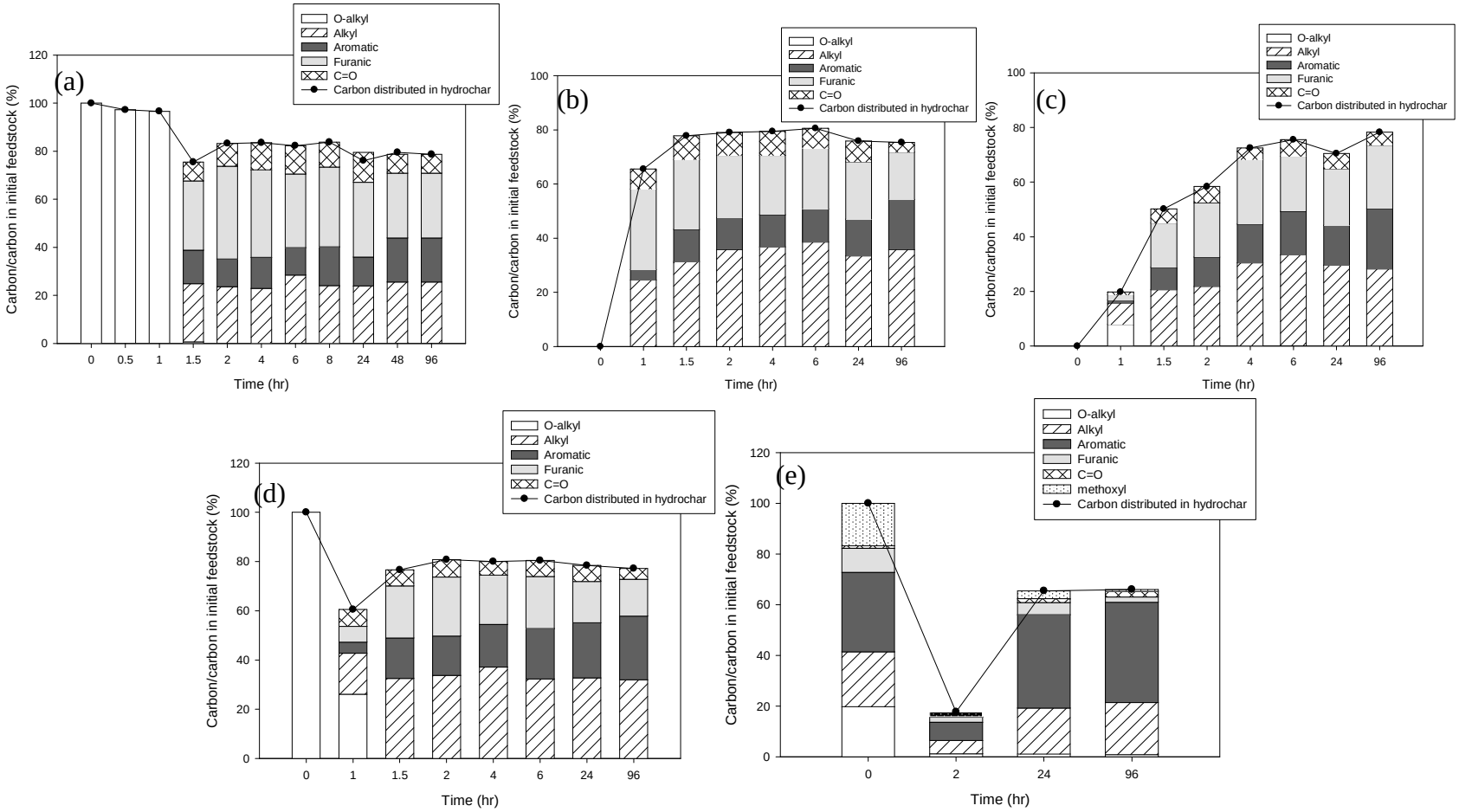

Figure 5.13 Solid-phase carbon distribution data derived from ^{13}C NMR data over time from: (a) cellulose, (b) glucose, (c): xylose, (d) starch, and (e) lignin.

an increase of aromatic compounds is observed. Increases in aromatic compounds are likely a result of the condensation of bonds in polyfuran (such as α-α and β-β) (Falco et al., 2011). The oxygen content of the furanics also decreases, possibly resulting in the formation of polyaromatic hydrocarbons (Falco et al., 2011).

Unlike cellulose, glucose, and xylose, lignin contains aliphatic, methoxyl, O-alkyl, aromatics, O-aromatics and carboxyl/carbonyl compounds (Figure 5.13). Results indicate that the methoxyl and O-alkyl groups associated with lignin decrease with time (Figure 5.13), indicating the O-C bonds in lignin decompose during carbonization. O-aromatic compounds in initial lignin, which represent the C3 and C4 in phenolic alcohol units also decrease with time, indicating a loss of oxygen substitutes on the aromatic rings. The amount of aliphatic, aromatic and C=O compounds are more resistant and remain stable over time.

A ratio to describe the relative condensation extent of the collected solids was developed, as illustrated in equation 1:

$$R = \frac{F + O\text{-}A}{nonO\text{-}A} \qquad (1)$$

where F is the relative amount of α- and β-carbon in furanic compounds, O-A represents the aromatic carbon that is attached to oxygen, and nonO-A represents the relative amount of carbon in aromatic rings that are not connected to oxygen. The relative amounts of F, O-A and nonO-A are calculated using the area of peaks in ^{13}C NMR spectra. The ratio of (F+O-A)/nonO-A reflects the relative amount of less stable or condensed carbon (carbon in F and O-A) to that of more condensed (carbon in nonO-A), and is applied here to describe the condensation extent of the recovered solids. This ratio is based on the assumptions that: (1) the conversion of the furanic compounds to aromatic

compounds in the recovered solids results in a more condensed solid (Falco et al., 2011), and (2) during carbonization of the lignin-containing feedstocks (lignin, mixture of cellulose, lignin, and xylose, and wood), the oxygen in the O-A from the initial feedstocks is likely eliminated (reduced nonO-A), resulting in more condensed aromatic structures.

The (F+O-A)/nonO-A ratios calculated for the recovered solids indicate that greater aromatization/condensation occurs when carbonizing starch (ratio = 0.6), while less aromatization/condensation results when carbonizing glucose (0.9), xylose (1.0), and cellulose (1.5). The larger extent of aromatization/condensation associated with starch is in accord with its highest extent of carbon densification (Figure 5.3).

The solids recovered from the carbonization of lignin have the smallest (F+O-A)/nonO-A ratio (0.1). Interestingly, the solids recovered from lignin after 96 hours contain mainly aromatic and aliphatic compounds, which are likely native to initial lignin structure (Preston et al., 1998). These solids contain no or negligible furanic compounds and more aromatic compounds native to lignin, suggesting little carbonization occurred. This result is consistent with the carbon densification data (little densification was observed, (Figure 5.3) and ADL measurements (Figure 5.4), suggesting little lignin was carbonized/converted.

5.3.4.2 Mixtures of pure compounds and complex feedstocks

The changes in the O-alkyl, furanic, aromatic, aliphatic and C=O containing compounds in the solids recovered over time resulting from the carbonization of the mixture of cellulose, xylose and lignin are similar to that observed when carbonizing pure

cellulose and xylose (Figure 5.14). The observed change in the methoxyl groups is similar to that observed when carbonizing lignin.

Initial wood contains aromatic, O-aromatic and aliphatic compounds resulting from the presence of lignin and O-alkyl from the presence of cellulose, hemicelluloses and lignin (Figure 5.14). The O-alkyl compounds decrease with time as a result of carbonization, similar to the trend observed when carbonizing pure cellulose, hemicelluloses (xylose), and lignin (Figure 5.14). The amount of O-aromatic compounds increases with time, which is likely a result of the formation of furanic compounds from the carbonization of the cellulose and hemicellulose components of the material. Aromatic compounds in the recovered solids do not show a clear increasing trend, as observed when carbonizing cellulose and xylose. Unlike with the pure compounds, a decrease of furanic compounds following their initial formation is observed in the solids recovered from the carbonization of wood. The solids recovered from the carbonization of wood at 96 hrs have the largest (F+O-A)/nonO-A among the solids recovered from all feedstocks evaluated (1.6), indicating the lowest extent of aromatization/condensation.

Initial paper contains O-alkyl compounds as the only functional group detected by ^{13}C NMR, indicating cellulose and hemicellulose as the predominant components, with negligibly identified lignin. There is an observed decrease of furanic compounds coupled with increase of aromatic compounds at longer reaction times when carbonizing paper (Figure 5.14). Accordingly, the (F+O-A)/nonO-A ratio of the recovered solids from the carbonization of paper after 96 hours is 1.5, which is close to ratios associated with the solids recovered from pure cellulose (1.5) and higher than that associated with xylose (1.0).

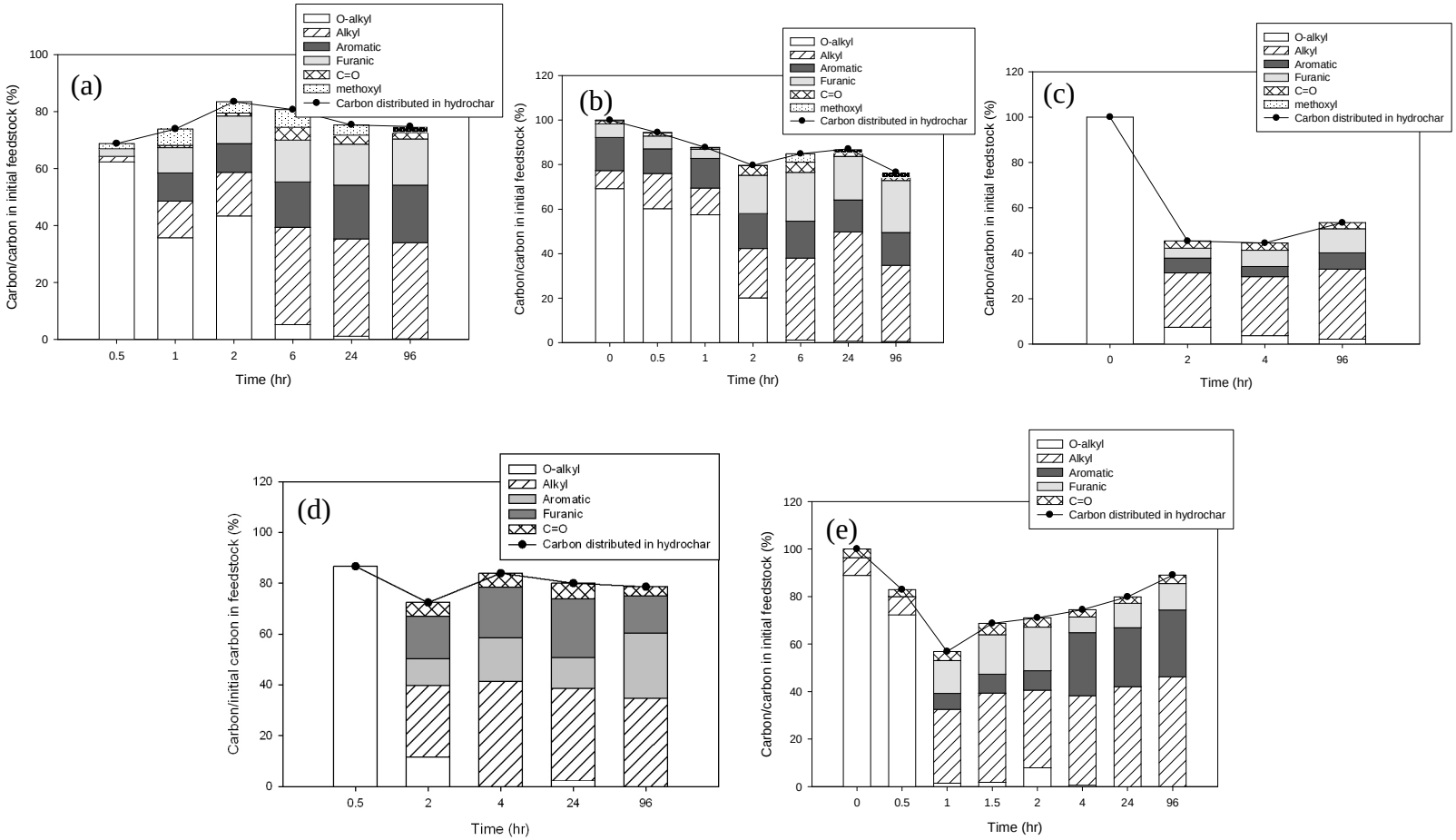

Figure 5.14 Solid-phase carbon distribution data derived from ^{13}C NMR data over time from: (a) mixture of cellulose, xylose and lignin, (b) wood, (c) paper, (d) mixture of starch and glucose, and (e) sweet corn.

The changes of functional groups in the solids recovered from the mixture of starch and glucose and sweet corn are similar to those observed when carbonizing starch and glucose alone (Figure 5.13 and Figure 5.14). The (F+O-A)/nonO-A ratio of the solids recovered from carbonization of the starch and glucose mixture after 96 hours (0.6) is similar to that of the solids recovered form the carbonization of starch (0.6) and lower than those associated with the solids formed during the carbonization of glucose (0.9). The solids recovered from the conversion of sweet corn after 96 hours have a relative high extent of aromatization/condensation, with a (F+O-A)/nonO-A ratio of 0.4, the lowest ratio among all the feedstocks evaluated, except lignin.

5.3.4.3 Prediction of functional groups

The data obtained from the carbonization of the pure compounds, coupled with the known chemical composition of the mixtures of pure compounds and complex feedstocks, were used to predict the functional groups in the mixtures of pure compounds and complex feedstocks present at a reaction time of 96 hours. Results from this analysis are shown in Table 5.3. When predicting the compounds initially containing lignin ((1) mixture of cellulose, xylose, and lignin, (2) paper, and (3) wood), the aromatic, furanic/O-aromatic and carboxyl/carbonyl compounds are overpredicted (Table 5.3), while aliphatic portion is underpredicted. The prediction errors associated with the mixtures of pure compounds are smaller than those associated with the complex feedstocks. These results suggest the complex feedstocks undergo a lesser extent of condensation than can be predicted with the pure compounds carbonized in this study and assuming a linear relationship. Based on results from previous predictions, this result is not surprising. When predicting the functional groups resulting from the carbonization of

the mixture of starch and glucose and corn, the portion of aliphatic compounds is closely approximated (Table 5.3).

The majority of the errors associated with the predictions of functional groups are significantly greater than those associated with predictions of solid yields and carbon masses in each phase. These results suggest that prediction of solids functional groups resulting from carbonization of these feedstocks cannot be predicted using results from the carbonization of pure compounds. It is likely that more detailed chemical characteristics and/or feedstock structural properties are required to make such a prediction.

5.4 CONCLUSIONS

Changes in feedstock composition and complexity influence carbonization product properties. Carbonization product characteristics were predicted using results from the carbonization of pure compounds and indicate that recovered solids energy contents are more accurately predicted than solids yields, and carbon masses in each phase, while predictions associated with solid functional groups are most difficult to predict accurately. These results suggest that suggesting energy content is not as sensitive to changes in feedstock chemical/structural characteristics as other predicted carbonization products. To more correctly predict other carbonization products, compounds more accurately representing the complex feedstocks need to be used as the basis for the predictions.

5.5 SUPPLEMENTARY INFORMATION

This supplementary information section presents Carbonization Product Prediction Calculations.

Calculations based on experimental results from the carbonization of pure compounds (i.e., lignin, cellulose, xylose, starch, glucose) were performed to predict the characteristics associated with the recovered solids from the experiments associated with the mixtures (e.g., cellulose + xylose + lignin and starch + glucose) and mixed feedstocks (i.e., wood, paper, corn). All predictions are based on the assumption that there is a linear relationship between carbonization product characteristics and feedstock type and concentration.

The relationship used for the prediction of solids yields is presented in equation 1:

$$P_{yield,1} = f_{cellulose} Y_{cellulose} + f_{lignin} Y_{lignin} + f_{hemicellulose} Y_{xylose} + f_{starch} Y_{starch} + f_{sugars} Y_{glucose} \quad (1)$$

where, $P_{yield,1}$ represents the predicted ash-free yield at a specific reaction time, $f_{cellulose}$, f_{lignin}, $f_{hemicellulose}$, f_{starch}, f_{sugars}, f_{ash} represent the fraction of each of these compounds in the compound mixtures or complex feedstocks, and $Y_{cellulose}$, Y_{lignin}, Y_{xylose}, Y_{tarch}, $Y_{glocose}$ are the ash-free solid yields measured from the carbonization of these pure compounds at the specific reaction time. Note that the hemicellulose fraction is modeled in these experiments with xylose and sugars are represented by glucose. It was also assumed that no starch or sugar was in the wood or paper and no cellulose, hemicellulose, or lignin is present in the corn. These calculations assume that the mass of ash remains constant throughout the duration of each experiment.

Similar calculations were performed to predict the carbon mass in the solid, liquid and gas-phases as a result of the known chemical composition. The gas-phase volumes were also predicted. These relationships are defined in equations 2 to 5:

$$C_s = f_{cellulose}C_{s,cellulose} + f_{lignin}C_{s,lignin} + f_{hemicellulose}C_{s,xylose} + f_{starch}C_{s,starch} + f_{sugars}C_{s,glucose} \quad (2)$$

$$C_l = f_{cellulose}C_{l,cellulose} + f_{lignin}C_{l,lignin} + f_{hemicellulose}C_{l,xylose} + f_{starch}C_{l,starch} + f_{sugars}C_{l,glucose} \quad (3)$$

$$C_g = f_{cellulose}C_{g,cellulose} + f_{lignin}C_{g,lignin} + f_{hemicellulose}C_{g,xylose} + f_{starch}C_{g,starch} + f_{sugars}C_{g,glucose} \quad (4)$$

$$V = f_{cellulose}V_{cellulose} + f_{lignin}V_{lignin} + f_{hemicellulose}V_{xylose} + f_{starch}V_{starch} + f_{sugars}V_{glucose} \quad (5)$$

where, C_s is the carbon mass in the solid-phase (g), $C_{s,lignin}$, $C_{s,cellulose}$, $C_{s,xylose}$, and $C_{s,glucose}$ are the masses of carbon measured in the solid-phase when carbonizing the pure feedstocks, $C_{l,lignin}$, $C_{l,cellulose}$, $C_{l,xylose}$, and $C_{l,glucose}$ are the masses of carbon measured in the liquid-phase when carbonizing the pure feedstocks, $C_{g,lignin}$, $C_{g,cellulose}$, $C_{g,xylose}$, and $C_{g,glucose}$ are the masses of carbon measured in the gas-phase when carbonizing the pure feedstocks, and V_{lignin}, $V_{cellulose}$, V_{xylose}, and $V_{glucose}$ are the gas volumes measured when carbonizing the pure feedstocks. It should be noted that these predictions only account for the chemical compounds measured; other compounds are not taken into account in these predictions.

Recovered solids energy contents were predicted using a similar technique, as outlined in equation 6:

$$E_{s,t} = f_{cellulose}E_{cellulose} + f_{lignin}E_{lignin} + f_{hemicellulose}E_{hemicellulose} + f_{starch}E_{starch} + f_{sugar}E_{sugar} \quad (6)$$

where, $E_{s,t}$ represents the predicted ash-free solids energy content at a specific reaction time and $E_{cellulose}$, E_{lignin}, E_{xylose}, E_{starch}, $E_{glocose}$ are the ash-free solid energy contents measured from the carbonization of these pure compounds at the specific reaction time. Note that the hemicellulose fraction is modeled in these experiments with xylose and sugars are represented by glucose. It was also assumed that no starch or sugar was in the wood or paper and no cellulose, hemicellulose, or lignin is present in the corn.

The percent of carbon in forms of different function groups are predicted by the following equation:

$$f_i = \frac{\left(f_{cellulose} C_{s,cellulose,i} + f_{lignin} C_{s,lignin,i} + f_{hemicellulose} C_{s,xylose,i} + f_{starch} C_{s,starch,i} + f_{sugars} C_{s,glucose,i} \right)}{C_{feed}} \quad (7)$$

where, f_i represents the percent of carbon in form of functional group i in the recovered solids, $C_{cellulose,i}$, $C_{s,lignin,i}$, $C_{s,xylose,i}$, $C_{s,starch,i}$, and $C_{s,glucose,i}$ are the mass of carbon in functional group i measured in the recovered solids from these pure compounds, and C_{feed} represents the total mass of carbon present in the initial feedstock.

5.6 ACKNOWLEDGEMENTS

This material is based upon work supported by the National Science Foundation under Grant No. 1055327. Any opinions, findings, and conclusions or recommendations expressed in this material are those of the author(s) and do not necessarily reflect the views of the National Science Foundation.

CHAPTER 6.

CONCLUSIONS AND RECOMMENDATIONS

6.1 CONCLUSIONS

Hydrothermal carbonization is an environmentally beneficial means to convert waste materials to value-added products, including carbon-rich, energy-dense solids and nutrient and chemical rich liquids. A series of experiments were conducted to determine how reaction conditions and heterogeneous compound mixtures (representative of municipal wastes) influence hydrothermal carbonization processes. These experiments were designed to: (1) determine how carbonization product properties are manipulated by controlling feedstock composition, process conditions, and catalyst addition; (2) determine if carbonization of heterogeneous mixtures follows similar pathways as that with pure feedstocks; and (3) evaluate and compare the carbon and energy-related implications associated with carbonization products with those associated with other common waste management processes for solid waste. The main findings associated with this work include:

- Feedstock type influences the properties of the generated hydrochar material. Solid yields have a linear relationship with the carbon content of feedstock, with

yields increasing with increasing feedstock carbon content.. In addition, the chemical composition of the solids generated from the carbonization of cellulose, xylose, glucose and starch contain mainly furanic, aromatic and aliphatic compounds, while solids generated from the carbonization of lignin is composed mainly of aromatics (with and without substitute oxygen) and aliphatic compounds. Solids generated from the carbonization of mixed feedstocks (e.g., wood) have compositions similar to those comprising their chemical composition.

- Feedstock type also appears to influence solids formation. Solids formation appears to be slower for mixed and complex feedstocks that of the corresponding pure feedstocks evaluated, except for lignin.
- Using data from the carbonization of the model compounds, the carbonization product characteristics associated with the mixtures of pure compounds and complex feedstocks were predicted. Results from this analysis indicate solids recoveries and carbon mass in the solids are predicted reasonably well for the mixture of pure compounds (< 20% error associated with the prediction). However, differences between the measured and predicted values for the carbon masses in the liquid and gas as well as the solids functional groups are significant for these mixtures, suggesting compound interaction may be occurring.
- Reaction time and temperature influence carbonization product composition. At early times, feedstocks are solubilized and subsequently form reactive intermediates, which are converted to more stable products in solid, liquid and gas. Higher temperatures and longer reaction times generally result in the increase of solids energy content, production of CO_2 and hydrocarbons in gas phase.

- Catalyst addition influences carbonization. Changes in the properties of initial process water (e.g., pH, ionic strength and organics) impart a kinetic effect, on carbonization, with little influence on final products. These qualities of process water have most significant influence on final carbon distributed in gas. $CaCl_2$ at 0.5 N (highest concentration in the present study) has more significant influence final product properties, probably due to its passivation effect on the generated solid surfaces.
- The environmental implications associated with the carbonization of waste materials depend on the ultimate use of hydrochar. If carbon in hydrochar remains stored after its utilization (such as soil amendment, catalyst, etc), HTC releases less GHG than other current used waste management processes (landfill, composting and incineration) and may serve as an effective and sustainable process for carbon sequestration.
- When hydrochar from waste materials is used as a solid fuel, no carbon remains sequestered. In addition, the hydrochar generated from waste materials has the potential to generate energy than that associated with collected landfill gas.

6.2 Recommendations for Future Work

Hydrothermal carbonization of wastes is still in developing. A greater understanding associated with the potential implications associated with energy generation from the solids and the environmental implications of the gas and liquid products is needed. Further study of the application of hydrochar is necessary. The stability of hydrochar in nature will show the ultimate potential for carbon sequestration

via carbonization. Energetic application of hydrochar requires more detailed information, such as combustion behaviours, requirement for facility of combustion or co-combustion with coal. A life cycle analysis will provide a macroscopic understanding of environmental impact and the energetic application of HTC, as well as other current used waste management techniques. This analysis is the next step in providing the information necessary to allow more informed scale-up of the process.

In addition, more detailed analyses evaluating carbonization are required. Development of a conceptual model of HTC will help to better understand specific carbonization mechanisms and ultimately allow the prediction of carbonization product characteristics under different experimental conditions (such as feedstock type, temperature and time). A kinetic analysis is required to quantitatively investigate the effect of reaction time and temperature on HTC process. Understanding how feedstock complexity influences carbonization is also important and should be evaluated in more detail in future studies.

REFERENCE

http://online.sfsu.edu/tripp/SFSU/Chem335/Entries/2011/4/15_Presentations_files/Dihydroxyacetone.pdf

Municipal Waste Streams. *Environmental Science & Technology*, 45, 5696-5703.

Aggarwal, P., Dollimore, D., 1996. A comparative study of the degradation of different starches using thermal analysis. *Talanta*, 43, 1527-1530.

Akiya, N., Savage, P.E., 2002. Roles of water for chemical reactions in high-temperature water. *Chemical Reviews*, 102, 2725-2750.

Antal Jr, M.J., Mok, W.S., Richards, G.N. 1990. Four-carbon model compounds for the reactions of sugars in water at high temperature. *Carbohydrate Research*, 199(1), 111-115.

Asghari, F.S., Yoshida, H. 2006. Acid-catalyzed production of 5-hydroxymethyl furfural from D-fructose in subcritical water. *Industrial & Engineering Chemistry Research* 45(7), 2163-2173.

Atalla, R.H., Vanderhart, D.L., 1984. Native cellulose: A composite of two distinct crystalline forms. Science, 223, 283-285.

Baccile, N., Laurent, G., Babonneau, F., Fayon, F., Titirici, M.-M., Antonietti, M., 2009. Structural characterization of hydrothermal carbon spheres by advanced solid-state MAS 13C NMR investigations. *Journal of Physical Chemistry C*, 113, 9644 –9654.

Barlaz, M.A., 1998. Carbon storage during biodegradation of municipal solid waste components in laboratory-scale landfills. *Global Biogeochemical Cycles*, 12, 373-380.

Berge, N.D., Reinhart, D.R., Batarseh, E.S., 2009. An assessment of bioreactor landfill costs and benefits. *Waste Management*, 29, 1558-1567.

Berge, N.D., Ro, K.S., Mao, J.D., Flora, J.R.V., Chappell, M.A., Bae, S.Y., 2011. Hydrothermal Carbonization of Municipal Waste Streams. *Environmental Science & Technology*, 45 (13), 5696-5703.

Berggren, R., Berthold, F., Sjoholm, E., Lindstrom, M., 2003. Improved methods for evaluating the molar mass distributions of cellulose in Kraft pulp. *Journal of Applied Polymer Science*, 88, 1170-1179.

Bergius, F., 1913. Formation of anthracite. *Zeitschrift Fur Elektrochemie Und Angewandte Physikalische Chemie*, 19, 858-860.

Bogner, J.E., Spokas, K.A., Chanton, R.P., 2011. Seasonal Greenhouse Gas Emissions (Methane, Carbon Dioxide, Nitrous Oxide) from Engineered Landfills: Daily, Intermediate, and Final California Cover Soils. *Journal of Environmental Quality*, 40, 1010-1020.

Bosmans, A., Vanderreydt, I., Geysen, D., Helsen, L., 2010. The crucial role of Waste-to-Energy technologies in enhanced landfill mining: a technology review. *Journal of Cleaner Production*, 55, 10-23.

Bridgwater, T., 2006. Biomass for energy. *Journal of the Science of Food and Agriculture*, 86, 1755-1768.

Buah, W.K., Cunliffe, A.M., Williams, P.T., 2007. Characterization of products from the pyrolysis of municipal solid waste. *Process Safety and Environmental Protection*, 85, 450-457.

Cao, D., Sun, Y., Wang, G., 2007. Direct carbon fuel cell: Fundamentals and recent developments. *Journal of Power Sources*, 167, 250-257.

Cao, X.Y., Ro, K.S., Chappell, M., Li, Y.A., Mao, J.D., 2011. Chemical Structures of Swine-Manure Chars Produced under Different Carbonization Conditions Investigated by Advanced Solid-State C-13 Nuclear Magnetic Resonance (NMR) Spectroscopy. *Energy & Fuels*, 25, 388-397.

Carrier, M., Loppinet-Serani, A., Absalon, C., Aymonier, C., Mench, M., 2012. Degradation pathways of holocellulose, lignin and α-cellulose from Pteris vittata fronds in sub- and super critical conditions. *Biomass and Bioenergy*, 43, 65-71.

Chang, Y.H., Chen, W.C., Chang, N.B., 1998. Comparative evaluation of RDF and MSW incineration. *Journal of Hazardous Materials*, 58, 33-45.

Channiwala, S.A., Parikh, P.P., 2002. A unified correlation for estimating HHV of solid, liquid and gaseous fuels. Fuel, 81, 1051-1063.

Chen, J., Chen, Z., Wang, X., Li, X. 2012. Calcium-assisted hydrothermal carbonization of an alginate for the production of carbon microspheres with unique surface nanopores. *Mater Lett*, 67, 365-368.

Chuntanapum, A., Matsumura, Y. 2009. Formation of Tarry Material from 5-HMF in Subcritical and Supercritical Water. *Industrial & Engineering Chemistry Research*, 48(22), 9837-9846.

Cui, X.J., Antonietti, M., Yu, S.H., 2006. Structural effects of iron oxide nanoparticles and iron ions on the hydrothermal carbonization of starch and rice carbohydrates. *Small*, 2, 756-759.

Debzi, E.M., Chanzy, H., Sugiyama, J., Tekely, P., Excoffier, G., 1991. The Iα → Iβ transformation of highly crystalline cellulose by annealing in various mediums. *Macromolecules*, 24, 6816-6822.

Demir-Cakan, R., Baccile, N., Antonietti, M., Titirici, M.-M., 2009. Carboxylate-Rich Carbonaceous Materials via One-Step Hydrothermal Carbonization of Glucose in the Presence of Acrylic Acid. *Chemistry of Materials*, 21, 484-490.

Demirbas, A., 2000. Mechanisms of liquefaction and pyrolysis reactions of biomass. *Energy Conversion and Management*, 41, 633-646.

Dinjus, E., Kruse, A., Tröger, N., 2011. Hydrothermal Carbonization – 1. Influence of Lignin in Lignocelluloses. *Chemical Engineering & Technology*, 34, 2037-2043.

Dudley, R.L., Fyfe, C.A., Stephenson, P.J., Deslandes, Y., Hamer, G.K., Marchessault, R.H., 1983. High resolution carbon 13C CP/MAS NMR spectra of solid cellulose oligomers and the structure of cellulose II. *Journal of the American Chemical Society*, 105, 2469 – 2472.

Duodu, K.G., Tang, H., Grant, A., Wellner, N., Belton, P.S., Taylor, J.R.N., 2001. FTIR and solid state ^{13}C NMR spectroscopy of proteins of wet cooked and popped sorghum and maize. *Journal of Cereal Science*, 33, 261-269.

Eleazer, W.E., Odle, W.S., Wang, Y.S., Barlaz, M.A., 1997. Biodegradability of municipal solid waste components in laboratory-scale landfills. *Environmental Science & Technology*, 31, 911-917.

Enthaler, S., J. von Langermann, Schmidt, T., 2010. Carbon idoxide and formic acid - the couple for environmental-friendly hydrogen storage? *Energy & Environmental Science*, 3(9), 1207-1217.

Erlach, B., Harder, B., Tsatsaronis, G., 2012. Combined hydrothermal carbonization and gasification of biomass with carbon capture. *Energy*, 45, 329-338.

Escala, M., Zumbuehl, T., Koller, C., Junge, R., Krebs, R., 2013. Hydrothermal Carbonization as an Energy-Efficient Alternative to Established Drying Technologies for Sewage Sludge: A Feasibility Study on a Laboratory Scale. *Energy & Fuels*, 27, 454-460.

Falco, C., Baccile, N., Titirici, M.-M., 2011. Morphological and structural differences between glucose, cellulose and lignocellulosic biomass derived hydrothermal carbons. *Green Chemistry*, 13, 3273-3281.

Falco, C., Caballero, F.P., Babonneau, F., Gervais, C., Laurent, G., Titirici, M.-M., Baccile, N. 2012. Hydrothermal Carbon from Biomass: Structural Differences between Hydrothermal and Pyrolyzed Carbons via C-13 Solid State NMR. *Langmuir*, 27(23), 14460-14471.

Fang, Z., Tang, K.B., Lei, S.J., Li, T.W., 2006. CTAB-assisted hydrothermal synthesis of Ag/C nanostructures. *Nanotechnology*, 17, 3008-3011.

Ferguson, J. E., Dickinson, D. B., Rhodes, A. M., 1979. Analysis of endosperm sugars in a sweet corn inbred (Illinois 677a) which contains the sugary enhancer (se) gene and comparison of se with other corn genotypes. *Plant physiology*, 63, 416-420.

Fuertes, A.B., Arbestain, M.C., Sevilla, M., Macia-Agullo, J.A., Fiol, S., Lopez, R., Smernik, R.J., Aitkenhead, W.P., Arce, F., Macias, F., 2010. Chemical and structural properties of carbonaceous products obtained by pyrolysis and hydrothermal carbonisation of corn stover. *Australian Journal of Soil Research*, 48, 618-626.

Flora, J.F.R., Lu, X., Li, L., Flora, J.R.V., Berge, N.D. 2013. The effects of alkalinity and acidity of process water and hydrochar washing on the adsorption of atrazine on hydrothermally produced hydrochar. *Chemosphere*, 93(9), 1989-1996.

Funke, A., Ziegler, F., 2009. Hydrothermal carbonization of biomass: a literature survey focusing on its technical application and prospects. 17th European biomass conference and Ezhibition, Hamburg, Germany, pp. 1037-1050.

Funke, A., Ziegler, F., 2010. Hydrothermal carbonization of biomass: A summary and discussion of chemical mechanisms for process engineering. *Biofuels Bioproducts & Biorefining-Biofpr*, 4, 160-177.

Gao, Y., Wang, X.-H., Yang, H.-P., Chen, H.-P., 2012. Characterization of products from hydrothermal treatments of cellulose. *Energy*, 42, 457-465.

Goto, M., Obuchi, R., Hiroshi, T., Sakaki, T., Shibata, M., 2004. Hydrothermal conversion of municipal organic waste into resources. *Bioresource Technology*, 93, 279-284.

Hao, W., Björkman, E., Lilliestråle, M., Hedin, N., 2013. Activated carbons prepared from hydrothermally carbonized waste biomass used as adsorbents for CO_2. *Applied Energy*, 112, 562-532.

Hatfield, R., Fukushima, R. S., 2005. Can lignin be accurately measured? *Crop science*, 45, 832-839.

He, M., Xiao, B., Liu, S., Guo, X., Luo, S., Xu, Z., Feng, Y., Hu, Z., 2009. Hydrogen-rich gas from catalytic steam gasification of municipal solid waste (MSW): Influence of steam to MSW ratios and weight hourly space velocity on gas production and composition. *International Journal of Hydrogen Energy*, 34, 2174-2183.

Hermann, B.G., Debeer, L., De Wilde, B., Blok, K., Patel, M.K., To compost or not to compost: Carbon and energy footprints of biodegradable materials' waste treatment. *Polymer Degradation and Stability*, 96, 1159-1171.

Hoekman, S.K., Broch, A., Robbins, C., 2011. Hydrothermal Carbonization (HTC) of Lignocellulosic Biomass. *Energy & Fuels*, 25, 1802 – 1810.

Hoover, R., 2001. Composition, molecular structure, and physicochemical properties of tuber and root starches: a review. *Carbohydrate Polymers*, 45, 253-267.

Horvat, J., Klaic, B., Metelko, B., Sunjic, V. 1985. Mechanism of levulinic acid formation. *Tetrahedron Letters*, 26(17), 2111-2114.

Hosoya, T., Kawamoto, H., Saka, S., 2009. Role of methoxyl group in char formation from lignin-related compounds. *Journal of Analytical and Applied Pyrolysis*, 84, 79-83.

Huber, G. W., J. N. Chheda, et al. (2005). Production of liquid alkanes by aqueous-phase processing of biomass-derived carbohydrates. *Science,* 308(5727), 1446-1450.

Hwang, I.H., Aoyama, H., Matsuto, T., Nakagishi, T., Matsuo, T. 2012. Recovery of solid fuel from municipal solid waste by hydrothermal treatment using subcritical water. *Waste Management*, 32(3), 410-416.

Hwang, I.H., Matsuto, T., Nakagishi, T., Matsuo, T., 2010. Recovery of solid fuel from municipal solid waste using hydrothermal treatment Third International symposium on Energy from Biomass and WAste, Venice, Italy.

Iiyama, K., Lam, T.B.T., Stone, B.A., 1994. Covalent cross-links in the cell wall *Plant Physiology*, 104, 315-320.

Kammann, C., Ratering, S., Eckhard, C., Muller, C., 2012. Biochar and hydrochar effecrs on greenhouse gas (carbon dioxide, nitrous oxide, and methane) fluxes from soil. *Journal of Environmental Quality*, 41, 1052-1066.

Kang, S., Li, X., Fan, J., Chang, J., 2012. Characterization of Hydrochars Produced by Hydrothermal Carbonization of Lignin, Cellulose, d-Xylose, and Wood Meal. *Industrial & Engineering Chemistry Research*, 51, 9023-9031.

Kang, S., Li, X., Fan, J., Chang, J., 2013. Hydrothermal conversion of lignin: A review. *Renewable and Sustainable Energy Reviews* 27, 546-558.

Khawam, A., Flanagan, D.R., 2006. Solid-state kinetic models: Basics and mathematical fundamentals. *Journal of Physical Chemistry B,* 110, 17315-17328.

Knežević, D., van Swaaij, W.P.M., Kersten, S.R.A. 2009. Hydrothermal Conversion of Biomass: I, Glucose Conversion in Hot Compressed Water. *Industrial & Engineering Chemistry Research*, 48(10), 4731-4743.

Knežević , D., van Swaaij, W., Kersten, S., 2010. Hydrothermal Conversion Of Biomass. II. Conversion Of Wood, Pyrolysis Oil, And Glucose In Hot Compressed Water. *Industrial & Engineering Chemistry Research*, 49, 104 –112.

Kono, H., Yunoki, S., Shikano, T., Fujiwara, M., Erata, T., Takai, M., 2002. CP/MAS C-13 NMR study of cellulose and cellulose derivatives. 1. Complete assignment of the CP/MAS C-13 NMR spectrum of the native cellulose. *Journal of the American Chemical Society*, 124, 7506-7511.

Kobayashi, N., Okada, N., Hirakawa, A., Sato, T., Kobayashi, J., Hatano, S., Itaya, Y., Mori, S., 2008. Characteristics of Solid Residues Obtained from Hot-

Compressed-Water Treatment of Woody Biomass. *Industrial & Engineering Chemistry Research*, 48, 373-379.

Kruse, A., Funke, A., Titirici, M.-M., 2013. Hydrothermal conversion of biomass to fuels and energetic materials. *Current Opinion in Chemical Biology*, 17, 515-521.

Kulkarni, N., Shendye, A., Rao, M., 1999. Molecular and biotechnological aspects of xylanases. *Fems Microbiology Reviews*, 23, 411-456.

Lehmann, J., Joseph, S., 2009. Biochar for environmental management - science and technology Earthscan, London.

Levis, J.W., Barlaz, M.A., 2011. Is Biodegradability a Desirable Attribute for Discarded Solid Waste? Perspectives from a National Landfill Greenhouse Gas Inventory Model. *Environmental Science & Technology*, 45, 5470-5476.

Levis, J.W., Barlaz, M.A., Themelis, N.J., Ulloa, P., 2010. Assessment of the state of food waste treatment in the United States and Canada. *Waste Management*, 30, 1486-1494.

Libra, J.A., Ro, K.S., Kammann, C., Funke, A., Berge, N.D., Neubauer, Y., Titirici, M.M., Fühner, C., Bens, O., Jürgen, K., K.-H., E., 2011. Hyddrothermal carbonization of biomass residuals: a comparative review of the chemistry, processes and applications of wet and dry pyrolysis. *Biofuels*, 2, 89-124.

Li, L., Diederick, R., Flora, J.R.V., Berge, N.D., 2013. Hydrothermal carbonization of food waste and associated packaging materials for energy source generation. *Waste Management*, 33, 2478-2492.

Li, L.X., Portela, J.R., Vallejo, D., Gloyna, E.F. 1999. Oxidation and hydrolysis of lactic acid in near-critical water. *Industrial & Engineering Chemistry Research*, 38(7), 2599-2606.

Liu, Z.G., Zhang, F.S., Wu, J.Z., 2010. Characterization and application of chars produced from pinewood pyrolysis and hydrothermal treatment. *Fuel*, 89, 510-514.

Liu, Z., Quek, A., Kent Hoekman, S., Balasubramanian, R., 2013. Production of solid biochar fuel from waste biomass by hydrothermal carbonization. *Fuel*, 103, 943-949.

Lu, X., Jordan, B., Berge, N.D. 2012. Thermal conversion of municipal solid waste via hydrothermal carbonization: Comparison of carbonization products to products from current waste management techniques. *Waste Management*, 32(7), 1353-1365.

Lu, L., Namioka, T., Yoshikawa, K., 2011. Effects of hydrothermal treatment on characteristics and combustion behaviors of municipal solid wastes. *Applied Energy*, 88, 3659-3664.

Lu, X., Pellechia, P., Flora, Joseph R. V., Berge, Nicole, 2013. Influence of reaction time and temperature on product formation associated with the hydrothermal carbonization of cellulose. *Bioresource Technology* 138. 180-190.

Lynam, J.G., Coronella, C.J., Yan, W., Reza, M.T., Vasquez, V.R. 2011. Acetic acid and lithium chloride effects on hydrothermal carbonization of lignocellulosic biomass. *Bioresource Technology*, 102(10), 6192-6199.

Lynam, J.G., Toufiq Reza, M., Vasquez, V.R., Coronella, C.J. 2012. Effect of salt addition on hydrothermal carbonization of lignocellulosic biomass. *Fuel*, 99(0), 271-273.

Malghani, S., Gleixner, G., Trumbore, S.E., 2013. Chars produced by slow pyrolysis and hydrothermal carbonization vary in carbon sequestration potential and greenhouse gases emissions. *Soil Biology & Biochemistry*, 62, 137-146.

Ming, J., Wu, Y., Liang, G., Park, J.B., Zhao, F., Sun, Y.K. 2013. Sodium salt effect on hydrothermal carbonization of biomass: a catalyst for carbon-based nanostructured materials for lithium-ion battery applications. *Green Chem*, 15, 2722-2726.

Mumme, J., Eckervogt, L., Pielert, J., DiakitÃ©, M., Rupp, F., Kern, J.r., 2011. Hydrothermal carbonization of anaerobically digested maize silage. *Bioresource Technology*, 102, 9255-9260.

Muthuraman, M., Namioka, T., Yoshikawa, K., 2010. A comparative study on co-combustion performance of municipal solid waste and Indonesian coal with high ash Indian coal: A thermogravimetric analysis. *Fuel Processing Technology*, 91, 550-558.

Newsome, D.S., 1980. The water-gas shift reaction. *Catalysis Reviews Science and Engineering*, 21(2), 275-318.

Oates, C.G., 1997. Towards an understanding of starch granule structure and hydrolysis. *Trends in Food Science & Technology*, 8, 375-382.

Paraknowitsch, J.P., Thomas, A., Antonietti, M., 2009. Carbon Colloids Prepared by Hydrothermal Carbonization as Efficient Fuel for Indirect Carbon Fuel Cells. *Chemistry of Materials*, 21, 1170-1172.

Patil, S.K.R., Lund, C.R.F. 2011. Formation and Growth of Humins via Aldol Addition and Condensation during Acid-Catalyzed Conversion of 5-Hydroxymethylfurfural. *Energy & Fuels*, 25(10), 4745-4755.

Patwardhan, P.R., Satrio, J.A., Brown, R.C., Shanks, B.H. (2010). Influence of inorganic salts on the primary pyrolysis of cellulose. *Bioresource Technol*, 101, 4646-4655.

Phan, A.N., Ryu, C., Sharifi, V.N., Swithenbank, J., 2008. Characterisation of slow pyrolysis products from segregated wastes for energy production. *Journal of Analytical and Applied Pyrolysis*, 81, 65-71.

Pińkowska, H., Wolak, P., Zlocińska, A., 2011. Hydrothermal decomposition of xylan as a model substance for plant biomass waste - Hydrothermolysis in subcritical water. *Biomass & Bioenergy*, 35, 3902-3912.

Preston, C.M., Trofymow, J.A., Niu, J., Fyfe, C.A., 1998. ^{13}CPMAS-NMR spectroscopy and chemical analysis of coarse woody debris in coastal forests of Vancouver Island. *Forest Ecology and Management*, 111, 51-68.

Ramsurn, H., Kumar, S., Gupta, R.B. 2011. Enhancement of biochar gasification in alkali hydrothermal medium by passivation of inorganic components using Ca(OH)2. *Energ Fuel*, 25, 2389-2398.

Ramke, H.G., Blöhse, D., Lehmann, H.J., Fettig, J., 2009. Hydrothermal carbonization of organic waste. *20th International Waste Management and Landfill Symposiu*.

Remsing, R.C., Swatloski, R.P., Rogers, R.D., Moyna. G. 2006. Mechanism of cellulose dissolution in the ionic liquid 1-n-butyl-3-methylimidazolium chloride: a ^{13}C and $^{35/37}$Cl NMR relaxation study on model systems. *Chem Comm*, 23, 1271-1273.

Ro, K.S., Cantrell, K.B., Hunt, P.G., Ducey, T.F., Vanotti, M.B., Szogi, A.A., 2009. Thermochemical conversion of livestock wastes: Carbonization of swine solids. *Bioresource Technology*, 100, 5466-5471.

Román, S., Valente Nabais, J.M., Ledesma, B., Gonzalez, J.F., Laginhas, C., Titirici, M.M. 2013. Production of low-cost adsorbents with tunable surface chemistry by conjunction of hydrothermal carbonization and activation processes. *Micropor Mesopor Mat*, 165, 127-133.

Román, S., Nabais, J.M.V., Laginhas, C., Ledesma, B., Gonzalez, J.F., 2012. Hydrothermal carbonization as an effective way of densifying the energy content of biomass. *Fuel Processing Technology*, 103, 78 – 83.

Ryu, C., Sharifi, V.N., Swithenbank, J., 2007. Waste pyrolysis and generation of storable char. *International Journal of Energy Research*, 31, 177-191.

Sasaki, M., Fang, Z., Fukushima, Y., Adschiri, T., Arai, K. 2000. Dissolution and hydrolysis of cellulose in subcritical and supercritical water. *Industrial & Engineering Chemistry Research*, 39(8), 2883-2890.

Sasaki, M., Kabyemela, B., Malaluan, R., Hirose, S., Takeda, N., Adschiri, T., Arai, K. 1998. Cellulose hydrolysis in subcritical and supercritical water. *Journal of Supercritical Fluids*, 13(1-3), 261-268.

Saulnier, L., Marot, C., Chanliaud, E., Thibault, J.F., 1995. Cell wall polysaccharide interactions in maize bran. *Carbohydrate Polymers*, 26, 279-287.

Scallet, B.L., Gardner, J.H. 1945. Formation of 5-Hydroxymethylfurfural from D-Glucose in Aqueous Solution1. *Journal of the American Chemical Society*, 67(11), 1934-1935.

Scheutz, C., Samuelsson, J., Fredenslund, A.M., Kjeldsen, P., 2011. Quantification of multiple methane emission sources at landfills using a double tracer technique. *Waste Management*, 31, 1009-1017.

Schuhmacher, J.P., Huntjens, F.J., Vankrevelen, D.W., 1960. Chemical structure and properties of coal XXVI: Studies on artificial coalification. *Fuel*, 39, 223-234.

Sevilla, M., Fuertes, A.B., 2009a. Chemical and structural properties of carbonaceous products obtained by hydrothermal carbonization of saccharides. *Chem. Eur. J* , 15, 4195-4203.

Sevilla, M., Fuertes, A.B., 2009b. The production of carbon materials by hydrothermal carbonization of cellulose. *Carbon*, 47, 2281-2289.

Sevilla, M., Fuertes, A.B., 2011. Sustainable porous carbons with a superior performance for CO2 capture. *Energy & Environmental Science*, 4, 1765-1771.

Sevilla, M., Fuertes, A.B., Mokaya, R., 2011a. High density hydrogen storage in superactivated carbons from hydrothermally carbonized renewable organic materials. *Energy & Environmental Science*, 4, 1400-1410.

Sevilla, M., Macia´-Agullo´, J.A., Fuertes, A.B., 2011b. Hydrothermal carbonization of biomass as a route for the sequestration of CO_2: Chemical and structural properties of the carbonized products. *Biomass and Bioenergy*, 35, 3152-3159.

Siskin, M., Katritzky, A.R., 2001. Reactivity of organic compounds in superheated water: General background. *Chemical Reviews*, 101, 825-835.

Shen, J., and Wyman, C.E. 2012. Hydrochloric acid-catalyzed levulinic acid formation from cellulose: data and kinetic model to maximize yields. *AIChE J*, 58, 236-246.

Spokas, K., Bogner, J., Chanton, J.P., Morcet, M., Aran, C., Graff, C., Moreau-Le Golvan, Y., Hebe, I., 2006. Methane mass balance at three landfill sites: What is the efficiency of capture by gas collection systems? *Waste Management*, 26, 516-525.

Srokol, Z., Bouche, A.G., van Estrik, A., Strik, R.C.J., Maschmeyer, T., Peters, J.A. 2004. Hydrothermal upgrading of biomass to biofuel: studies on some monosaccharide model compounds. *Carbohydrate Research*, 339(10), 1717-1726.

Staley, B.F., Barlaz, M.A., 2009. Composition of Municipal Solid Waste in the United States and Implications for Carbon Sequestration and Methane Yield. *Journal of Environmental Engineering*, 135, 901-909.

Stemann, J., Putschew, A., Ziegler, F. 2013. Hydrothermal carbonization: process water characterization and effects of water recirculation. *Bioresource Technology*, 143, 139-146.

Sweet, M.S., Winandy, J.E., 1999. Influence of degree of polymerization of cellulose and hemicellulose on strength loss in fire-retardant-treated southern pine. *Holzforschung*, 53, 311-317.

Tchobanoglous, G., Theisen, H., Vigil, S., J. , 1993. Integrated solid waste management: engineering principles and management issues. McGraw-Hill, Inc.

Titirici, M.M., Antonietti, M. 2010. Chemistry and materials options of sustainable carbon materials made by hydrothermal carbonization. *Chemical Society Reviews*, 39(1), 103-116.

Titirici, M.M., Antonietti, M., Baccile, N., 2008. Hydrothermal carbon from biomass: a comparison of the local structure from poly- to monosaccharides and pentoses/hexoses. *Green Chemistry*, 10, 1204-1212.

Titirici, M.M., White, R.J., Falco, C., Sevilla, M. 2012. Black perspectives for a green future: hydrothermal carbons for environment protection and energy storage. *Energy & Environmental Science*, 5(5), 6796-6822.

Titirici, M.M., Thomas, A., Antonietti, M. 2007a. Back in the black: hydrothermal carbonization of plant material as an efficient chemical process to treat the CO_2 problem? *New Journal of Chemistry*, 31(6), 787-789.

Titirici, M.M., Thomas, A., Yu, S.-H., Muller, J.-O., Antonietti, M. 2007b. A Direct Synthesis of Mesoporous Carbons with Bicontinuous Pore Morphology from Crude Plant Material by Hydrothermal Carbonization. *Chemistry of Materials*, 19(17), 4205-4212.

USEPA, 1998. Solid waste disposal, fifth ed. USEPA.

USEPA, 2005. Landfill gas emissions model (LandGEM) version 3.02 user's guide. USEPA.

USEPA, 2006. Municipal solid waste in the United States: 2005 facts and figures. USEPA.

USEPA, 2011. 2011 US greenhouse gas inventory report. USEPA.

Waigh, T.A., Donald, A.M., Heidelbach, F., Riekel, C., Gidley, M.J., 1999. Analysis of the native structure of starch gra nules with small angle x-ray microfocus scattering. *Biopolymers*, 49, 91-105.

Wang, Q., Li, H., Chen, L.Q., Huang, X.J., 2001. Monodispersed hard carbon spherules with uniform nanopores. *Carbon*, 39, 2211-2214.

Wang, Z., McDonald, A.G., Westerhof, R.J.M., Kersten, S.R.A., Cuba-Torres, C.M., Ha, S., Pecha, B., Garcia-Perez, M., 2013. Effect of cellulose crystallinity on the formation of a liquid intermediate and on product distribution during pyrolysis. *Journal of Analytical and Applied Pyrolysis*, 100, 56-66.

Watanabe, A., Morita, S., Ozaki, Y., 2007. Temperature-dependent changes in hydrogen bonds in cellulose I alpha studied by infrared spectroscopy in combination with perturbation-correlation moving-window two-dimensional correlation spectroscopy: Comparison with cellulose I beta. *Biomacromolecules*, 8, 2969-2975.

Watanabe, M., Sato, T., Inomata, H., Smith, R.L., Arai, K., Kruse, A., Dinjus, E., 2004. Chemical reactions of C-1 compounds in near-critical and supercritical water. *Chemical Reviews*, 104, 5803-5821.

Weingarten, R., Cho, J., Xing, R., Conner, W.C., and Huber, G.W. 2012. Kinetics and Reaction Engineering of Levulinic Acid Production from Aqueous Glucose Solutions. *ChemSusChem*, 5, 1280-1290.

Williams, P.T., Onwudili, J., 2006. Subcritical and supercritical water gasification of cellulose, starch, glucose, and biomass waste. *Energy & Fuels*, 20, 1259-1265.

Wu, C.H., Chang, C.Y., Lin, J.P., Hwang, J.Y., 1997. Thermal treatment of coated printing and writing paper in MSW: pyrolysis kinetics. *Fuel*, 76, 1151-1157.

Xiao, L., Shi, Z., Xu, F., R., S., 2012. Hydrothermal carbonization of lignocellulosic biomass. *Bioresource Technology*, 118, 619 – 623

Xie, F., Yu, L., Chen, L., Li, L., 2008. A new study of starch gelatinization under shear stress using dynamic mechanical analysis. *Carbohydrate Polymers*, 72, 229-234.

Yamamoto, H., Horii, F., 1993. CP/MAS 13C NMR analysis of the crystal transformation induced for Valonia cellulose by annealing at high temperatures. *Macromolecule*s, 26, 1313-1317.

Yao, C., Shin, Y., Wang, L.-Q., Windisch, C.F., Jr., Samuels, W.D., Arey, B.W., Wang, C., Risen, W.M., Jr., Exarhos, G.J. 2007. Hydrothermal dehydration of aqueous fructose solutions in a closed system. *Journal of Physical Chemistry C*, 111(42), 15141-15145.

Yan, W., Acharjee, T.C., Coronella, C.J., Vásquez, V.R., 2009. Thermal pretreatment of lignocellulosic biomass. *Environmental Progress & Sustainable Energy*, 28, 435-440.

Yasuda, S., Fukushima, K., Kakehi, A., 2001. Formation and chemical structures of acid-soluble lignin I: sulfuric acid treatment time and acid-soluble lignin content of hardwood. *Journal of wood science*, 47, 69-72.

Yin, S., A. K. Mehrotra, Tan, Z.,. 2012. Direct formation of gasoline hydrocarbons from cellulose by hydrothermal conversion with in situ hydrogen. *Biomass & Bioenergy*, 47, 228-239.

Yu, S.H., Cui, X.J., Li, L.L., Li, K., Yu, B., Antonietti, M., Cölfen, H., 2004. From Starch to Metal/Carbon Hybrid Nanostructures: Hydrothermal Metal-Catalyzed Carbonization. *Advanced Materials*, 16, 1636-1640.

Zhang, L., Xu, C., Champagne, P., Overview of recent advances in thermo-chemical conversion of biomass. *Energy Conversion and Management*, 51, 969-982.

Zobel, H.F., Young, S.N., Rocca, L.A., 1988. Starch gelatinization: An X-ray diffraction study. *Cereal Chemistry*, 65, 443-446.

APPENDIX A

MANUSCRIPT PERMISSIONS

ELSEVIER LICENSE
TERMS AND CONDITIONS

Feb 19, 2014

This is a License Agreement between xiaowei lu ("You") and Elsevier ("Elsevier") provided by Copyright Clearance Center ("CCC"). The license consists of your order details, the terms and conditions provided by Elsevier, and the payment terms and conditions.

All payments must be made in full to CCC. For payment instructions, please see information listed at the bottom of this form.

Supplier	Elsevier Limited The Boulevard,Langford Lane Kidlington,Oxford,OX5 1GB,UK
Registered Company Number	1982084
Customer name	xiaowei lu
Customer address	300 main street COLUMBIA, SC 29201
License number	3316850474658
License date	Jan 26, 2014
Licensed content publisher	Elsevier
Licensed content publication	Waste Management
Licensed content title	Thermal conversion of municipal solid waste via hydrothermal carbonization: Comparison of carbonization products to products from current waste management techniques
Licensed content author	Xiaowei Lu,Beth Jordan,Nicole D. Berge
Licensed content date	July 2012
Licensed content volume number	32
Licensed content issue number	7
Number of pages	13
Start Page	1353
End Page	1365
Type of Use	reuse in a thesis/dissertation
Intended publisher of new work	other
Portion	full article
Format	both print and electronic
Are you the author of this Elsevier article?	Yes
Will you be translating?	No
Title of your thesis/dissertation	UNDERSTANDING HYDROTHERMAL CARBONIZATION OF MIXED FEEDSTOCKS FOR WASTE CONVERSION
Expected completion date	Jan 2014

ELSEVIER LICENSE
TERMS AND CONDITIONS

Feb 19, 2014

This is a License Agreement between xiaowei lu ("You") and Elsevier ("Elsevier") provided by Copyright Clearance Center ("CCC"). The license consists of your order details, the terms and conditions provided by Elsevier, and the payment terms and conditions.

All payments must be made in full to CCC. For payment instructions, please see information listed at the bottom of this form.

Supplier	Elsevier Limited The Boulevard,Langford Lane Kidlington,Oxford,OX5 1GB,UK
Registered Company Number	1982084
Customer name	xiaowei lu
Customer address	300 main street COLUMBIA, SC 29201
License number	3317120088158
License date	Jan 27, 2014
Licensed content publisher	Elsevier
Licensed content publication	Bioresource Technologyt
Licensed content title	Influence of reaction time and temperature on product formation and characteristics associated with the hydrothermal carbonization of cellulose
Licensed content author	Xiaowei Lu,Perry J. Pellechia,Joseph R.V. Flora,Nicole D. Berge
Licensed content date	July 2013
Licensed content Volume number	32
Licensed content issue number	None
Number of pages	11
Start Page	180
End Page	190
Type of Use	reuse in a thesis/dissertation
Intended publisher of new work	other
Portion	full article
Format	both print and electronic
Are you the author of this Elsevier article?	Yes
Will you be translating?	No
Title of your thesis/dissertation	UNDERSTANDING HYDROTHERMAL CARBONIZATION OF MIXED FEEDSTOCKS FOR WASTE CONVERSION
Expected completion date	Jan 2014

ELSEVIER LICENSE
TERMS AND CONDITIONS

Feb 19, 2014

This is a License Agreement between xiaowei lu ("You") and Elsevier ("Elsevier") provided by Copyright Clearance Center ("CCC"). The license consists of your order details, the terms and conditions provided by Elsevier, and the payment terms and conditions.

All payments must be made in full to CCC. For payment instructions, please see information listed at the bottom of this form.

Supplier	Elsevier Limited The Boulevard,Langford Lane Kidlington,Oxford,OX5 1GB,UK
Registered Company Number	1982084
Customer name	xiaowei lu
Customer address	300 main street COLUMBIA, SC 29201
License number	3316850338558
License date	Jan 26, 2014
Licensed content publisher	Elsevier
Licensed content publication	Bioresource Technology
Licensed content title	Influence of process water quality on hydrothermal carbonization of cellulose
Licensed content author	Xiaowei Lu,Joseph R.V. Flora,Nicole D. Berge
Licensed content date	February 2013
Licensed content Volume number	154
Licensed content issue number	None
Number of pages	11
Start Page	229
End Page	239
Type of Use	reuse in a thesis/dissertation
Portion	full article
Format	both print and electronic
Are you the author of this Elsevier article?	Yes
Will you be translating?	No
Title of your thesis/dissertation	UNDERSTANDING HYDROTHERMAL CARBONIZATION OF MIXED FEEDSTOCKS FOR WASTE CONVERSION
Expected completion date	Jan 2014